

SHINING A LIGHT  
ON THE FUTURE  
OF BIOPHOTONICS

VII.  
**ICOB**  
**2024**

International  
Congress on  
Biophotonics

**3 – 7 March**  
Jena | Germany

**POSTER ABSTRACTS**

Organized by:



Funded by:



in cooperation with:



Presented by:



# General data pipeline for MALDI – TOF/ IMS and statistical analysis

Mou Adhikari<sup>a,b</sup>, Thomas Bocklitz<sup>a,b,c</sup>

<sup>a</sup> *Institute of Physical Chemistry, Friedrich Schiller University, University of Jena, 07743 Jena, Germany*

<sup>b</sup> *Leibniz Institute of Photonic Technology, Member of Research Alliance “Leibniz Health Technologies”, 07745 Jena, Germany*

<sup>c</sup> *Institute of Computer Science, University of Bayreuth, 95447 Bayreuth, Germany*

Matrix-assisted laser desorption/ ionization and time-of-flight/ imaging (MALDI-TOF/ IMS) mass spectrometry is a label-free technology for biological and chemical analysis [1]. However, processing the MALDI-TOF/ IMS data presents challenges, including background noise, intensity variations, and precise mass determination for each peak [1]. Making the right computational decisions is crucial because a MALDI-TOF/ IMS experiment involves a huge number of mass spectra [2]. In order to address this challenge, a proper data processing pipeline is essential.

Our data processing pipeline is structured into two primary stages: pre-processing, and analysis. We conduct an initial examination of spectra in the pre-processing phase, whereas classification is the primary objective of the analysis section. The pre-processing workflow consists of the following steps: peak alignment, baseline correction, smoothing, peak picking, peak binning, normalization, and dimension reduction.

As the correct choice of pre-processing parameters has a significant effect on the performance of further analytical steps, we investigated the effect of binning width on classification outcomes. Binning describes the process of reducing the number of points in the spectrum by combining neighboring mass-to-charge ratios ( $m/z$ ) into a single same-mass bin [1]. This is motivated by the fact that MALDI peak positions are often similar but not identical due to several factors, like instrumental precision (especially the TOF detection), isotopic variants, or matrix effects [2]. We have explored both fixed-width peak binning (using five bin widths) and adaptive binning together with the Gaussian Naive Bayes algorithm. The trained models were validated using leave-one-patient-out cross-validation. Our initial findings indicate that classification accuracy improves as the binning width increases for fixed-width binning, while adaptive binning outperforms all fixed binning methods.

While the classification accuracy may not be exceptionally high, our future research will focus on conducting a systematic investigation of classification in the context of highly imbalanced MALDI data sets with respect to binning width.

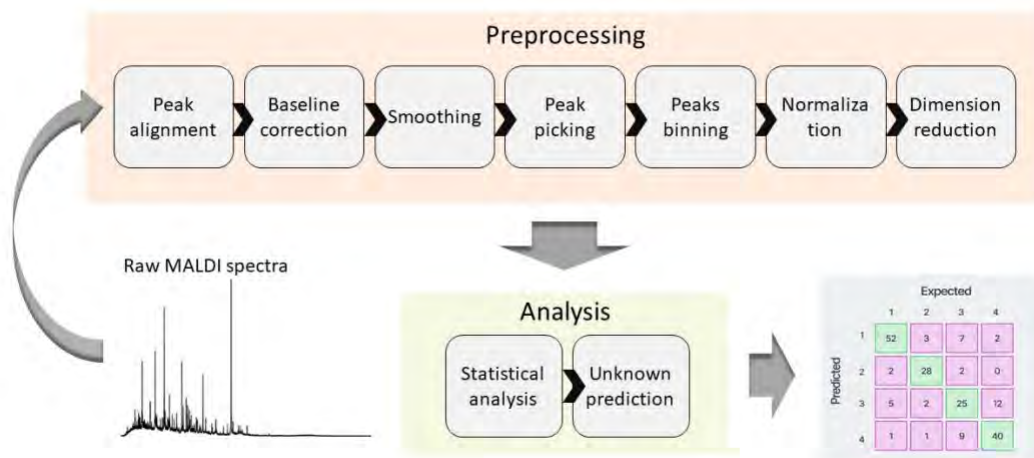


**Figure 1** Schematic diagram of MALDI data analysis pipeline. The data analysis step is divided into mainly two parts. The 1<sup>st</sup> part is pre-processing, and the 2<sup>nd</sup> part is analysis. The pre-processing consists of several steps to make data more understandable, and these steps are shown in the above figure.

## ACKNOWLEDGMENTS

This work is supported by the BMBF, funding program Photonics Research Germany (13N15719 (LPI-BT5)) and is integrated into the Leibniz Center for Photonics in Infection Research (LPI). The LPI initiated by Leibniz-IPHT, Leibniz-HKI, Friedrich Schiller University Jena, and Jena University Hospital is part of the BMBF national roadmap for research infrastructures.

## REFERENCES

- [1] “Alexandrov T. BMC Bioinformatics. 2012;13 Suppl 16, S11. doi: 10.1186/1471-2105-13-S16-S11.
- [2] P. Ràfols *et al.*, *Mass Spectrom. Rev* 2018., 37, 3, 281–306, doi: 10.1002/mas.21527.

# Investigation of data fusion pipelines for correlation of photonic and clinical data

Kazi Sultana Farhana Azam<sup>a,b</sup>, Oleg Rybchykov<sup>a,b</sup>, Thomas W. Bocklitz<sup>a,b,c</sup>

<sup>a</sup> *Leibniz Institute of Photonic Technology, Member of Leibniz Health Technologies, Member of the Leibniz Centre for Photonics in Infection Research (LPI), Albert-Einstein-Strasse 9, 07745 Jena, Germany.*

<sup>b</sup> *Institute of Physical Chemistry (IPC) and Abbe Center of Photonics (ACP), Friedrich Schiller University Jena, Member of the Leibniz Centre for Photonics in Infection Research (LPI), Helmholtzweg 4, 07743 Jena, Germany.*

<sup>c</sup> *Institute of Computer Science, Faculty of Mathematics, Physics & Computer Science, University Bayreuth Universitaetsstraße 30, 95447 Bayreuth, Germany.*

Data fusion aims to provide a more accurate sample description than a single data type alone and it minimizes the uncertainty of the results by combining data from multiple sources. Specific data fusion pipelines usable in the context of the medical and biomedical fields depend on the task and the investigated data types. These pipelines are designed to combine images, spectra [1], demographic information, clinical values, etc.

As a part of our investigation of data fusion, we investigate both instance-level and local-level fusion approaches.

For instance-level data fusion, we designed the workflow where different types of data (images, spectra, discrete and continuous data) will be combined after the preprocessing routine with subsequent feature extraction and weighting. The data weighting step is especially important in the case of heterogeneous data types to balance the contribution of different sources. The balanced features can then be used to construct the model.

To continue our study on data fusion, we investigated the early detection of sepsis combining Raman spectra and clinical data. With plans to incorporate Raman spectra and clinical data in subsequent stages of the study, we have currently combined clinical data with Raman predictions from the optimal model of individual Raman spectra classification (see Figure 1). We performed both combined and single-mode data analysis and applied two-level cross-validation (CV) [2] to obtain a realistic estimation of the model performance. In the analysis, we optimize our models in the inner CV and only test the model in the outer CV. We also investigated the influence of different scaling methods in the inner CV. After conducting analyses on combined and both single modalities, the results indicate that the combined model significantly outperformed the single modalities.

Another important objective is to investigate the potential improvements when combining different data sources. We aim to enhance the analysis preciseness by incorporating data fusion in more studies. Therefore, we ensured the code reusability

for future projects by designing a flexible and user-friendly pipeline compatible with various machine-learning methods.

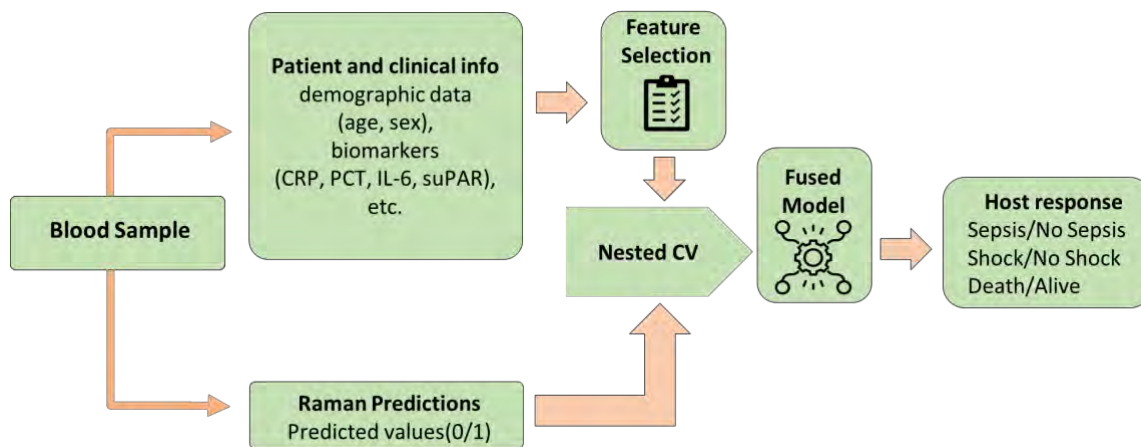


**Figure 1** Data fusion pipeline for combining photonic and clinical data. The general workflow for early detection of sepsis combines Raman spectra and clinical values and here we use Raman predictions instead of Raman spectra where Raman predictions are generated from single-mode Raman data analysis, and we select the best model's predictions according to CV. The developed systematic evaluation workflow can now also be applied to the analysis of other data such as cellular data.

## ACKNOWLEDGMENTS

Financial support from the EU, the TMWWDG, the TAB, the BMBF, the DFG, the Carl-Zeiss Foundation, and the Leibniz Association is greatly acknowledged. This work is supported by the BMBF, funding program Photonics Research Germany (13N15715 (LPI-BT4-FSU) and 13N15710 (LPI-BT3-FSU)) and is integrated into the Leibniz Center for Photonics in Infection Research (LPI). The LPI initiated by Leibniz-IPHT, Leibniz-HKI, Friedrich Schiller University Jena, and Jena University Hospital is part of the BMBF national roadmap for research infrastructures.

## REFERENCES

1. Azam, Kazi Sultana Farhana, Oleg Ryabchykov, and Thomas Bocklitz. "A Review on Data Fusion of Multidimensional Medical and Biomedical Data." *Molecules* 27.21 (2022): 7448.
2. Guo, Shuxia, et al. "Common mistakes in cross-validating classification models." *Analytical Methods* 9.30 (2017): 4410-4417.



# Graphene Photonic Heterostructure Device for Biosensing

Emir Aznakayev<sup>a</sup>, Victor Zadorozhnii<sup>b</sup>

<sup>a</sup>National Aviation University, Liubomyra Huzara Avenue 1, Kyiv, Ukraine, [aznakayev1@yahoo.com](mailto:aznakayev1@yahoo.com)

<sup>b</sup>Taras Shevchenko National University of Kyiv, 64/13, Volodymyrska Street, Ukraine, [v.i.zador@gmail.com](mailto:v.i.zador@gmail.com)

The Surface Plasmon Resonance technique is extremely surface sensitive method that allows detecting and examining biological species being attached to the surface of biosensor. It allows the real-time and label-free detection and analysis due to the interfacial refractive index changes which is associated with binding of biomolecules in the tested substances with biosensor surface. Recently, there has been significant progress in the use of graphene as transparent electrodes in various optoelectronic devices [1, 2]. In this research, we present a photonic heterostructure device for biosensing applications using an electrically controlled liquid crystal (LC). Liquid crystal with graphene electrodes controlling the sensory structure properties, as well as the in-plane black phosphorus [3] and a distributed Bragg reflector (DBR) for the detection of biological agents in the terahertz frequency range are being considered. Based on a previously proposed scheme of a photonic device for control of terahertz radiation [4], a new scheme of biosensor for environmental analysis is proposed. Modeling of the detection process is been carried out with use the transfer-matrix method [5, 6]. The transfer matrix method is based on the fact that, according to Maxwell's equations, there are simple conditions for the continuity of the electric field across boundaries of DBR from one medium to another. If the input electromagnetic field intensity of the layer is known, the output electromagnetic field intensity of the layer can be obtained using a simple matrix operation. The stack of layers can then be thought of as a system matrix, which is the product of the matrices of the individual layers. The last step of the method involves converting the system matrix back into reflection and transmission coefficients. As the object of research we consider messenger ribonucleic acid (mRNA). The influence of changing the parameters of the photonic device and the characteristics of detected biological agents on the spectral properties of the photonic device was studied for bioobjects classification. The change in the intensity of the radiation transmitted into the biosensor and reflected from it in the presence of biomolecules on the surface of BP depends on the type and number of biomolecules  $N_{bio}$  on the BP sensing surface (Fig. 1, 2). For example, reflectivity of radiation as a function of wavelength at the Plasmon Resonance Phenomena at the detection of some type of biomolecules (mRNA) is presented in Figures 1, 2. The characteristics of the reflected electromagnetic wave determination make it possible to detect the type of biological agent.

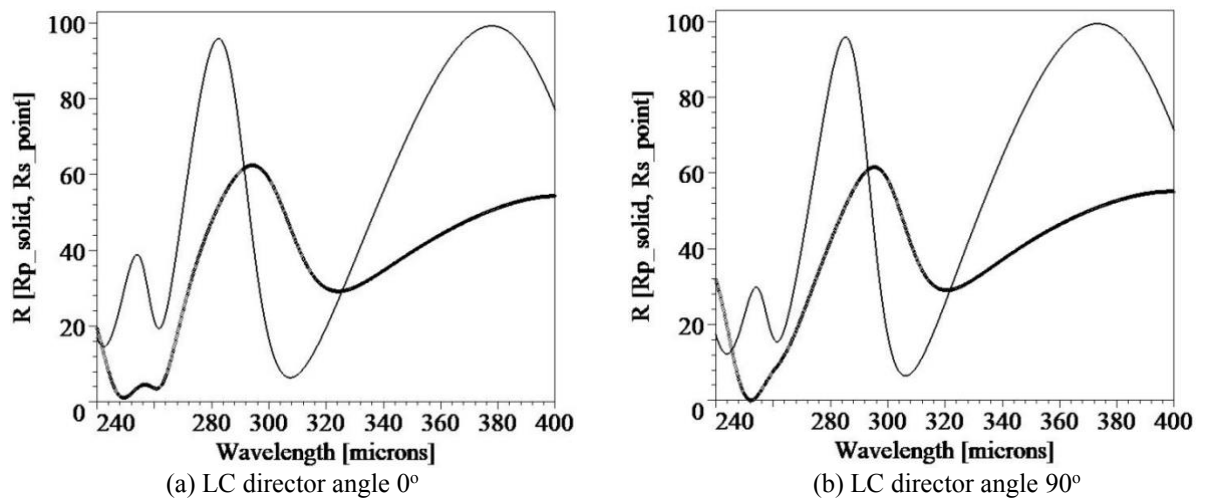


**Figure 1.** Reflectance  $R(\%)$  for two polarizations  $p$  (solid line) and  $s$  (point line), when mRNA molecules are far from the black phosphorus sensing surface

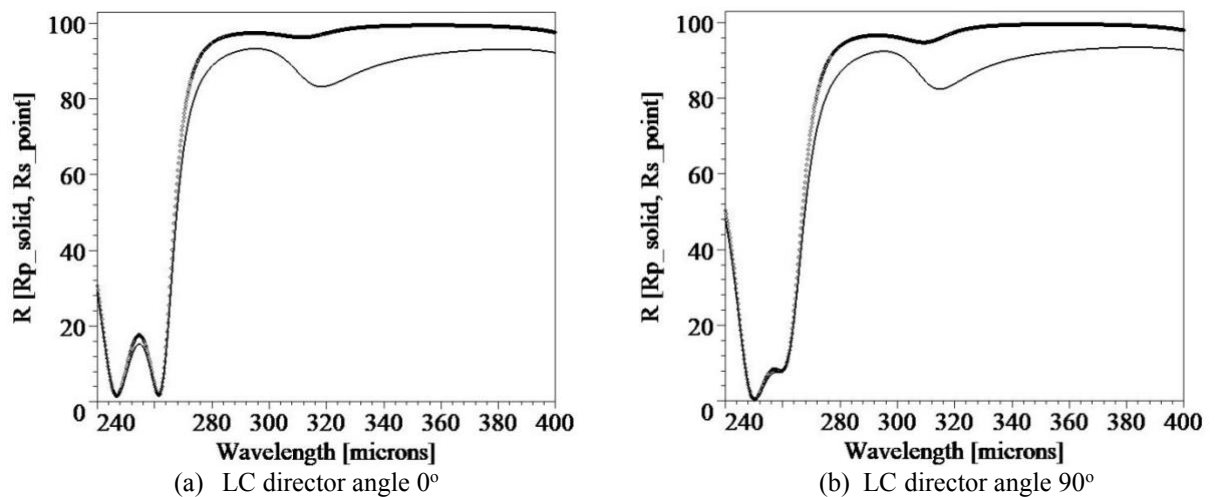


**Figure 2.** Reflectance  $R(\%)$  for two polarizations  $p$  (solid line) and  $s$  (point line), when mRNA molecules are on the black phosphorus surface and the number of biomolecules  $N_{bio} = 23500$  on sensing surface is close to the maximum value

## REFERENCES

1. Y. S. Woo, *Micromachines* (Basel), 2019, **10**, 13, 1-27.
2. A.D. Boardman, Yu. G. Rapoport, D.E. Aznakayeva, E.G. Aznakayev, V. V. Grimalsky; Mei Zhang (Ed.). *Graphene Metamaterial Electron Optics: Excitation Processes and Electro-Optical Modulation: Handbook of Graphene: Volume 3*, Wiley Publ., 492 p., USA, 2019.
3. J. Pan, W. Zhu, H. Zheng, J. Yu, Y. Chen, H. Guan, H. Lu, Y. Zhong, Y. Luo, and Z. Chen, *Optics Express*, 2020, **28**, 13443-13454.
4. V.I. Zadorozhnyi, *Molecular Crystals and Liquid Crystals*, 2022, **747**, 23-29.
5. T. Zhan, Xi Shi, Y. Dai, X. Liu and J. Zi, *J. Phys.: Condensed Matter*, 2013, **25**, 215301, 1-10.
6. M. C. Troparevsky, A. S. Sabau, A. R. Lupini, Z. Zhang, *Optics Express*, 2010, **18**, 24715-24721.

# Nonlinear multimodal imaging towards endoscopic applications

Hyeonsoo Bae<sup>a,b</sup>, Matteo Calvarese<sup>a,b</sup>, Tobias Meyer-Zedler<sup>a,b</sup>, Anna Mühlig<sup>c</sup>, Chenting Lai<sup>d</sup>, Karl Reichwald<sup>d</sup>, Bernhard Messerschmidt<sup>d</sup>, Orlando Guntinas-Lichius<sup>c</sup>, Michael Schmitt<sup>a</sup>, Juergen Popp<sup>a,b</sup>

<sup>a</sup> *Institute of Physical Chemistry and Abbe Center of Photonics, FSU Jena, Germany*

<sup>b</sup> *Leibniz Institute of Photonic Technology (IPHT), Member of Leibniz Health Technologies, Member of the Leibniz Centre for Photonics in Infection Research (LPI), Jena, Germany*

<sup>c</sup> *Department of Otorhinolaryngology, Jena University Hospital, Jena, Germany*

<sup>d</sup> *GRINTECH GmbH, Otto-Eppenstein-Str. 7 Jena, Germany*

Since the advent of the scanning Coherent Anti-Stokes Raman Scattering (CARS) microscope in the 1980s, the field of CARS microscopy has diversified, exploiting its remarkable capacity for label-free imaging of molecular species distributions. A key development in this area is the incorporation of ultra-short pulse lasers, enabling the concurrent capture of other nonlinear imaging modalities, such as Second Harmonic Generation (SHG) and Two Photon Excited Fluorescence (TPEF). However, the adaptation of nonlinear imaging techniques for endoscopic use — positioning them as viable *in vivo* diagnostic imaging tools in clinical settings — requires overcoming substantial obstacles. These include minimizing background noise in the delivery fiber, refining probe miniaturization, enhancing light transmission efficiency for both excitation and detection, and improving data processing across various imaging techniques.

In light of these challenges, we developed distinct nonlinear endoscopic systems [1]-[3], and introduce here mainly two endoscopes as shown in Figure 1 below. The first, a multicore fiber-based imaging probe [1], employs proximal remote scanning, obviating the need for electro-mechanical moving parts at the distal fiber end. A custom image reconstruction algorithm is employed to improve the interpretability of images, which are otherwise constrained by the inherent pixelation from the core distribution. This endoscope produces multimodal images of bulk tissue samples with a level of detail that satisfies the operational demands of clinical applications, offering a comparable alternative to images obtained from traditional nonlinear microscopes at a resolution of tissue level.

The second system is predicated on a double-core double-clad (DCDC) fiber [2], designed for background-free operation and high-efficiency in laser light delivery and epi-directional signal collection. The system's all-fiber architecture synergistically combines a fiber laser source with a robust coupling unit and a compact endoscopic tube, complete with a piezo fiber scanner. This configuration permits the endoscope to



deliver high-resolution images, delineating single cells and their sub-cellular components, including cell nuclei.

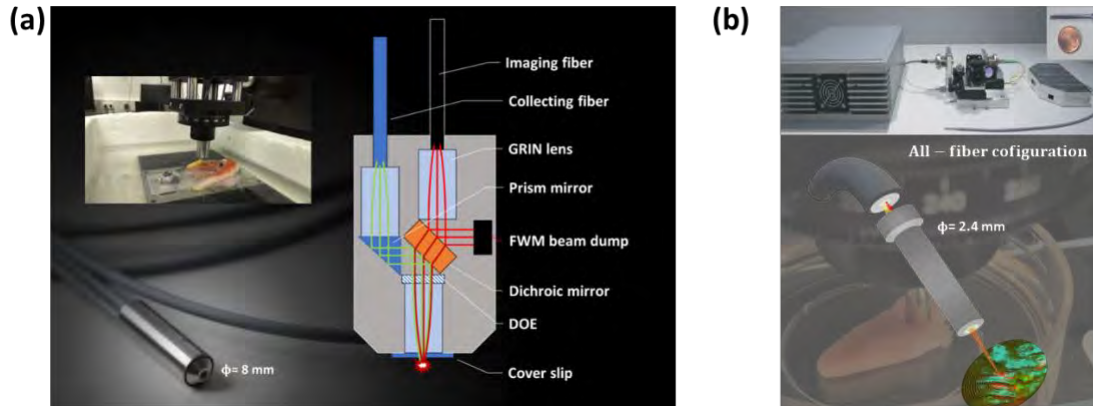


**Figure 1** (a) Imaging Fiber Probe: Proximal scanning is transferred to distal end by multicore fiber. The figure presents the internal optics design of the probe head, which mimics the conventional laser scanning microscope (b) DCDC fiber nonlinear endoscopic imaging probe. The pulse laser and the endoscope with the DCDC fiber is set in all-fiber connection by the coupling unit. Due to the separated delivery of two pulses (pump / Stokes) into two cores, FWM background (from delivery fiber) free imaging is realized.

## ACKNOWLEDGMENTS TIMES

The work presented has received funding from the European Union's Horizon 2020 research and innovation programme under grant agreements No 101016923 (CRIMSON) and No. 860185 (PHAST). This work is supported by the BMBF projects TheraOptik (FKZ 13GW0370E) and the funding program Photonics Research Germany (FKZ: 13N15464.) and is integrated into the Leibniz Center for Photonics in Infection Research (LPI). The LPI initiated by Leibniz-IPHT, Leibniz-HKI, UKJ and FSU Jena is part of the BMBF national roadmap for research infrastructures.

## REFERENCES

1. Bae, H., Rodewald, M., Meyer-Zedler, T. et al. *Sci Rep*, 2023, **13**, 13779.
2. Pshenay-Severin, E., Bae, H., Reichwald, K. et al., *Light Sci Appl*, 2021, **10**, 207.
3. Lai, C., et al., 2023, **28**(6), 066004.

# Intraoperative Tumor Diagnosis in Head and Neck Cancer with Raman Spectroscopy: The Prospective Clinical Trial RAMAN-HNSCC

Ayman Bali<sup>a</sup>, Thomas Bitter<sup>a</sup>, Ines Latka<sup>b</sup>, Florian Windirsch<sup>b</sup>, Mussab Kouka<sup>a</sup>, Jonas Ballmaier<sup>a</sup>, Katja Otto<sup>a</sup>, Katja Scherf<sup>a</sup>, Nikolaus Gaßler<sup>c</sup>, Anna Mühlig<sup>a</sup>, David Pertzborn<sup>a</sup>, Jürgen Popp<sup>b,d</sup>, Ferdinand von Eggeling<sup>a</sup>, Iwan W. Schie<sup>b,e</sup>, Orlando Guntinas-Lichius<sup>a</sup>

<sup>a</sup> Department of Otorhinolaryngology, Jena University Hospital, Jena, Germany

<sup>b</sup> Leibniz Institute of Photonic Technology, Jena, Germany

<sup>c</sup> Department of Pathology

<sup>d</sup> Institute of Physical Chemistry and Abbe Centre of Photonics, Friedrich Schiller University Jena, Germany

<sup>e</sup> Department for Medical Engineering and Biotechnology, University of Applied Sciences Jena, Germany

Head and neck cancer is the seventh most prevalent cancer type globally, with approximately 890,000 new cases diagnosed annually, leading to approximately 450,000 deaths. Traditionally, these malignancies were primarily associated with alcohol and tobacco use. However, in recent years, there has been an increase in cases linked to human papillomavirus (HPV) for oropharyngeal cancer. Surgical resection is a predominant treatment modality, with the primary objective of achieving complete tumor removal while minimizing morbidity and preserving functional and aesthetic aspects [1].

Head and neck cancer originates from epithelial tissues, and their location on internal body surfaces allows for direct visual, endoscopic, or microscopic examination. The conventional methods involve white-light inspection, which lacks the capacity to reliably distinguish between tumorous tissue, precancerous lesions, benign alterations, and inflammation. In the context of surgery for head and neck squamous-cell carcinoma (HNSCC), the successful outcome heavily depends on complete tumor excision. The standard approach involves biopsies and subsequent histological examination, which is both time-consuming and subjective for intraoperative decision-making [2].

Biophotonic techniques, including Raman spectroscopy, a non-invasive, non-ionizing, and contrast agent-free technique, have demonstrated the ability to differentiate between tumorous and non-tumorous tissues *ex vivo* [3, 4, 5].

The primary objective of this prospective monocentric clinical trial RAMAN-HNSCC (DRKS00028114) is to assess the feasibility of utilizing Raman spectroscopy for a real-time *in vivo* tumor differentiation and comparing the results with histopathological findings. Secondary objectives encompass validating measurement properties, ensuring safety, and assessing ease of use. Furthermore, the study aims to evaluate the accuracy and precision of Raman spectroscopy as a diagnostic method, providing insights into its overall efficacy.

This study has the potential to improve intraoperative tumor diagnostic in head and neck cancer, addressing the pressing need for an objective, real-time assessment of tumor margins during surgical procedures. The findings could positively impact patient

outcomes by improving the precision of tumor resection and preserving critical functional and aesthetic elements.

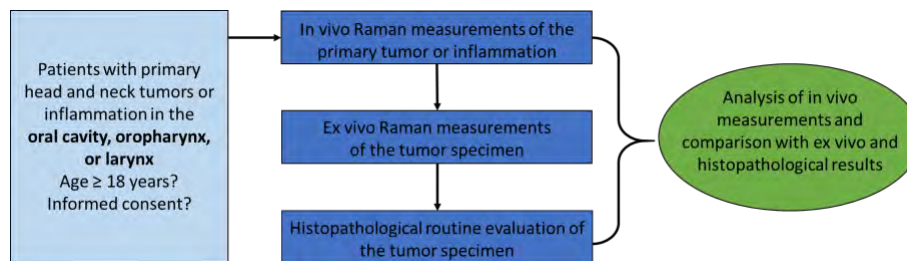


**Figure 1.** Workflow for the clinical study RAMAN-HNSCC



**Figure 2.** Recording Raman spectra in an oropharyngeal carcinoma using the Raman probe developed at the Leibniz Institute of Photonic Technology, Jena, Germany

## ACKNOWLEDGMENTS

We acknowledge funding from the Carl Zeiss Foundation, CRIMSON – Coherent Raman Imaging for the molecular study of origin of diseases (EU Horizon 2020-ICT, grant number 101016923), CHARM – Chemometric Histopathology via Coherent Raman Imaging for precision medicine (HORIZON-EIC-2021-TRANSITIONCHALLENGES-01, grant number 101058004), TROPHY – ulTRafast hOlograPHic FTIR microscopY (HORIZON-EIC-2021-PATHFINDER-OPEN-01, grant number 101047137) and QUANCER – Quantum microscopy with non-detected light for chemical-selective imaging of tumor tissue in a clinical setting (BMBF FKZ: 13N16444).

## REFERENCES

1. Chow, L.Q.M.; Head and Neck Cancer. *N Engl J Med*, 2020. 382(1): p. 60-72.
2. Pertzborn, D., Nguyen H.N., Hüttmann K., Prengel J., Günther E., Guntinas-Lichius O., von Eggeling F., Hoffmann F.; *Cancers (Basel)*, 2022. 15(1).
3. Cordero E., Latka I., Matthäus C., Schie I.W., Popp J.; *J. Biomed. Opt.* 23(7) 071210.
4. Ortega, S., Halicek M., Fabelo H., Callico G.M., Fei B.; *Biomed Opt Express*, 2020. 11(6): p. 3195-3233.
5. Bocklitz T., Bräutigam K., Urbanek A., Hoffmann F., von Eggeling F., Ernst G., Schmitt M., Schubert U., Guntinas-Lichius O., Popp J.; *Anal Bioanal Chem.* 2015 Oct;407(26):7865-73.

ICOB-P-06

# Label-free Surface Enhanced Raman Scattering (SERS) of Different Proteins

Shrobona Banerjee<sup>a</sup>, Lars Dannenberg<sup>a</sup>, Janina Kneipp<sup>a</sup>

<sup>a</sup> Department of Chemistry, Humboldt-Universität zu Berlin, Brook-Taylor-Str. 2, 12489 Berlin, Germany

Surface-enhanced Raman scattering (SERS) spectra of nanoparticle-protein aggregates are valuable in characterizing the interaction of proteins with nanomaterials<sup>1</sup>. The structure and interaction of proteins in aqueous environments and in particular, their interaction with nanostructures is difficult to probe. Proteins are large molecules with a variety of functional groups, and their structure can be affected also by the slight changes in local microenvironment. Since the spectral information from SERS is affected already by small changes in the interaction of proteins with the nanostructures, brought about by slight variation in properties of the system such as concentration or changes in surface potential, it is important to compare the SERS spectra of proteins collected under different experimental conditions. Moreover, it is known that the amino acid sequence of proteins influences their secondary structure in biological and artificial environments.

We collected SERS spectra of different proteins using the same plasmonic substrate in an aqueous environment, so that we can observe the variations in SERS solely due to differences in protein structure and conformation. Thereafter, we performed a statistical analysis of a large number of spectra of different proteins and relate it to protein size, amino acid content and sequence<sup>2</sup>, as well as concentration. The results can provide insight into obtaining details of protein structure and protein-nanoparticle interactions in biological and/or biomimetic systems, which in turn can pave the way for better nanostructure fabrication as well as interpretation of SERS variations.

## ACKNOWLEDGEMENTS

S.B. and J.K. gratefully acknowledge funding by EU MSCA-DN 101072818 (DYNAMO). L.D. acknowledges funding by a short-term research grant of the School of Analytical Sciences Adlershof (SALSA STF23-04).

## REFERENCES

1. Szekeres, G.P., Kneipp, J., *Front. Chem.*, **2019**, *7*, 30
2. Szekeres, G.P.; Kneipp, J., *Analyst*, **2018**, *143*, 6061-6068

# Investigating microbiome-host interactions by combining marker-independent imaging with machine learning approaches in an Organ-on-a-Chip application

Emanuel Behling<sup>a</sup>, Daniel Carvajal-Berrio<sup>a</sup>, Benjamin Suchalla<sup>a</sup>, Eduardo Bras<sup>b,c</sup>, Bernhard Krismer<sup>d</sup>, Peter Loskill<sup>b,c</sup>, Katja Schenke-Layland<sup>a,b</sup>, Julia Marzi<sup>a,b</sup>

<sup>a</sup>*Institute of Biomedical Engineering, Department for Medical Technologies & Regenerative Medicine, Eberhard Karls University Tübingen, Germany*

<sup>b</sup>*NMI Natural and Medical Sciences Institute at the University of Tübingen, Reutlingen, Germany*

<sup>c</sup>*Institute of Biomedical Engineering, Department for Microphysiological Systems, Eberhard Karls University Tübingen, Germany*

<sup>d</sup>*Interfaculty Institute for Microbiology and Infection Medicine, Infection Biology Unit, Eberhard Karls University Tübingen, Germany*

The human microbiome plays a crucial role for human health and predisposition to a variety of diseases. Early identification of life-threatening pathogens as well as understanding their interactions with the microbiome will enable the development of novel treatments, potentially overcoming limitations by multi-resistant strains. However, static culture of nasal microbiome for in vitro testing remains challenging and conventional readouts to study host-microbiome interactions such as gene and protein expression requires time-consuming and destructive sample preparation.

Therefore, we used Raman generated spectral fingerprints to i) show the progression of bacteria-host interaction at the example of an infection with the opportunistic pathogen *C. aurimucosum* and to ii) investigate the potential of microbiome editing by adding competitive strains. Combined with machine learning approaches, Raman imaging was implemented to discriminate different bacteria strains and to characterize their metabolites as well as subcellular components of the mucosal cells. A support vector machine classification identified the different strains in a complex 3D environment with high accuracy.

With this work, we aim to contribute to solve the growing problem of antibiotic resistance by combining label-free live-imaging with machine learning approaches to investigate microbiome-host interactions. The data shows that Raman microspectroscopy is a versatile method, enabling quick targeted readouts at high spatial resolution.

# Surface-enhanced Raman scattering of ergothioneine in biological samples.

Stefano Fornasaro<sup>a</sup>, Valter Sergo<sup>b</sup>, Alois Bonifacio<sup>b</sup>

<sup>a</sup> *Department of Chemical and Pharmaceutical Sciences, University of Trieste, Via Giorgieri 1, 34100 Trieste, Italy*

<sup>b</sup> *Department of Engineering and Architecture, University of Trieste, Via Valerio 6a, 34100 Trieste, Italy*

Ergothioneine, a natural amino acid, has gained recent prominence due to its unique properties and roles in various health conditions. This poster presentation presents its relevance in the context of label-free Surface Enhanced Raman Scattering (SERS). Intense SERS spectra of ergothioneine are achieved using near-infrared excitation on various Ag and Au substrates. A distinctive spectral pattern, characterized by a prominent band at 480-486  $\text{cm}^{-1}$ , remains consistent across diverse substrate types [1].

This same spectral pattern is observed in SERS spectra of filtered erythrocyte lysates, affirming the presence of this metabolite within these cells. The presence of ergothioneine bands in label-free SERS spectra of serum and plasma, as documented by multiple authors in the literature, is examined, underscoring the significance of this amino acid in the interpretation of SERS spectra from these biological fluids [2]. Furthermore, results from a SERS quantification study of this metabolite in serum are reported.

## REFERENCES

1. Fornasaro et al. *Spectrochim Acta A Mol Biomol Spectrosc*, **2021**, 246:119024
2. Fornasaro et al. *FEBS Lett*, **2022**, 596(10):1348-1355.



# Fusion of food profiling data from various analytical techniques

K. C. Brettschneider, S. Seifert

*University of Hamburg, Hamburg School of Food Science, Grindelallee 117, 20146 Hamburg*

The growing consumer desire for safe, authentic and high-quality food products is increasing the demand for analytical methods to verify these properties. For this reason, numerous approaches based on various analytical techniques have been developed. All of these approaches, however, only focus on a specific part of the complex composition of food. To obtain a more comprehensive view, it can therefore be useful to combine different data sets in data fusion approaches.

Data fusion can be performed in a variety of ways depending on the use case and the available data to improve prediction performance or to better understand the complex data of individual approaches. In general, the different approaches can be divided into three different groups [1,2]: The first group is called low-level fusion. Here, the data sets are preprocessed individually and combined immediately afterwards.. Mid-level data fusion combines only relevant information of the individual data sets determined by an additionally applied selection method, while high-level fusion combines models that have been trained on the individual data sets.

Here we present a review on the state of the art of data fusion for food profiling using data from spectroscopic and other analytical techniques. The applied approaches will be compared and critically analyzed, and their applicability and feasibility will be evaluated.

## ACKNOWLEDGMENTS

This IGF Project of the FEI is supported via AiF (German Federation of Industrial Research Association, AiF project 22909N) within the program for promoting Industrial Collective Research (IGF) of the Federal Ministry of Economic Affairs and Climate Action (BMWK), based on a resolution of the German Parliament.

## REFERENCES

1. T. Casian, B. Nagy, B. Kovács, D.L. Galata, E. Hirsch, A. Farkas, *Molecules*, 2022, **27**, 1-41.
2. E. Borrás, J. Ferre, R. Boque, M. Mestres, L. Acena, O. Busto, *Analytica Chimica Acta*, 2015, **891** 1-14.

# Label-free Cancer Cell Death Monitoring by Stimulated Raman Microscopy

Maryam Rezaei<sup>a</sup>, Kai Moritz Eder<sup>2</sup>, Felix Neumann<sup>a</sup>, Björn Kemper<sup>2</sup>, Jürgen Schnekenburger<sup>2</sup>, Tim Hellwig<sup>a</sup>, Max Brinkmann<sup>a</sup>

<sup>a</sup> *Refined Laser Systems GmbH, Mendelstr. 11, 48149 Münster, Germany*

<sup>b</sup> *Biomedizinisches Technologiezentrum, Mendelstraße 17, 48149 Münster, Germany*

Label-free imaging techniques are valuable tools in biomedical research for minimally-invasive monitoring of biological processes without the need for exogenous labels. In the field of cancer research, it is crucial to differentiate between healthy and dying cells, as cancer therapies aim to induce apoptosis only in cancer cells while minimizing harm to healthy cells. However, current imaging methods often rely on exogenous labels that can interfere with cellular processes.

This study applies the label-free imaging technique stimulated Raman scattering for monitoring of cell death in MCF7 breast cancer cells. SRS detects intrinsic molecule specific information. Cell death was induced using the drug staurosporine, typically used in preclinical research to induce apoptosis and as a lead compound in drug discovery. Our novel SRS imaging setup rapidly acquires multispectral datasets with high chemical specificity by scanning the spectral range of 700-3100 1/cm in just 100 ms, providing a tenfold increase in acquisition speed over state-of-the-art systems. Therewith, it enabled clear visualization of changes in the shapes of the nucleus and cytoplasm during cell death. A spectral phasor analysis additionally revealed spectral changes and facilitated the differentiation of lipid droplet types based on their chemical composition.

Taken together, label-free imaging with SRS contribute to a deeper understanding of cell death in cancer research by minimally-invasive monitoring while preserving cellular integrity and minimizing interference from exogenous labels. The novel system offers new applications for SRS in high throughput screening of drug induced cellular effects.

# Rigid endomicroscopic system for cancer diagnosis and tissue removal

Matteo Calvarese<sup>1</sup>, Hyeonsoo Bae<sup>1</sup>, Chenting Lai<sup>3</sup>, Elena Corbetta<sup>1,2</sup>, Tobias Meyer-Zedler<sup>1,2</sup>, Bernhard Messerschmidt<sup>3</sup>, Ayman Bali<sup>4</sup>, David Pertzborn<sup>4</sup>, Anna Mühlig<sup>4</sup>, Orlando Guntinas-Lichius<sup>4</sup>, Thomas Bocklitz<sup>1,2,5</sup>, Micheal Schmitt<sup>2</sup>, Juergen Popp<sup>1,2</sup>

<sup>1</sup> Leibniz Institute of Photonic Technology, Member of Leibniz Health Technologies, Jena, Germany

<sup>2</sup> Institute of Physical Chemistry and Abbe Center of Photonics, Friedrich Schiller University, Jena, Germany

<sup>3</sup> GRINTECH GmbH, Otto-Eppenstein-Str. 7 Jena, Germany

<sup>4</sup> Department of Otorhinolaryngology Jena University Hospital, Jena, Germany

<sup>5</sup> Institute of Computer Science, Faculty of Mathematics, Physics & Computer Science, University Bayreuth Universitaetsstraße 30, 95447 Bayreuth, Germany

A major challenge in modern medicine is the effective prevention, diagnosis and treatment of cancer. However, diagnostic and surgical tools for early detection and minimally invasive treatment are still lacking. Laser-based endoscopy is among the most promising technologies to improve cancer diagnostics. Endoscopic probes allow the implementation of non-invasive imaging modalities into compact platforms and can potentially integrate laser systems for tissue ablation. Incorporating molecular selective spectroscopy in endoscopy allows to image besides the tissue morphology also its molecular composition. To assess the tissue chemical composition, we combine several nonlinear imaging techniques, as coherent anti-Stokes Raman scattering (CARS), second harmonic generation (SHG) and two-photon excited fluorescence (TPEF) in a single rigid endomicroscopic system for head and neck cancer diagnosis. The use of multiple imaging modalities allows the detection of molecular changes at early stage of disease progression and enables distinguishing cancer from healthy tissue. Alongside the imaging capability, we integrate the system with

a high-power femtosecond laser to implement fs-laser ablation and remove tumorous parts of tissue.

A complete endomicroscopic system featuring a wide field of view (FOV) of approximately 650  $\mu\text{m}$  and a lateral resolution of 1  $\mu\text{m}$  has been developed and investigated [1]. The device has been tested with ex-vivo measurements on head and neck tissue slices from 13 patients, using multimodal nonlinear microscopy to diagnose cancer. The measurements have demonstrated high signal quality and the ability to distinguish various tissue compositions. Machine learning methods are being developed to quantitatively validate the device's diagnostic capability in comparison to standard histopathology methods (H&E). Furthermore, the device has demonstrated robustness in transmitting the high-energy ultrashort pulses required for tissue fs-ablation.

## **ACKNOWLEDGEMENTS**

Funding from the European Community's Horizon 2020 Programme under the grant agreement No. 860185 (PHAST) and from the German Federal Ministry of Education and Research (BMBF): within the project TheraOptik (FKZ 13GW0370E) is acknowledged.

## **REFERENCES**

[1] Lai, C., Calvarese, M., Reichwald, K., Bae, H., Vafaeinezhad, M., Meyer-Zedler, T., Hoffmann, F., Mühlig, A., Eidam, T., et al., *Journal of Biomedical Optics*, 2023, **28(06)**.

# Fluorescence dynamics of Tb-DPA complexes

Cristina Consani<sup>a</sup>, Christoph Leithold<sup>a</sup>, Wolfgang Lakata<sup>a</sup>, Gerald Auböck<sup>a</sup>

<sup>a</sup> Photonics Systems, Sensor Systems, Silicon Austria Labs GmbH, Europastr. 12, 9524 Villach, Austria

Dipicolinic acid (DPA), bound to calcium (Ca), is a main component of bacterial endospores. CaDPA enhances the spore resistance to dry heat and desiccation and plays a role in the photoprotection of the spore DNA [1]. CaDPA is released from the spores during germination and conversion to fully active cells. Due to its large concentration in the spores, constituting up to the 20% of the dry-weight of spore core, DPA is among the main biomarkers for bacterial spores, with applications spanning from imaging to biohazard detection. The most common optical detection method for DPA relies on the formation of strongly fluorescent species upon complexation with lanthanide ions or lanthanide-based compounds, in particular based on Terbium (Tb) or Europium (Eu). Upon excitation of the DPA moiety, energy transfer takes place and fluorescence from the lanthanide ion is observed. Lanthanide complexes with DPA (and other biomolecules) are also extensively used as luminescence labels in cell imaging applications [2].

In this contribution, we investigate deeper the fluorescence dynamics of TbDPA complexes. It was previously reported [3] that DPA can form different complexes in presence of Tb, namely  $\text{TbDPA}^+$ ,  $\text{Tb(DPA)}_2^-$  and  $\text{Tb(DPA)}_3^{3-}$ , all characterized by high fluorescence yields. The three compounds have different excited state lifetimes, being 0.66 ms, 1.4 ms and 2.0 ms, respectively [3]. Interestingly, contradicting reports are present in the literature regarding the rise-time of Tb fluorescence in these species. Hindle and Hall [4] could not detect a rise of the fluorescence in  $\text{Tb(DPA)}^+$  on a timescale of some tens of  $\mu\text{s}$ , Rosen and coworkers reported a fluorescence risetime of a few hundred  $\mu\text{s}$  in  $\text{Tb(DPA)}_3^{3-}$  [3], while Makoui [5] reported a 0.4 ms risetime of fluorescence in  $\text{TbDPA}^+$ . While the risetime of fluorescence is not the measurable on which most applications are based, a precise knowledge of the dynamics of the ligand-to-metal energy transfer process can enable more appropriate DPA detection schemes.

Here we report on measurements of the fluorescence risetime in  $\text{TbDPA}^+$  and  $\text{Tb(DPA)}_3^{3-}$  with a sub-100 ns time resolution upon photoexcitation of DPA at 266 nm. The sample was photoexcited by the fourth harmonic of a Nd:YAG laser (Polaris, New wave photonics), providing 6 ns pulses at 266 nm with a repetition rate of 20 Hz. Due to the overlapping signal of the buffer and pure DPA signal (green curve in the inset of figure 1), data were evaluated after approximately 70 ns. The sample was flushed through a 3x3 mm flow cell to minimize photodamage. Due to the photolability of DPA, which can form several photoproducts upon UV illumination, a very large sample quantity was used to ensure virtually single-pass detection during the measurement

time. The collected fluorescence was focused onto an avalanche photodiode (Thorlabs, APD430A2) and read-out by an oscilloscope (LeCroy Wavepro 7ZI).

Results for the  $\text{TbDPA}^+$  and  $\text{Tb(DPA)}_3^{3-}$  complexes are shown in Figure 1. Both species decay monoexponentially with a decay time that depends on the concentration of the complex and on the ionic strength of the buffer, as previously described [3]. For both species, and independent of the concentration of the complex, fluorescence appears within the first 70 ns, showing no additional rise.

Our results show that the energy transfer between the photoexcited DPA and the  $\text{Tb}^{3+}$  fluorophore occurs on timescales more than 1000 times faster than previously believed.

Our results have practical implications in the field of DPA sensors and cell imaging. In particular, they show that such applications can benefit from employing time-resolved fluorescence detection, particularly by time-gating the fluorescence collection over much shorter timescales as previously believed, opening the way towards faster and more sensitive endospore detection and cell imaging schemes.

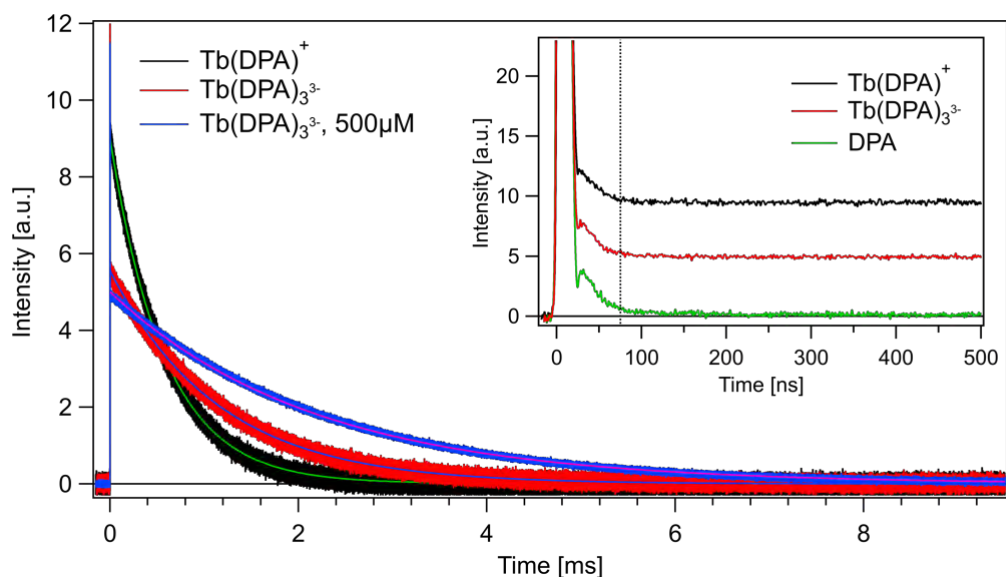


**Figure 1** Time-resolved fluorescence of  $\text{TbDPA}^+$  (black) and  $\text{Tb(DPA)}_3^{3-}$  (red) in pH 8 Trizma buffer with a concentration of 50  $\mu\text{M}$  DPA, including their exponential fit. The blue curve shows the fluorescence decay for  $\text{Tb(DPA)}_3^{3-}$  at higher DPA concentrations (600 $\mu\text{M}$ ). The inset shows time traces recorded over the first 500 ns for the 50 $\mu\text{M}$  samples. The green curve shows the signal from the DPA in buffer.

## REFERENCES

1. B. Setlow, S. Atluri, R. Kitchel, K. Koziol-Dube and P. Setlow, *J. Bacteriol.*, 2006, **188**, 3740-3747
2. U. Cho and J. K. Chen, *Cell Chemical Biology*, 2020, **27**, 921-936
3. D.L. Rosen and S. Niles, *Appl. Spectroscopy* 2001, **55**, 208-216.
4. A. A. Hindle and E. A. H. Hall, *Analyst*, 1999, **124**, 1599-1604
5. A. Makoui, PhD Thesis, 2007, *University of South Florida*, <https://digitalcommons.usf.edu/etd/2271>.



# Uncertainty Quantification in AI using Monte Carlo Dropout for Raman Spectra Classification

Jhonatan Contreras<sup>1,2</sup>, Thomas Bocklitz<sup>1,2,3,\*</sup>

<sup>1</sup>Leibniz Institute of Photonic Technology, Member of Leibniz Health Technologies, Member of the Leibniz Centre for Photonics in Infection Research (LPI), Albert-Einstein-Strasse 9, 07745 Jena, Germany.

<sup>2</sup>Institute of Physical Chemistry (IPC) and Abbe Center of Photonics (ACP), Friedrich Schiller University Jena, Member of the Leibniz Centre for Photonics in Infection Research (LPI), Helmholtzweg 4, 07743 Jena, Germany

<sup>3</sup>Institute of Computer Science, Faculty of Mathematics, Physics & Computer Science, University Bayreuth Universitaetsstraße 30, 95447 Bayreuth, Germany

\* Corresponding author: [Thomas.bocklitz@uni-jena.de](mailto:Thomas.bocklitz@uni-jena.de)

Artificial Intelligence (AI) has become an indispensable tool in classification tasks due to its enhanced capabilities. However, the opacity inherent in its decision-making processes remains a significant challenge, particularly when encountering inputs beyond its training space. This is often observed in models based on Raman spectra due to the pronounced variability across biological samples and measurement setups.

This research presents a methodology that combines the Monte Carlo Dropout (MCD) method [1]-[2] with deep neural networks (DNNs). MCD integrates a dropout mechanism, typically used during DNN training, into the inference phase. This allows for a generation of diverse predictions, thus quantifying model uncertainty. Our analysis of the prediction distributions assesses the model confidence and reliability, emphasizing a balance between decision accuracy and outcome confidence.

The proposed methodology clusters unseen data based on prediction certainty using established thresholds, the significance of uncertainty quantification becomes evident. Data characterized by low uncertainty showcases a much higher balance and overall accuracy than those with elevated uncertainty values as shown in Figure 1. Our results underscore a distinction between the predicted classification's confidence levels and traditional probability scores. With high certainty in 40.7% of the data, correct decisions range from 79.10% to 95.31%.

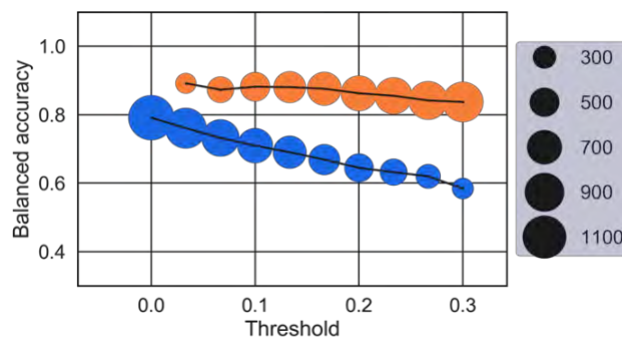


**Figure 1** Balanced Accuracy vs. Uncertainty Threshold. A representation of the relationship between various uncertainty thresholds and the balanced accuracy of data segmented as 'Certain' and 'uncertain'. As the threshold is reduced, there's an improvement in the accuracy of the 'Certain' group.

## ACKNOWLEDGMENTS

This work is supported by the BMBF, funding program Photonics Research Germany (13N15466 (LPI-BT1-FSU), 13N15710 (LPI-BT3-FSU)) and is integrated into the Leibniz Center for Photonics in Infection Research (LPI). The LPI initiated by Leibniz-IPHT, Leibniz-HKI, Friedrich Schiller University Jena and Jena University Hospital is part of the BMBF national roadmap for research infrastructures.

## REFERENCES

- [1] G. E. Hinton, N. Srivastava, A. Krizhevsky, I. Sutskever, and R. R. Salakhutdinov, "Improving neural networks by preventing co-adaptation of feature detectors," *arXiv preprint arXiv:1207.0580*, 2012.
- [2] Y. Gal and Z. Ghahramani, "Dropout as a bayesian approximation: Representing model uncertainty in deep learning," in *international conference on machine learning*, PMLR, 2016, pp. 1050–1059.

# Image evaluation method to optimize uneven illumination corrections in multimodal microscopy

Elena Corbetta<sup>a,b</sup>, Matteo Calvarese<sup>b</sup>, Hyeonsoo Bae<sup>b</sup>, Chenting Lai<sup>d</sup>, David Pertzborn<sup>e</sup>, Tobias Meyer-Zedler<sup>a,b</sup>, Bernhard Messerschmidt<sup>d</sup>, Anna Mühlige<sup>e</sup>, Orlando Guntinas-Lichius<sup>e</sup>, Micheal Schmitt<sup>a</sup>, Juergen Popp<sup>a,b</sup>, Thomas Bocklitz<sup>a,b,c</sup>

<sup>a</sup> *Institute of Physical Chemistry (IPC) and Abbe Center of Photonics (ACP), Friedrich Schiller University Jena, Member of the Leibniz Centre for Photonics in Infection Research (LPI), Helmholtzweg 4, 07743 Jena, Germany*

<sup>b</sup> *Leibniz Institute of Photonic Technology, Member of the Leibniz Centre for Photonics in Infection Research (LPI), Albert-Einstein-Strasse 9, 07745 Jena, Germany.*

<sup>c</sup> *Institute of Computer Science, Faculty of Mathematics, Physics & Computer Science, University Bayreuth Universitaetsstraße 30, 95447 Bayreuth, Germany*

<sup>d</sup> *GRINTECH GmbH, Otto-Eppenstein-Str. 7 Jena, Germany*

<sup>e</sup> *Department of Otorhinolaryngology Jena University Hospital, Jena, Germany*

Uneven illumination is an artifact affecting all measurements acquired by optical microscopes. It is a non-uniform illumination of the field of view (FOV) due to misalignments in the optical path and aberrations, that impacts multicolor and nonlinear imaging techniques. Uneven illumination generates vignetting in single FOVs and mosaicking structures in composite images of large samples.<sup>1,2</sup> Various algorithms have been developed<sup>2,3</sup> to reduce uneven illumination artifacts that can prevent correct interpretation of the measurement and reduce the performance of analysis algorithms. However, determining the quality of the corrected images is not trivial, and an established workflow for the evaluation of raw and processed images is not available in the literature.<sup>1</sup>

To optimize the evaluation of raw and corrected images, we implemented a method for the quantitative assessment of different correction methods and the selection of the best processed result. We inspected the removal of the mosaicking structure and the reduction of vignetting in single FOVs. In addition, we evaluated the overall image quality through the estimation of resolution, contrast, and presence of smoothing and noise. We tested the evaluation method on the multimodal measurements of human head and neck tissue slices composed of three different channels: Coherent Anti-Stokes Raman Scattering (CARS), Second Harmonic Generation (SHG) and Two Photon Excited Fluorescence (TPEF)<sup>4</sup>. Each raw channel has been corrected with different custom algorithms and evaluated with no-reference quality metrics. Then, the best combination of corrected channels was selected to generate the best enhanced multimodal image for further analysis tasks.

Our method enables the quantitative evaluation of raw and processed images and the selection of the best correction algorithm without manual inspection of the images. In the presence of multiple channels, the evaluation can be utilized to obtain an improved multimodal image by selecting the best correction algorithm for separate channels. In addition, automatic generation of the best corrections can be exploited to improve further processing and analysis tasks, such as image registration, segmentation, and classification.

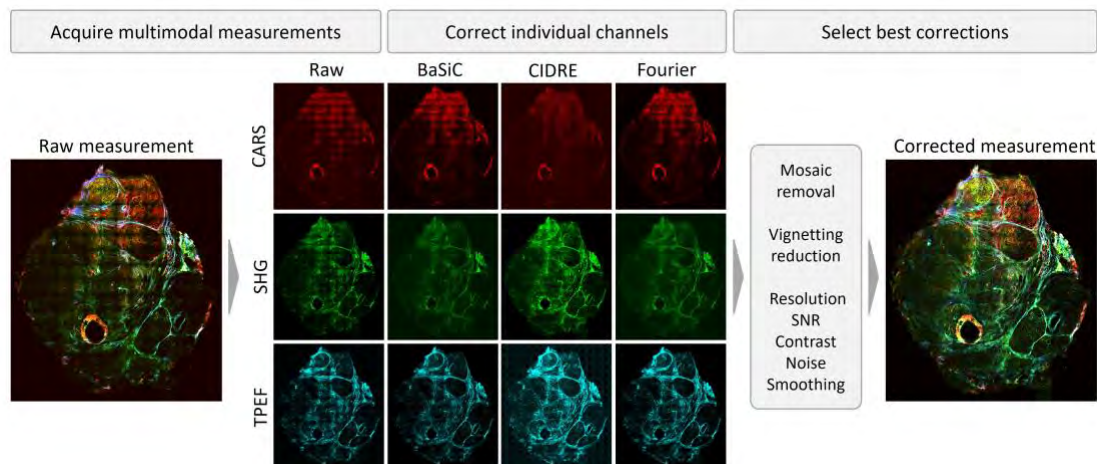


**Figure 1** Example workflow for the evaluation of correction methods for multimodal images affected by uneven illumination. The raw acquisition of a head and neck tissue slice is split into individual channels and each image is corrected with three different methods (BaSiC<sup>3</sup>, CIDRE<sup>2</sup> and Fourier<sup>1</sup> corrections). The final corrected RGB image is generated with the corrections selected after automatic quality evaluation.

## ACKNOWLEDGMENTS

This work is supported by the BMBF, funding program Photonics Research Germany (13N15706 (LPI-BT2-FSU), 13N15719 (LPI-BT5)) and is integrated into the Leibniz Center for Photonics in Infection Research (LPI). The LPI initiated by Leibniz-IPHT, Leibniz-HKI, Friedrich Schiller University Jena and Jena University Hospital is part of the BMBF national roadmap for research infrastructures. The work presented has received funding from the European Union's Horizon 2020 research and innovation programme under grant agreement No. 860185 (PHAST).

## References

1. Chernavskaja, O., et al., *Journal of Chemometrics*, 2017, **31**, e2901.
2. Smith, K., et al., *Nat Methods*, 2015, **12**, 404-406.
3. Peng, T., et al., *Nat Commun*, 2017, **8**, 14836.
4. Lai, C., et al., *Journal of Biomedical Optics*, 2023, **28**, 066004.

# Confocal Raman spectroscopic analysis of pathogen biofilms

Dongyu Cui<sup>1,2,3</sup>, Petra Rösch<sup>1,2,3</sup>, Jürgen Popp<sup>1,2,3</sup>

([dongyu.cui@uni-jena.de](mailto:dongyu.cui@uni-jena.de))

<sup>1</sup> Institute of Physical Chemistry and Abbe Center of Photonics, Friedrich Schiller University, Jena, Germany

<sup>2</sup> InfectoGnostics Research Campus Jena, Center of Applied Research, Jena, Germany

<sup>3</sup> Leibniz Institute of Photonic Technology, Member of Leibniz Health Technologies, Jena, Germany

## Abstract

Biofilms are complex community systems with high cell density, consisting mainly of aggregated microorganisms and the extracellular polymeric substances (EPS) they secrete. EPS mainly consists of polysaccharides, eDNA, proteins and lipids. The composition of EPS varies from species to species. There is currently no way to attribute specific components of EPS to a particular species in the community, nor is it possible to effectively control the amount and composition of EPS<sup>[1]</sup>.

The development of biofilms can be divided into three phases at least: attachment, maturation, and detachment<sup>[2]</sup>. Compared to planktonic microorganisms, members in the biofilm have stronger antibiotic resistance that disappears when the cells are detached from the biofilm. Biofilms formed by pathogens are a common clinical cause of infection. Although compounds with *in vitro* anti-biofilm activity have been reported, there are still no clinically efficient solutions for biofilm infections. Therefore, *in situ* investigation of pathogenic biofilms is necessary to propose effective clinical treatment options.

Raman spectroscopy is a label-free optical detection tool with potential for clinical applications. Vibrational information of biological macromolecules can be detected at the single-cell level by Raman spectroscopy. Compared to other techniques, Raman spectroscopy in microbiology has many advantages including high resolution, low sample demand, non-destructive<sup>[3]</sup>. Confocal Raman spectroscopy has better axial spatial resolution, enabling the acquisition of Raman signals in a specific volume<sup>[4]</sup>. Hence, Raman spectroscopy is one of the ideal techniques for studying the overall structure and formation details of biofilms.

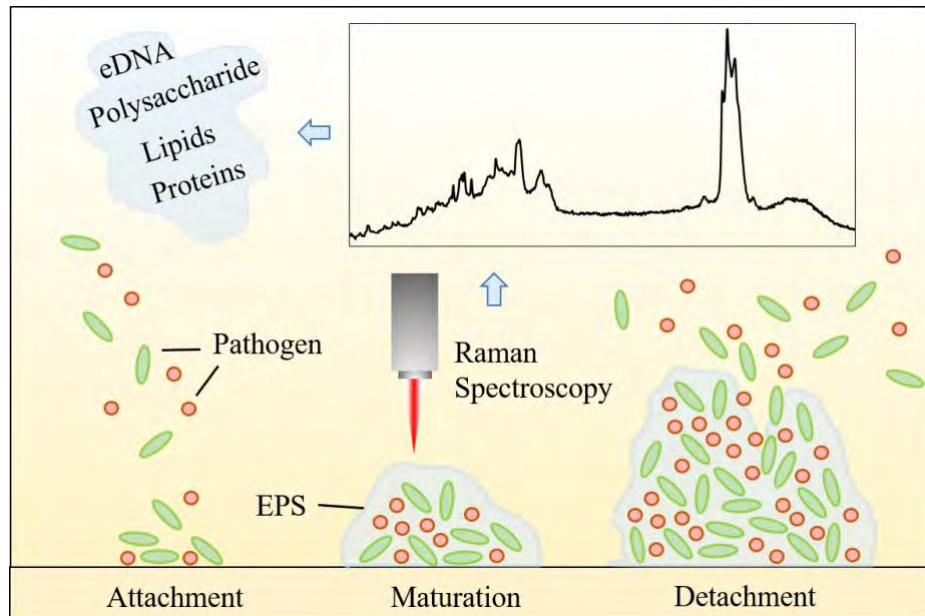


**Figure 1.** Confocal Raman spectroscopic analysis of pathogen biofilms

## Acknowledgments

Financial support from the China Scholarship Council (CSC) for D.C.

## References

- [1] Seviour, T., Derlon, N., Dueholm, M.S., Flemming, H.C., Girbal-Neuhausser, E., Horn, H., Kjelleberg, S., van Loosdrecht, M.C.M., Lotti, T., Malpei, M.F., Nerenberg, R., Neu, T.R., Paul, E., Yu, H.Q. and Lin, Y.M. Extracellular polymeric substances of biofilms: Suffering from an identity crisis. *Water Research*. 2019. 151, 1-7.
- [2] Otto, M. Staphylococcal infections: Mechanisms of biofilm maturation and detachment as critical determinants of pathogenicity. *Annual Review of Medicine*. 2013. 64, 175-188
- [3] Cui, D.Y., Kong, L.C., Wang, Y., Zhu, Y.Q. and Zhang, C.L. *In situ* identification of environmental microorganisms with Raman spectroscopy. *Environmental Science and Ecotechnology*. 2022. 11, 100187.
- [4] Cialla-May, D., Krafft, C., Rosch, P., Deckert-Gaudig, T., Frosch, T., Jahn, I.J., Pahlow, S., Stiebing, C., Meyer-Zedler, T., Bocklitz, T., Schie, I., Deckert, V. and Popp, J. Raman spectroscopy and imaging in bioanalytics. *Analytical Chemistry*. 2022. 94(1), 86-119.



# Comprehensive Evaluation of Color Transformation Methods for H&E and Multimodal Images: A Focus on Stability

Fatemeh Zahra Darzi<sup>a,b</sup>, Thomas W. Bocklitz<sup>a,b,c</sup>

<sup>a</sup> *Leibniz Institute of Photonic Technology, Member of Leibniz Health Technologies, Member of the Leibniz Centre for Photonics in Infection Research (LPI), Albert-Einstein-Strasse 9, 07745 Jena, Germany.*

<sup>b</sup> *Institute of Physical Chemistry (IPC) and Abbe Center of Photonics (ACP), Friedrich Schiller University Jena, Member of the Leibniz Centre for Photonics in Infection Research (LPI), Helmholtzweg 4, 07743 Jena, Germany.*

<sup>c</sup> *Institute of Computer Science, Faculty of Mathematics, Physics & Computer Science, University Bayreuth Universitaetsstraße 30, 95447 Bayreuth, Germany.*

In medical imaging, image registration is crucial for aligning images from different sources to make meaningful comparisons. Color transformation is a vital part of this, ensuring consistent and accurate color reproduction for tasks like image analysis and diagnostics. This study examines various color transformation methods, focusing on their stability in preserving color accuracy for hematoxylin and eosin (H&E) stained and multimodal images [1, 2].

The assessment of color transformation methods involves multiple steps. First, data is collected, followed by color transformation. Then the images are registered by the Lucas-Kanade method, extracting two windows. Keypoint detection is then used to identify and match keypoints. This is the second keypoint detection instance, also used during image registration. Finally, we plot the distances between matched keypoints, calculate mean, standard deviation (SD), and median absolute deviation (MAD) distances.

To tackle color discrepancies between H&E and multimodal images, an extra step inverts all multimodal images. Color transformation is performed bidirectionally for each method, using H&E as the source and inverted multimodal as the target in one direction, and vice versa in the other. The five methods under scrutiny include Reinhard, Vahadane, Macenko, CycleGAN, and StainNet.

The comparison of stability among these methods uses box plots based on SD and MAD distances. A lower SD means that matched keypoints are closely grouped around the mean distance, indicating stable matching. Similarly, a lower MAD suggests most data points are near the median, showing consistency around a central value and indicating stability. Results show that CycleGAN is the most stable, while Reinhard is the least stable.

In conclusion, this study provides insights into color transformation method stability, improving our understanding of their suitability for maintaining color accuracy in

different image tasks. The structured workflow becomes a foundational resource for future research, especially in multimodal image registration. These findings contribute significantly to advancing methodologies in medical image processing and analysis, enhancing the reliability and accuracy of diagnostic procedures and quantitative assessments.

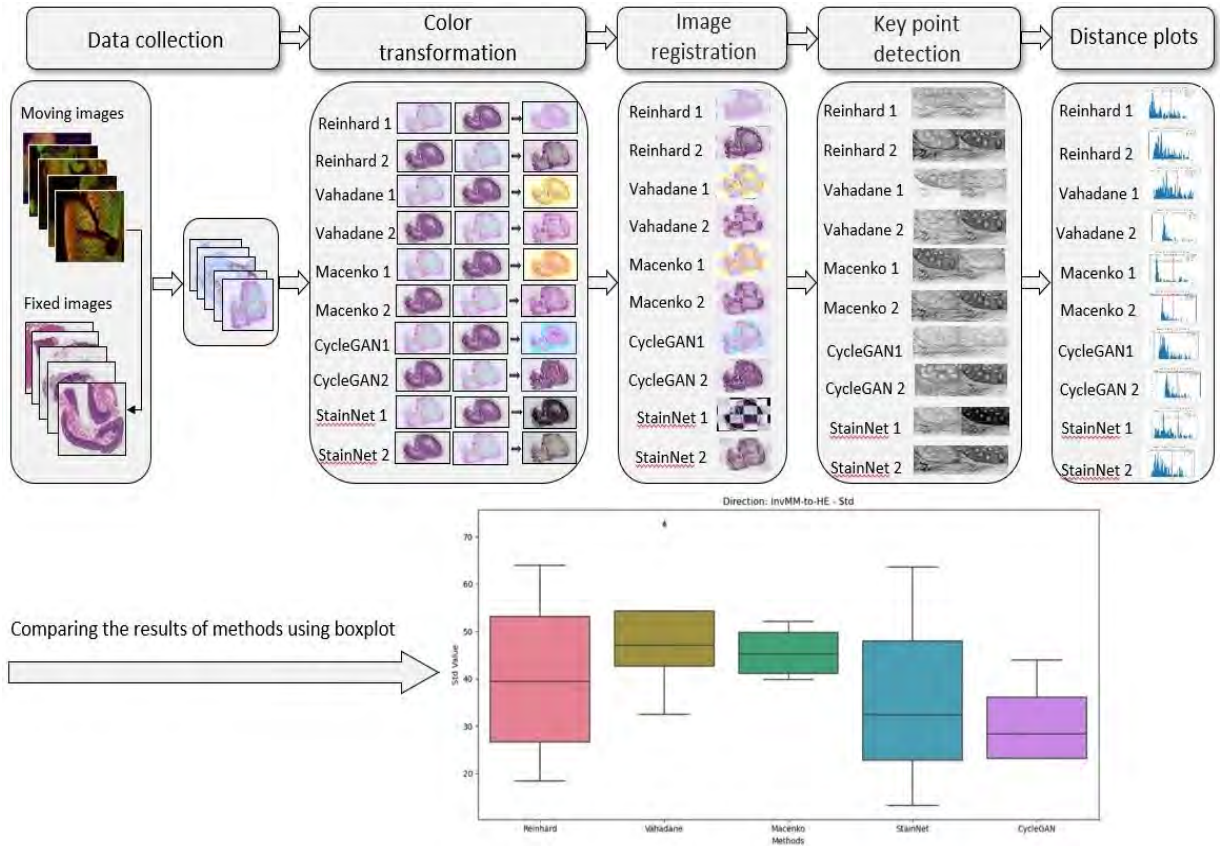


**Figure 1** This figure outlines the study's workflow, which thoroughly examines color transformation methods for H&E and multimodal images. The analysis centers on stability and involves six crucial steps: data collection, color transformation, image registration, keypoint detection, and distance calculation. Five methods are compared, and box plots based on Std and MAD distances are used for stability comparison. CycleGAN stands out as the most stable method, with Reinhard identified as the least stable.

## ACKNOWLEDGMENTS

This work is supported by the BMBF, funding program Photonics Research Germany (13N15710 (LPI-BT3-FSU)) and is integrated into the Leibniz Center for Photonics in Infection Research (LPI). The LPI initiated by Leibniz-IPHT, Leibniz-HKI, Friedrich Schiller University Jena and Jena University Hospital is part of the BMBF national roadmap for research infrastructures.

## REFERENCES

- [1] Bocklitz, T. W., et al. (2016). Pseudo-HE images derived from CARS/TPEF/SHG multimodal imaging in combination with Raman-spectroscopy as a pathological screening tool. *BMC cancer*, 16(1), 1-11.
- [2] Chernavskaia, O., Heuke, S., Vieth, M., Friedrich, O., Schürmann, S., Atreya, R., ... & Popp, J. (2016). Beyond endoscopic assessment in inflammatory bowel disease: real-time histology of disease activity by non-linear multimodal imaging. *Scientific Reports*, 6(1), 29239

# A systematic investigation of image pre-processing on image classification

Pegah Dehbozorgi<sup>a,b</sup>, Oleg Ryabchykov<sup>a,b</sup>, Thomas W. Bocklitz<sup>a,b,c</sup>

<sup>a</sup> *Leibniz Institute of Photonic Technology, Member of Leibniz Health Technologies, Member of the Leibniz Centre for Photonics in Infection Research (LPI), Albert-Einstein-Strasse 9, 07745 Jena, Germany.*

<sup>b</sup> *Institute of Physical Chemistry (IPC) and Abbe Center of Photonics (ACP), Friedrich Schiller University Jena, Member of the Leibniz Centre for Photonics in Infection Research (LPI), Helmholtzweg 4, 07743 Jena, Germany.*

<sup>c</sup> *Institute of Computer Science, Faculty of Mathematics, Physics & Computer Science, University Bayreuth Universitaetsstraße 30, 95447 Bayreuth, Germany.*

In the field of healthcare, AI-powered image analysis has arisen as a groundbreaking technology, holding promise for enhancing diagnostics and patient care. Precise evaluations of medical images, including X-rays, MRIs, and Optical Coherence Tomography (OCT) scans, play a pivotal role in assisting healthcare professionals in disease detection, anomaly identification, and treatment planning. Yet, the medical imaging domain presents challenges related to inherent noise and visual inconsistencies during image acquisition. These issues can adversely impact image quality, rendering them less suitable for robust AI-driven decisions.

A variety of strategies can be employed to tackle the challenges in medical image analysis. Notably, image pre-processing techniques are exceptionally effective solutions. These methods encompass adjusting pixel values to enhance image quality and mitigate noise, revealing vital information concealed within the images. As a result, with improved image data quality and, most importantly, the extraction of essential features, AI-assisted healthcare decisions can attain higher levels of accuracy, resilience, and dependability.

This study thoroughly analyzes the impact of image pre-processing on the performance of binary classification models, utilizing three distinct datasets: hematoxylin and eosin (H&E)-stained tissue images, chest X-ray images, and retina OCT images. Our primary objective was to underscore the key role of pre-processing methods in model performance and emphasize the importance of selecting and optimizing these steps. The careful selection of the pre-processing techniques markedly improved the mean sensitivity across all three image modalities, highlighting the essential contribution of these methods in elevating model accuracy and reliability.

Furthermore, we explored two distinct pre-processing sequences for the execution of pre-processing steps. One followed the sequence of consecutive adjustment, filtering, and normalization, while the other featured an altered sequence where filtering took place before adjustment and normalization. This approach allowed us to assess the impact of pre-processing and investigate the influence of the order in which these steps were applied. Notably, these modified sequences resulted in minimal effects,

highlighting a consistent performance improvement, irrespective of the selected sequence.

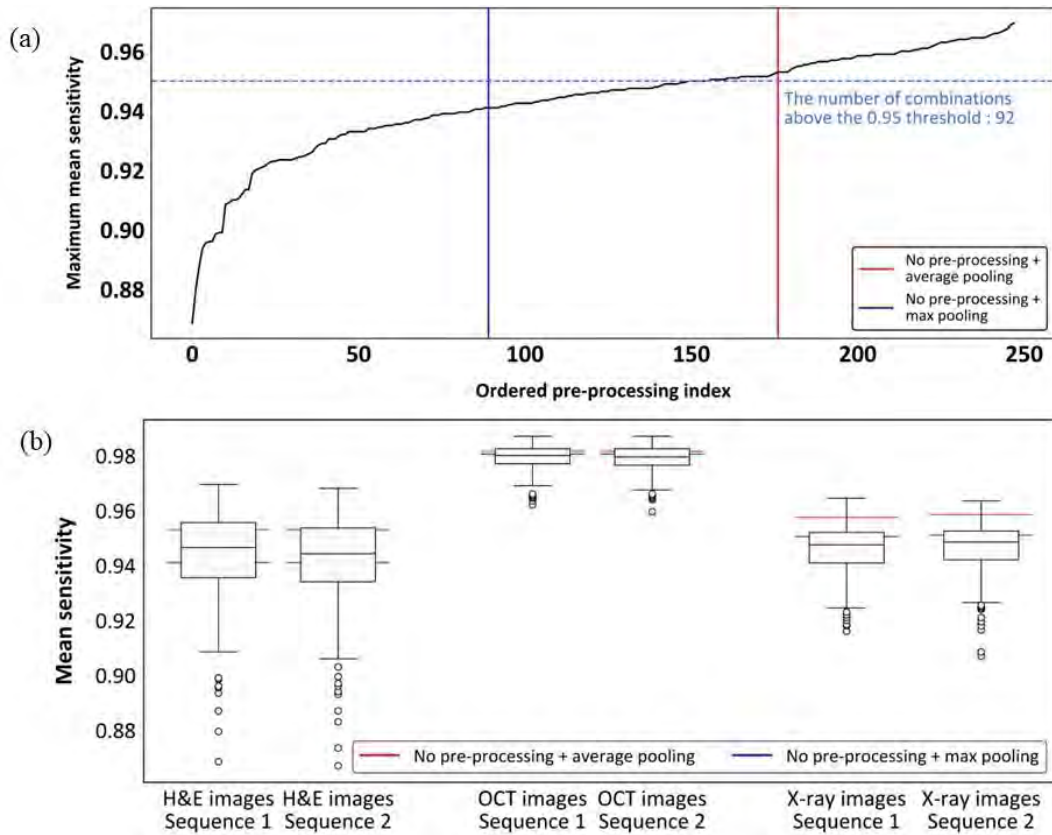


**Figure 1** Exploring the impact of pre-processing combinations and sequence on model performance. (a) Shows how pre-processing selection can positively affect the performance of binary classification models to increase mean sensitivity from 0.8 to more than 0.96. This observation also holds true for the other investigated image modalities, including the Chest X-ray and OCT datasets. Considering 0.95 as a critical threshold for making diagnostic decisions in practical applications, fine-tuning of the pre-processing combinations led to an exceptional outcome: 92 models surpassed this crucial threshold, signifying an outstanding observation. (b) Offers a summary of the findings derived from the H&E, Chest X-ray, and OCT images through the application of two different pre-processing sequences, referred to as Sequence 1 and Sequence 2. This comparative analysis demonstrates that the selection of the pre-processing sequence has minimal influence on the overall performance of the classification models.

## ACKNOWLEDGMENTS

This work is supported by the BMBF, funding program Photonics Research Germany (13N15710 (LPI-BT3-FSU)) and is integrated into the Leibniz Center for Photonics in Infection Research (LPI). The LPI initiated by Leibniz-IPHT, Leibniz-HKI, Friedrich Schiller University Jena and Jena University Hospital is part of the BMBF national roadmap for research infrastructures.

# Raman-based Detection of Natural Products in Microbial Communication

Tony Dib<sup>a,b</sup>, Simone Edenhart<sup>c,d</sup>, Aradhana Dwivedi<sup>a,b</sup>, Dana Cialla-May<sup>a,b</sup>, Axel A. Brakhage<sup>c,d</sup>, Juergen Popp<sup>a,b</sup>

<sup>a</sup> Leibniz-Institute of Photonic Technology, Member of Leibniz-Health Technologies, Member of the Leibniz-Centre for Photonics in Infection Research (LPI), Jena Germany

<sup>b</sup> Institute of Physical Chemistry and Abbe Center of Photonics, Friedrich Schiller University Jena, Member of the Leibniz-Centre for Photonics in Infection Research (LPI), Jena, Germany

<sup>c</sup> Leibniz Institute for Natural Product Research and Infection Biology (Leibniz-HKI), Jena, Germany

<sup>d</sup> Institute of Microbiology, Friedrich Schiller University Jena, Jena, Germany

The critical role of the interaction between prokaryotic and eukaryotic microorganisms in ecosystem functionality is well recognized, yet our understanding of the mechanisms underlying these microbial community interactions is limited. Polyketides derived from arginine, known as arginoketides, are produced by *Streptomyces* species and play a key role in mediating cross-kingdom microbial interactions with *Aspergillus* fungi, leading to the production of natural products. These arginoketides can either be cyclic, such as monazomycin and desertomycin A, or linear, like lydicamycin and linearmycin A, all of which produced by *Streptomyces iranensis* and have been found to stimulate the orsellinic acid gene cluster in *Aspergillus nidulans*.<sup>1</sup> The characterization and detection of natural products by surface-enhanced Raman spectroscopy (SERS) is expected to shed light on how they are released and transported through the environment, and how they trigger responses in other microorganisms.<sup>2</sup>

SERS measurements were carried out using a dendritic silver substrate fabricated on a silicon wafer by means of galvanic replacement of silver and sulfur ions. At the nanoscale, the branches of the tree-like structure form sharp angles and narrow gaps that are supposed to turn into “hot spots” where the Raman signal of the target molecules should be enhanced.

Raman and SERS spectra of the bacterial secondary metabolites monazomycin, desertomycin A, lydicamycin, and linearmycin A and the fungal products orsellinic and lecanoric acids were characterized in terms of assigning marker modes, thus enabling their detection and identification in the microbial culture.

## ACKNOWLEDGMENTS

Funded by the Deutsche Forschungsgemeinschaft (DFG, German Research Foundation) under Germany’s Excellence Strategy – EXC 2051 – Project-ID 390713860.



## REFERENCES

1. M.K. Krespach, M.C. Stroe, T. Netzker, M. Rosin, L.M. Zehner, A.J. Komor, ... & A.A. Brakhage, *Nature Microbiology*, 2023, 8, 1348–1361.
2. D. Cialla-May, C. Krafft, P. Rösch, T. Deckert-Gaudig, T. Frosch, I.J. Jahn, S. Pahlow, C. Stiebing, T. Meyer-Zedler, T. Bocklitz, I. Schie, V. Deckert, and J. Popp, *Analytical Chemistry*, 2022, 94 (1), 86-119.

# Temporal analysis of Alkyne tagged DNA using surface enhanced Raman spectroscopy on silver dendritic structures

Aradhana Dwivedi<sup>a</sup>, Vladimir Sivakov<sup>a</sup>, Juergen Popp<sup>a,b</sup>, Dana-Cialla May<sup>a,b</sup>

<sup>a</sup> Leibniz-Institute of Photonic Technology, Member of Leibniz-Health Technologies, Member of the Leibniz-Centre for Photonics in Infection Research (LPI), Jena Germany

<sup>b</sup> Institute of Physical Chemistry and Abbe Center of Photonics, Friedrich Schiller University Jena, Member of the Leibniz-Centre for Photonics in Infection Research (LPI), Jena, Germany

In complex biological systems, detection accuracy can be hindered by the overlap of Raman bands between typical reporters and interfering molecules. Alkynes provide a solution as they display a distinct and strong Raman scattering peak in the 1800–2800  $\text{cm}^{-1}$  silent region, which minimizes signal overlap with cellular components. Despite their potential, the weak Raman scattering response of alkynes restricts their widespread use. Furthermore, the vibrational modes of alkynyl groups fluctuate depending on substitution patterns, thus providing versatility in applications [1]. This approach enhances the applicability of alkyne tags in biological analyses, addressing challenges associated with weak Raman responses [2].

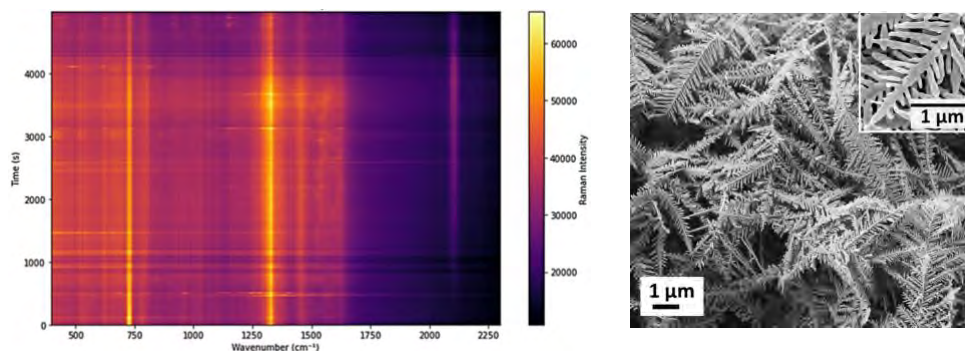


**Figure 1** (a) Mapping of time-dependent SERS response of Alkyne tagged DNA, (b) SEM image of silver dendrite

Silver sulfate acted as a precursor for generating silver dendrites, which possess outstanding properties for use in SERS applications owing to their large surface area and distinctive plasmonic behaviour [3]. Synchrotron-based XPS was employed to discover the oxidation states of nanostructures, which shed light on their chemical composition. Silver structures evaluated as SERS substrates using 4-mercaptobenzoic acid (4MBA) as a model molecule showed excellent performance. This evaluation was subsequently extended to include SERS evaluation of alkyne-labelled DNA strands. This demonstrates the versatility of our fabricated substrates.

We studied the evolution of the alkyne mode ( $\text{-C}\equiv\text{C-}$ ) in alkyne-labelled DNA as function of time by recording SERS spectra every second. This temporal analysis provides valuable insights into the dynamics of DNA and its interaction with plasmonic structures. Our investigation provides a solid foundation for the design and preparation of SERS substrates with enhanced stability, sensitivity and flexibility, opening up opportunities for diverse applications in chemical and biological sensing and the use of alkynes in complex biological matrices.

## **ACKNOWLEDGMENTS**

The authors gratefully acknowledge the financial support provided by the DFG (German Research Foundation) for projects 465289819 (CI344/3-1) and SI1893/30-1.

## **REFERENCES**

1. Si, Y., Bai, Y., Qin, X., Li, J., Zhong, W., Xiao, Z., Li, J. and Yin, Y., 2018, *Analytical chemistry*, 90(6), pp.3898-3905.
2. Dodo, K., Fujita, K. and Sodeoka, M., 2022, *Journal of the American Chemical Society*, 144(43), pp.19651-19667.
3. Zhang, Y., Sun, S., Zhang, X., Tang, L., Song, X. and Yang, Z., 2014, *Physical Chemistry Chemical Physics*, 16(35), pp.18918-18925.

# ***In silico* analytics in vibrational spectroscopy**

**Tarek Eissa**<sup>a,b,c</sup>, Kosmas V. Kepesidis<sup>a,b</sup>, Mihaela Zigman<sup>a,b</sup>, Marinus Huber<sup>a,b</sup>

<sup>a</sup> Ludwig Maximilian University of Munich, Department of Laser Physics, Germany

<sup>b</sup> Max Planck Institute of Quantum Optics, Laboratory for Attosecond Physics, Germany

<sup>c</sup> Technical University of Munich, School of Computation, Information and Technology, Germany

Vibrational spectroscopy provides a robust and efficient means of analyzing the chemical composition of molecularly complex samples. Although widely applied in research and practical domains, the prospects and limitations of the molecular fingerprinting approach are yet to be fully understood. The challenge is that a variety of technical and data acquisition aspects impact measured spectra. At the same time, any analyzed sample matrix may exhibit an inherent level of molecular variability, further challenging the success of an application of interest. Characterizing the impact of diverse sources of measurement variability is critical for interpreting the informational content of spectra and understanding the practical limitations of the analytical approach.

To this end, we introduced an *in silico* model that generates synthetic spectra that model varying experimental paradigms [1]. With the flexibility to fine-tune simulation parameters, our approach offers a versatile and time-efficient means to explore how a range of experimental setups may lead to improved measurement sensitivity. Focusing on infrared spectroscopy of cell-free blood-based samples, our applications of the model address different clinical questions, such as cancer detection and the prospects of personalized medicine. Our work presents a new platform to strengthen our understanding of spectral fingerprinting and expose opportunities to advance its applications.

## **REFERENCES**

1. T. Eissa, K. V. Kepesidis, M. Zigman, and M. Huber, “Limits and prospects of molecular fingerprinting for phenotyping biological systems revealed through *in silico* modeling,” *Analytical Chemistry*, vol. 95, no. 16. pp. 6523–6532, 2023. doi: 10.1021/acs.analchem.2c04711.

## Drug distribution and metabolism via label-free molecular fingerprint

Samir F. El-Mashtoly<sup>a</sup>, Anne De Paepe<sup>b</sup>, Rainer E. Martin<sup>b</sup>, Uwe Grether<sup>b</sup>, Karina Weber<sup>a</sup>, Christoph Krafft<sup>a</sup>, and Jürgen Popp<sup>a</sup>

<sup>a</sup>Leibniz Institute of Photonic Technology (IPHT), Jena, Germany

<sup>b</sup>Roche Pharma Research and Early Development, Roche Innovation Center Basel, Basel, Switzerland

Raman microscopy is an emerging bioanalytical tool for the characterization and imaging of different types of specimens, such as cells and tissues, and it is a non-destructive and label-free approach. Tyrosine kinase receptors are one of the major targets in cancer therapy. They play an essential role in the modulation of growth factor signaling and can induce cell proliferation and growth. Targeting epidermal growth factor receptor (EGFR) is one of the effective strategies to suppress tumors in advanced stages. Tyrosine kinase inhibitors (TKIs) bind to tyrosine kinase receptors and exhibit anti-tumor activity. However, little is known about their detailed cellular uptake and metabolism.

Imaging the uptake, distribution, and metabolism of drug candidates in living systems can measure the physicochemical properties of drug candidates and provide a mechanistic understanding of the observed biological response.<sup>1-3</sup> Here, we follow the uptake, intracellular spatial distribution, and metabolism of several TKIs within different cancer cells using label-free spontaneous Raman micro-spectroscopy. The strategy follows the previous published research on neratinib,<sup>3</sup> where the uptake and distribution of the cyano group was monitored by Raman microscopic imaging as shown in Figure 1. New metabolites were detected and a combination of Raman microscopy and density functional theory calculations was used to identify the chemical structure of these metabolites.

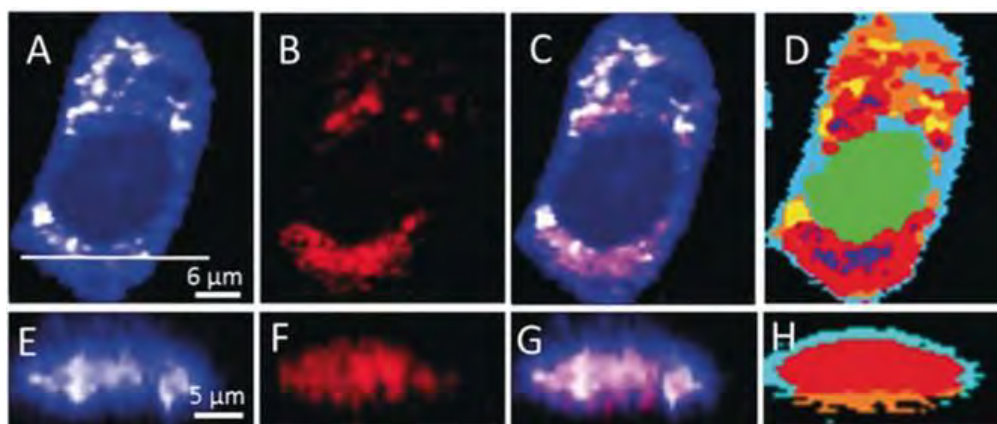


**Figure 1** Raman imaging of SK-BR-3 cells treated with 5  $\mu$ M neratinib for 8 h. Raman images reconstructed from the C–H deformation (A) and C $\equiv$ N stretching (B) intensities. C) Overlay of Panels

A and B. E–G) Cross-section Raman images of the same cell measured along the  $x$ – $z$  axis. Scanning positions are indicated by the white line in Panel A. D,H) HCA results based on the Raman data shown in Panels A and E.<sup>3</sup>

We have also monitored the distribution and metabolism of alkyne- and cyano-based drug candidates with the optical photothermal IR microscope (O-PTIR) with its submicrometer spatial resolution and simultaneous Raman measurements. This method delivers information on cellular molecular composition and drug–cell interaction, showing the potential of O-PTIR in drug development.

## ACKNOWLEDGMENTS

We thank Hoffmann La-Roche for funding.

## REFERENCES

1. S.F. El-Mashtoly, *J. Medicinal Chemistry*, 2020, **63**, 3472-3474.
2. S.F. El-Mashtoly and K. Gerwert, *Analytical Chemistry*, 2022, **94**, 120142.
3. K. Aljakouch, T. Lechtonen, H.K. Yosef, M. K. Hammoud, W. Alsaïdi, C. Kötting, C. Mügge, R. Kourist, S. F. El-Mashtoly, K. Gerwert, *Angewandte Chemie International Edition*, 2018, **57**, 7250-7254.

# Cloud-Based System for Digital Pathology Image Analysis

Rodrigo Escobar Díaz Guerrero<sup>a,b</sup>, Rui Jesus<sup>c</sup>, José Luis Oliveira<sup>b,c</sup>,  
Thomas Bocklitz<sup>a,d,e</sup>

<sup>a</sup> Leibniz Institute of Photonic Technology Jena, Albert-Einstein-Straße 9, 07745 Jena, Germany

<sup>b</sup> DETI/IEETA, University of Aveiro, 3810-193 Aveiro, Portugal.

<sup>c</sup> BMD Software, PCI - Creative Science Park, 3830-352 Ilhavo, Portugal.

<sup>d</sup> Institute of Physical Chemistry and Abbe Center of Photonics (IPC), Friedrich-Schiller-University, Germany.

<sup>e</sup> Faculty of Mathematics, Physics and Computer Science, University of Bayreuth (UBT), Nürnberger Str. 38, D-95440 Bayreuth, Germany

Digital Pathology (DP) image analysis is a process that involves detecting, segmenting, labeling, and classifying elements present in tissue samples using computer algorithms. Currently, DP images are acquired through Whole Slide Imaging (WSI) scanners, which provide complete whole slide images with very high resolution<sup>1</sup>. Early WSI systems only produced bright-field microscopy images, but new WSI systems can be used with more microscopy modes, such as fluorescence and spectroscopic imaging<sup>2</sup>.

Analyzing DP images is a complex task due to several challenges. These challenges include significant sample variability, encompassing biological, pathological, and technological variations, making the interpretation of tissue images difficult<sup>3</sup>. Additionally, the resolution of digital pathology images, often reaching gigapixel dimensions, poses storage and analysis complexities. A critical challenge is the scarcity of high-quality annotations, which are crucial for advanced analysis methods. However, obtaining such annotations is difficult and expensive, as it requires expertise, and the sensitivity of histopathological images often prevents their public release.

To address these challenges, we have developed a flexible system that facilitates the integration of specialized algorithms through plug-ins, tailored to specific scenarios. This cloud-based system comprises three key components, as depicted in Figure 1. The first component, an Archive and Indexer, serves as a repository for storing and indexing images in the DICOM format. The second component, a Whole Slide Image Viewer, empowers users to navigate through images and create manual annotations as needed. Lastly, the third component, a Data Analysis Provider, enables the management of various algorithms for image analysis. Notably, we have designed and tested a couple of artificial intelligence algorithms for tasks such as nuclei detection and classification. In Figure 2, an example showcases the detection of lymphocytes using one of these algorithms.

In summary, our innovative cloud-based Digital Pathology (DP) image analysis system represents a significant advancement in addressing the complex challenges of this field.



Comprising three key components, including an Archive and Indexer for image storage, a Whole Slide Image Viewer for manual annotations, and a Data Analysis Provider for managing specialized algorithms, our system offers a comprehensive solution.

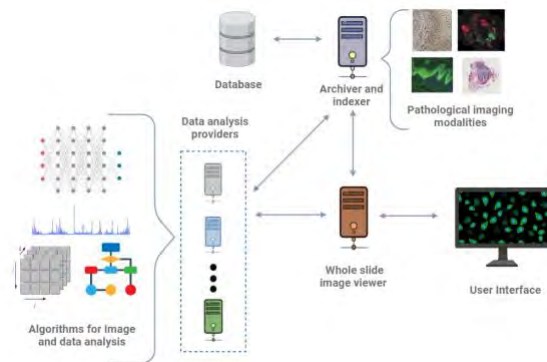


**Figure 1.** Representation of the cloud-based digital pathology image analysis system

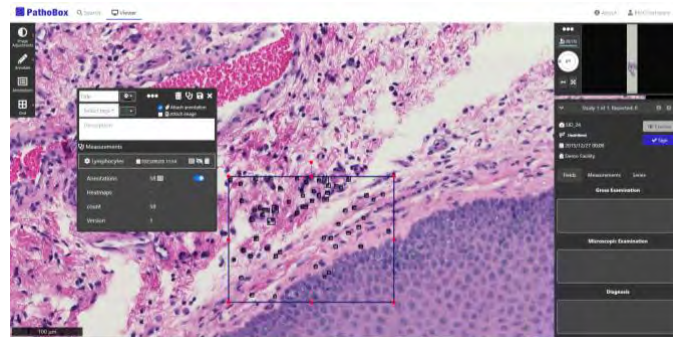


**Figure 2.** AI algorithm example: Lymphocyte detection in a tissue stained with Hematoxylin and Eosin.

## ACKNOWLEDGMENTS

This work was supported by the Marie Skłodowska Curie ITN - EID, Horizon 2020 project IMAGE-IN (grant agreement No 861122). This work is further supported by the BMBF, funding program Photonics Research Germany (13N15710 (LPI-BT3-FSU)) and is integrated into the Leibniz Center for Photonics in Infection Research (LPI). The LPI initiated by Leibniz-IPHT, Leibniz-HKI, Friedrich Schiller University Jena and Jena University Hospital is part of the BMBF national roadmap for research infrastructures.

## REFERENCES

1. Farahani N, Parwani A, Pantanowitz L, Pathology and Laboratory Medicine International, 2015, **7**, 23-33.
2. Ghaznavi F, Evans A, Madabhushi A, Feldman M, Annual Review of Pathology: Mechanisms of Disease. 2013, **8**, 331-359.
3. Ponzio F, Urgese G, Ficarra E, Di Cataldo S, Electronics (Switzerland), 2019, **8(3)**, 256.

# Raman microspectroscopy for detecting head and neck tumour markers in body liquids

Edoardo Farnesi<sup>1,2</sup>, Chen Liu<sup>1,2</sup>, Orlando Guntinas-Lichius<sup>3</sup>, Dana Cialla-May<sup>1,2</sup>, Michael Schmitt<sup>1</sup>, Juergen Popp<sup>1,2,4</sup>

<sup>1</sup> *Institute of Physical Chemistry and Abbe Center of Photonics, Friedrich Schiller University Jena, Member of the Leibniz-Centre for Photonics in Infection Research (LPI), Jena, Germany*

<sup>2</sup> *Leibniz-Institute of Photonic Technology, Member of Leibniz-Health Technologies, Member of the Leibniz-Centre for Photonics in Infection Research (LPI), Jena Germany*

<sup>3</sup> *Department of Otorhinolaryngology Jena University Hospital, Jena, Germany*

<sup>4</sup> *Research Campus Infectognostic, Jena, Germany*

Traditional methods for head and neck cancer diagnostics, which include clinical examination, white light endoscopy, radiological imaging, and fine-needle aspiration cytology, for example, may have a limited diagnostic accuracy. Gold standard for proof of malignancy is a histopathological examination of tissue biopsies. Taking into consideration that such investigations generally are performed when the tumor is already clinically obvious, and are not reliable for head and neck cancer screening, novel, non-invasive, rapid diagnostics, especially to detect early cancer in a point-of-care (POC) setting are warranted. The analysis of body liquids (urine, serum, sputum) by Raman spectroscopy offers great potential as non- or less invasive approach for a rapid screening of cancer markers in an early stage. Here, we report about the development of spectral acquisition protocols for Raman spectroscopic measurements of body fluids to detect head and neck cancer markers.

One crucial point in investigating body liquids via Raman spectroscopy is the development of appropriate sample preparation methods. Thus, to reach the aforementioned goals, we develop standardized sampling approaches leading to reproducible Raman analysis of body liquids. In order to enhance the intrinsic weak Raman signal, surface enhanced Raman spectroscopy (SERS) can be applied by employing powerful plasmonic-active nanostructured sensing surfaces.

The recorded SERS spectra of the body fluids (urine, serum, sputum) are dominated by the contribution of well-known medical target molecules as lysozyme, phenylalanine and tryptophan in saliva or hypoxanthine, urea and xanthopterin in urine. [1] In Fig. 1, the workflow for the SERS-based detection of salivary tumor markers in combination with molecular dynamic simulations is illustrated. The researched spectral acquisition protocols will be implemented in an automated POC measuring protocol. Further goals of this study are the development of custom-made chemometric data evaluation protocols, involving the most innovative and efficient machine learning algorithms. This will result in standard operating procedures (SOPs) for the POC Raman spectroscopic analysis of body fluids to detect tumour markers, leading to an improved personalized treatment of patients. Additionally, the potential for early cancer detection

will be evaluated, even before the onset of symptoms, with just a few drops of body fluid.

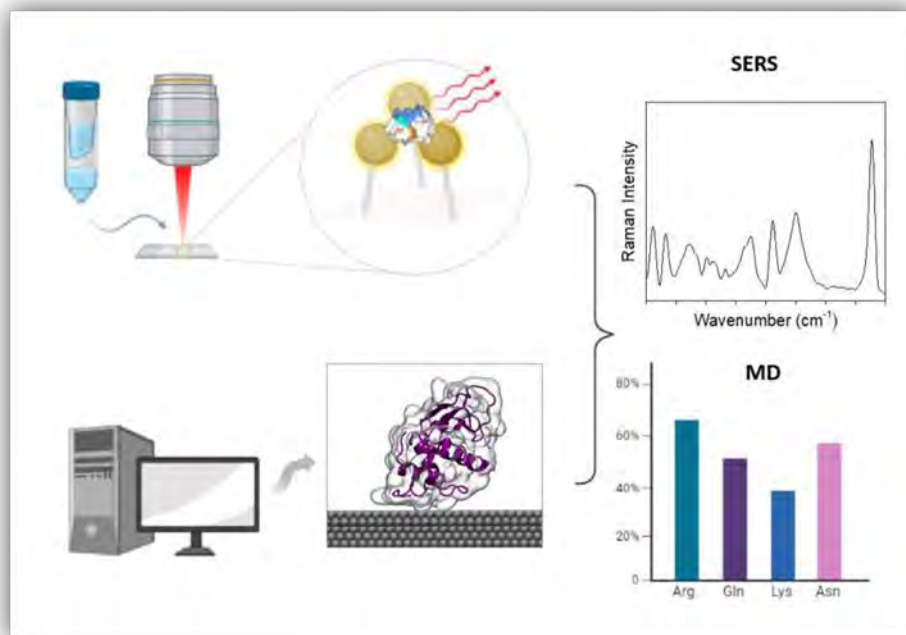


**Figure 1.** SERS/ Molecular dynamic (MD) simulation combined workflow for identification of salivary tumor markers.

## ACKNOWLEDGMENTS

The authors acknowledge financial support from European Union's Horizon 2020 research and innovation programme under the Marie Skłodowska-Curie grant agreement No 860185 (PHAST = Photonics for Healthcare: multiscale cancer diagnosis and Therapy)

## REFERENCES

1. Farnesi, E., Rinaldi, S., Liu, C., Ballmaier, J., Guntinas-Lichius, O., Schmitt, M., Cialla-May, D. & Popp, J. (2023). Label-Free SERS and MD Analysis of Biomarkers for Rapid Point-of-Care Sensors Detecting Head and Neck Cancer and Infections. *Sensors*, 23(21), 8915.

# Exploring analytical parameters in profiling of liquid human biofluids with infrared molecular fingerprinting

Frank Fleischmann<sup>a,b</sup>, Tarek Eissa<sup>a,b</sup>, Guanting Guo<sup>a</sup>, Jacqueline Hermann<sup>a</sup> and Mihaela Žigman<sup>a,b</sup>

<sup>a</sup> Faculty of Physics, Ludwig-Maximilians Universität München (LMU), Am Coulombwall 1, Garching, Germany;

<sup>b</sup> Max Planck Institute of Quantum Optics (MPQ), Hans-Kopfermann-Straße 1, Garching, Germany.

We are developing and applying infrared spectroscopy as a new strategy for quantitative probing of liquid human biofluids at the molecular level. Our previous work has demonstrated the stability of infrared fingerprinting within individuals over time<sup>1</sup>, the feasibility of using this approach to capture common cancers<sup>2</sup>, and an exploration of the impact of biological noise versus measurement variability<sup>3</sup>.

In the current presentation, we are conducting a thorough and robust investigation of potential sources of variability that could potentially limit the application of the approach for the analysis of human blood serum and plasma in the context of *in vitro* diagnostics. Our goal is to devise an efficient way to probe human health and disease. To achieve this, we are leveraging the analyses of infrared spectroscopic fingerprinting of variety of measured samples collected across several experiments and studies conducted in our laboratories. This examination allows us to explore the diverse parameters and settings that can contribute to and standardize relevant variables.

Our investigation encompasses several key areas. Firstly, we are delving into the effects of clinical peripheral venous blood sampling and standard operating procedures for preparing and managing serum and plasma samples, respectively. Secondly, we are evaluating pre-analytical effects of differences in sample preparation, sample storage, the number of freeze-thaw cycles and the consumables applied, all of which could play a role in infrared molecular fingerprinting.

Furthermore, we are investigating how various Fourier transform infrared spectrometer-related aspects impact the captured spectral measurements. This analysis includes examining potential measurement drifts and variations due to factors like the measurement cuvette and path length.

Altogether, we show that several analytical parameters and minor sample handling variations have a direct impact on measured spectra. This, in turn, may impact the applications of machine learning models – from masking away useful information to introducing dataset bias. The discussion will center around the clinical, pre-analytical and analytical parameters and protocols that hold implications for the future design and performance of cell-free blood-based infrared molecular fingerprinting platform. This platform offers a promising avenue for multi-molecular *in vitro* profiling, enhancing our understanding and diagnostic capabilities in the field of analytics in healthcare.

## ACKNOWLEDGMENTS

We thank our study nurses Carola Spindler, Sabine Witzens and Ewelina Wozniak-Bauer for sample collection and blood processing and Viola Zóka and Daniel Meyer for technical assistance with sample management and FTIR measurements.

## REFERENCES

1. M. Huber, K.V. Kepesidis, L. Voronina, M. Božić, M. Trubetskov, N. Harbeck, F. Krausz, M. Žigman. Nature Communications 2021, 12, 1511, <https://doi.org/10.1038/s41467-021-21668-5>.

2. M. Huber, K.V. Kepesidis, L. Voronina, F. Fleischmann, E. Fill, J. Hermann, I. Koch, K. Milger-Kneidinger, T. Kolben, G.B. Schulz, F. Jokisch, J. Behr, N. Harbeck, M. Reiser, C. Stief, F. Krausz, M. Žigman, *eLife*, 2021, **10**, e68758, <https://doi.org/10.7554/elife.68758>.
3. T. Eissa, K.V. Kepesidis, M. Žigman, M. Huber, *Analytical Chemistry*, 2023, **95**, 6523–6532, <https://doi.org/10.1021/acs.analchem.2c04711>

# Isolation of Bacteria from Wastewater and Identification by Raman Spectroscopy

Sandra Baaba Frempong<sup>1,2</sup>, Annette Wagenhaus<sup>1,2</sup>, Sophie Girnus<sup>1,2</sup>, Petra Rösch<sup>1,2</sup> Jürgen Popp<sup>1,2,3</sup> (sandra.frempong@uni-jena.de)

1 Institute of Physical Chemistry and Abbe Center of Photonics, Friedrich Schiller University, Jena, Germany

2 InfectoGnostics Research Campus Jena, Center of Applied Research, Jena, Germany

3 Leibniz Institute of Photonic Technology, Member of Leibniz Health Technologies, Jena, Germany

## Abstract

Wastewater from healthcare facilities is a significant reservoir of nosocomial infectious agents, including facultative pathogenic Gram-negative bacteria like *E. coli*, *enterococci*, and *Pseudomonas aeruginosa*, which can lead to persistent outbreaks [1-3]. Monitoring hospital wastewater is therefore useful as an additional strategy for infection outbreak prevention and control. Meanwhile, conventional microbiological techniques for identifying bacteria in wastewater are labour-intensive and time-consuming, and the microbial species composition in samples can vary depending on sampling methods or location [4]. In addition, only a fraction of the bacteria in the overall diversity of nature are cultivable in the laboratory [5, 6]. Consequently, there is a need for culture-free identification methods that do not limit the wide range of bacteria strains that may be identified.

Raman spectroscopy is a powerful, non-destructive analytical technique that offers rapid, precise, and label-free identification of microorganisms by exploiting the interaction between their molecular vibrations and light. However, because wastewater is a complex and diverse medium that is constantly changing, this has an influence on bacterial cellular adaptations in response to environmental fluctuations, thus consequently on the Raman spectra [2]. Moreover, wastewater varies from day to day and from one house to the next, which adds more complexity to the bacterial identification process. Therefore, it is essential to develop robust and reliable methods for isolating and identifying bacteria from wastewater. In this work, we present an approach for isolating single bacterial cells from wastewater and a subsequent identification using Raman spectroscopy.

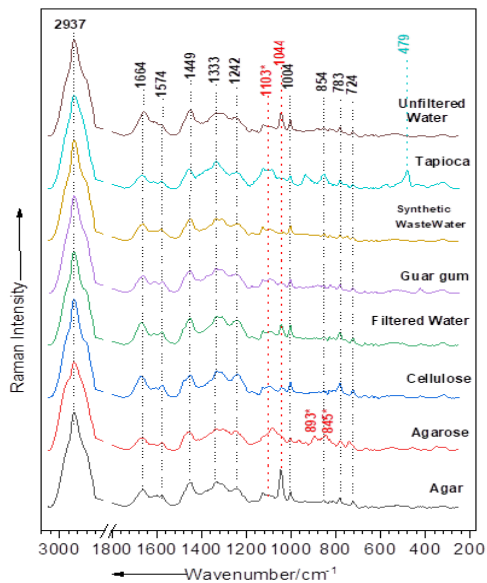


**Figure 1:** Raman spectra of *E. coli* cultivated in different simulated wastewater media using different suspended matter.

## Acknowledgments

Financial support of the Federal Ministry of Education and Research, Germany (Bundesministerium für Bildung und Forschung (BMBF), Deutschland) in the project FastAlert (13GW0460B).

## References

1. Exner, M., et al., *Anforderungen der Hygiene an abwasserführende Systeme in medizinischen Einrichtungen*. Bundesgesundheitsblatt-Gesundheitsforschung-Gesundheitsschutz, 2020. **4**: p. 484.
2. Wichmann, C., et al., *Simulating a reference medium for determining bacterial growth in hospital wastewater for Raman spectroscopic investigation*. Spectrochimica Acta Part A: Molecular and Biomolecular Spectroscopy, 2023: p. 123425.
3. Pistiki, A., et al., *Application of Raman spectroscopy in the hospital environment*. Transl. Biophotonics, 2022: p. e202200011.
4. Baritau, J.C., et al., *A study on identification of bacteria in environmental samples using single-cell Raman spectroscopy: feasibility and reference libraries*. Environ. Sci. Pollut. Res. Int., 2016. **23**(9): p. 8184-91.
5. Amann, R.I., W. Ludwig, and K.-H. Schleifer, *Phylogenetic identification and in situ detection of individual microbial cells without cultivation*. Microbiological reviews, 1995. **59**(1): p. 143-169.
6. Hofer, U., *The majority is uncultured*. Nature Reviews Microbiology, 2018. **16**(12): p. 716-717.



# Raman spectroscopic platform for the characterization of bacterial blood stream infections

**Richard Grohs<sup>a,d</sup>**, Marie-Luise Enghardt<sup>a,d</sup>, Anja Silge<sup>a,d</sup>, Uwe Glaser<sup>a</sup>, Karina Weber<sup>a,d</sup>, Oleg Ryabchykov<sup>a,d,e</sup>, Franziska Hornung<sup>c</sup>, Stefanie Deinhardt-Emmer<sup>c</sup>, Bettina Löffler<sup>c</sup>, Jürgen Popp<sup>a,b,c,d</sup>

<sup>a</sup>Leibniz Institute of Photonic Technology, Member of Leibniz Health Technologies, Member of the Leibniz Centre for Photonics in Infection Research (LPI), Jena Germany

<sup>b</sup>Institute of Physical Chemistry (IPC) and Abbe Center of Photonics (ACP), Friedrich Schiller University Jena, Member of the Leibniz Centre for Photonics in Infection Research (LPI), Helmholtzweg 4, 07743 Jena, Germany

<sup>c</sup>Institute of Medical Microbiology, Jena University Hospital, Am Klinikum 1, 07747, Germany

<sup>d</sup>InfectoGnostics Research Campus Jena, Center of Applied Research, Philosophenweg 7, 07743 Jena, Germany

<sup>e</sup>Biophotonics Diagnostics GmbH, Am Wiesenbach 30, 07751 Jena, Germany

Antibiotic resistances are a growing problem in modern medicine. Treatment of infectious diseases is thereby becoming more complicated and sometimes impossible having serious medical and financial implications. [1] A crucial way to counteract the spread of existing resistances and stop the evolution of new resistances is rapid antimicrobial susceptibility testing. Raman spectroscopy is a powerful tool for probing pathogens phenotypical response to antibiotic treatment [2]. Vital bacteria, *Escherichia coli* and *Staphylococcus aureus*, isolated from positive blood cultures were exposed to appropriate antibiotic concentrations and analyzed by On-Chip Raman spectroscopy. Spectroscopic changes are detectable after only 90 min of bacteria-antibiotic interaction while total test duration is  $\leq 3$  h. Using photonic data analysis, the spectral signals are translated into antibiograms.

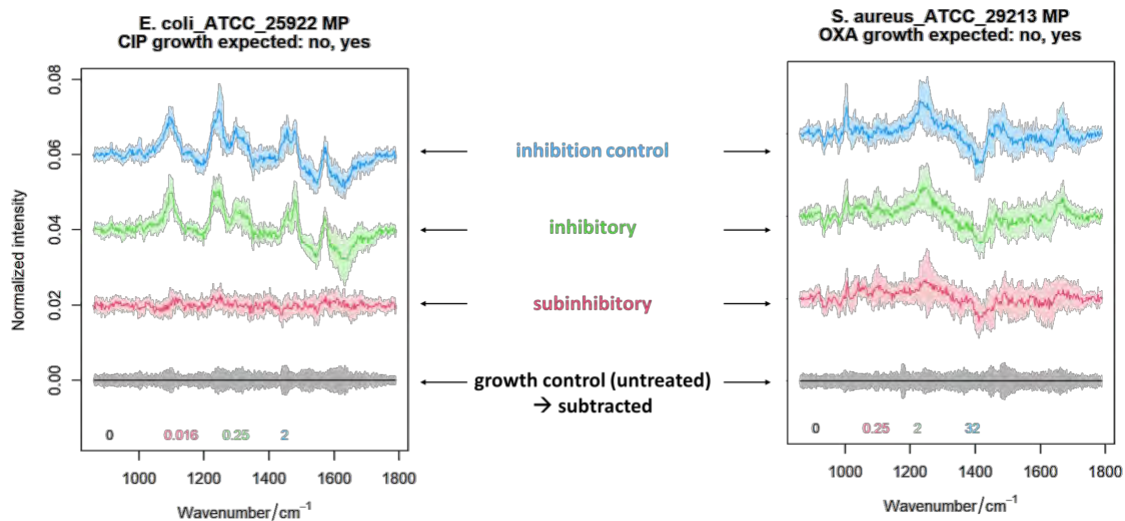


**Figure 1** Difference Raman-spectra of *Escherichia coli* treated with Ciprofloxacin (left) and *Staphylococcus aureus* treated with Oxacillin (right) in various concentration below and above minimal inhibitory concentration. Distinct variations in difference spectra of sufficiently treated (blue and green spectra) in comparison to insufficiently treated (red and black spectra) are visible due to molecular changes caused by the antibiotic after only 90 min of bacteria-antibiotic interaction time, respectively.

## ACKNOWLEDGMENTS

Federal Ministry of Education and Research (BMBF): Project InfectoXplore (13GW0459A)

Federal Ministry of Education and Research (BMBF): Funding program Photonics Research Germany and is integrated into the Leibniz Center for Photonics in Infection Research LPI-BT2-IPHT: 13N15704.

Microverse Imaging Center funded by the Deutsche Forschungsgemeinschaft: German Exzellenz Strategy– EXC 2051 – Project-ID 390713860

## REFERENCES

- [1] Dadgostar, P. 2019. Antimicrobial Resistance: Implications and Costs. *Infection and drug resistance* 12, 3903–3910.
- [2] Kirchoff, J., Glaser, U., Bohnert, J. A., Pletz, M. W., Popp, J., and Neugebauer, U. 2018. Simple Ciprofloxacin Resistance Test and Determination of Minimal Inhibitory Concentration within 2 h Using Raman Spectroscopy. *Analytical chemistry* 90, 3, 1811–1818.

# Advancing Cardiac Diagnostics: Exploring Non-Invasive Optical Modalities for Myocardial Tissue Characterization

Alexander Gumbel<sup>a</sup>, Christian Krüger<sup>a</sup>, David L. Vasquez<sup>b</sup>, Iwan W. Schie<sup>a,b</sup>,

<sup>a</sup> *Department for Medical Engineering and Biotechnology, University of Applied Sciences Jena, Germany*

<sup>b</sup> *Leibniz Institute of Photonic Technology, Jena, Germany*

The investigation of pathological tissue changes in the myocardium is crucial due to a wide range of possible causes, including ischemic and non-ischemic cardiomyopathies, as well as infiltrative and inflammatory diseases. Accurately understanding these changes is essential for precise diagnosis and effective treatment planning. Currently, endomyocardial biopsy (EMB) is the gold standard for diagnosing myocardial alterations. However, this method is associated with significant risks, such as the potential for cardiac tamponade, arrhythmias, and tricuspid valve damage. Additionally, its invasive nature and the need for specialized clinical facilities limit its widespread use.

Optical modalities have become well-established in clinical practice, encompassing everything from visual inspection of structural tissue changes and high-resolution microscopy to in vivo endoscopy for diagnosing a variety of pathologies. Emerging optical modalities, including optical coherence tomography, UV-excited autofluorescence, and near-infrared spectroscopy, have been applied broadly for tissue characterization and in enhancing the diagnosis of pathological tissue changes. However, there are currently only a limited number of clinical studies that investigate optical techniques for cardiac tissue characterization.

In this research, we investigate optical modalities suitable for non-invasive, marker-free, and non-destructive characterization of structural changes in the myocardium, regardless of the underlying pathology. Our study aims to assess the potential of these modalities, particularly through dedicated multimodal endoscopic imaging, to identify specific tissue changes in the myocardium. This technology could greatly assist healthcare professionals in cardiac diagnostics, enabling more targeted therapy and adherence to the guidelines of the European Society of Cardiology regarding the diagnosis of the cause and severity of pathological tissue changes in the myocardium.

## ACKNOWLEDGMENTS

We acknowledge funding by the Carl Zeiss Foundation, OptoCarDi – Research and translation of a multimodal optical catheter for the diagnosis of myocarditis, (CZS, grant number P2022-07-003), the project OpenLab-KI - Application of AI and explainable AI for cross-domain processing of OCT-Images (BMBF, FKZ: 16DKWN111); EASYprobe - Multimodal, endoscopic, fiber optic probes for clinical imaging diagnostics - new concepts and manufacturing technologies (BMBF, FKZ: 13FH578KX1).

# Systematic investigation on device drift for Raman spectroscopy and quality control

Shuxia Guo<sup>a, b</sup>, Anuradha Ramoji<sup>a, b</sup>, Oleg Ryabchykov<sup>a, b</sup>, Anja Silge<sup>a, b</sup>,  
Jürgen Popp<sup>a, b</sup>, Thomas Bocklitz<sup>\*a, b, c</sup>

<sup>a</sup> Leibniz Institute of Photonic Technology, Member of Leibniz Health Technologies, Member of the Leibniz Centre for Photonics in Infection Research (LPI), Albert-Einstein-Strasse 9, 07745 Jena, Germany.

<sup>b</sup> Institute of Physical Chemistry (IPC) and Abbe Center of Photonics (ACP), Friedrich Schiller University Jena, Member of the Leibniz Centre for Photonics in Infection Research (LPI), Helmholtzweg 4, 07743 Jena, Germany

<sup>c</sup> Institute of Computer Science, Faculty of Mathematics, Physics & Computer Science, University Bayreuth Universitätsstraße 30, 95447 Bayreuth, Germany

\* Corresponding author: [Thomas.bocklitz@uni-jena.de](mailto:Thomas.bocklitz@uni-jena.de)

By indirectly detecting molecular vibrations, Raman spectroscopy provides the unique fingerprints of molecular components under measurement [1]. Together with machine learning techniques, which translate the spectral fingerprints into interpretable knowledge, Raman spectroscopy has obtained more and more attention in biological, medical, and clinical investigations. Its broader application, however, is by large hindered by the substantial variations between devices and over time [2, 3]. A machine learning model built on one device is often inapplicable on the other. A systematic investigation of such variations is in urgent need.

In this study, we measured weekly 13 substances as quality control references over 10 months on one Raman setup to investigate the instrumental variations and its time-dependence. The 13 substances were selected to be stable and span a broad range of solvents, lipids, and carbohydrates. From each substance 50 Raman spectra were acquired every measurement day. All spectra were preprocessed to remove spikes and fluorescence baselines. Thereafter, we characterized the spectral variations of each substance over the measurement period based on the correlation coefficient, the peak position shift of well-defined Raman bands, as well as the peak intensity ratios. As a comparison, the analysis was conducted in cases of with and without wavenumber calibration [4]. According to Figure 1, the spectral variations are substantial even after the wavenumber calibration. We also observed that the variations are different among substances and for different Raman bands. This study aims to explore the hidden patterns of these spectral variations as a guide for better setup calibration.

## ACKNOWLEDGMENTS

We thank the financial support from the EU funded project Telegraft (No. 101057673). This work is also supported by the BMBF, funding program Photonics Research Germany (FKZ:13N15466 (BT1)) and is integrated into the Leibniz Center for Photonics in Infection Research (LPI). The LPI initiated by Leibniz-IPHT, Leibniz-

HKI, UKJ and FSU Jena is part of the BMBF national roadmap for research infrastructures.

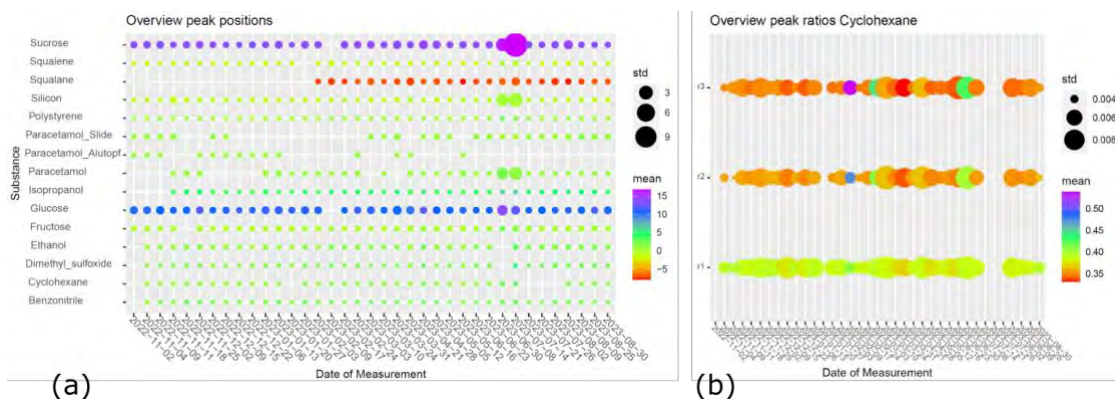


**Figure 1** (a) peak position drift of each substance over the measurement days. (b) peak intensity ratios calculated from Cyclohexane between three Raman bands ( $1028.3$ ,  $1266.4$ ,  $1444.4$   $\text{cm}^{-1}$ ) and the fourth ( $801.3$   $\text{cm}^{-1}$ ).

## REFERENCES

1. Bocklitz, T. W.; Guo, S.; Ryabchykov, O.; Vogler, N.; Popp, J. r., Raman based molecular imaging and analytics: a magic bullet for biomedical applications!? *Analytical chemistry* 2016, 88 (1), 133-151.
2. S. Guo, J. Popp, T. Bocklitz, *Nature Protocols* 16, 5426–5459 (2021).
3. S. Guo, C. Beleites, U. Neugebauer, et al., *Analytical Chemistry*, 2020, 92, 15745–15756.
4. T.W. Bocklitz, T. Dörfer, R. Heinke, M. Schmitt, and J. Popp, *Spectrochim. Acta. A. Mol. Biomol. Spectrosc.* 5, 544–549 (2015)

# Characterization of Toll-like Receptor Activation of Monocytes using Raman Microscopy

Leah M. H. Haase<sup>1,2</sup>, Max Naumann<sup>2,3</sup>, Rustam R. Guliev<sup>2</sup>, Natalie Arend<sup>2</sup>, Uwe Glaser<sup>2</sup>, David L. Vasquez-Pinzon<sup>2</sup>, Iwan Schie<sup>2</sup>, Aikaterini Pistiki<sup>2,3</sup>, Ramya Motganhalli<sup>2</sup>, Jürgen Popp<sup>2,3</sup>, Ute Neugebauer<sup>2,3,4</sup>

<sup>1</sup> Friedrich Schiller University Jena, Faculty of Physics and Astronomy, Jena, Germany

<sup>2</sup> Leibniz Institute of Photonic Technology (Member of Leibniz Health Technologies, Member of the Leibniz Center for Photonics in Infection Research, LPI), Jena, Germany

<sup>3</sup> Friedrich Schiller University Jena, Institute of Physical Chemistry and Abbe Center of Photonics, Jena, Germany

<sup>4</sup> Jena University Hospital, Center for Sepsis Control and Care and Department of Anesthesiology and Intensive Care Medicine, Jena, Germany

Monocytes function as part of the immune system by patrolling the bloodstream for invading pathogens. They sense infection using receptors, e.g. Toll-like receptors (TLRs), that identify components of bacteria and viruses, so-called pathogen-associated molecular patterns (PAMPs). Upon activation, signaling pathways are triggered and the cellular metabolism changes. The activation state of monocytes can be investigated using Raman spectroscopy [1]. The objective of this study is to detect and characterize the activation states induced by different stimuli and to establish Raman microscopy as a biophotonic technology for distinguishing between the non-activated and activated cells as well as between the stimuli.

In this work, we stimulated THP-1 monocytes with receptor-specific stimuli for four hours. We used stimuli which are characteristic for Gram-positive or Gram-negative bacteria or for viruses. ELISA was performed to assess the activation of the cells. Single cell and High Throughput Raman microscopy indicated the spectral differences between non-activated and activated monocytes and the different TLR activation profiles. Unsupervised and supervised learning algorithms were used for differentiation between stimuli.

## Literature:

[1] Töpfer, N. et al. *Integrative Biology* 2019, 11(3), 87–98.

## Acknowledgement:

This work is supported by the BMBF, funding program Photonics Research Germany (FKZ: BT4 Leibniz-IPHT13N15713, BT4 UKJ: 13N15716) and is integrated into the Leibniz Center for Photonics in Infection Research (LPI). L. H. acknowledges the "Honours Programme for Future Researchers" at the Friedrich Schiller University Jena (Germany).

# Detection of protein modification in biological tissue caused by physical plasma as a tool to optimize label-free spectroscopic visualization of plasma effects *in vivo*

Hasse, Sybille<sup>1</sup>, Völter, Melissa Joana<sup>2</sup>, Meyer, Tobias<sup>3</sup>, Schmitt, Michael<sup>3</sup>, von Woedtke, Thomas<sup>1,2</sup>

<sup>1</sup>Leibniz Institute for Plasma Science and Technology (INP), Greifswald, Germany\*

<sup>2</sup>Greifswald University Medicine, Institute for Hygiene and Environmental medicine, Greifswald, Germany

<sup>3</sup>Leibniz-Institute of Photonic Technology Jena, Jena, Germany\*

\*a member of the Leibniz Research Alliance Leibniz Health Technology

Research and application of cold atmospheric plasma (CAP) for therapeutic purposes established the field of plasma medicine. CAP emerged as a promising tool in the treatment of hard-to-heal and infected wounds. Other fields like cancer treatment are under investigation. Biological CAP effects can be attributed to reactive oxygen and nitrogen species (ROS/RNS) that in turn react readily with cellular structures. So far, the anticipated protein modifications were studied *in vitro* both with amino acids (e.g. cysteine) and model proteins (e.g. ovalbumin) (1-3).

The aim of this study was to visualize CAP-caused oxidative protein modifications directly in biological tissue (*in situ*). Therefore, tissue samples from porcine ear skin were treated with the argon-driven atmospheric pressure plasma jet kINPen® (neoplas med, Greifswald, Germany) for different time intervals and with different gas admixtures to vary its ROS/RNS content. In addition, the outermost protective skin layer (stratum corneum) was removed to ease species penetration into deeper tissue layers. Redox modification was visualized by labelling oxidized cysteine residues with immune fluorescence technique. This method allows for semi-quantitative detection and localization of CAP-caused protein modifications within different skin layers.

Previously, it has been demonstrated that spectroscopic methods, such as CARS, FLIM, SHG etc. and particularly combinations of them are powerful tools to visualize plasma triggered changes in skin sections without any label (4). The labelling technique presented here will be used to establish and further optimize this label-free visualization of redox-based protein modifications with temporal and spatial resolution *in situ* (i.e. skin or wound tissue). The future aim is to upgrade CAP treatment devices to treatment systems including a continuous and real-time monitoring of the target that is treated to enhance the molecular understanding and help to improve the outcome and effectiveness of CAP-based therapies (5).



## References

1. Wende K, Bruno G, Lalk M, Weltmann KD, von Woedtke T, Bekeschus S, Lackmann JW. On a heavy path - determining cold plasma-derived short-lived species chemistry using isotopic labelling. *Rsc Adv* 2020;10(20):11598-607.
2. Lackmann JW, Wende K, Verlackt C, Golda J, Volzke J, Kogelheide F, et al. Chemical fingerprints of cold physical plasmas - an experimental and computational study using cysteine as tracer compound. *Scientific reports* 2018;8(1):7736.
3. Clemen R, Freund E, Mrochen D, Miebach L, Schmidt A, Rauch BH, et al. Gas Plasma Technology Augments Ovalbumin Immunogenicity and OT-II T Cell Activation Conferring Tumor Protection in Mice. *Adv Sci (Weinh)* 2021;8(10):2003395.
4. Meyer T, Bae H, Hasse S, Winter J, Woedtke TV, Schmitt M, et al. Multimodal Nonlinear Microscopy for Therapy Monitoring of Cold Atmospheric Plasma Treatment. *Micromachines (Basel)* 2019;10(9).
5. von Woedtke T, Emmert S, Metelmann H-R, Rupf S, Weltmann K-D. Perspectives on cold atmospheric plasma (CAP) applications in medicine. *Physics of Plasmas* 2020;27(7).

# Development of a filter-based spectral imaging system for position- and wavelength-dependent detection of localized surface plasmons

André Heewig<sup>a</sup>, Jonathan Frohn<sup>b</sup>, Manal al Maoush<sup>c</sup>, Andrea Csáki<sup>a</sup>,  
Wolfgang Fritzsche<sup>a</sup>

<sup>a</sup> Leibniz-Institute of Photonics Technologies, Albert-Einstein-Str. 9 07745 Jena, Germany

<sup>b</sup> Ernst-Abbe-Hochschule Jena, Carl-Zeiss-Promenade 2 07745 Jena, Germany

<sup>c</sup> Friedrich-Schiller-Universität, Fürstengraben 1 07743 Jena, Germany

Localized surface plasmon resonance (LSPR) based sensorics is an elegant method for label-free testing in future bioanalytics. In these, plasmonic nanostructures such as nanoparticles form the optical signal transducers. Depending on the surrounding refractive index, they show a spectral response in the visible wavelength region, which can be used as sensoric principle for the presence of molecules. By arranging not just one spot of nanoparticles modified with selectively binding receptor molecules, but an array of spots, multiplexed testing can be realized. To spectroscopically readout the array, we decided to use imaging spectrometry methods [1]. Here, we describe a setup using a liquid crystal tunable filter (LCTF) [2] in order to expose the particles subsequently with light of different wavelengths, the resulting image stack is then utilized to reconstruct a spectrum for each image pixel, and allows to monitor the spectral behavior of the nanoparticle spots.

A common method to determine the optical signal of a single transducer spot is to use spectrometer in transmission. The advantage of this setup is a high measurement accuracy and fast measured value acquisition, whereby binding kinetics can be also detected. However, a position-dependent resolution of LSPR signal is not possible. To meet the ever-increasing demands of bioanalytics, an imaging system for spatial and multiplex detection of LSPR were developed [3]. Since both experimental setups rely on different optical readout's for LSPR detection, the main challenge is to develop an adapted evaluation to compare both methods. Another challenge is the selection of a suitable light source. This should have the broadest possible spectrum with sufficient intensity, long-term stability and low heat generation. Because different nanoparticles

can be used as transducers, it is necessary to ensure that the resonance lines are situated within the spectrum of the light source in order to detect it.

In general, for an optimal sensor setup all these factors have to be considered to establish a reproducible detection technique for future diagnostic issues.



**Figure 1** Prototype of the measurement device for plasmonic micro arrays

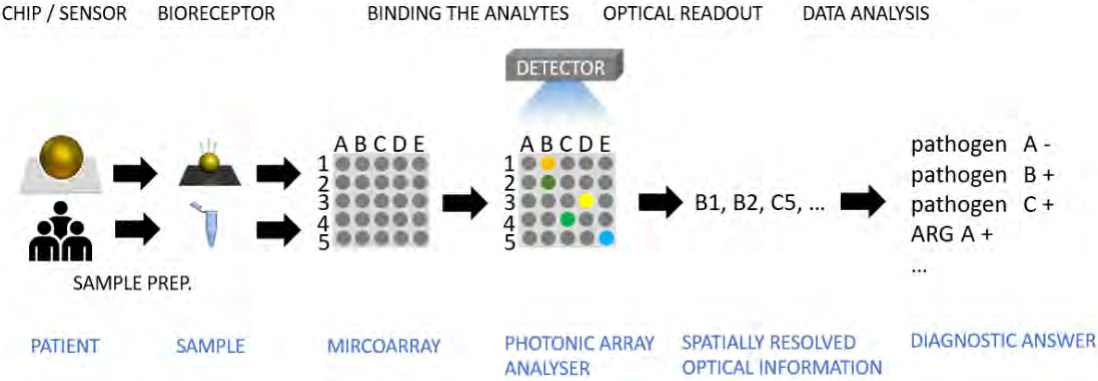


**Figure 2** Sensing principle for pathogens using plasmonic micro array analyser

## **Acknowledgments**

Funding by the Free State of Thuringia with funds from the European Union within the framework of the European Regional Development Fund, grant number 2018 FE 9038 (2018 VF0015), and the Federal Ministry of Education and Research in the frame of the Leibniz Center for Photonics in Infection Research (LPI), Grand number 13N15717), is gratefully acknowledged.

## **References**

1. ElMasry, G., & Sun, D.-W., *Hyperspectral Imaging for Food Quality Analysis and Control*, 2010, *Principles of Hyperspectral Imaging Technology*, 3–43.
2. Lu, G., & Fei, B., *Journal of Biomedical Optics*, 2014, *Medical hyperspectral imaging: a review.*, 19
3. Zopf, D., Pittner, A., Dathe, A., Grosse, N., Csáki, A., Arstila, K., ... Stranik, O., *ACS Sensors*, 2019, *Plasmonic nanosensor array for multiplexed DNA-based pathogen detection.*

# High-throughput multimodal imaging and spectroscopy system for the analysis of cells

S M Miftahul Islam<sup>a</sup>, Kristina Worch<sup>b</sup>, Antje Burse<sup>b</sup>, Jürgen Popp<sup>a,c</sup>, and Iwan W. Schie<sup>a,b</sup>

<sup>a</sup> *Leibniz Institute of Photonic Technology, Member of Leibniz Health Technologies, member of the Leibniz Centre for Photonics in Infection Research (LPI), Jena, Germany*

<sup>b</sup> *Department for Medical Engineering and Biotechnology, University of Applied Sciences –Jena, Germany*

<sup>c</sup> *Institute of Physical Chemistry and Abbe Centre of Photonics, Friedrich Schiller University Jena, Germany*

The investigation of cellular processes poses a significant challenge due to their inherent complexity. High throughput systems (HTS), based on fluorescence labeling in combination with imaging microscopy offer promising solutions in this context. HTS has received considerable attention in biomedical research and drug discovery, providing comprehensive data about complex biological systems, such as eukaryotic cells [1]. Moreover, HTS can be used as an in vitro tool to prioritize compounds for toxicological and mechanistic studies [2]. However, there are also label-free modalities, which have significant potential to provide complementary information, allowing multiple properties of the sample to be probed simultaneously. Therefore, a multimodal high-throughput system has the potential to address complex biological questions in many aspects of research and clinical studies.

We present the development of a fully automated multimodal optical system for high-throughput analysis of cells that incorporates phase-contrast (PC) microscopy, fluorescence microscopy, and brightfield (BF) microscopy with Raman spectroscopy. The integration of multiple modalities into a single system can extend possible applications for single cell analysis, as each modality provides a complementary type of specific information. Our system is controlled by a custom-written LabVIEW program, which enables high-throughput imaging and spectra collection by utilizing image processing methods to detect cells and obtain spectroscopic information on those indicated locations. The integration of Raman spectroscopy, phase-contrast microscopy, and fluorescence microscopy holds significant potential for the noninvasive examination and real-time tracking of the physiological processes within individual cells [3].

Simultaneous detection of Raman spectra and imaging with several microscopy methods enable detailed spectral and spatial information of the samples. Molecular specific information can be obtained by fluorescence microscopy, while phase-contrast microscopy provides images with high contrast to facilitate identification of internal cellular structures along with brightfield imaging. Finally, Raman spectroscopy provides the composition of molecules in the samples and the results can be validated

from the individual cells in combination with fluorescence microscopy. Moreover, the combination of Raman spectroscopy and phase-contrast microscopy could provide changes in refractivity to specific molecular changes [3]. The data acquisition process is shown in figure 1.

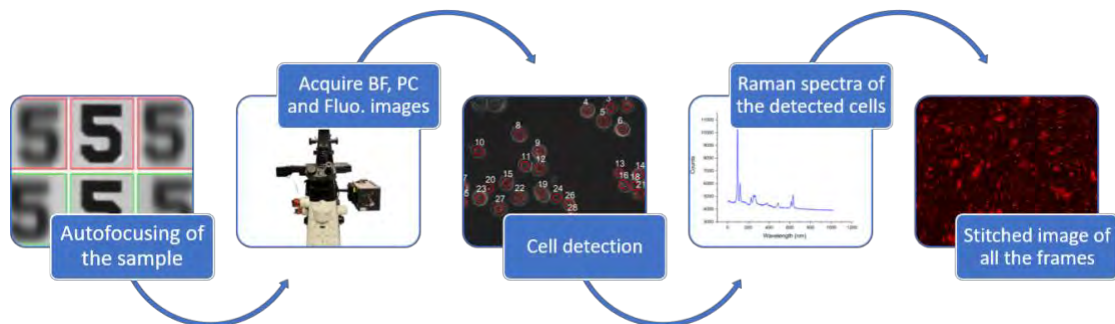


**Figure 1** Workflow of the automated measurement

## ACKNOWLEDGMENTS

This work is supported by the BMBF (Federal Ministry of Education and Research) and is integrated into the Leibniz Center for Photonics in Infection Research (LPI). The LPI initiated by Leibniz-IPHT, Leibniz-HKI, UKJ and FSU Jena is part of the BMBF national roadmap for research infrastructures.

## REFERENCES

1. Schie, I., Rüger J., Mondol, A. *et al.* High-throughput screening Raman spectroscopy (HTS-RS) platform for label-free cellomics. *Analytical Chemistry*. 90. 10.1021/acs.analchem.7b04127 (2017).
2. Li, S., Xia, M. Review of high-content screening applications in toxicology. *Arch Toxicol* 93, 3387–3396 (2019)
3. Kong, L., Zhang, P., Wang, G. *et al.* Characterization of bacterial spore germination using phase-contrast and fluorescence microscopy, Raman spectroscopy and optical tweezers. *Nat Protoc* 6, 625–639 (2011).

# Identification of Pathogenic Microbials by Digital Live-Cell Reporter Assays

Duyguhan Kozal<sup>a\*</sup>, Cornelia Reuter<sup>a</sup>, Mark Kielpinski<sup>a</sup>, Thomas Henkel<sup>a</sup>

<sup>a</sup> Leibniz Institute of Photonic Technology, Albert-Einstein-Str. 9, 07745 Jena, Germany, member of the Leibniz Centre for Photonics in Infection Research (LPI), Jena, Germany

Microbial pathogens have consistently prompted a significant threat to human health by causing severe diseases. As a consequence of the rising needs to more rapid, convenient and high throughput microbial detection applications, droplet-based microfluidic assays have been implemented as one of the most promising techniques [1]. Droplet-based microfluidics is a unique tool focusing the generation of uniformly-sized droplets as microreactors that brings together point-of-care diagnostics and biotechnological applications. These systems make achievable to precisely and automated handle of minute volumes of liquids [2]. In addition to the increasing sensitivity, not only multiple experiments in parallel can be conducted, but also the reaction time is diminished. Within the scope of this study, the specialized reader system combining of colorimetric and fluorometric imaging will be utilized for the detection and characterization of pathogenic bacteria which metabolize reporter substrate. Here we report on the implementation of a reader for this class of assays and give examples on measurements and data processing workflow. The reader is optimized for the readout of chip devices as given in Figure 1. A readout example for a chromogenic reporter assay is shown in Figure 2.



**Figure 1** Chip device with droplet generator and incubation channel.



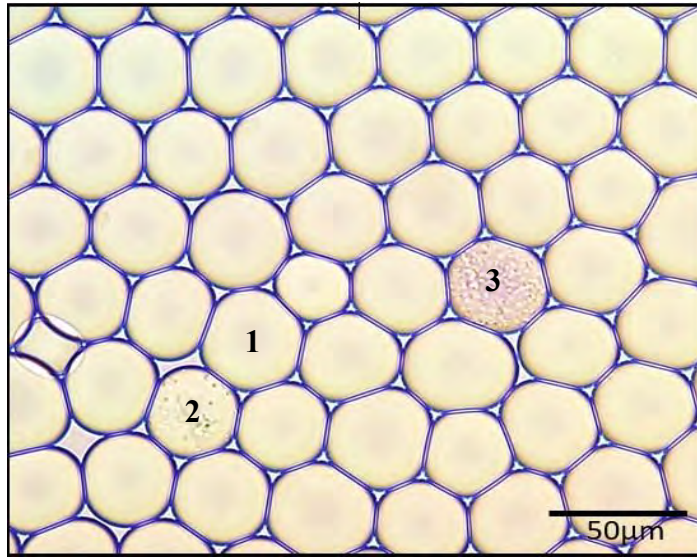


**Figure 2** Droplets in incubation channel as (1) empty droplets, (2) cell growth without colour change, (3) cell growth with colour change.

## ACKNOWLEDGMENTS

This work is supported by the BMBF, funding program Photonics Research Germany (13N15704) and is integrated into the Leibniz Center for Photonics in Infection Research (LPI). The LPI initiated by Leibniz-IPHT, Leibniz-HKI, JUH and FSU Jena is part of the BMBF national roadmap for research infrastructures.

## REFERENCES

1. Kaminski, T. S., Scheler, O., & Garstecki, P., *Lab on a Chip*, 2016, **16(12)**, 2168-2187.
2. Scheler, O., Postek, W., & Garstecki, P., *Current opinion in biotechnology*, 2019, **55**, 60-67.

# Integrating Hyperspectral Imaging with Mixed Reality for Enhanced Medical Diagnostics and Treatment Planning

Christian Krüger<sup>a</sup>, Alexander Gumbel<sup>a</sup>, Abed Assad<sup>a</sup>, Iwan W. Schie<sup>a,b</sup>,

<sup>a</sup> *Department for Medical Engineering and Biotechnology, University of Applied Sciences Jena, Germany*

<sup>b</sup> *Leibniz Institute of Photonic Technology, Jena, Germany*

Hyperspectral imaging (HSI) has become a highly sensitive and cost-effective technology in biomedical research, offering non-invasive, detailed spectral analysis of biological tissues. This method, capturing a broad spectrum of light beyond primary colors, enables identification and analysis of materials through their spectral signatures. HSI is particularly effective in detecting and delineating tumor tissues, identifying tumor margins, and providing insights into wound healing. It assesses tissue oxygenation and perfusion, measuring oxygen saturation levels crucial in evaluating blood circulation efficiency during surgeries and in critical care.

Recently, augmented (AR) and mixed reality (MR) technologies, propelled by the gaming industry, have made significant strides in advanced data visualization, especially in medicine. Mixed reality merges physical and digital realms, creating an interactive environment for medical professionals to visualize and interact with complex data intuitively and immersively. In medical imaging and diagnostics, MR transforms two-dimensional images into three-dimensional models, enhancing surgeons' ability to examine anatomical structures and plan surgeries more precisely and safely.

This research explores the integration of HSI data on perfusion with mixed reality to enhance diagnostic accuracy and patient care. We're developing a multisensor platform that combines biomedical sensors with mixed reality visualization through Microsoft HoloLens 2. This platform enables real-time vital data exchange between microcontrollers connected to biosensors and mixed reality glasses, using the Open Sound Control network protocol for data transmission. Designed to be transportable and largely independent of the internet or servers, and operating on rechargeable batteries, this system is particularly valuable in emergency medicine scenarios, offering a novel approach to medical diagnostics and treatment planning.

## ACKNOWLEDGMENTS

We acknowledge funding by the Carl Zeiss Foundation of ZAKI - Center for Applied AI; and OptoCarDi – Research and translation of a multimodal optical catheter for the diagnosis of myocarditis, (CZS, grant number P2022-07-003); the project OpenLab-KI - Application of AI and explainable AI for cross-domain processing of OCT-Images (BMBF, FKZ: 16DKWN111); EASYprobe - Multimodal, endoscopic, fiber optic probes for clinical imaging diagnostics - new concepts and manufacturing technologies (BMBF, FKZ: 13FH578KX1).

# SERS-based detection of antibiotics and metabolites in pharmaceutical formulations and clinical-relevant matrices

Chen Liu<sup>a,b</sup>, Jürgen Popp<sup>a,b</sup>, Dana Cialla-May<sup>a,b</sup>

<sup>a</sup>Leibniz Institute of Photonic Technology, Member of Leibniz Health Technologies, Member of the Leibniz Centre for Photonics in Infection Research (LPI), Albert-Einstein-Straße 9, 07745 Jena, Germany.

<sup>b</sup>Institute of Physical Chemistry (IPC) and Abbe Center of Photonics (ACP), Friedrich Schiller University Jena, Member of the Leibniz Centre for Photonics in Infection Research (LPI), Helmholtzweg 4, 07743 Jena, Germany

Raman spectroscopy and surface enhanced Raman spectroscopy (SERS) are widely utilized in the detection of drugs and metabolites aiming its application in a clinical environment. [1] However, due to the strong competition in high complex matrices for free binding sites on the surface of SERS-active sensors, customizing the sample preparation strategy to reduce the interference of the Raman marker modes of the target analytes with them of the matrix molecules for successful SERS applications is essential.

In the case of the detection of the antibiotic ciprofloxacin (CIP) in pharmaceutical formulations i.e., eye drop, ear drop, dextrose and sodium chloride infusion solution, the SERS-based quantification of CIP is impeded by the presence of matrix components such as benzalkonium chloride, mannitol or similar ingredients. Raman spectroscopy can be performed directly when the spectral background of the pharmaceutical formulations does not overlap with the spectral marker bands of the analyte molecule. For formulations with strong Raman background, we mixed the entire sample with water employing a ratio of 1:5000. Moreover, SERS as analytical tool is applied and due to the dilution, less competition for SERS-active sites is achieved for the target analyte CIP. Thus, the developed workflow has a high potential in quality control approaches in pharmaceutical technology or pharmacies. [2]

Moreover, in real clinical sample applications, such as whole blood or blood plasma samples, the hotspots of the SERS substrate are expected to be blocked by a protein corona due to its high affinity to nanostructures. Using the example of the antibiotic ceftriaxone (CRO) and its detection in blood plasma, the requirement for precipitation of the proteins became evident, which is achieved by the application of acetonitrile. Thus, protein-bound drugs are released and accessible for detection allowing the estimation of the whole drug plasma concentration. On the other hand, the application of microdialysis to separate the free fraction of antibiotics from the blood plasma with subsequent SERS-based detection illustrates the potential of this method in clinical settings such as intensive care units.

Finally, functionalized SERS-active nanostructures are applied to selectively enrich the metabolite pyrazinoic acid (POA) from a matrix containing its pro-drug pyrazinamide (PZA) administered to patients in case of tuberculosis. The schematic diagram was shown in Figure 1. Here, POA is interacting with iron(II) ions of the Prussian blue functionalization layer and is detected via SERS, allowing its estimation down to the relevant concentration range to distinguish between sensitive and resistant *M. tuberculosis* strains. [3]

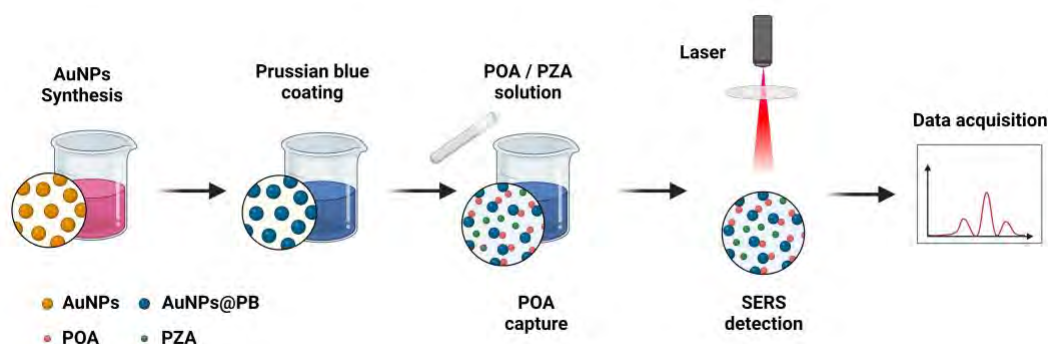


**Figure 1** Illustration diagram of SERS-based detection of POA using gold nanoparticles (AuNPs) adorned with a Prussian blue (PB) coating.

## ACKNOWLEDGMENTS

We thank the funding of the project InfectoGnostics (13GW0096F) by BMBF, Germany, as well as the project 465289819 by German Research Foundation (DFG).

## REFERENCES

1. Liu C, Weber S, Peng R, Wu L, Zhang W-s, Luppia PB, et al., *TrAC Trends in Analytical Chemistry*, **2023**, 164, 117094.
2. Liu C, Müller-Bötticher L, Liu C, Popp J, Fischer D, Cialla-May D. *Talanta*, 2022, **250**, 123719.
3. Liu C, Jiménez-Avalos G, Zhang W-s, Sheen P, Zimic M, Popp J, et al., *Talanta*, 2024, **266**, 125038.

# Deep Learning based 3D Raman Spectral Data Analysis for Colorectal Tissue Diagnosis

Ruihao Luo<sup>a,b</sup>, Shuxia Guo<sup>a,b</sup>, Thomas Bocklitz<sup>a,b,c</sup>

<sup>a</sup> Institute of Physical Chemistry and Abbe Center of Photonics, Friedrich-Schiller-Universität Jena, Helmholtzweg 4, Jena, Germany

<sup>b</sup> Leibniz Institute of Photonic Technology, Albert-Einstein-Straße 9, Jena, Germany

<sup>c</sup> Institute of Computer Science, Universität Bayreuth, Universitätsstraße 30, Bayreuth, Germany

The rise of artificial intelligence has led to deep learning algorithms playing an increasingly important role in various traditional fields of research. In recent years, they have also become popular tools in the field of data analysis for Raman spectroscopy and especially Raman imaging[1]. However, most current methods only use 1-dimensional (1D) spectral data for classification, instead of considering any spatially neighbouring information. Despite some successes, these of methods does not use the 3-dimensional (3D) structure of Raman imaging scans to their advantage.

Therefore, to investigate the feasibility of containing the spatial information of Raman imaging for data analysis, we have applied 3D deep learning algorithms to a murine colorectal tissue dataset [2]. This dataset contains Raman scans of normal & hyperplastic tissue as well as adenoma and carcinoma tissue samples. Firstly, a network modified from the 3D U-Net [3] is utilised for segmentation; secondly, another CNN network using 3D Raman patches is utilised for classification. Both methods are compared with the conventional 1D CNN method, which serves as baseline.

Based on the experiments of both segmentation and classification, it is shown that using the spatial information of 3D Raman scans can increase the performance of deep learning models, although it might also hugely increase the complexity of network training.

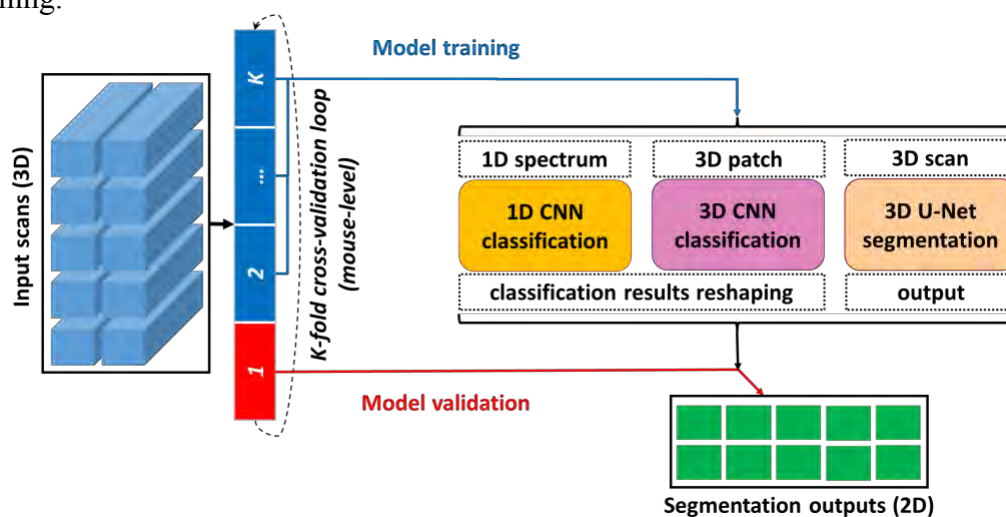


**Figure 1** Overall dataflow of this study. With the input Raman scans, an external K-fold cross-validation loop was implemented based on a mouse-level dataset split. The training subsets were sent to 3 deep learning networks (1D CNN, 3D CNN and 3D U-Net). Afterwards, the validation subset was used to evaluate the trained models based on the 2D segmentation outputs.

## **ACKNOWLEDGMENTS**

This work is supported by the BMBF, funding program Photonics Research Germany (13N15466 (LPI-BT1)) and is integrated into the Leibniz Center for Photonics in Infection Research (LPI). The LPI initiated by Leibniz-IPHT, Leibniz-HKI, Friedrich Schiller University Jena and Jena University Hospital is part of the BMBF national roadmap for research infrastructures.

## **REFERENCES**

1. Luo, R. et al., *Analytica* 2022, **3**, 287 - 301.
2. Vogler, N. et al. *J. Biophotonics* 2015, **9**, 1 - 9.
3. Çiçek, Ö. et al. *MICCAI* 2016, **9901**, 424 - 432.

# Spectroscopic Analysis through Spider Plots: Harnessing Pre-trained Networks for Raman Classification

Azadeh Mokari<sup>a,b</sup>, Thomas Bocklitz<sup>a,b,c</sup>

<sup>a</sup> Leibniz Institute of Photonic Technology, Member of Research Alliance "Leibniz Health Technologies", 07745 Jena, Germany

<sup>b</sup> Institute of Physical Chemistry, Friedrich Schiller University Jena, 07743 Jena, Germany

<sup>c</sup> Institute of Computer Science, Universität Bayreuth, Universitätsstraße 30, Bayreuth, Germany

In the realm of spectroscopic analysis, the limited availability of pre-trained networks hinders the rapid classification of diverse datasets. Addressing this challenge, our study introduces an innovative approach to convert spectral data into image form using spider plots as shown in Figure 1. After pre-processing the collected Raman data, each spectral variable is mapped to a radial line on the plot. The line's length is determined by the intensity on the respective wavenumber position. When interconnected, these lines form a spider or radar plot reflecting the sample's spectral signature. To enrich the image representation, the inner sections of the spider are also color-coded based on their intensities, adding another dimension of information to the image. With these converted spectra, it is possible to leverage image-focused pre-trained networks originally developed for traditional image datasets by adapting them to classify diverse Raman data sets ranging from bacterial to oil signatures.

In our approach, we utilized seven different pre-trained networks for classification. Among them, EfficientNetB7 showed the highest performance. To evaluate our method's effectiveness, we assessed it using a Raman data set containing six classes of bacteria, by comparing its performance against the traditional spectral classification method PCA-LDA applied directly to spectra. Preliminary findings showed EfficientNetB7 achieved a balanced accuracy of  $0.88 \pm 0.01$ . In contrast, PCA-LDA registered a balanced accuracy score of  $0.90 \pm 0.024$ . These results show that our image transformation technique performs on par with traditional approaches. Expanding on this, we evaluated our method on a separate Raman dataset containing eight different classes of oils. In this rigorous evaluation using 10-fold cross-validation, our approach using EfficientNetB7 achieved a balanced accuracy of  $0.99 \pm 0.02$  while PCA-LDA achieved a value of  $0.94 \pm 0.02$ . Here, our approach notably outperformed the PCA-LDA.

Our findings underline the potential of image-based spectral data representations and highlight the adaptability of deep learning architectures in spectroscopic applications. This research offers a promising alternative for spectra, opening up the possibility of repurposing the wide field of existing image processing neural networks across diverse scientific fields.



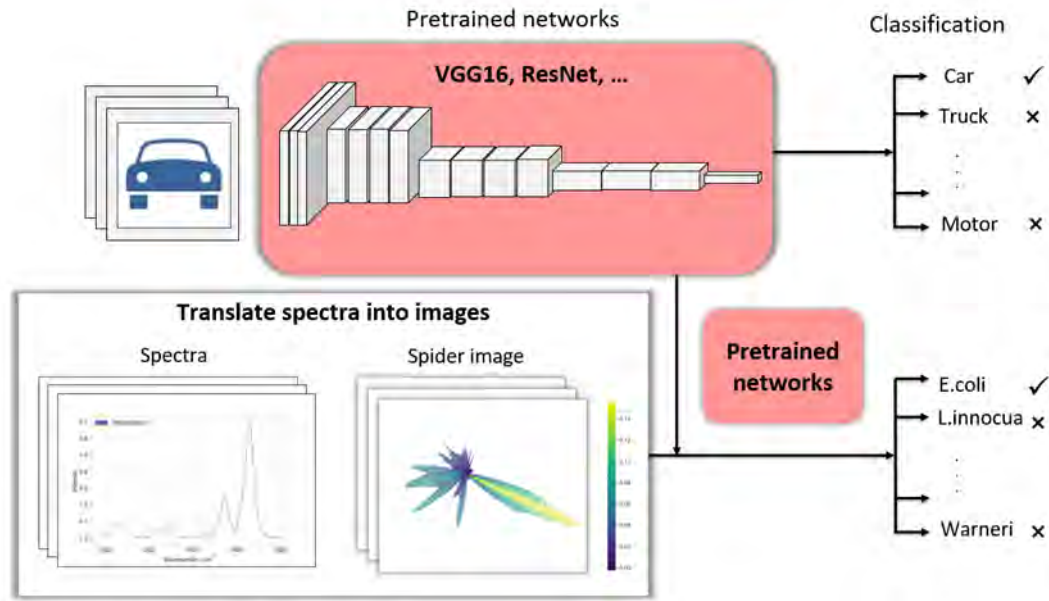


**Figure 1** Adapting pre-trained networks for spectra classification. In a basic analogy, consider various vehicles being classified using pre-trained networks: Given an image, the network can determine, for instance, that the image depicts a car. Using a similar rationale, to classify bacterial Raman data, we first transform these data into an image representation. Then, leveraging the pre-trained networks, we can identify the specific bacterial type represented by the input.

## ACKNOWLEDGMENTS

This work is supported by the BMBF, funding program Photonics Research Germany (13N15466 (LPI-BT1)) and is integrated into the Leibniz Center for Photonics in Infection Research (LPI). The LPI initiated by Leibniz-IPHT, Leibniz-HKI, Friedrich Schiller University Jena and Jena University Hospital is part of the BMBF national roadmap for research infrastructures.

## REFERENCES

- [1] Tan, Mingxing, and Quoc Le., International conference on machine learning. PMLR, 2019.
- [2] Gareau, T. P., Smith, R. G., Barbercheck, M. E., & Mortensen, J. Extension, 2010, 48(5).

# Siamese neural networks used in bacteria classification analysed by Raman Spectroscopy

Sara Mostafapour<sup>a</sup>, Jhonatan Contreras<sup>a,b</sup>, Thomas Bocklitz<sup>a,b,c</sup>

<sup>a</sup>*Institute of Physical Chemistry (IPC) and Abbe Center of Photonics (ACP), Friedrich Schiller University Jena, Helmholtzweg 4, 07743 Jena, German*

<sup>b</sup>*Leibniz Institute of Photonic Technology, Albert Einstein Straße 9, 07745 Jena, Germany*

<sup>c</sup>*Institute of Computer Science, Faculty of Mathematics, Physics & Computer Science, University Bayreuth, Universitaetsstraße 30, 95447 Bayreuth, Germany*

Pattern recognition methods can be used for identification of substances from their Raman spectrum. However, most pattern recognition methods require pre-processing of the data like cosmic ray removal, smoothing and baseline correction [1]. In contrast, it was shown that convolutional neural networks (CNNs) are successfully used in Raman spectra classification without the need for pre-processing as CNNs have inherent pre-processing abilities. A CNN without additional pre-processing showed higher classification accuracy than conventional machine learning algorithms with pre-processing. However, CNN models need large training sets and retraining to detect and classify targets not represented by the training data set, which is time-consuming and bothersome [2,3].

In comparison, a Siamese neural network (SNN) does not need retraining to work on untrained targets. This architecture consists of two CNN networks with the same structure and a final network that acts as a distance metric between the CNNs. Therefore, in a Siamese network the classification problem is converted into a similarity problem and the issue of limited available data for training is CNN is solved.

We explored this architecture on a Raman dataset including six bacterial species, cultivated in nine independent biological replicates (9 batches), totaling 5420 single bacteria spectra. Using two batches as a test set and applying a 70/30% training/validation split to the other batches, we examined the data set by PCA-LDA, CNN (2 models) and SNN (2 models). The models achieved test accuracies of 79.41%, 84.13%, 82.80%, 82.65% and 83.61% respectively. These results show that CNNs and SNNs outperform the classical method PCA-LDA and that the Siamese network performs on par with a “normal” CNN, while it offers the additional advantages mentioned above. SNNs therefore present a promising approach for spectral analysis of biological data sets.

## ACKNOWLEDGMENTS

This study is part of the Collaborative Research Centre AquaDiva of the Friedrich Schiller University Jena, funded by the Deutsche Forschungsgemeinschaft (DFG, German Research Foundation) – SFB 1076 – Project Number 218627073. This work is further supported by the BMBF, funding program Photonics Research Germany

(13N15466 (LPI-BT1-FSU)) and is integrated into the Leibniz Center for Photonics in Infection Research (LPI). The LPI initiated by Leibniz-IPHT, Leibniz-HKI, Friedrich Schiller University Jena and Jena University Hospital is part of the BMBF national roadmap for research infrastructures.

## **REFERENCES**

1. S. Guo, J. Popp, T. Bocklitz, *Nature protocols*, 2021, **16**, 5426–5459
2. R. Luo, J. Popp, T. Bocklitz, *Analytica*, 2022, **3**, 287-301
3. P. Pradhan, S. Guo, O. Ryabchykov, J. Popp, T. Bocklitz, *Journal of Biophotonics*. 2020, **13**, e201960186.

# Broadband CARS hyperspectral imaging of cells and tissues using a deep-learning NRB removal approach

Ryan Muddiman<sup>a</sup> and Bryan Hennelly<sup>a,b</sup>

<sup>a</sup> *Department of Electronic Engineering, Maynooth University, Co. Kildare, Ireland*

<sup>b</sup> *Department of Computer Science, Maynooth University, Maynooth, Co. Kildare, Ireland*

Raman hyperspectral imaging (HSI) has long been known to be capable of imaging cells using vibrational contrast from the molecular composition of the sample. While Raman HSI is frequently used for single cell phenotyping and spatio-chemical analysis, the application of this technique is time consuming, and HSI data is typically recorded at a rate of 5-10 minutes per cell [1]. The application of broadband coherent anti-Stokes Raman scattering (BCARS) circumvents slow acquisition times, with the drawback of requiring a specific treatment of the nonresonant background (NRB). We have shown that deep learning can remove the NRB and denoise single spectra simultaneously [2]. Here, we show this approach when applied to BCARS HSI datasets, permits an unsupervised and label-free chemical imaging of cells and tissues.

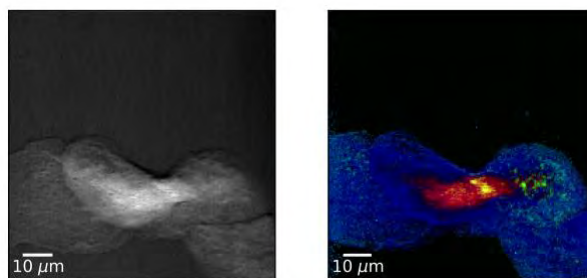


**Figure 1** BCARS image of a buccal cell on a coverslip, left: total intensity, right: cars spectrally unmixed 3-band pseudocolor.

## ACKNOWLEDGMENTS

The authors would like to acknowledge the support of Science Foundation Ireland under Grant Numbers 15/CDA/3667, 19/FFP/7025, and 16/RI/3399.

## REFERENCES

1. R. J. Swain and M. M. Stevens, *Biochem. Soc. Trans.*, 2007, 35, 544–549
2. Muddiman R, O' Dwyer K, Camp CH Jr, Hennelly B. *Anal Methods*. 2023, 15, 4032-4043

# DNA microarray-based detection of target genes in Vancomycin resistant Enterococci

**Ibukun Elizabeth Osadare<sup>1,2,3</sup>, Stefan Monecke<sup>1,2,3</sup>, Annett Reissig<sup>1,2,3</sup>, Elke Müller<sup>1,2,3</sup>, Maximilian Collatz<sup>1,2,3</sup>, Sascha Braun<sup>1,2,3</sup>, Wulf Schneider-Brachert<sup>4</sup>, Katrin Frankenfeld<sup>5</sup>, Dominik Gary<sup>5</sup>, Ralf Ehricht<sup>1,2,3</sup>**

1 Leibniz Institute of Photonic Technology (IPHT), Jena, Germany

2 Institute of Physical Chemistry, Friedrich-Schiller University, Jena, Germany

3 InfectoGnostics Research Campus, Jena, Germany

4 University Hospital Regensburg, Regensburg, Germany

5 Forschung Zentrum für Medizintechnik und Biotechnologie (fzmb) GmbH

Today, there is a continuous battle worldwide against antimicrobial resistance and alongside there is the need for methods that can adequately and quickly detect transmission chains in outbreaks. Molecular typing methods like deoxyribonucleic acid (DNA) microarray technology are, therefore, important for these purposes and just as was previously demonstrated for Staphylococci, the focus in this study is the use of the same technology in detecting resistance, virulence and other target genes in Enterococci. Bioinformatic analysis was initially performed to select target genes and to design target-specific oligonucleotide sequences. This involved the collection of high-quality annotated sequence data of Enterococcal strains, and the creation of an in-house database from which individual target genes were selected, manually analyzed and aligned. Using these oligonucleotides, microarrays were manufactured by an industrial partner. Genomic DNA from VRE strains was isolated, followed by a primer extension reaction that labelled amplicons with biotin. DNA – DNA hybridization was performed in which labelled sample DNA can bind to the specific probes immobilized on the array surface. The incorporated labels triggered a dye precipitation at those probes where hybridization occurred. This resulted in visible spots on the array and its image was analyzed for the presence or absence of target genes using a dedicated reader and software. Validation involved obtaining the genome sequence data of the strains used in the actual experiments. Probe sequences were then searched for within the genome in order to check whether the target genes were present or not. Comparison between these theoretical results and the practical data from the microarray for all experiments confirmed that this was the case, so that the system can henceforth be used for typing “unknown” strains. In conclusion; DNA microarray technology can be used to fast and economically detect resistance, virulence and other target genes in Enterococci, as well as obtain genetic signatures for typing purposes.

# Droplet microfluidics autosampler for multimodal imaging microscopy

**Fabian Ott<sup>1,2</sup>, Tobias Meyer-Zedler<sup>1,2</sup>, Jürgen Popp<sup>1,2</sup>**

<sup>1</sup>Leibniz Institute of Photonic Technology, Spectroscopy / Imaging, Jena, Germany

<sup>2</sup>Friedrich Schiller University Jena, Institute of Physical Chemistry and Abbe Center of Photonics, Jena, Germany

The further development of droplet microfluidics in the past decades has opened up a wide range of applications, covering life sciences, biomedical analysis, material sciences, biology and chemistry. However, many of these applications have a very small-time frame related to inline analysis, which makes imaging challenging.

To open the time window for multimodal imaging, we have developed an image-based feedback algorithm that allows targeted positioning of picolitre droplets in a microfluidic chip for a few seconds. The algorithm can be tailored to different chip layouts, channel width as well as droplet size.

The method of operation is as follows: The regions of interest are imaged by a monochrome camera. A threshold is applied to the grayscale images, and the generated binary images are used to detect droplet contours. The shapes, velocities and positions are extracted from the contour information. These parameters are passed to a fuzzy logic control, which calculates the input and output pressure for the pressure controller which is connected to the microfluidic chip.

Once the droplet is placed, a full range of imaging techniques can be applied. As an example, a hyperspectral snapshot image is acquired and a corrected three-dimensional data cube is generated. In the next step, the microscope switches from brightfield to confocal laser scanning mode to acquire multimodal nonlinear coherent anti-Stokes Raman scattering (CARS) and two-photon excited fluorescence (TPEF) images. The microscope returns to brightfield mode and the cycle begins again.

# Label-free differentiation of antimicrobial resistance groups using Raman spectroscopy

Aikaterini Pistiki<sup>a,b</sup>, Oleg Ryabchykov<sup>a,b</sup>, Annette Wagenhaus<sup>a,b</sup>, Thomas W Bocklitz<sup>b</sup>, Steffanie Deinhard-Emmer<sup>d</sup>, Bettina Löffler<sup>d</sup>, Petra Rösch<sup>a</sup>, Juergen Popp<sup>a,b,c</sup>

<sup>a</sup> Institute of Physical Chemistry and Abbe Center of Photonics, Friedrich Schiller University, Lessingstraße 10, 07743 Jena, Germany

<sup>b</sup> Leibniz Institute of Photonic Technology Jena, Albert-Einstein-Str. 9, 07745 Jena, Germany

<sup>c</sup> InfectoGnostics Research Campus Jena, Center of Applied Research, Jena, Germany

<sup>d</sup> Institute of Medical Microbiology, Jena University Hospital, Jena, Germany

Antimicrobial resistance (AMR) is a major medical challenge. Due to the extensive time required by routine laboratory diagnostic methods to deliver results, physicians are forced to administer empirical treatment, without any information about the pathogens AMR. Thus, a need exists for the development of fast and inexpensive clinical laboratory methods that provide physicians with strain-specific AMR-information, allowing the administer of proper antibiotic treatment shortly after infection diagnosis. Label-free Raman spectroscopy can be an important player in this field, since it provides an overall biochemical profile of the bacterial cells, including AMR-related information [1, 2].

This is the first attempt to determine bacterial resistance groups using Raman spectroscopy. Two Raman methods were tested, UV-resonance Raman spectroscopy (UVR) using 244nm excitation and Raman fiber probe directly on the culture dish using 785 nm excitation. 56 clinical isolates were analyzed, belonging to the pathogen species *Acinetobacter baumannii*, *Escherichia coli*, *Citrobacter freundii*, *Enterococcus faecium*, *Klebsiella pneumoniae* and *Klebsiella oxytoca*. In the Gram-negative isolates 3 resistance groups were tested, namely susceptible, Extended-spectrum beta-lactamases producers (ESBL) and carbapenem-resistant Enterobacterales (CRE). The *Enterococcus faecium* isolates were vancomycin susceptible (VSE) and vancomycin resistant (VRE). In the data analysis, first a classification of the species was performed, followed by classification of the resistance group in each species separately, using chemometrics methods. Further research is required to develop this method for clinical application however, these first results show that Raman spectroscopy has the potential to provide physicians with resistance-related information they would not have access to otherwise and this is done in a label-free way, without the need for expensive consumables and within 16 h after sample intake.



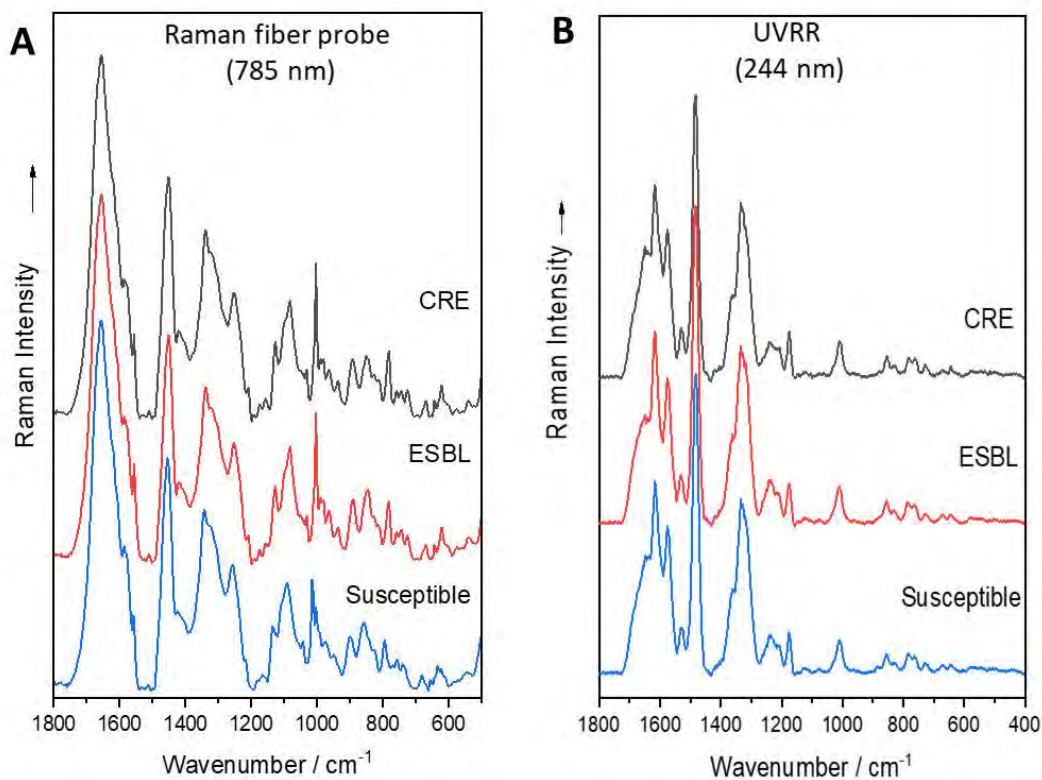


**Figure 1.** Differentiation of AMR groups using Raman spectroscopy. (A) Mean Raman spectrum *E. coli* resistance groups using Raman fiber probe method (B) Mean Raman spectrum of *Acinetobacter baumannii* resistant groups using UVRR method.

## ACKNOWLEDGMENTS

Financial support of the Federal Ministry of Education and Research, Germany (Bundesministerium für Bildung und Forschung (BMBF), Deutschland) in the project FastAlert (13GW0460B).

## References

1. A. Nakar, A. Pistiki, O. Ryabchykov, T. Bocklitz, P. Rösch and J. Popp, "Detection of multi-resistant clinical strains of *E. coli* with Raman Spectroscopy", *Anal. Bioanal. Chem.* **2022**, *414*, 1481-1492.
2. A. Pistiki, S. Monecke, H. Shen, O. Ryabchykov, T. Bocklitz, P. Rösch, R. Ehricht and J. Popp, "Comparison of different label-free Raman spectroscopy approaches for the discrimination of isogenic MRSA and MSSA clinical isolates", *Microbiol. Spectrum* **2022**, *10*, e0076322.

# Stability of the fluorescence of DNA-stabilized silver clusters

<sup>1</sup>Uwe Pliquett, <sup>1</sup>Daniel Martin, <sup>1</sup>Katharina Schieke, <sup>2</sup>Patrick Witzel, <sup>2</sup>Marina Gárdonyi, <sup>2</sup>Jürgen Meinhardt

<sup>1</sup>Institut für Bioprozess- und Analysenmesstechnik, Heilbad Heiligenstadt, Germany

<sup>2</sup>Fraunhofer Institut für Silikatforschung, Würzburg, Germany

The formation of stable silver clusters on single-stranded DNA (Ag:DNA) leads to bright fluorescence in the visible range, depending on the DNA-sequence. This fluorescence shows high sensitivity to environmental variables such as pH or the ionic composition of electrolytes. Ag:DNA clusters can usually be stored refrigerated for several weeks. However, depending on the DNA sequence, a decrease in fluorescence may occur within a few days. Here two linear structures with 28 bp and 19bp single stranded DNA were compared. A joint feature of both sequences is a cytosine-rich region where the silver atoms are stabilized.

The fluorescence at  $\lambda_{em} = 640$  nm of the 28 bp sequence, excited at  $\lambda_{ex} = 600$  nm, is significantly more stable than that of the 19 bp-DNA ( $\lambda_{em} = 685$  nm). After 3 days there is almost no drop in fluorescence of the 28 bp-DNA, but then there is a sudden loss of fluorescence up to 11% within one day. In contrast, the fluorescence of the 19 bp Ag:DNA drops by half after just 3 days. When excited with shorter wavelengths, a completely different picture emerges. When excited at  $\lambda_{ex} = 540$  nm, 28 bp shows an emission at 710 nm and at  $\lambda_{ex} = 495$  nm even 2 peaks at 585 nm and 675 nm. While the fluorescence drops by about half at  $\lambda_{ex} = 540$  nm, both peaks excited at 495 nm decline up to 70% within 4 days. For 19 bp with a peak at 590 nm (575 nm at  $\lambda_{ex} = 495$  nm), the fluorescence loss is only 30% within 4 days. During the same time, the absorption only decreased by 8% around 600 nm, but otherwise remained stable.

# Digital droplet-based microfluidic reporter assays for live cell analysis

Cornelia Reuter<sup>a</sup>, Mark Kielpinski<sup>a</sup>, Duyguhan Kozal<sup>a</sup>, Thomas Henkel<sup>a</sup>, Karina Weber<sup>a</sup>, Juergen Popp<sup>a,b,c</sup>

<sup>a</sup> Leibniz Institute of Photonic Technology, Member of Leibniz Health Technologies, Member of the Leibniz Centre for Photonics in Infection Research (LPI), Jena, Germany

<sup>b</sup> Institute of Physical Chemistry and Abbe Center of Photonics, Friedrich Schiller University Jena, Member of the Leibniz Centre for Photonics in Infection Research (LPI), Jena, Germany

<sup>c</sup> InfectoGnostics Research Campus Jena, Center for Applied Research, Jena, Germany

Droplet-based microfluidics for microbial research is emerging as ability to generate and monitor droplets inoculated with single cells or small populations of pathogenic bacteria in a highly parallel manner [1,2]. Digital, droplet-based assays minimize the assay volume and are highly sensitive [3]. This allows the identification and differentiation of rare pathogens from patient samples with a in a large microbiome (e.g., swabs from the mouth and throat).

This work presents a microfluidic chip-based implementation of digital microbial single-cell reporter assays (including pathogen-drug interaction assays) with colorimetric and fluorometric readout and absolute quantification. Due to the droplet-based assay methodology, each pathogen strain develops in its droplet independently of other droplets and its interaction with additional noxious agents can be investigated. Chromogenic or fluorogenic reporter substrates are added for growth detection. The associated enzyme and metabolic activities generate stained or fluorescence-active products and are evaluated by optical image reading and data processing. Selectivity and specificity can be variably adjusted based on the reporter substrate [4, 5]. We demonstrate a microbial digital droplet assays coupled with a robust optical setup applicable for pathogenic bacteria enumeration.

**Keywords:** Photonic interaction assays, bacterial cultivation, microfluidics

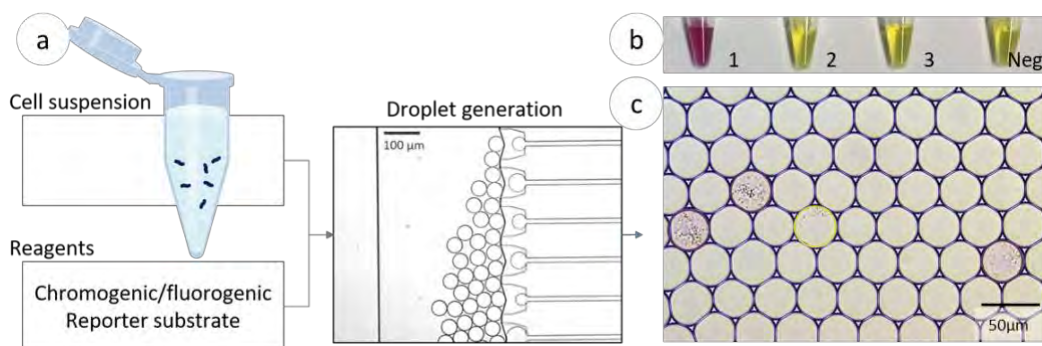


**Figure 1** Concept of the digital microbial assay a) the cells were mixed with chromogenic/fluorogenic substrate and bacteria single-cell encapsulation through the microfluidic chip is performed. b) The substrate is metabolized by specific bacteria, c) for mixed populations monoclonal growth of different bacterial species is observed and confirmed by the chromogenic reporter assays.

## ACKNOWLEDGMENTS

This work is supported by the BMBF, funding program Photonics Research Germany (FKZ: 13N15704) and is integrated into the Leibniz Center for Photonics in Infection Research (LPI). The LPI initiated by Leibniz-IPHT, Leibniz-HKI, UKJ and FSU Jena is part of the BMBF national roadmap for research infrastructures.

## REFERENCES

1. Liu D, et al. *Analyst*, 2022, **147**(11), 2294-2316.
2. Kaminski, T. S. et al. *Lab on a Chip*, 2016, **16**, 2168-2187
3. Reuter, C.; et al. *Appl. Microbiol. Biotechnol.*, 2020, **104**(1), 405–415.
4. Streett, H., et al. *Current Opinion in Biotechnology*, 2021, **71**, 151-163.
5. Goddard, J. P., & Reymond, J. L., *TRENDS in Biotechnology*, 2004. **22**(7), 363-370.

1 *Poster*

## 2 **Quantum efficiency analysis of Raman signal** 3 **enhancement by a cratered gold colloid**

4 **Iuliia Riabenko** <sup>1\*</sup>

5 <sup>1</sup> V.N. Kharkiv Karazin National University

6 \* Correspondence: jriabenko@karazin.ua;

7 **Abstract:** Investigation into the impact of gold nanoparticle morphology [1] on Raman signal  
8 enhancement was conducted through the development of a simulation using Ansys Lumerical  
9 Software. Specifically, a fixed spherical gold nanoparticle with an air cone crater was analyzed to  
10 induce a quadrupole mode within the nanoparticle.

11 The FDTD method was selected to discretize Maxwell's equations with minimal error, particularly  
12 when incorporating a PML. This method offers the convenience of selecting various wavelengths  
13 for the eigenvalues of frequencies.

14 The analysis of mode effective refractive index dispersion revealed that the propagation constant is  
15 minimal at a light wavelength of 785 nm [2] when the effective coefficient [3] approaches 0.1.  
16 Consequently, this resulted in the formation of a quadrupole mode, characterized by a radiation  
17 absorption-to-scattering ratio of approximately 0.9 by the nanoparticle. In the lower frequency  
18 range, a notable enhancement in the efficiency metric was observed [4].

19 The spatial distribution of fields in the proximity of a nanoparticle possessing a crater, under light  
20 propagation along the Z axis within the YZ plane, demonstrated field localization as a dipole [5],  
21 while a quadrupole mode manifested in the XY plane. Consequently, when estimating the electric  
22 and magnetic fields within a granule featuring a crater, consideration of quadrupole term is  
23 essential.

### 24 **References**

- 25 1. Riabenko I.; Shulga S. Permittivity Model Selection Based on Size and Quantum-Size Effects in Gold Films.  
26 *East European Journal of Physics* **2023**, *3*, 406-412,  
27 DOI 10.26565/2312-4334-2023-3-44. Available online: <https://periodicals.karazin.ua/ejpp/article/view/22154>  
28 (accessed on 04.09.2023).
- 29 2. Beloshenko K.; Shulga S. Myasthenia Gravis Diagnosis with Surface-enhanced Raman Spectroscopy. *arXiv*  
30 *preprint arXiv* **2022**, 2208.02014 DOI 10.48550/arXiv.2208.02014. Available online:  
31 <https://arxiv.org/abs/2208.02014> (accessed on 01.08.2022).
- 32 3. Riabenko I.; Shulga S. Calculation of the relative permittivity of Rhodamine 6G using the quantum  
33 mechanical method. *Biophysical Bulletin* **2023**, *50*, 7-16,  
34 DOI 10.26565/2075-3810-2023-50-01. Available online:  
35 <https://periodicals.karazin.ua/biophysvisnyk/article/view/22030> (accessed on 19.12.2023).
- 36 4. Riabenko I., Detection of traces of biotoxins using Raman spectroscopy. PhD thesis, V.N. Kharkiv Karazin  
37 National University, Kharkiv, Ukraine, February 8, 2024.
- 38 5. Beloshenko M.; Makarovskiy I. Resonance light absorption of granular aluminium and silver films placed  
39 on a rough sublayer of multilayered ZnS. *Ukrainian journal of physical optics* **2019**, *20*, 10-15,  
40 DOI 10.3116/16091833/20/1/10/2019. Available online: [http://nbuv.gov.ua/UJRN/UJPO\\_2019\\_20\\_1\\_4](http://nbuv.gov.ua/UJRN/UJPO_2019_20_1_4)  
41 (accessed on 30.06.2019).

# Biomedical Applications of Metabolic Two-Photon Excited Fluorescence Lifetime Microscopy.

Marko Rodewald<sup>a,b</sup>, Stella Greiner<sup>a</sup>, Tobias Meyer-Zedler<sup>a,b</sup>, Michael Schmitt<sup>a</sup>, Ute Neugebauer<sup>a,b</sup>, Orlando Guntinas-Lichius<sup>c</sup>, Franziska Hornung<sup>d</sup>, Bettina Löffler<sup>d</sup>, Stefanie Deinhardt-Emmer<sup>d</sup>, Juergen Popp<sup>a,b</sup>

<sup>a</sup> Institute of Physical Chemistry and Abbe Center of Photonics, FSU Jena, Germany

<sup>b</sup> Leibniz Institute of Photonic Technology (IPHT), Member of Leibniz Health Technologies, Member of the Leibniz Centre for Photonics in Infection Research (LPI), Jena, Germany

<sup>c</sup> Department of Otorhinolaryngology, Jena University Hospital, Jena, Germany

<sup>d</sup> Institute of Medical Microbiology, FSU Jena, Germany

Fluorescence lifetime imaging microscopy (FLIM) is a powerful tool for visualizing minute changes in the chemical makeup of biological samples in a spatially resolved manner. While most fluorophores show only minor changes in their emission spectra as a response to differences in their chemical environment, their lifetimes typically react much more sensitively. Furthermore, spectrally overlapping species can be separated and quantified using the additional informational dimension. Combining these general aspects of FLIM with a two-photon excitation scheme has proven to be particularly beneficial as it provides larger penetration depth, less out-of-focus bleaching, intrinsic z-resolution, and no overlap of excitation light with the fluorophores' emission. Additionally, the necessary hardware allows the easy implementation of complimentary multi-photon imaging techniques such as second harmonic generation. Here, we present three applications of this concept from the field of biomedicine: (1) detection of tumor tissue in head and neck cancer samples, (2) sepsis characterization in mouse kidney tissue, and (3) characterization of the host response to influenza infection in lung tissue. These applications rely on the autofluorescence of NADH and FAD, two important molecules in the energy metabolism of cells. Their lifetimes, relative concentrations, the amounts found in free and protein-bound forms – differentiable only by the respective lifetimes – and spatial distributions are considered important markers for the state of a tissue and subject to change upon disease. Recording these data has been coined 'metabolic imaging' and holds great promises for disease detection.

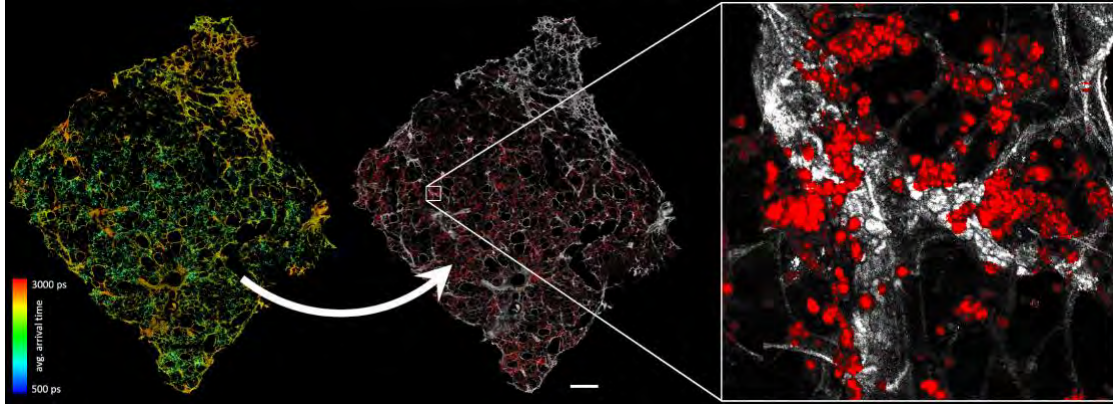


**Figure 1** Immune cells in human lung tissue, identified by FLIM. Scale bar: 1 mm.

## ACKNOWLEDGMENTS

The work presented has received funding by the BMBF, funding program Photonics Research Germany (FKZ: 13N15464.) and is integrated into the Leibniz Center for Photonics in Infection Research (LPI). The LPI initiated by Leibniz-IPHT, Leibniz-HKI, UKJ and FSU Jena is part of the BMBF national roadmap for research infrastructures.



# Raman spectroscopic analysis of aerobic *Bacillus* and anaerobic *Clostridium* species

Markus Salbreiter<sup>1,2</sup>, Annette Wagenhaus<sup>1,2</sup>, Petra Rösch<sup>1,2</sup> Jürgen Popp<sup>1,2,3</sup>  
([markus.salbreiter@uni-jena.de](mailto:markus.salbreiter@uni-jena.de))

<sup>1</sup> Institute of Physical Chemistry and Abbe Center of Photonics, Friedrich Schiller University, Jena, Germany

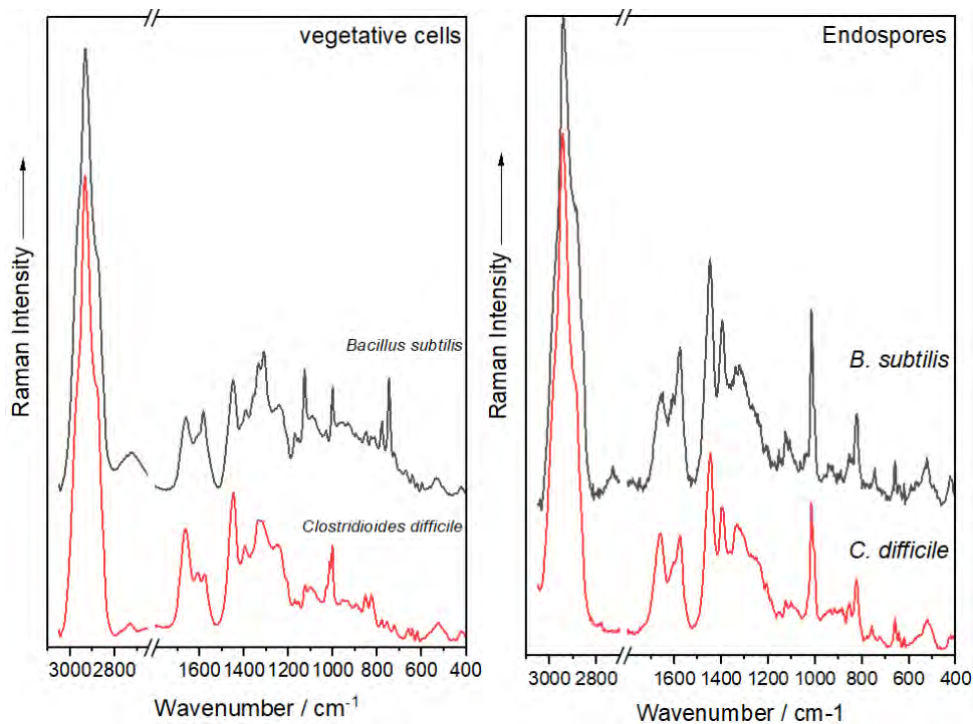
<sup>2</sup> InfectoGnostics Research Campus Jena, Center of Applied Research, Jena, Germany

<sup>3</sup> Leibniz Institute of Photonic Technology, Member of Leibniz Health Technologies, Jena, Germany

## Abstract

Aerobic *Bacillus* and anaerobic *Clostridium* species are Gram-positive bacteria that are found all over the world. Because they produce endospores, they may survive in the environment for prolonged periods of time[1]. Many *Bacillus* species and genera are not human pathogens in general, however there are a few exceptions: Anthrax is caused by *B. anthracis*, whereas food poisoning is caused by *B. cereus*. In contrast, the genus *Clostridium* is extremely diverse, with *C. tetani* (tetanus), *C. botulinum* (botulism), *C. perfringens* (gas gangrene), and *C. difficile* (antibiotic-associated diarrhoea and pseudomembranous colitis) all causing toxin-mediated illnesses[1,2].

Rapid and reliable detection methods for pathogenic *Clostridium* species are currently critical in the medical industry, and fresh ways must be studied and developed. Raman spectroscopy is an analytical method that can capture the target's vibrational information in form of a spectrum, which enables for the characterisation and identification of the microorganism[3,4]. This method is then applied to classify *Bacillus* and *Clostridium* species based on phylogenetic relatedness, growth conditions, and capacity to create endospores. The study's purpose was to amass a huge library of Raman spectra from vegetative cells and endospores of pathogenic and non-pathogenic *Bacillus* and *Clostridium* species.



## Acknowledgments

Financial support of the Federal Ministry of Education and Research, Germany (Bundesministerium für Bildung und Forschung (BMBF), Deutschland) in the project FastAlert (13GW0460B).

## References

1. Madigan, M.T.; Bender, K.S.; Buckley, D.H.; Sattley, W.M.; Stahl, D.A. *Brock Biology of Microorganisms*; Pearson Education Limited 2022: 2020.
2. Riedel, S.; Hobden, J.A.; Miller, S.; Morse, S.A.; Mietzner, T.A.; Detrick, B.; Mitchell, T.G.; Sakanari, J.A.; Hotez, P.; Mejia, R. In *Jawetz, Melnick, & Adelberg's Medical Microbiology, 28e*; McGraw-Hill Education: New York, NY, 2019.
3. Pistiki, A.; Salbreiter, M.; Sultan, S.; Rösch, P.; Popp, J. Application of Raman spectroscopy in the hospital environment. *Translational Biophotonics* **2022**, *n/a*, e202200011, doi:<https://doi.org/10.1002/tbio.202200011>.
4. Salbreiter, M.; Pistiki, A.; Cialla-May, D.; Rösch, P.; Popp, J. Raman Spectroscopy for Infection Diagnosis. In *Raman Spectroscopy in Human Health and Biomedicine*; pp. 337-410.

# A Deep Learning approach for detecting single division events of bacteria in microfluidic droplets imaged by angle-resolved scattered light imaging

Arjun Sarkar<sup>1,2</sup>, Carl-Magnus Svensson<sup>1</sup>, Martina Graf<sup>2,3</sup>, Anne-Sophie Munser<sup>4</sup>, Marc Thilo Figge<sup>1,2</sup>, Miriam A. Rosenbaum<sup>2,3</sup>

<sup>1</sup> *Applied Systems Biology, Leibniz Institute for Natural Product Research, and Infection Biology – Hans-Knöll-Institute, Jena, Germany*

<sup>2</sup> *Friedrich Schiller University, Jena, Germany*

<sup>3</sup> *Bio Pilot Plant, Leibniz Institute for Natural Product Research, and Infection Biology – Hans-Knöll-Institute, Jena, Germany*

<sup>4</sup> *Fraunhofer Institute for Applied Optics and Precision Engineering IOF, Jena, Germany*

Angle-Resolved Scattered (ARS) light imaging gives fast and highly resolved information about structures and objects that otherwise would only be visible by very specific microscopy techniques. We employ ARS to picoliter-sized droplets in flow to detect cell growth on a single-cell level. This approach allows for detailed information about the content of the droplets where we can screen thousands of droplets each hour.

To interpret and decode the information in the droplets, we extract features from the complex scatter light images using a pre-trained Convolutional Neural Network (CNN) called EfficientNet [1] and then employ various unsupervised and supervised deep learning methods. These models help us realize the fastest exposure time that can be used for imaging without hindering the overall classification accuracy. We demonstrate the efficiency of the model by performing microbial growth experiments and fast antibiotic susceptibility testing.

Current phenotypic methods need high cell densities resulting in relatively long incubation times of 24 hours. Newer and faster approaches mainly rely on genotypic predictions, which are not guaranteed to represent the true antibiotic resistance of a sample. With our method, employing deep learning-based regression models, we can detect cell growth on a few-cell level after a short incubation period. A few cell divisions are already enough to detect growth or growth inhibition [2] and in the droplet-based system this occurs in a matter of hours. In the future, we intend to increase the multiplexing of the system by coupling it to a fluorescence detector, which allows us to code different experimental conditions using fluorescence.

## Detection of different cell concentrations with the scattered light sensor

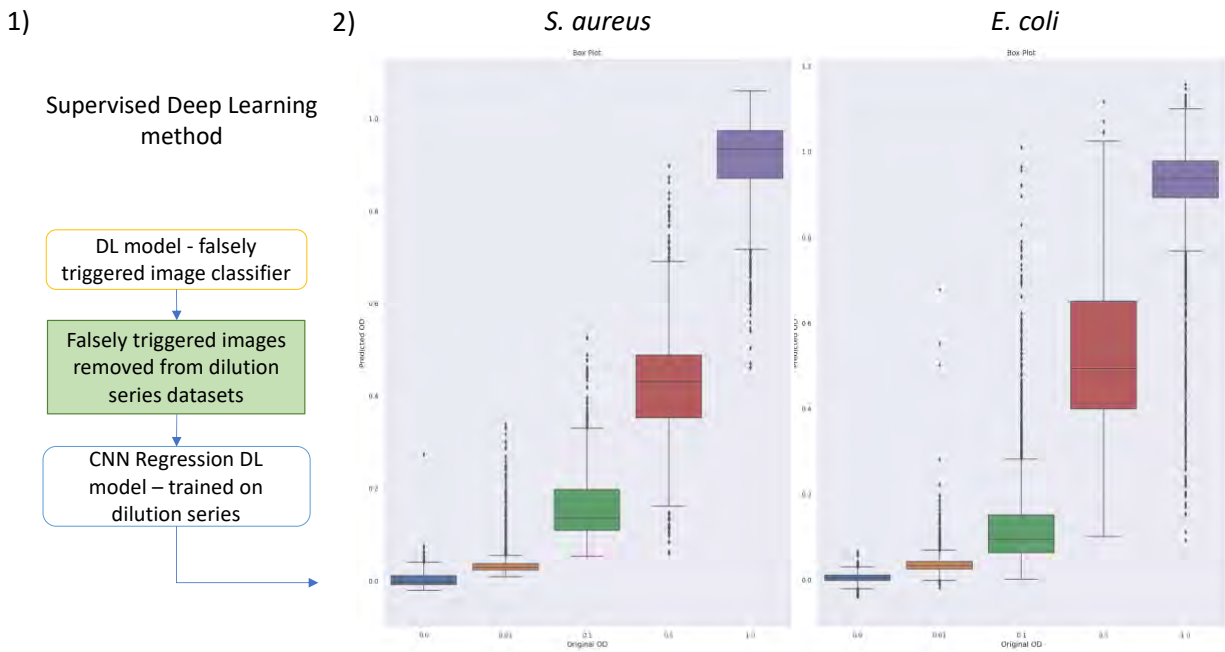


**Figure 1:** 1) Overview of the analysis steps of ARS images. 2) Predicted OD (Optical Density) distributions versus actual mean ODs of 5 different droplet populations with *S. aureus*/*E. coli* cells.

### Growth detection of *S. aureus* cells

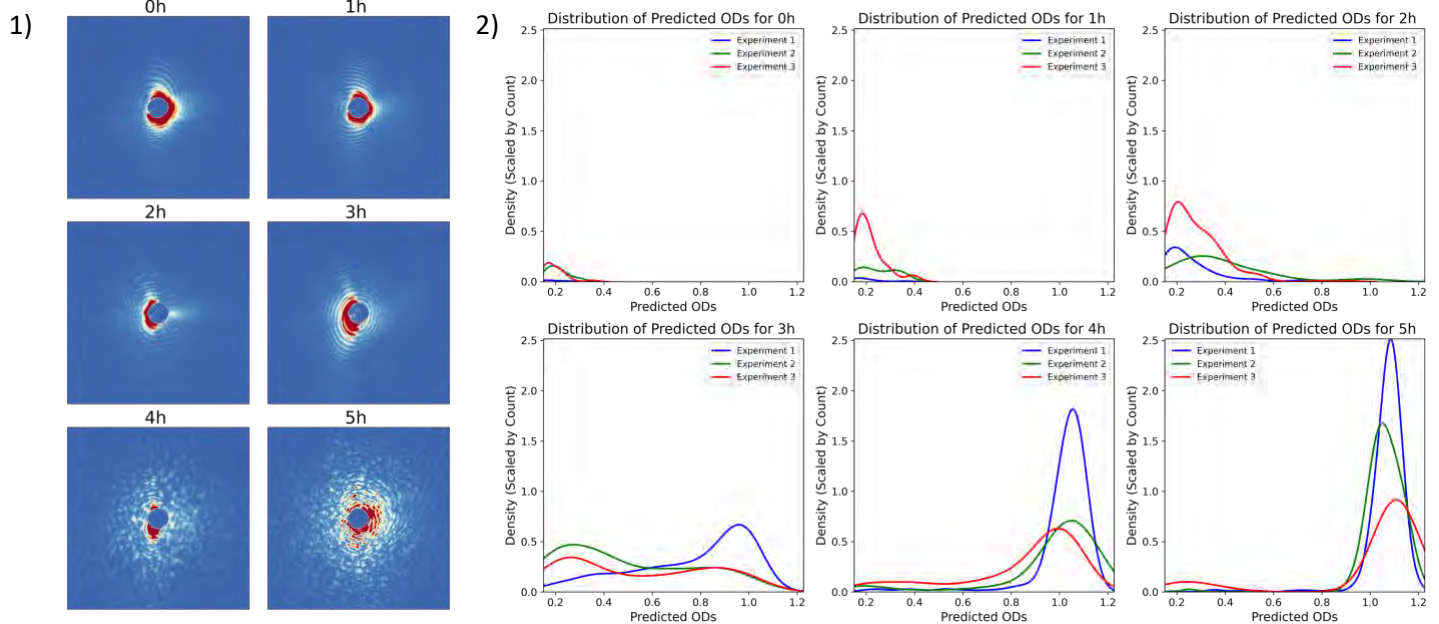


**Figure 2:** 1) Exemplary images of growth experiment of *S. aureus* over 5 h. Starting OD = 0.003 (1 cell per droplet 90 % empty). Droplets were incubated at 37 °C. 2) Predicted ODs above detection threshold (0.15) at every timepoint across 3 different experiments.

## References

1. Tan, W. & Le, Q.V. (2019) EfficientNet: Rethinking Model Scaling for Convolutional Neural Networks. [arxiv.org/abs/1905.11946](https://arxiv.org/abs/1905.11946)
2. Wohlfeil, S., et al. (2019) Optical fiber-based light scattering detection in microfluidic droplets. 41. [10.1117/12.2509248](https://doi.org/10.1117/12.2509248)

# Exploring the wavenumber silent region for biological issues

Constanze Schultz<sup>a</sup>, Tobias Meyer-Zedler<sup>a,b</sup>, Michael Schmitt<sup>b</sup>, Juergen Popp<sup>a,b</sup>

<sup>a</sup> *Leibniz-Institute of Photonic Technology, Member of Leibniz Health Technologies, Member of the Leibniz-Center for Photonics in Infection Research (LPI), Jena, Germany*

<sup>b</sup> *Institute of Physical Chemistry and Abbe Center of Photonics, Friedrich Schiller University Jena, Member of the Leibniz-Center for Photonics in Infection Research (LPI), Jena, Germany*

Many biological processes are essentially influenced by small molecules of less than  $1000 \text{ g mol}^{-1}$ . The elucidation of mechanistic core steps or the discovery of anomalies within a biological process of interest not only involves the identification of such small molecules but also the determination of their distribution pattern, metabolization, and organism interplay. Thus, a selective and non-destructive identification of small molecular targets within diverse and complex biological environments is crucial and poses several requirements on imaging techniques that can be met using vibrational Raman spectroscopy combined with a smart tag concept (Figure 1).

Triple bond and deuterium markers are particularly well suited as vibrational labels because they feature bands in the otherwise wavenumber silent region of the spectrum. As a consequence, rapid on-site evaluation is possible and drastically reduces the required post-processing cost and time. Incorporation strategies of vibrational tags into biomolecules under study are diverse. They range from intrinsic label-free approaches<sup>1,2</sup> to artificial and individually tunable labels for e.g. multiplexing experiments and few-molecule detection schemes.

We here present the application of triple bond and deuterium labels as vibrational tags in linear and coherent nonlinear Raman spectroscopy for biological needs. Despite Raman scattering itself being an insensitive process, the application of tagged molecules in biologically acceptable concentrations of the low three-figure micromolar range succeeds for real biological systems due to the accumulation at certain positions, e.g., in lipid droplets, nuclei, or membranes. Coherent nonlinear vibrational techniques, such as narrow- and broadband coherent anti-Stokes Raman spectroscopy (CARS), and stimulated Raman scattering (SRS), can additionally overcome some of the well-known obstacles of spontaneous Raman imaging, eventually enabling time-resolved or large-area screenings.

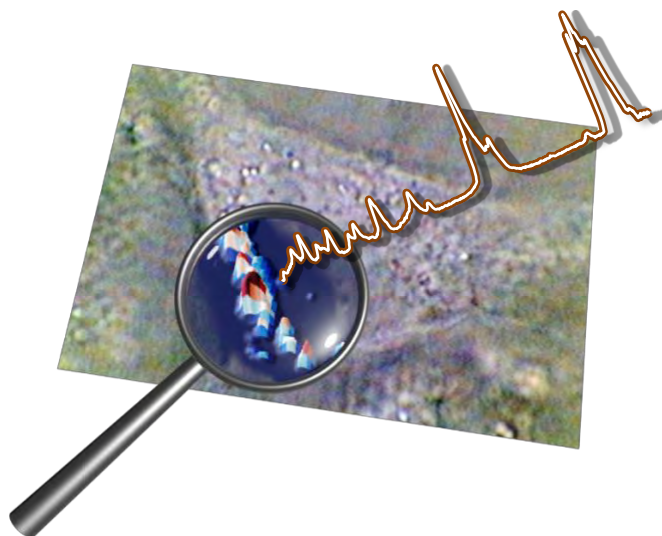


**Figure 1** Graphical abstract of the presented work. Artistic representation of the detection of a vibrationally-tagged fatty acid inside a macrophage cell by Raman spectroscopic techniques.

## ACKNOWLEDGMENTS

This work was supported by the Leibniz ScienceCampus InfectoOptics Jena, which is financed by the funding line Strategic Networking of the Leibniz Association and by the European Union's Horizon 2020 research and innovation program under grant agreement No. 101016923 (CRIMSON). Funding from the Deutsche Forschungsgemeinschaft (DFG, German Research Foundation) within the Collaborative Research Center SFB 1127 ChemBioSys - Project-ID 239748522) and under Germany's Excellence Strategy - EXC 2051 - Project-ID 390713860 is gratefully acknowledged.

## REFERENCES

1. V. Hotter, D. Zopf, HJ. Kim et al., *Proc. Natl Acad. Sci USA* **2021**, *118*(33), 1-9.
2. B. Dose, T. Thongkongkaew, D. Zopf, HJ. Kim et al., *Chem Bio Chem* **2021**, *22*, 2901.



# Liquid crystal tunable filter and imaging-based localized surface plasmon resonance spectrometry utilizing DNA-based recognition elements

Florian Seier<sup>a</sup>, André Heewig<sup>a</sup>, Manal Al-Maoush<sup>a</sup>, Andrea Csáki<sup>a</sup>,  
Wolfgang Fritzsche<sup>a</sup>

<sup>a</sup> Leibniz Institute of Photonic Technology, Albert-Einstein-Straße 9, 07745 Jena. Germany

Humanity is facing severe dangers caused by wide diversity of pathogenic organisms such as viruses and bacteria. These organisms are capable of rapid mutations, potentially leading to the development of resistances against commonly used treatment methods. Therefore, it is of utmost importance to be able to identify these resistances as fast as possible in order to properly treat infections <sup>[1]</sup>. In addition to speed, the sensitivity, the adaptability, the cost, and ease of use are other important qualities <sup>[2,3]</sup>. Localized surface plasmon resonance (LSPR) spectroscopy is a promising tool, utilizing incident light exciting the free electrons of noble metal nanoparticles and causes them collectively oscillate. This oscillation leads to strong absorption and scattering of the incident light at a certain frequency. The absorbed wavelength is strongly dependent on the local refractive index of the surroundings <sup>[3,4]</sup>. However, nanoparticles on their own show no specificity, thus a recognition element is needed. DNA has the capability to specifically detect many different target molecules in the form of single stranded DNA by hybridizing the target <sup>[1]</sup> or by forming aptamers to catch <sup>[2]</sup>. To be able to test for many different targets at the same time, plasmonic microarrays pose a suitable sensor type. For the optical readout an image-based approach incorporating a camera and a liquid-crystal-tunable-filter (LCTF), allowing to create a stack of images taken at different wavelengths set by the LCTF, were developed <sup>[5]</sup>. By fitting the gray values of the nanoparticle spots inside the image stack and tracking the wavelength of the center of mass over time binding events to the nanoparticle's recognition element can be observed and the presence or absence of the target can be confirmed.



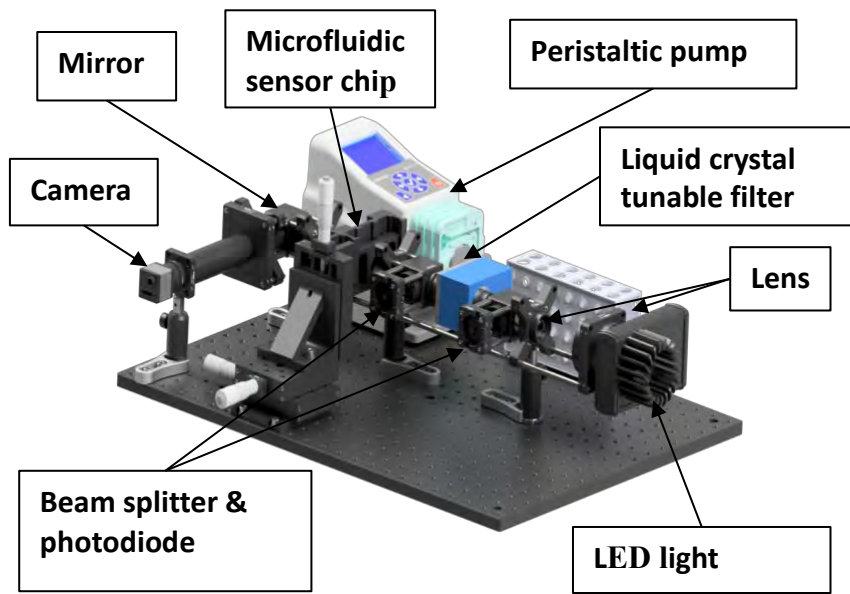


Figure 1: 3D render of an imaging-base localized surface plasmon resonance spectrometry setup with liquid crystal tunable filter for measuring plasmonic nanoarrays, by André Heewig.

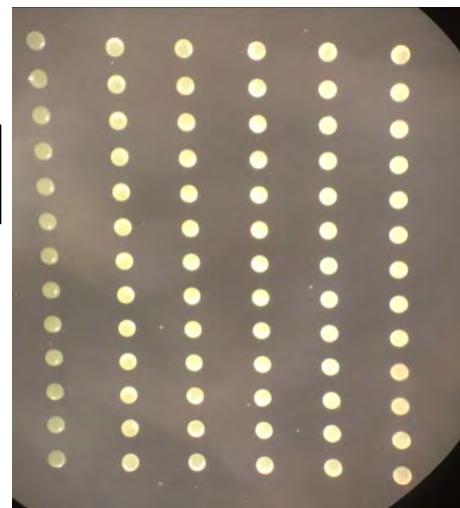


Figure 2: Plasmonic microarray with 80 nm Au-spheres with 80x, 160x, 240x, 320x, 400x, and 480x concentrated particles (left to right).

## REFERENCES

- [1] Kastner, Stephan, et al. *Small* 19 (2023)
- [2] Galhano, Beatriz SP, et al. *Microorganisms* 9.5 (2021): 923
- [3] Zopf, David, et al. *ACS Sensors* 4.2 (2019): 335-343
- [4] Soares, Leonor, et al. *Analyst* 139.19 (2014): 4964-4973
- [5] Pittner, Angelina, et al. *Analytical and Bioanalytical Chemistry* 411 (2019): 1537-1547

# Development and Application of a High-Throughput Raman Spectroscopy System for Rapid Detection and Characterization of Microplastics

Shiwani Shiwani<sup>a</sup>, Jürgen Popp<sup>a,b</sup>, Christoph Krafft<sup>a</sup> and Iwan W. Schie<sup>a,c</sup>

<sup>a</sup>*Leibniz Institute of Photonic Technology, Albert-Einstein-Straße 9, 07745 Jena, Germany*

<sup>b</sup>*Institute of Physical Chemistry and Abbe Centre of Photonics, Friedrich Schiller University Jena, Helmholtzweg 4, 07743 Jena*

<sup>c</sup>*Department for Medical Engineering and Biotechnology, University of Applied Sciences–Jena, Carl-Zeiss-Promenade 2, 07745 Jena, Germany*

The degradation of plastics over time, through chemical and biological processes, results in the release of microplastics (MPs), which are tiny plastic fragments up to 5 mm in size [1]. These particles are particularly concerning because of their persistence in the environment and their ability to accumulate in human bodies.

MPs have been detected in various everyday items, including our food supply [2], drinking water [3], and the air we breathe [4], making ingestion and inhalation primary pathways for human exposure. Human biomonitoring studies have found MPs in human tissues such as lungs [5], blood [6] and breastmilk [7]. The accumulation of MPs in the body is linked to potential adverse health effects, with evidence pointing to possible impairment of the cardiovascular [6], digestive [8], and respiratory systems [4]. Additionally, the risk posed by MPs is not only a matter of their presence but also their characteristics, including size, concentration, shape, and surface charge, as well as their ability to attract and carry other harmful organic and inorganic substances [9]. Given their ubiquity, there is an urgent need for efficient analytical techniques for the identification of MPs.

Addressing this, we have developed a high-throughput Raman system (HTS-RS) for rapidly assessing the presence and types of microplastics, even at low concentrations, on various substrates. By optimizing the optical design parameters, we were able to maximize information throughput while maintaining the highest possible optical resolution. This has resulted in a system with a large field-of-view, while maintaining high spatial resolution, enabling quick MP detection and proving particularly beneficial for samples with low MP density, such as present in biological samples. The implementation of our system is illustrated in Figure 1, which depicts a schematic of the HTS-RS setup. The system is designed to quickly capture high-resolution images with a size of 3.2x2.2 mm<sup>2</sup> at approximately 2 μm spatial resolution, facilitating the rapid detection of MPs. Our system can handle different types, shapes, and size of microplastics, bridging micro and macro-level, by integrating several automatic detection techniques. Figure 1 provides an example of the system's capabilities, presenting the spectra of different microplastic particles detected on a substrate. For

particle measurement, we used an acquisition time of 0.5 s Raman scan time per particle. An inset showcases an image of the filter substrate with MPs on it.

Our approach offers a repeatable and time-efficient strategy for the detailed morphological and chemical characterization of microplastics, enabling their quick detection and identification.

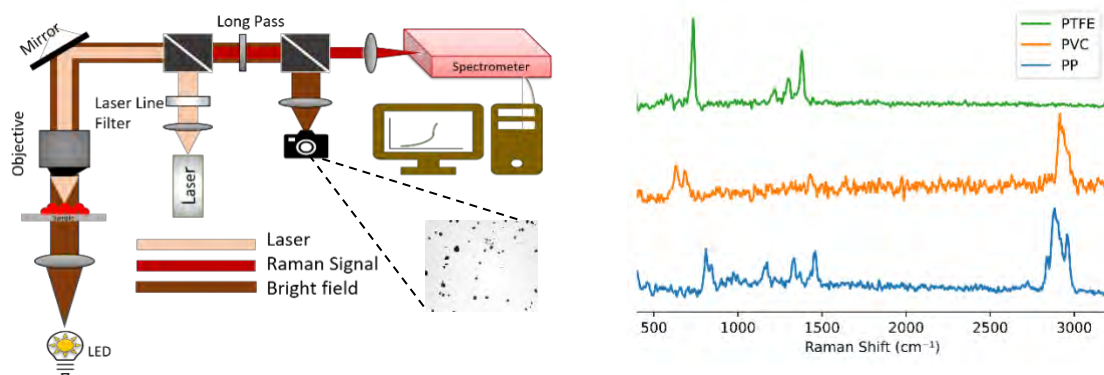


**Figure 1** Schematic of HTS-RS system for MP detection. Inset shows CaF<sub>2</sub> slide with MPs. Raman spectra of detected MPs is shown on the right side.

## ACKNOWLEDGMENTS

This project has received funding from the European Union's Horizon 2020 research and innovation program under the Marie Skłodowska-Curie grant agreement No 860775.

## REFERENCES

1. Wright SL, Thompson RC, Galloway TS. *Environ Pollut.* 2013;178:483-92.
2. Farrell P, Nelson K. *Environ Pollut.* 2013;177:1.
3. Dalmau-Soler J, Ballesteros-Cano R, Ferrer N, Boleda MR, Lacorte S. *Water Environ J.* 2021;36:292-298.
4. Gasperi J, Wright SL, Dris R, Collard F, Mandin C. *Curr Opin Environ Sci Health.* 2018;1:1-5.
5. Jenner LC, Rotchell JM, Bennett RT, Cowen M, Tentzeris V, Sadofsky LR. *Sci Total Environ.* 2022;831:154907.
6. Leslie HA, van Velzen MJM, Brandsma SH, Vethaak AD, Garcia-Vallejo JJ, Lamoree MH. *Environ Int.* 2022;163:107199.
7. Ragusa A, Notarstefano V, Svelato A, Belloni A, Gioacchini G, Blondeel C, Zucchelli E, De Luca C, D'Avino S, Gulotta A. *Polymers.* 2022;14:2700.
8. Banerjee A, Shelver WL. *Sci Total Environ.* 2021;755(Pt 2):142518.
9. Xu K. *BMC Genomics.* 2022;23:203.

## Evaluation of 3D light sheet microscopy for visualization of corneal morphological changes and qualitative assessment of the entire eye.

Axel Stoecker<sup>1</sup>, Diana Pinkert-Leetsch<sup>2</sup>, Timea Koch<sup>3</sup>, Roland Ackermann<sup>3</sup>, Stefan Nolte<sup>3,4</sup>, Christian van Oterendorp<sup>5</sup>, Jeannine Missbach-Guentner<sup>2</sup>, Christoph Russmann<sup>1,6</sup>

<sup>1</sup>University of Applied Science and Arts, Faculty of Engineering and Health, 37085 Goettingen, Germany

<sup>2</sup>Department of Diagnostic and Interventional Radiology, University Medical Center; 37075 Goettingen, Germany

<sup>3</sup>Institute of Applied Physics, Abbe Center of Photonics, Friedrich-Schiller-University, 07745 Jena, Germany

<sup>4</sup>Fraunhofer Institute for Applied Optics and Precision Engineering IOF Jena, 07745 Jena, Germany

<sup>5</sup>Department of Ophthalmology, University Medical Center, 37075 Goettingen, Germany

<sup>6</sup>Molecular-Biomarkers-Nanoimaging Laboratory (MBNI), Brigham & Women's Hospital/Harvard Medical School/Boston/MA/USA

To study rigidity-related diseases such as keratoconus, it is necessary to comprehensively visualize the complex morphologic changes in their entire anatomic context. The aim of this study is to utilize 3D light sheet fluorescence microscopy (LSFM) to visualize whole, unlabeled porcine eyeballs and corneal tissue samples in three dimensions, discerning whether alterations in corneal stiffness can be represented qualitatively with this technique.

The collagen autofluorescence signals [1] within the unlabeled and undestroyed porcine eyeball facilitated the clear identification of the 2D and 3D anatomy of the entire eye. Furthermore, different techniques were applied to corneal tissue samples in order to induce collagen cross-linking. The degree of cross-linking was measured by induced autofluorescence [2], since cross-linking and stiffening within the collagen matrix occur via Schiff bases between individual molecules [3]. After LSFM scans, the altered corneal stiffening was depicted due to specific changes in autofluorescence signals of the corneal stroma. Conventional histology confirmed the identified anatomical features and morphological alterations of the cornea. LSFM analysis of porcine whole eye and corneal tissue samples enables label-free 3D evaluation of overall morphology, anatomical relationships and tissue composition due to their autofluorescence properties. Therefore, it provides the technical foundation for comprehensive analyses of pathologically altered cornea, thus facilitating ophthalmologic studies of corneal diseases relying on modified tissue stiffness, with significant potential for clinical translation.

References

- [1] H. L. Zhao, C. P. Zhang, H. Zhu, Y. F. Jiang, and X. B. Fu, *Skin Res Technol* **23**, 588–592 (2017).
- [2] U. Leischner, A. Schierloh, W. Zieglgänsberger, and H.-U. Dodt, *PLoS One* **5**, e10391 (2010).
- [3] A. L. Kwansa, R. de Vita, and J. W. Freeman, *Matrix Biol* **34**, 161–169 (2014).

# Characterization of the interaction of SARS-CoV-2 viruses and ACE2 receptor using surface plasmon resonance

**Astrid Tannert<sup>1,2</sup>, Franziska Hornung<sup>3</sup>, Gina Sophie Merkel<sup>1</sup>, Magdalena Čapková<sup>4</sup>, Sandor Nietzsche<sup>5</sup>, Jiří Homola<sup>4</sup>, Stefanie Deinhardt-Emmer<sup>3</sup>, Ute Neugebauer<sup>1,2</sup>**

<sup>1</sup> Leibniz Institute of Photonic Technology (Member of Leibniz Health Technologies, Member of the Leibniz Center for Photonics in Infection Research, LPI), Jena, Germany

<sup>2</sup> Jena University Hospital, Center for Sepsis Control and Care and Department of Anesthesiology and Intensive Care Medicine, Jena, Germany

<sup>3</sup> Jena University Hospital, Medical Microbiology, Jena, Germany

<sup>4</sup> UFE Institute of Photonics and Electronics, The Czech Academy of Sciences, Prague, Czech Republic

<sup>5</sup> Jena University Hospital, Electron Microscopy Centre, Jena, Germany

Viral infections present substantial global threats to human health, exemplified by the recent SARS-CoV-2 pandemic. A comprehensive understanding of virus interactions with host cell receptors is pivotal for unraveling the mechanisms of viral entry, a critical step in the infection process. This knowledge is essential for the development of targeted therapeutic strategies, including novel viral inhibitors. Surface plasmon resonance (SPR) biosensors emerge as a potent tool in this endeavor, providing real-time and high-sensitivity analysis of molecular binding events.

In this study, we introduce an SPR assay designed to characterize the binding of SARS-CoV-2 viruses, including the Omicron and Delta variants, to the human ACE2 receptor. To achieve this, SPR gold substrates were initially functionalized to bind biotinylated ACE2 receptors, utilizing the specific streptavidin-biotin interaction. Non-specific binding interactions on the ACE2 receptor or subjacent layers were studied and minimized. Binding curves of different viruses were analyzed using a six-channel SPR system, revealing variations in binding efficiency between SARS-CoV-2 variants (Omicron and Delta) and influenza A viruses. Successful visualization of virus binding on the SPR surface was further confirmed through electron microscopy post-measurements.

Acknowledgement:

This work is supported by the BMBF, funding program Photonics Research Germany (FKZ: LPI-BT4 Leibniz-IPHT13N15713, and SARS-CoV-2Dx, FKZ: 13N15745) and is integrated into the Leibniz Center for Photonics in Infection Research (LPI).



# Parameters Influencing Metabolic Imaging of White Blood Cells

Astrid Tannert<sup>a,b</sup>, Max Naumann<sup>a</sup>, Simone Eiserloh<sup>a,b</sup>, Ute Neugebauer<sup>a,b</sup>

<sup>a</sup> *Leibniz-Institute of Photonic Technology, Albert-Einstein-Straße 9, Jena, Germany*

<sup>b</sup> *Center for Sepsis Control and Care, Jena University Hospital, Am Klinikum 1, Jena, Germany*

The energy metabolic state is a parameter that can yield information on pathological alterations of cells and tissues. While in a healthy environment the oxidative phosphorylation is more prominent, the metabolism can shift towards glycolysis due to hypoxia and insufficient mitochondrial capacity in various pathological conditions, like cancer and infection. Nicotinamide adenine dinucleotide (NADH) acts as the main coenzyme for electron transport in cellular metabolism and together with Flavin adenine dinucleotide (FADH<sub>2</sub>) it reflects the oxidation state of the whole metabolism.

Fluorescence lifetime imaging microscopy (FLIM) of the autofluorescent forms of the electron transporters, the reduced NADH and the oxidized FAD is a sensitive tool to monitor the metabolic state of cells and tissues. During oxidative phosphorylation, the unbound NAD exists mainly in its non-fluorescent oxidized form NAD<sup>+</sup>, and the measured fluorescence life time is dominated by protein bound NADH with life times around 2500 ps. In glycolysis, the reduced form of unbound NADH with shorter lifetimes of about 400 ps predominates, resulting in overall shorter mean fluorescence lifetimes (Schaefer et al 2021). The opposite behavior exists for FAD. Here, the protein-bound form shows shorter while the free form shows longer fluorescence lifetimes.

Changes in the energy metabolism of the body under various pathophysiological conditions can be detected directly by FLIM of NADH and FAD measured on white blood cells. However, these measurements are time consuming and not always possible immediately after sample retrieval. During storage and measurement duration the metabolic state of these cells might change. Therefore, we evaluated how the NADH/FAD fluorescence lifetime is influenced by different media composition as well as by freezing the sample and thawing it after storage. While the presence of FCS in the measurement medium seems to have only minor effects on the measured metabolic state, freezing and thawing the sample seems to shift the fluorescence lifetime of NADH in some cells to shorter values indicating increased glycolysis (see figure 1). This is probably due to damage during freezing/thawing. We conclude that frozen/thawed samples still reflect differences between individual samples when samples have been prepared in the same way. However, one should be careful about directly comparing values obtained from fresh samples to that of frozen/thawed samples.

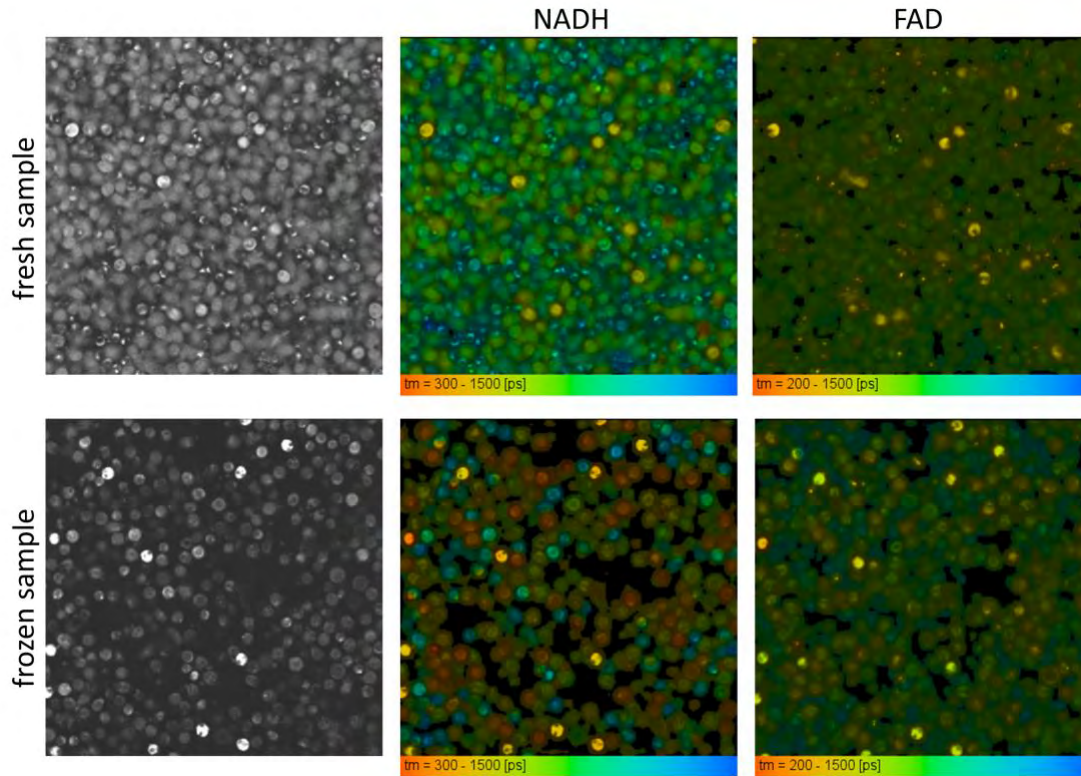


**Figure 1** Comparison of mean NADH and FAD fluorescence lifetime of a white blood cells directly after isolation and after freezing, storage at  $-80^{\circ}\text{C}$  and thawing. The intensity image reflects the intensity value for NADH. Both samples were measured using a 25x NA 1.1 oil immersion objective at room temperature in RPMI cell culture medium. Excitation was achieved using a pulsed (80 MHz) Ti:Sa laser (Chameleon, Coherent) and FLIM was detection was done using TCSPC controlled via SPCImage (Becker&Hickl). NADH was excited at 790 nm and detected using a 460/50 BP filter and FAD was excited and 890 nm and detected through a 525/50 band pass filter. Data were fitted to an incomplete bi- or triexponential decay model.

## ACKNOWLEDGMENTS

We acknowledge support from the Jena Biophotonics and Imaging Laboratory (JBIL).

## REFERENCES

1. P.M. Schaefer, S. Kalinina, A. Rueck, C.A.F. von Arnim, B. von Einem, *Cytometry A*, 2019, **95A**, 34-46.

# Multimodal Optical Imaging in Ear Diagnostics

Sven Urban<sup>a</sup>, Clara Kristen<sup>a</sup>, Jürgen Popp<sup>b,c</sup>, Orlando Guntinas-Lichius<sup>d</sup>  
Iwan W. Schie<sup>a,b</sup>,

<sup>a</sup> *Department for Medical Engineering and Biotechnology, University of Applied Sciences Jena, Germany*

<sup>b</sup> *Leibniz Institute of Photonic Technology, Jena, Germany*

<sup>c</sup> *Institute of Physical Chemistry and Abbe Centre of Photonics, Friedrich Schiller University Jena, Germany*

<sup>d</sup> *Department of Otorhinolaryngology, Jena University Hospital, Jena, Germany*

Non-invasive diagnosis and imaging of the ear, particularly the eardrum and middle ear, are crucial in otolaryngology, especially for assessing pediatric middle ear diseases. Recently, there has been significant interest in employing new biomedical optical tools for enhanced diagnostics of middle ear infections. Optical coherence tomography (OCT), for instance, offers noninvasive, rapid, and contact-free depth-resolved imaging and is widely used in ophthalmology. OCT's applications have expanded to include intravascular and esophagus imaging, as well as preclinical devices for skin, lower gastrointestinal tract, and ear imaging. Its simple, affordable, and compact design allows for high-resolution imaging that can be easily integrated into clinical workflows.

In this work, we explore optical design considerations for the multimodal combination of OCT with multispectral methods, aiming for a label-free and depth-resolved examination of ear structures. The multimodal OCT system is designed to produce high-resolution cross-sectional images of the ear, with the sample arm specifically tailored as a handheld module to enhance its use in pediatric cases. Additionally, multispectral imaging gathers data on the spectral distribution of reflected light, providing detailed analysis of tissue composition. This combination offers promising potential for characterizing ear structures, including distinguishing between different tissue types and identifying potential pathological changes.

This proposed system is poised to be a significant advancement in otolaryngology, potentially greatly improving the diagnosis and treatment of ear diseases, particularly in pediatric patients.

## ACKNOWLEDGMENTS

We acknowledge funding from the project PüDE - Promotion über Dreißig (BMBF, 03FHP175); OpenLab-KI - Application of AI and explainable AI for cross-domain processing of OCT-Images (BMBF, FKZ: 16DKWN111); EASYprobe - Multimodal, endoscopic, fiber optic probes for clinical imaging diagnostics - new concepts and manufacturing technologies (BMBF, FKZ: 13FH578KX1).

# Colorectal Cancer Discrimination Through Probes-based Raman Spectroscopy and Optical Coherence Tomography

David L. Vasquez<sup>a</sup>, Christian Röse<sup>b</sup>, Calvin Kreft<sup>b</sup>, Jürgen Popp<sup>a,c</sup>, Rene Mantke<sup>d</sup>, and Iwan W. Schie<sup>a,b</sup>

<sup>a</sup> *Leibniz Institute of Photonic Technology, Department Spectroscopy and Imaging, Albert-Einstein-Str. 9, 07745 Jena, Germany*

<sup>b</sup> *University of Applied Sciences - Jena, Department for Medical Engineering and Biotechnology, Carl-Zeiss-Promenade 2, 07745, Jena, Germany*

<sup>c</sup> *Institute of Physical Chemistry and Abbe Centre of Photonics, Friedrich Schiller University Jena, Germany*

<sup>d</sup> *University Clinics Brandenburg an der Havel, Medical University Brandenburg, Klinik für Allgemein- und Viszeralchirurgie, Hochstraße 29, 14770 Brandenburg an der Havel*

Colorectal cancer, a malignancy that develops within the large intestine, ranks among the leading causes of cancer-related mortality worldwide [1]. There is an increasing emphasis on developing rapid and personalized diagnostics and improved detection of this cancer. A prognostic factor for colorectal cancer is the extent of invasion and the occurrence of distant metastasis. Previous studies have documented the successful implementation of label-free techniques, such as Raman spectroscopy (RS) and optical coherence tomography (OCT), to distinguish between colonic adenocarcinoma and healthy tissue [2].

Our research focuses on the endoscopic probe-based integration of these techniques as a supplementary diagnostic tool for tumor tissue evaluation, aiming for future in-vivo translation. We outline the technical development for a probe-based implementation of OCT and RS for label-free molecular and morphological tissue characterization. Moreover, we evaluate machine learning models using spectroscopy and morphological information for tissue classification. The achieved results demonstrate comparable levels of sensitivity and specificity when compared to prior research utilizing large microscopy-based systems. With the endoscopic implementation, we take a significant step toward achieving accurate and minimally invasive cancer diagnosis.



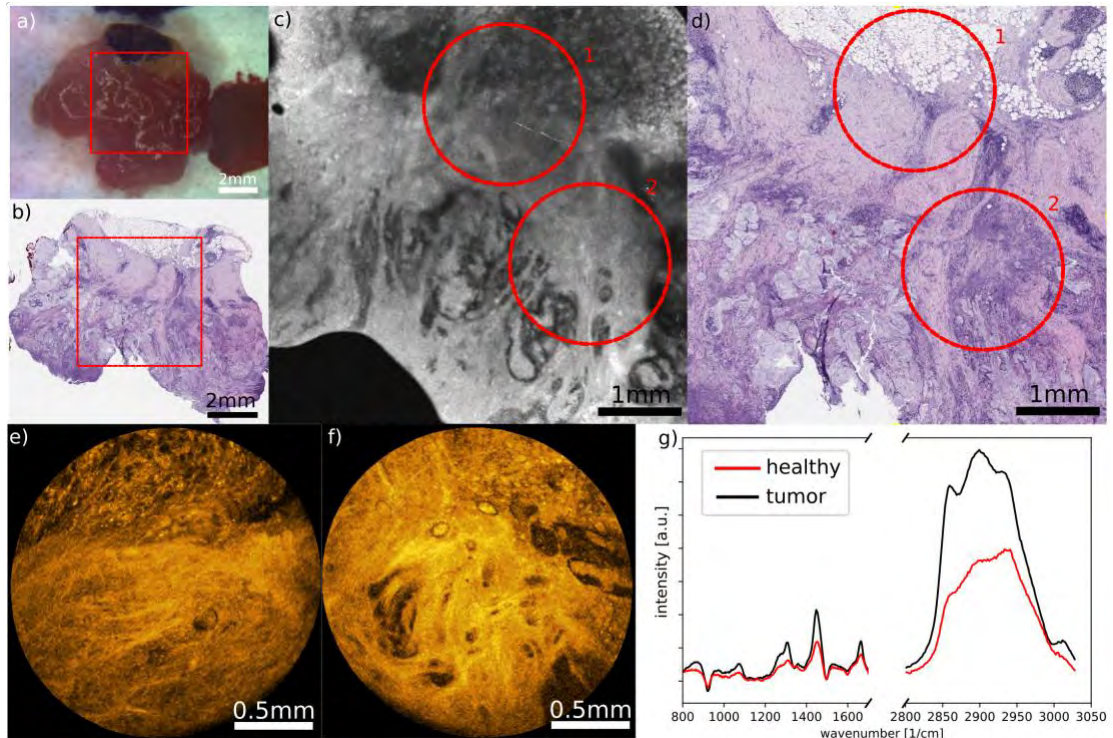


**Figure 1 Colorectal cancer sample** a) Bright field image of a colon biopsy showing the region of interest measured by the desktop OCT system and RS system , b) Sample H&E stain of captions, c) depth OCT image showing the region and field of view of the endoscopic view, e) and f) Probe OCT measurement from the region of interest 1 and 2 respectively, g) Mean RS spectra for healthy and tumour types of tissue.

## ACKNOWLEDGMENTS

We acknowledge funding from the project OpenLab-KI - Application of AI and explainable AI for cross-domain processing of OCT-Images (BMBF, FKZ: 16DKWN111); EASYprobe - Multimodal, endoscopic, fiber optic probes for clinical imaging diagnostics - new concepts and manufacturing technologies (BMBF, FKZ: 13FH578KX1)

## REFERENCES

1. Haggard FA, Boushey RP. Colorectal cancer epidemiology: incidence, mortality, survival, and risk factors. *Clin Colon Rectal Surg.* 2009;22(4):191–7. doi.org/10.1055/s-0029-12424 58.
2. Ashok PC, Praveen BB, Bellini N, Riches A, Dholakia K, Herrington CS. Multi-modal approach using Raman spectroscopy and optical coherence tomography for the discrimination of colonic adenocarcinoma from normal colon. *Biomed Opt Express.* 2013 Sep 16;4(10):2179-86. doi: 10.1364/BOE.4.002179.

## **Molecule transfer into mammalian cells by single sub-nanosecond laser pulses**

Rainer Wittig<sup>a</sup>, Florian Hausladen<sup>a</sup>, Petra Kruse<sup>a</sup>, Holger Wurm<sup>a</sup>, Thomas Stegmayer<sup>a</sup>, Karl Stock<sup>a</sup>, Marco Springer<sup>b</sup>, Rosemarie Preyer<sup>b</sup>, Wolf Seelert<sup>c</sup>

<sup>a</sup> *Institute for Laser Technologies in Medicine & Metrology (ILM) at Ulm University, Ulm, Germany*

<sup>b</sup> *GenID GmbH, Strassberg, Germany*

<sup>c</sup> *Coherent Laser Systems, Lübeck, Germany*

A rapid, precise, and viability-retaining high-throughput method for the spatially controlled transient poration of cells would provide new opportunities for cell engineering, particularly cytoplasmic molecule transfer in adherently growing cells but also e. g. 3D cell cultures or microfluidic applications like Organ-on-Chip. Routine methods suffer from either low throughput, lack of selectivity, requirement of helper compounds, predominant endosomal delivery, and/or are frequently restricted to specific molecule classes such as e. g. nucleic acids. In a proof-of-concept study we demonstrate efficient transfer of molecules from cell culture media in up to 40% of targeted adherent cells (CHO-K1 and THP-1) by applying single sub-nanosecond laser pulses to monolayers. Confocal laser scanning fluorescence microscopy and flow cytometry analyses revealed that variations of pulse energy, energy density, Rayleigh length and axial beam waist positioning in relation to a cell monolayer resulted in characteristic patterns of molecule transfer, but also to cell ablation and cell death. Future research seeks to further optimize laser pulse application schemes towards adherent monolayers for immune cell manipulation in personalized medicine approaches, but also to extend the application field towards spatially controlled manipulation of cells in (micro)fluidic systems as well as 3D cell cultures.

# Disease biomarker identification based on mid-infrared spectroscopy and machine learning

Leiying Xie<sup>a,b,d,e</sup>, Shuxia Guo<sup>a,b</sup>, Shaowei Wang<sup>d,e</sup>, Thomas Bocklitz<sup>a,b,c</sup>

<sup>a</sup> Leibniz Institute of Photonic Technology, Member of Leibniz Health Technologies, Member of the Leibniz Centre for Photonics in Infection Research (LPI), Albert-Einstein-Strasse 9, 07745 Jena, Germany.

<sup>b</sup> Institute of Physical Chemistry (IPC) and Abbe Center of Photonics (ACP), Friedrich Schiller University Jena, Member of the Leibniz Centre for Photonics in Infection Research (LPI), Helmholtzweg 4, 07743 Jena, Germany

<sup>c</sup> Institute of Computer Science, Faculty of Mathematics, Physics & Computer Science, University Bayreuth Universitaetsstraße 30, 95447 Bayreuth, Germany

<sup>d</sup> State Key Laboratory of Infrared Physics, Shanghai Institute of Technical Physics, Chinese Academy of Sciences, Shanghai 200083, China

<sup>e</sup> School of Physical Science and Technology, ShanghaiTech University, Shanghai 201210, China

As a rapid, label-free, and non-destructive technology, mid-infrared spectroscopy has been extensively used in the analysis of biological samples, including plasma, serum, tissue and cells. It is a versatile method being able to probe multiple molecular groups in parallel to characterize the changes of proteins, lipids, nucleic acids etc. To apply the technology in diagnostics, however, it is important and necessary to identify the specific biomarkers for a given disease under diagnostics.

In this work, we proposed to identify the disease-specific biomarkers for blood samples based on mid-IR in combined with machine learning methods. With this we aim for an easier and faster blood-based diagnosis for certain diseases. To do so, we compared the mid-IR spectra from the plasma samples to those from the cell lines based on correlative analysis. In this way we could identify the spectral features of the plasma samples that are discriminative between healthy and diseased samples. This method was verified by the detection of acute myeloid leukemia and abnormal immune status. In particular, significant changes were observed for the valleys at 1629, 1610, 1604, 1536 and 1528  $\text{cm}^{-1}$  and the peak at 1404  $\text{cm}^{-1}$  for acute myeloid leukemia according to the correlation analysis between patients' peripheral blood, bone marrow blood and the U937, HL-60, THP-1 cell lines. On the other hand, the abnormal immune status mainly caused the changes in the  $\beta$ -sheets/ $\alpha$ -helix and CD4+/CD8+ ratio based on the comparison between human total leukocytes and the CD4+ T cells, CD8+ T cells, CD19+ B cells, NK cells and the granulocytes.



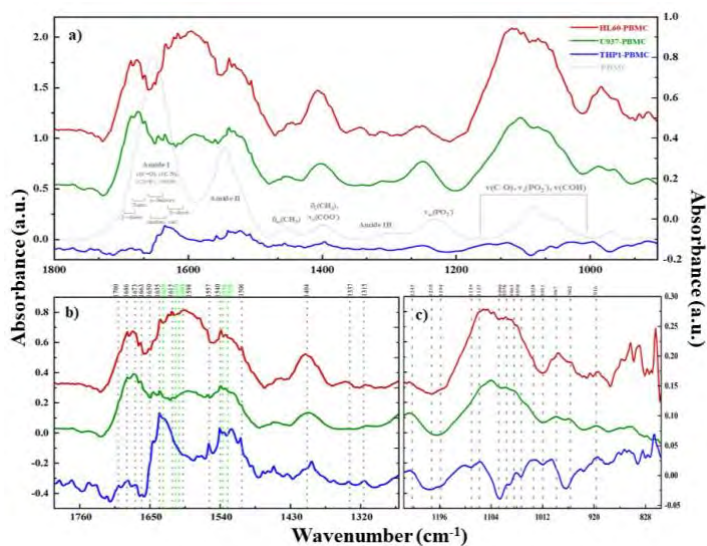


**Figure 1** The difference infrared spectra of acute myeloid leukemia

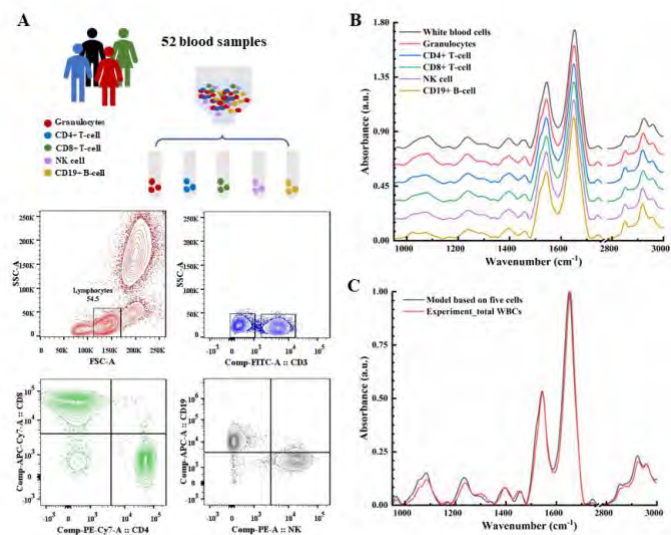


**Figure 2** The infrared spectra of leukocytes subpopulations

## ACKNOWLEDGMENTS

L.X is financially supported by China scholarship council (CSC).

## REFERENCES

1. Holly J Butler, *et. al.* Nature Protocal, 2016, 11(4).
2. Shuxia Guo, *et. al.* Nature Protocal, 2021, 16, 5426-5429.
3. Leiyong Xie, *et. al.* Journal of Pharmaceutical and Biomedical Analysis, 2023, 233, 115454.

## Spatial tissue protein MS modification mapping to facilitate spectroscopic approaches

Kristian Wende<sup>a</sup>, Sebastian Wenske<sup>a</sup>, Paula Marx<sup>a</sup>, Ramona Clemen<sup>a</sup>, Thomas von Woedtke<sup>a,b</sup>, Sander Bekeschus<sup>a,c</sup>

<sup>a</sup> Leibniz Institute for Plasma Science and Technology, Felix-Hausdorff-Str. 2, Greifswald, Germany\*

<sup>b</sup>Institute for Hygiene and Environmental Medicine, Greifswald University Medical Center, Greifswald, Germany

<sup>c</sup> Clinic and Policlinic for Dermatology and Venerology, Rostock University Medical Center, Rostock, Germany

\*a member of the Leibniz Research Alliance Leibniz Health Technology

Non-thermal atmospheric pressure gas discharges (physical plasmas) are applied to alleviate inflammatory disorders, including (chronic) wounds and (pre-) malignant conditions. Despite widespread use and ongoing medical research, the molecular mechanism is still under debate. Among other points, the penetration depth in a biological target remains controversial. Physical plasmas generate reactive chemical species, electrical fields, and light, ranging from vacuum UV to IR. Since all of these entities have different properties, and generating one without the other is notoriously difficult, a pragmatic approach is to analyze tissue samples after plasma exposure.

We decided to investigate the skin as the tissue with the most frequent contact to physical plasma. After plasma treatment of ex vivo skin, the samples were either analyzed by fluorescence and Raman microscopy (Poster Hasse, INP Greifswald/IPHT Jena) or via high-resolution mass spectrometry. By applying the tape strip assay,  $\approx 1\mu\text{m}$  thick layers of the epidermis were obtained, subjected to cleanup and protein digestion, and analyzed by nanoLC/HRMS (Thermo Exploris 480). Subsequent bioinformatics comprised ProteomeDiscoverer 2.4SP1 profiling of the proteome and ProteinMetrics Byonic v5.2.5 for identifying/mapping the post-translational oxidative modifications. A parallel workflow targets the lipids present in the samples (UHPLC/HRMS). Some samples were covered during plasma treatment with a VUV transparent  $\text{MgF}_2$  window in order to investigate the role of UV radiation specifically.

About 2000 proteins were identified from the tape strips, with some carrying oxidative modifications. Pilot experiments using model peptides successfully identified the main amino acid targets of physical plasma (aromatic, heterocyclic, and sulfur-containing amino acids) and the predominant oxidative modifications (oxPTMs) introduced (up to three oxygen atoms, deamidation, chlorination, nitration, ring cleavages). They allowed a targeted search algorithm and shorter computation times<sup>1,2</sup>. Subsequent changes in protein activity were identified<sup>3-5</sup>. In the skin samples, a small increase of oxPTMs was observed, with a slight emphasis on the outermost layers after plasma/UV treatment of thiol oxidation and oxidation of aromatic rings was observed<sup>6</sup>. A similar result was obtained when analyzing the lipid composition and oxidation products, respectively.

The workflows have been successfully established, allowing us to analyze stratified tissues quickly. Profound knowledge of physical plasma-introduced oxPTMs can be used to understand the underlying mechanism and guide microscopic or spectroscopic approaches. Indeed, the stratum corneum served as a strong barrier, preventing more extensive oxidation of the biomolecules, especially in the deeper layers of the tissue. This is in contrast to findings based on other approaches<sup>7,8</sup>, which, however, have not used mass spectrometry as highly sensitive and precision tool for protein analysis.

## ACKNOWLEDGMENTS

This work was supported by the German Ministry of Research and Education (BMBF), grant numbers 03Z22DN12 (to K.W.), 03Z22DN11 (to S.B.), and 03Z22Di1 (to S.B.).

## REFERENCES

- <sup>1</sup>S. Wenske, J. W. Lackmann, L. M. Busch, S. Bekeschus, T. von Woedtke and K. Wende, *J Appl Phys* **129** (19), 193305 (2021).
- <sup>2</sup>S. Wenske, J. W. Lackmann, S. Bekeschus, K. D. Weltmann, T. von Woedtke and K. Wende, *Biointerphases* **15** (6), 061008 (2020).
- <sup>3</sup>R. Clemen, L. Minkus, D. Singer, P. Schulan, T. von Woedtke, K. Wende and S. Bekeschus, *Antioxidants* **12** (11), 1936 (2023).
- <sup>4</sup>Z. Nasri, S. Memari, S. Wenske, R. Clemen, U. Martens, M. Delcea, S. Bekeschus, K. D. Weltmann, et al., *Chemistry – A European Journal* **27** (59), 14702-14710 (2021).
- <sup>5</sup>R. Clemen, E. Freund, D. Mrochen, L. Miebach, A. Schmidt, B. H. Rauch, J. W. Lackmann, U. Martens, et al., *Adv Sci (Weinh)* **8** (10), 2003395 (2021).
- <sup>6</sup>G. Bruno, S. Wenske, H. Mahdikia, T. Gerling, T. von Woedtke and K. Wende, *Frontiers in Physics* **9** (2021).
- <sup>7</sup>T. Wenzel, D. A. Carvajal Berrio, R. Daum, C. Reisenauer, K. D. Weltmann, D. Wallwiener, S. Y. Brucker, K. Schenke-Layland, et al., *ACS Appl Mater Interfaces* **11** (46), 42885-42895 (2019).
- <sup>8</sup>K. R. Liedtke, E. Freund, C. Hackbarth, C.-D. Heidecke, L.-I. Partecke and S. Bekeschus, *Clinical Plasma Medicine* **11**, 10-17 (2018).

# Label-free, chemically specific imaging with the Leica STELLARIS 8 CRS – a true multi-modal optical discovery instrument

Dr. Volker Schweikhard<sup>a</sup>

<sup>a</sup>Leica Microsystems CMS GmbH, Am Friedensplatz 3, 68165 Mannheim, Germany

Here, we report on a number of applications in label-free, chemically specific imaging using the STELLARIS 8 CRS – Leica’s hands-free Coherent Raman Scattering microscopy instrument. It offers the two popular CRS modalities – SRS and CARS – and allows for the simultaneous acquisition of two-photon fluorescence and second-harmonic generation signals. Importantly, the seamless integration of CRS with the STELLARIS visible confocal fluorescence microscopy platform results in a true multi-modal optical discovery instrument that is capable of capturing a unique combination of biochemical, biophysical and molecular contrasts. Here, we present a range of applications of SRS, including label-free morphochemical imaging in model organisms, the characterization of organoids and spheroids, and investigations of brain tissues for neurodegenerative disease research. We show specifically that SRS can provide novel insights into the biophysical properties and biochemical composition of Amyloid- $\beta$  plaques in a mouse model of Alzheimer’s disease. Our results highlight the potential of SRS to contribute to a deeper understanding of cell and tissue biology, and to serve as a powerful tool for preclinical and translational research.

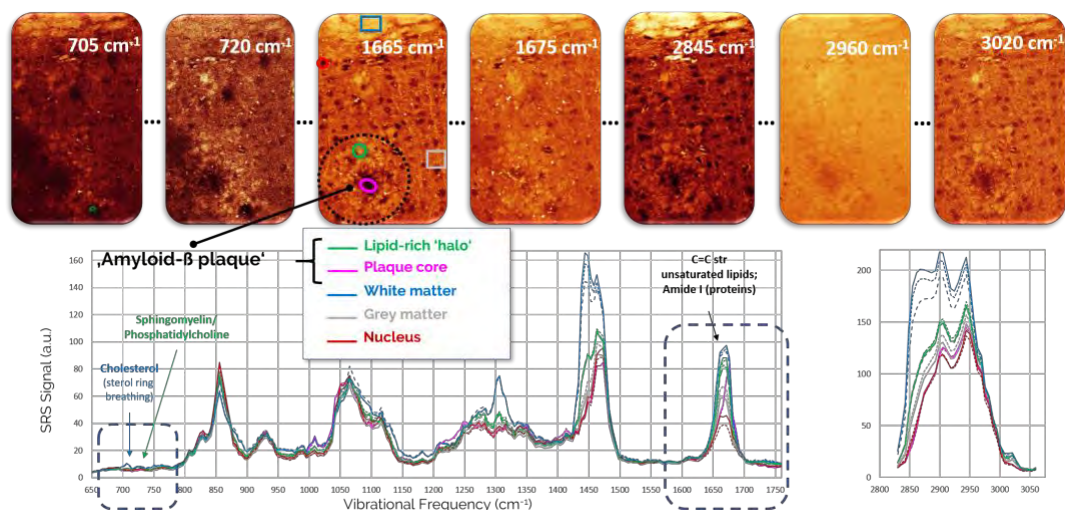


**Figure 1** Hyperspectral SRS imaging of mouse brain tissue allows label-free visualization of Amyloid- $\beta$  plaques and shows differential localization of lipid species to healthy and pathological brain structures [1].

## REFERENCES

1. V. Schweikhard *et al.*, bioRxiv 2019; <http://dx.doi.org/10.1101/789248>.

# Advancements in FLIM: Comparative Analysis and New Methods for High-Resolution, Rapid Microenvironmental Imaging

Thomas Kellerer<sup>a,b</sup>, Lukas Moser<sup>a</sup>, Janko Janusch<sup>a</sup>, Patrick Byers<sup>a</sup>, Joachim Rädler<sup>b</sup> and Thomas Hellerer<sup>a</sup>

<sup>a</sup> *Multiphoton Imaging Lab, Munich University of Applied Sciences, 80335 Munich, Germany*

<sup>b</sup> *Faculty of Physics, Soft Condensed Matter, Ludwig-Maximilians-University, 80539 Munich, Germany*

## Abstract:

Investigating various biological topics requires a comprehensive understanding not only of morphology but also of microenvironmental parameters like for example the pH-Value. For instance, in novel drug delivery systems based on lipid nanoparticles (LNPs), the pH-value governs the release process of messenger ribonucleic acid (mRNA) into the cytosol. An essential question in such studies is how to optically measure these microenvironmental properties. Among the methods available, specially designed fluorophores that display intensity fluctuations in response to changing properties like the pH-Value are notable. However, fluorescence lifetime imaging (FLIM) emerges as the superior technique for assessing these properties due to its robustness against changes in fluorophore concentration, photobleaching, and excitation intensity. Researchers typically need to choose between two predominant FLIM techniques depending on the requirement for speed or spatial resolution: Time Domain (TD) and Frequency Domain (FD). In this study, we discuss which microenvironmental parameters can be quantified using both TD and FD techniques, providing a comparative analysis. Additionally, we introduce innovative methods that synergize TD and FD's advantages, enabling rapid acquisition with enhanced spatial resolution. One of them integrates fluorescence lifetime measurement with a resonant galvo scanner, opening new pathways for rapid and high-resolution FLIM data.

## 1. Introduction:

Contemporary microscopy has greatly enhanced our capability to visualize the structure of living organisms. Yet, extending our insights beyond mere structure to include photophysical, chemical, and biological contexts, methodologies like fluorescence lifetime imaging microscopy (FLIM) stand out. Many conventional microscopy approaches, however, are limited due to their reliance on signal intensities. These intensities are not only influenced by the specifics of the experimental arrangement, like how efficiently a sample is excited or detected, but are also prone to problematic occurrences, such as the photo-bleaching of fluorescent markers—leading to measurements that can typically only assess relative shifts. What sets FLIM apart is its independence from the modality of excitation, whether through single-photon (1P) or two-photon (2P) interaction, nor does it require tuning the laser precisely to the fluorescence excitation peak of the examined material. Discrepancies in reported lifetime values from FLIM might convey an impression of unreliability; however, these are often attributable to variables directly affecting the sample, like concentration, pH-value, solvent polarity, and temperature - factors we studied in our previous work [1]. Although both established TD and FD-FLIM techniques have their merits and limitations, cutting-edge method arises when combining these two techniques. For example, the instantFLIM approach merges the rapid data collection feature of FD-FLIM with the superior optical resolution of TD-FLIM [2]. By including a lock-in amplifier in our setup we were able to expand this technique to



enable fluorescence lifetime measurements with a resonant galvo scanner. We call this technique speed up phase resolved fluorescence lifetime imaging microscopy (SUPER FLIM) based on previous results from another group [3].

## 2. Results:

One important result from our research is the matching lifetimes obtained using both FD- and TD-FLIM setups. FD-FLIM utilizes widefield, single-photon absorption, while TD-FLIM employs laser scanning with two-photon absorption. Testing with a  $10^{-2}$  M Rose Bengal solution in ethanol resulted in consistent lifetimes of approximately 0.85 ns across various wavelengths, modulation frequencies, and integration times.

Adjusting the microenvironment revealed that pH-value (Figure 1), along with potential quenching molecules and solvent polarity, significantly impacts the measured lifetime. Phasor plot analysis verified the mono-exponential decay of our samples, and a p-value test statistically validated the comparable accuracy of both FLIM methods.

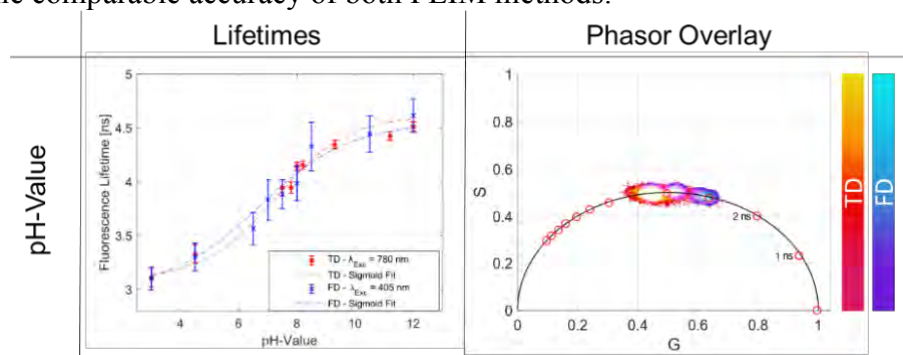


Figure 1: The pH dependent lifetime of Fluorescein in water ( $10^{-4}$  M) for pH values between 3 and 12 that follows a sigmoid function (left). The corresponding phasor plots for the TD- and FD-FLIM technique are shown on the right.

The excellent agreement between all four FLIM techniques - including instantFLIM and SUPER FLIM- was demonstrated by changing the solvent polarity as one of the strongest influencing factors (Figure 2). Although the measured lifetimes vary between 0.18 ns and 2.8 ns, all values determined by the different techniques match very well for each individual solvent.

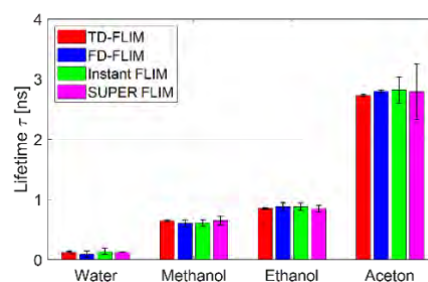


Figure 2: Fluorescence lifetimes for Rose Bengal for different solvent polarities measured with TD-FLIM (red), FD-FLIM (blue), instantFLIM (green) and with the new technique SUPER FLIM (magenta).

## 3. Discussion:

In this work we demonstrated that the results of a FD setup are comparable with the one of a TD setup and to that of an instantFLIM setup with statistical proof and without exception. We also showed which parameters have the greatest influence on the lifetime and should be mentioned in published data. Especially the results of instantFLIM and SUPER FLIM are promising for future lifetime measurements because the lifetime can be measured with high frame rates and all other benefits of two photon microscopy.

## **ACKNOWLEDGMENTS**

This research was funded by the Bundesministerium für Bildung und Forschung (BMBF) – SEMPA-Track (13N16300) and the Bavarian Academic Forum (BayWISS) – Doctoral consortium “Health Research”.

## **REFERENCES**

[1] Kellerer, Thomas, et al. "Comprehensive Investigation of Parameters Influencing Fluorescence Lifetime Imaging Microscopy in Frequency-and Time-Domain Illustrated by Phasor Plot Analysis." *International Journal of Molecular Sciences* 23.24 (2022): 15885.

[2] Zhang, Yide, et al. "Instant FLIM enables 4D in vivo lifetime imaging of intact and injured zebrafish and mouse brains." *Optica* 8.6 (2021): 885-897.

[3] Halip, Hafizah, et al. "Ultrashort laser based two-photon phase-resolved fluorescence lifetime measurement method." *Methods and Applications in Fluorescence* 8.2 (2020): 025003.



# Advancements in miRNA Detection: Harnessing the Potential of a Silicon Nitride Photonic Biosensing Platform

Florenta A. Costache<sup>a,b</sup>, David M. Smith<sup>b,c,e</sup>, Hendrik Reichelt<sup>b,c</sup>, Aarya Lakshmireddy<sup>b,d</sup>, Andreas Stoll<sup>a,b</sup>, Zhiqiu Lu<sup>a,b</sup>

<sup>a</sup> Fraunhofer Institute for Photonic Microsystems IPMS, Maria-Reiche Str. 2 01109, Dresden, Germany

<sup>b</sup> Fraunhofer Center for Microelectronic and Optical Systems for Biomedicine MEOS, Herman-Hollerith-Straße 3, 99099, Erfurt, Germany

<sup>c</sup> Fraunhofer Institute for Cell Therapy and Immunology IZI, Perlickstraße 1, 04103, Leipzig, Germany

<sup>d</sup> Fraunhofer Institute for Applied Optics and Precision Engineering IOF, Albert-Einstein-Straße 7, 07745 Jena, Germany

<sup>e</sup> University of Leipzig, Peter Debye Institute for Soft Matter Physics, Linnéstr. 5, 04103 Leipzig, Germany

Silicon photonic biosensors have shown potential in advancing biomedical applications requiring parallel detection of multiple biomolecules in portable and miniaturized systems [1, 2]. This paper presents a detailed investigation into the development of a scalable silicon nitride ( $\text{Si}_3\text{N}_4$ ) photonic biosensor platform designed specifically for biomedical use.

The work involved the development of a biosensor chip with novel  $\text{Si}_3\text{N}_4$  microring resonators (MRR) operating at a wavelength of 1550 nm. The sensors were fabricated on a PECVD  $\text{Si}_3\text{N}_4$  waveguide platform on 200-mm silicon wafers. The biosensor chip featured a  $1 \times 8$  MRR multiplexed architecture with 7 sensors and one reference. The chip was integrated into a system consisting of the biosensor chip itself (Fig. 1a), a custom-designed microfluidic cell combined with a fine-dosing pump, and a specially developed optical readout system featuring light in/out connection to the chip via optical fibers. This integrated setup enabled rapid, simultaneous, multi-channel acquisition of MRR transmission spectra. By monitoring the resonance wavelength shifts resulting from biomolecules captured on the sensor surface, the system facilitated the detection of these biomolecules from the analyte solution flowing over the chip.

The primary focus of this research was the detection of specific disease-indicating biomarkers, particularly transcriptomic microRNA (miRNA) biomarkers. These miRNA biomarkers, which are present in the bloodstream, hold significant potential for the rapid and minimally invasive diagnosis of neurodegenerative diseases such as Alzheimer's and Parkinson's [3] as well as many others including cancer and infectious diseases.

To detect miRNA biomarkers, DNA-based capture components were used in specially designed binding assays. The sensor surface was pre-functionalized with a silane layer, and complementary DNA strands were immobilized on it. This enabled controlled binding of miRNA-mimicking biomarkers from the analyte solution to the sensor surface. Additionally, the MRR sensors could be specifically functionalized using a

local spotting procedure with DNA strands (Figure 1b). This allowed parallel detection of several complementary miRNA biomarkers at the same time. Figure 1c illustrates the results of parallel detection of three different miRNA biomarkers using specific surface functionalized MRR sensors by wavelength shifts over time. The current setup allowed for simultaneous detection of up to 6 biomarkers with the same chip. The system demonstrated good sensitivity, with an estimated detection limit (without signal amplification) below the nanomolar (nM) range.

This work builds upon a previous study [4] and proposes further optimizations, including a new sensor design approach involving the deposition of selected oxide thin films on the silicon nitride waveguide core in the sensor region to enhance sensor sensitivity.

The development of this biosensor platform and the surface functionalization protocols demonstrated the potential for a common workflow in the detection of various disease-indicating biomarkers. This advancement holds promising opportunities for rapid and minimally invasive diagnostics, particularly for early onset and monitoring of diseases evolution.

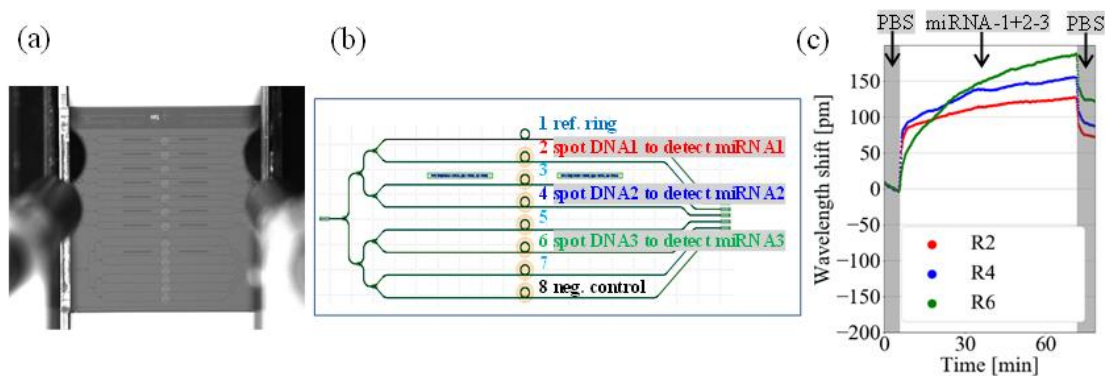


**Figure 1** MRR sensor chip with in/out light coupling via fibers and grating couplers. (a) 1x8 multiplexing scheme for 3 miRNAs. (c)  $\Delta\lambda$  change over time confirms biomarker detection after flowing miRNA mixture over DNA-functionalized chip.

## REFERENCES

1. E. Luan et al., *Sensors*, 2018, **18**, 3519.
2. P. Steglich et al., *Molecules*, 2009, **24**, 519.
3. B. Roy et al., *Genes*, 2022, **13**, 425.
4. F. Costache, Z. Wang, M. Namdari, Z. Lu, M. Blasl, D. Smith, H. Reichelt, C. Gessinger, A. Kölsch, *Sensors*, in preparation.

# Development of a fast Push-Broom Imaging Raman Micro-Spectrometer for biological tissue

Aguila-Castro, Fernando J.<sup>a\*</sup>, Hauswald, Walter<sup>a</sup>

<sup>a</sup> Leibniz-Institute of Photonic Technology, Albert-Einstein-Straße 9, D-07745 Jena, Germany, member of the Leibniz Centre for Photonics in Infection Research (LPI), Jena, Germany

\*fernando.aguila@leibniz-ipht.de

**Introduction.** In order to address biomedical questions related to infectious diseases, cancer diagnostics and other pathologies, powerful tools for the identification and characterization of bio-molecules, bioparticles, body fluids, and biological tissues are necessary. Molecular specificity as well as lateral resolution down to the sub-cellular level can be achieved through Raman micro-spectroscopy in a label free and non-invasive manner [1]. Nevertheless, due to the small Raman scattering cross-section, the Raman signal is easily overwhelmed by a fluorescence signal and typical image acquisition times can be significant due to the long integration times per spectrum, particularly for large regions of interest [2]. An increase of laser intensity is not an option, since thermal dissipation of light starts to modify or even destroy the sample [3]. Therefore, a confocal light-line Raman microscopy setup brings two advantages: low thermal degradation effects on the sample and increased spectral acquisition speed. In the present work a Push-Broom Imaging Raman Micro-Spectrometer (PBIRMS) is developed and assessed (Fig. 1).

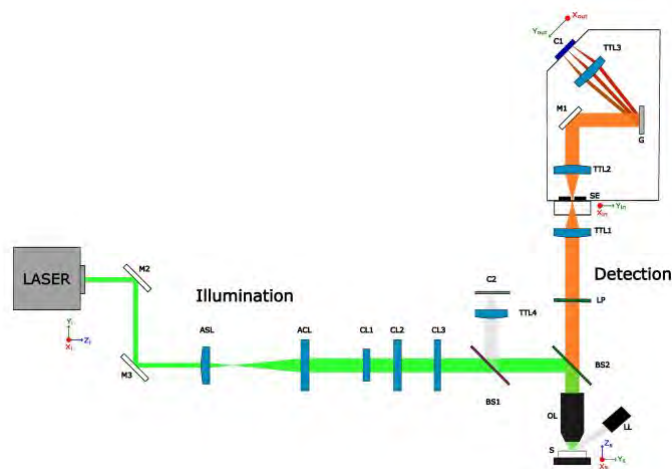


**Figure 1:** Optical setup diagram of the instrument.

**Experimental Setup.** The excitation light source used is a 532 nm DPSS laser. The spectrometer entrance consists of a slit mask composed of 140 rectangular holes of  $13 \times 47 \mu\text{m}$  separated 0.1 mm from one another. Our PBIRMS presents a uniform light-line sample illumination with dimensions  $0.75 \text{ mm} \times 0.665 \mu\text{m}$ , with a spectral resolution of  $5 \text{ cm}^{-1}$ . Image processing of the recorded data is performed using a self written data processing algorithm in Python, in order to correct the conical diffraction

of the spectrometer and retrieve the hyperspectral information from the sample. Assessment of the potential of the instrument for Raman spectroscopy was made through the analysis of a paracetamol tablet sample.

**Results.** The hyperspectral image of the paracetamol tablet obtained consists of 120 spectra measured simultaneously. Spectra from three sections of the sensor were compared against measurements of the same paracetamol tablet and of pure paracetamol (acetaminophen) performed with a reference Raman setup (Fig. 2). Spectra from the PBIRMS and reference Raman setup were similar and the identification of Raman bands corresponding to vibrations of the Phenyl ring and Acetamino molecule was possible [4].

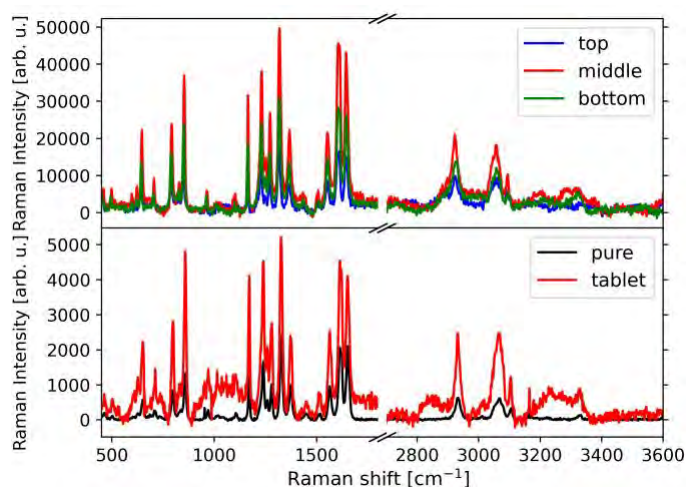


**Figure 2:** Measurement comparison of paracetamol sample. Top plot shows the results from the PBIRMS. Bottom plot shows the results from the reference Raman setup.

## ACKNOWLEDGMENTS

We thank Izabella Jahn for support and advice, Uwe Hübner and his team for fabricating the slit masks, Henry John for CAD construction, as well as Thomas Büttner and his team for manufacturing mechanical parts. This work is supported by the BMBF, funding program Photonics Research Germany (13N15464) and is integrated into the Leibniz Center for Photonics in Infection Research (LPI).

## REFERENCES

1. C. Kraft and J. Popp, *Analytical and Bioanalytical Chemistry*, 2015, **407**, 699-717.
2. C. Kraft et al, *Journal of Biomedical Optics*, 2012, **17.4**, 1-15.
3. W. Hauswald, R. Förster, J. Popp, and R. Heintzmann. *PLoS One*, 2019, **14**, 1-17.
4. A.M. Amado et al, *Spectrochimica Acta Part A: Molecular and Biomolecular Spectroscopy*, 2017, **183**.

# High resolution in hyperspectral data analysis from nanoscale IR spectroscopic imaging – a challenge!

Maryam Ali<sup>1</sup>, Sebastian Unger<sup>1,2</sup>, Selema Buzhala<sup>1,2</sup>, Christoph Krafft<sup>1,2</sup>, Rainer Heintzmann<sup>1,2</sup>, Robin Schneider<sup>2</sup>, Ute Neugebauer<sup>1,2,3</sup>, Daniela Täuber<sup>1,2</sup>.

<sup>1</sup> Friedrich Schiller University, Jena, Germany

<sup>2</sup> Leibniz Institute of Photonic Technology, Jena, Germany

<sup>3</sup> University Hospital Jena, Jena, Germany

Technical progress has triggered close to molecular resolution in the emerging field of infrared spectroscopic imaging methods. The access to chemical variation on the scale of few nm combined to high spectral resolution can reveal unprecedented spectroscopic details in biomaterials opening a new era in IR spectroscopic imaging. This requires also new approaches in data analysis. We applied mid-Infrared Photo-induced Force Microscopy (PiF-IR) to bacterial<sup>[1]</sup> and tissue<sup>[2]</sup> observing a unique spatial resolution  $\approx 5\text{nm}$  of the surfaces<sup>[1]</sup>. Here we compare the results of applying several approaches for hyperspectral data analysis of the obtained PiF-IR hyperspectra (Figure 1). The advantages and disadvantages of applying unguided Principal Component Analysis (PCA)<sup>[3]</sup>, Hierarchical Clustering Analysis (HCA)<sup>[4]</sup>, and Topological Data Analysis (TDA)<sup>[5]</sup> are discussed and compared to a guided approach using known spectral components.

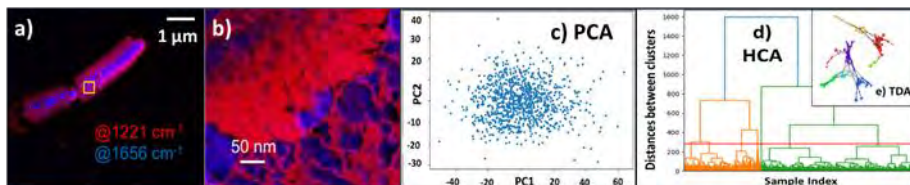


Figure 1: a, b) PiF-IR contrasts obtained from *Bacillus subtilis*<sup>[1]</sup>. c, d, e) Schematics comparing PCA, HCA, and TDA applied to a hyperspectral data set obtained via PiF-IR on *Bacillus subtilis* incubated with Vancomycin.

[1] N. Krishnakumar *et al.*, “Nanoscale chemical imaging of cell surface and core-shell nanoparticles using infrared excitation and detection by force microscopy,” in *70. Mosbacher Kolloquium - “High-resolution imaging of cells and molecules,”* Mosbach, 2019, p. 1. doi: 10.13140/RG.2.2.13191.06564.

[2] J. Joseph *et al.*, “Nanoscale chemical characterization of secondary protein structure of F-Actin using mid-infrared photoinduced force microscopy (PiF-IR),” *Spectrochimica Acta - Part A: Molecular and Biomolecular Spectroscopy*, vol. ECSBM2022, p. revision submitted.

[3] I. T. Jolliffe and J. Cadima, “Principal component analysis: a review and recent developments,” *Philosophical Transactions of the Royal Society A: Mathematical, Physical and Engineering Sciences*, vol. 374, no. 2065, p. 20150202, Apr. 2016, doi: 10.1098/rsta.2015.0202.

[4] L. Liu, G. Delnevo, and S. Mirri, “Unsupervised hyperspectral image segmentation of films: a hierarchical clustering-based approach,” *Journal of Big Data*, vol. 10, no. 1, p. 31, Mar. 2023, doi: 10.1186/s40537-023-00713-8.

[5] L. Duponchel, “Exploring hyperspectral imaging data sets with topological data analysis - ScienceDirect,” *Analytica Chimica Acta*, vol. 100, pp. 123–131, Feb. 2018.

# Photo-thermal Expansion of Nanostructured Surfaces in nano-IR spectroscopic imaging using Photo-induced Force Microscopy (PiF-IR)

Shohely Anindo<sup>a,d</sup>, Rainer Heintzmann<sup>b,c,d</sup>, Daniela Täuber<sup>b,c</sup>, Christin David<sup>a,d</sup>

<sup>a</sup> Institute of Condensed Matter Theory and Solid State Optics, FSU, Jena, Germany

<sup>b</sup> Institute of Physical Chemistry, FSU, Jena, Germany

<sup>c</sup> Institute Leibniz-IPHT, Jena, Germany

<sup>d</sup> Abbe Center of Photonics, Jena, Germany

Combinations of powerful infrared illumination with mechanical detection via force microscopy provide access to nanoscale infrared spectroscopic imaging [1]. One such method, mid-IR photo-induced force microscopy (PiF-IR) has already been applied in material and biological sciences [2]. In PiF-IR structural and dielectric characteristics of materials are revealed using pulsed IR-illumination and non-contact force microscopy. When the tip and sample are brought close to each other, a distance-dependent weak Van der Waals (VdW) force [3] starts to act between them. The pulsed IR-illumination causes absorbing materials to expand thermally as a result of the rise in local temperature. The measured force between the tip and the sample is then affected by this thermal expansion, yielding the PiF-IR signal [2]. The non-linear impact of material characteristics and surface shape on the tip-sample interaction, heat generation from the presence of a photo-induced electric field, and the associated thermal expansion at different illumination conditions are theoretically studied in this work.

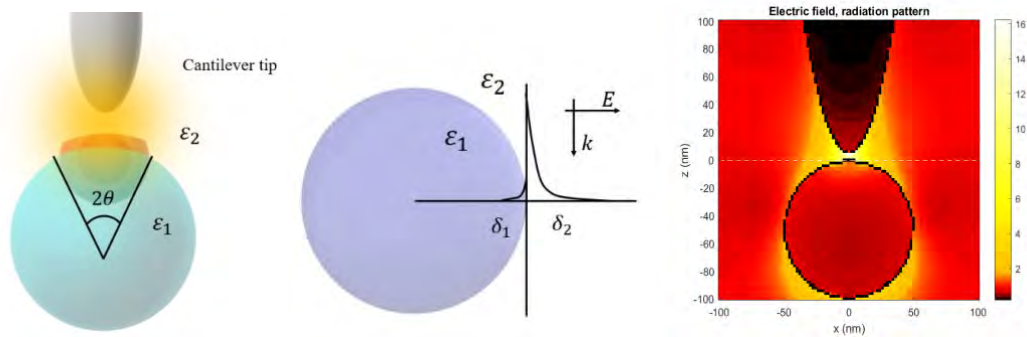


**Figure 1** Portion of the electric field that contributes to heat generation with (a) heat generation due to the electric field inside the nanosphere and enhanced field outside the nanosphere, (b) penetration depth inside the nanosphere and (c) tip-sample interaction at p-polarization.

## REFERENCES

1. H. Wang, D. Lee, and L. Wei, *Chemical & Biomedical Imaging*, 2023, **1(1)**, 3–17.
2. J. Jahng, B. Kim, and E. Seong Lee, *Phys. Rev. B*, 2022, **106**, 155424, 1–13.
3. D. Täuber, I. Trenkman, and C. von Borzyskowski, *Langmuir*, 2013, **29(11)**, 3583–3593.



## Infrared spectral biomarkers of hypoxia in 2D and 3D cultures of endothelial cells.

Anna Antolak<sup>a</sup>, Aleksandra Pragnaça<sup>a,b</sup>, Zuzanna Krysiak<sup>c</sup>, Monika Leśniak<sup>c</sup>, Robert Zdanowski<sup>c</sup>, Kamilla Małek<sup>a</sup>

<sup>a</sup> Jagiellonian University, Faculty of Chemistry, Department of Chemical Physics, Raman Imaging Group Krakow, Poland

<sup>b</sup> Jagiellonian University, Doctoral School of Exact and Natural Sciences, Krakow, Poland

<sup>c</sup> Military Institute of Medicine National Research Institute, Laboratory of Molecular Oncology and Innovative Therapies, Warsaw, Poland

Blood brain barrier (BBB) is a dynamic and highly regulated cellular system. Endothelial cells of the brain capillaries are highly specialized epithelial cells, which are primary component of the blood brain barrier<sup>1</sup>. Together with pericytes and astrocytes, they are being involved in sustaining and regulation of the BBB properties such as resistance and permeability<sup>2</sup>. Hypoxia is an *in vitro* model of oxygen deficiency in neurological dysfunctions. BBB dysfunction is direct indicator of the pathogenesis of neurovascular and degenerative diseases of the CNS<sup>3</sup>. Therefore, the research on BBB is of interest for multiple scientific disciplines evoking an ongoing need to ameliorate functional models of the human blood-brain barrier. The 3D spheroids, composed of brain endothelial cells, pericytes, and astrocytes, which mimic the spatial architecture and cell-cell interactions in BBB are concerned the most reliable model of the *in vivo* conditions<sup>4</sup>. However, not only reproducibility of *in vitro* barrier properties remains major challenges, but also rapid and non-destructive methods are required for complex analysis of the internal structure and biochemical effects inside the culture-based BBB models.

In this study, we aimed to generate a reproducible cellular spheroids and evaluate the potential of label-free imaging to find spectral biomarkers of hypoxic effects in 2D and 3D cell cultures. Cerebral microvascular endothelial cells (HBEC 5i) were purchased from ATCC (CRL-3245, USA) and cultured up to 9th passage. The CaF<sub>2</sub> Raman grade glass slides with seeded cells were placed in the incubator with the O<sub>2</sub> concentration of 1% for 24h. The mono-cellular spheroids were obtained by use of hanging drop method. Cells were fixed and subsequently evaluated by FT-IR imaging (Agilent 670-IR spectrometer combined with the 620-IR microscope). H&E and fluorescence staining were used as the reference method. Statistical and chemometric methods were used for data analysis.

Fluorescence microscopy revealed proper shape and interconnections between the cells, as well as visualized structures and formation of lipid droplets. Cells within the spheroid very tightly packed and the necrotic core was present. Analysis of the FT-IR spectra revealed distinct spectral characteristics of experimental groups. HCA and PCA analysis indicated spectral differences between cell groups and allowed for discrimination of the cell classes within the spheroid. Hypoxia induced major changes in protein-lipid system

and nucleic acids. The alternations in the lipid content and their saturation level were observed. The expression of proteins, structural changes and cross-linking was also affected by hypoxic effects. It was confirmed that hypoxia can cause stimulation or suppression of specific genes, leads to increased glycolysis as well as stimulation of angiogenesis in hypoxic tissues. Reduced oxygen levels cause degenerative changes in the endothelial membrane and subsequently affect vascular permeability<sup>5,6</sup>.

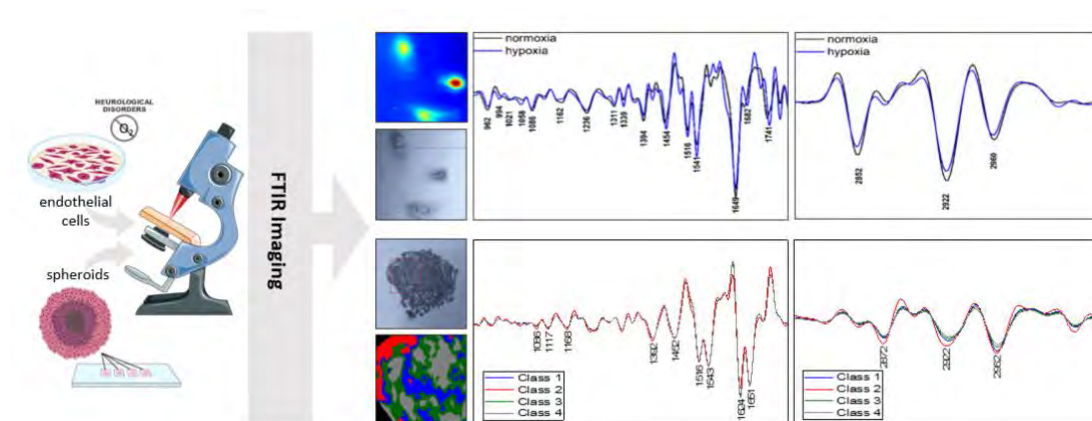


**Figure 1.** Scheme and exemplary results from spectroscopic analysis: protein distribution in cells and HCA cluster maps with respective second derivatives of average FT-IR spectra of the cell classes.

## ACKNOWLEDGMENTS

This work was supported by “Blood-brain barrier: A 3D cell model and its functionality assessed by a multimodal molecular platform” grant funded by the polish National Science Center (OPUS 21, grant No. 2021/41/B/ST4/02000).

## REFERENCES

1. A. Majewska, K. Wilkus, K. Brodaczewska, C. Kieda. *Int. J. Mol. Sci.* 2021, **22**, 520
2. T. Ruck T, S. Bittner, S.G. Meuth SG, *Neural Regen Res*, 2015, **10**(6), 889-891.
3. G. Nzou, R.T. Wicks, N.R., VanOstrand, *et al.*, *Sci Rep*, 2020, **10**, 9766
4. C.F. Cho, J.M. Wolfe, C.M. Fadzen, D. Calligaris, K. Hornburg, E.A. Chiocca, N.Y.R. Agar, B.L. Pentelute, S.E. Lawler. *Nat Commun*, 2017, **139**, 44, 15628–15631
5. A.A. Tirpe, D. Gulei, S.M. Ciortea, C. Crivii, I. Berindan-Neagoe. *Int J Mo. Sci*, 2019, **20**, 6140
6. K.A Witt, K.S. Mark, J. Huber, T.P. Davis, *J Neurochem*, 2005, **92**(1), 203-14

# DFT study, Vibrational frequency, and biological analysis on Methyl 2-hydroxy-4-methoxy benzoate

B Shinthiya Mystica<sup>a,b</sup>, Johanan Christian Prasana<sup>a,b\*</sup>, S. Muthu<sup>c,d\*</sup>

<sup>a</sup> Department of Physics, Madras Christian College, East Tambaram, Chennai 600059, Tamil Nadu India.

<sup>b</sup> University of Madras, Chennai 600005 Tamil Nadu, India.

<sup>c</sup> Department of Physics, Arignar Anna Govt. Arts College, Cheyyar 604407, Tamil Nadu, India.

<sup>d</sup> Department of Physics, Puratchi Thalaivar DR.MGR. Govt. Arts and Science College, Uthiramerur-603406, Tamilnadu, India.

\*Corresponding author: reachjcp@gmail.com

Methyl 2-hydroxy-4-methoxybenzoate (M2H4MB) is a chemical compound used in a wide range of healthcare and biological applications [1]. The title compound consists of 23 atoms, and the molecular formula is C<sub>9</sub>H<sub>10</sub>O<sub>4</sub>. Its primary function is to prevent the growth of blood clots, which have the potential to induce ischaemic stroke, heart damage, liver cirrhosis, and pulmonary embolism. Its antifibrotic properties make it effective in breaking blood clots [2]. Ongoing research on M2H4MB has the potential to facilitate the progress of pharmaceutical drug development.

Methyl 2-hydroxy-4-methoxybenzoate (**M2H4MB**), an organic compound, derivative of benzoic acid, belongs to the class of ester and was studied theoretically in terms of structural, vibrational (FT-IR, FT-RAMAN), electronic (UV-Vis), optical (NLO), and biological properties. Using Density Functional Theory, B3LYP/6-311++G (d, p) basis set, the optimized geometry (bond length and bond angle), and vibrational frequencies of (**M2H4MB**), were computed. Further, FT-IR and FT-Raman spectra were scaled, and prominent peaks were analyzed in detail, comparing the results with experimental data. Vibrational assignments (%PED) were performed for all 63 modes of vibration of the title compound under study. UV-Vis spectra were obtained using the TD-DFT technique for different solvents, and the peaks were identified. HOMO and LUMO energy levels of the title compound were identified using Frontier Molecular Orbital Analysis. These results were used to calculate the energy gap and global reactivity parameters. The stability and non-toxicity of M345TMB have been checked using FMO studies. Multiwfn software was used to study topological analyses such as RDG, MEP, ELF, and LOL. Intermolecular and intramolecular interactions were determined using Natural Bond Orbital (NBO). Non-linear Optics (NLO) properties were shown based on first-order hyperpolarizability calculations. To determine whether a compound has the potential to be a pharmaceutical drug, Lipinski's rule of five is employed. For the title compound, all the drug-likeness parameters fall within the desired range, confirming its suitability as an effective oral medication. Molecular docking studies with the protein 1SR5 (anti-fibrinolytic) were done on the title compound (M2H4MB) and with a standard drug (Cilostazol) to treat Ischaemic strokes. M2H4MB shows a binding energy of -5.5 kcal/mol and the standard drug shows a binding energy of -5.1 kcal/mol. When comparing, the title compound shows good binding energy against the standard drug. This predicts that M2H4MB may be a suitable drug to treat Ischaemic stroke.

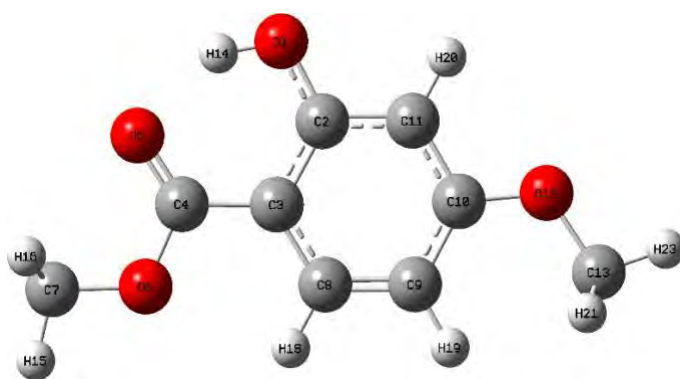


**Figure 1-** The optimized geometrical structure of the M2H4MB.

## REFERENCES

1. Leopold Jirovetz, *Journal of Essential Oil Research*, 2002;14:6,437-438.
2. Carl-Erik Dempfle, *Fibrinolytic Treatment of Acute Ischemic Stroke*, 2011;32:616–619

# About 10x faster image acquisition and two orders of magnitude faster tuning in SRS microscopy including the fingerprint region of relevant biological samples

Ingo Rimke<sup>a</sup>, Gero Stibenz<sup>a</sup>, Stefan Popien<sup>a</sup>, Peter Trabs<sup>a</sup>, Lenny Reinkensmeier<sup>b</sup>, Rene Siegmund<sup>b</sup>, Alexander Egner<sup>b</sup>, Sandro Heuke<sup>c</sup>

<sup>a</sup> APE Angewandte Physik & Elektronik GmbH, Berlin 13053, Germany

<sup>b</sup> Department of Optical Nanoscopy, Institute for Nanophotonics Göttingen, Göttingen, Germany

<sup>c</sup> Aix Marseille Univ, CNRS, Centrale Marseille, Institut Fresnel, Marseille 13013, France

We have successfully developed an advanced light source tailored for Coherent Raman microscopy and other nonlinear microscopy modalities, including SHG and multiphoton fluorescence. In comparison to the prevailing SRS light source available in the market (APE's picoEmerald S [1]), our innovative solution offers several notable enhancements.

One prominent advantage of the new light source lies in its significantly accelerated tuning speed. We have achieved a 100-fold increase for random wavelength access, including laser output power control and dispersion compensation. Switching to different Raman bands now takes about 1 second. As is state of the art, the light source setup includes both spatial and temporal overlap of Stokes and Pump laser beams to provide the application with a single laser beam. The temporal overlap can automatically adjust to the dispersion properties of the external optical setup (microscope).

To speed up image acquisition and improve signal, we have changed the repetition rate from 80 MHz to 40 MHz, resulting in doubled pulse energy. This in combination with a subharmonic modulation frequency of 20 MHz leads to a significant reduction of the pixel dwell time. The theoretical improvement is a factor of 8 all while maintaining the same Signal-to-noise ratio within the image [2]. The laser is based on proven solid state OPO technology and thus intrinsically shot noise limited from 5 MHz onwards. The output pulse lengths and bandwidths of 2 ps and about 10 cm<sup>-1</sup> respectively combine optimum spectral resolution with high sensitivity.

The OPO's redesigned optical cavity also allows for a wider wavelength coverage. The Signal beam is now tunable from 660 nm to 1020 nm (up from previously 700 nm to 990 nm) which corresponds to an Idler tuning range of 1040 nm to 2340 nm (up from 1080 nm to 1950 nm). To enhance SHG and TPF efficiencies even further, the new light source now allows to selectively increase the output bandwidth, which offers the opportunity to compress the pulse duration down to a few 100 fs.

We directly compare the image quality of the two light sources side by side coupled into the same microscope and will present CH- and fingerprint images of relevant biological samples.

## REFERENCES

1. Xu, H., Zhao, Y., Suo, Y. et al., "A label-free, fast and high-specificity technique for plant cell wall imaging and composition analysis," *Plant Methods*, 2021, **17**, 29.
2. Sandro Heuke, Xavier Audier, and Hervé Rigneault, "Double-modulation stimulated Raman scattering: how to image up to 16-fold faster," *Opt. Lett.*, 2023, **48**, 423-426.

# Tailoring the Cavity-Induced Interplay of Modes to Enhance Four-Wave Mixing over a Broadband Molecular Fingerprint Regime

Abhik Chakraborty<sup>1,2</sup>, Parijat Barman<sup>1,2</sup>, Ankit Kumar Singh<sup>2</sup>, Xiaofei Wu<sup>2</sup>, Denis A. Akimov<sup>2</sup>, Tobias Meyer-Zedler<sup>1,2</sup>, Stefan Nolte<sup>3,4</sup>, Carsten Ronning<sup>5</sup>, Michael Schmitt<sup>1</sup>, Jürgen Popp<sup>1,2</sup>, Jer-Shing Huang<sup>1,2</sup>

<sup>1</sup>Institute of Physical Chemistry and Abbe Center of Photonics, Friedrich Schiller University Jena, Helmholtzweg 4, 07743 Jena, Germany

<sup>2</sup>Leibniz Institute of Photonic Technology, Albert-Einstein Str. 9, 07745 Jena, Germany

<sup>3</sup>Institute of Applied Physics, Abbe Center of Photonics, Friedrich Schiller University Jena, Albert-Einstein-Str. 15, 07745 Jena, Germany

<sup>4</sup>Fraunhofer Institute for Applied Optics and Precision Engineering IOF, Center of Excellence in Photonics, Albert-Einstein-Str. 7, 07745 Jena, Germany

<sup>5</sup>Institute of Solid State Physics, Friedrich Schiller University Jena, Max-Wien-Platz 1, 07743 Jena, Germany

Four-wave mixing (FWM) signal originates from the instantaneously polarized electronic resonances inherent in matter. [1] However, the enhancement of said signal depends on the resonant enhancement enforced by the cavity. [1] For the most efficient use of complex nanostructures, a rigorous optimization of the interplay between the electromagnetic modes enforced by the different cavity geometries involved is critical. The ACG consists of a series of eccentrically displaced rings (grooves) that provides it with a continuously varying grating periodicity. This, in turn, offers the necessary phase-matching conditions capable of mediating the near field and the far field over a broad range of wavelengths via the enforcement of the specific order of diffraction responsible for producing in-plane lattice modes at certain wavelength-period combinations. [1-3] These modes essentially allow the plasmonic platform to host plasmonic surface lattice resonances (PSLR) which are characterized by sharp Fano lineshape in both the spectral domain and the non-spectral parametric domain [1]. In addition to that, the V-shaped grating grooves individually act as hosts of plasmonic hot spots, thereby, facilitating field enhancement and frequency conversion by virtue of their mode confinement and broadband momentum distribution, respectively. [1] With broadband FWM experiments and full-wave analysis, we shed light on the interplay between the groove-dependent localized surface plasmon resonance (LSPR) and the period-dependent PSLR to demonstrate the generation and enhancement of broadband FWM in complex periodic systems.

[1] A. Chakraborty *et al.*, Laser Photonics Rev. 17, 2200958 (2023).

[2] L. Ouyang *et al.*, ACS Nano 15, 809-818 (2021).

[3] P. Barman, A. Chakraborty *et al.*, Nano Lett. 22, 9914-9919 (2022).



# Precision-Engineered Nanostar Arrays for Enhanced SERS Analysis

Alexandre Chícharo<sup>a,b</sup>, Alexandra Teixeira<sup>a</sup>, Diogo Moreira<sup>a</sup>, Maria Relvas<sup>a</sup>, Marta Aranda-Palomer<sup>a</sup>, Jérôme Borme<sup>a</sup>, Lorena Diéguez<sup>a</sup>, Sara Abalde-Cela<sup>a</sup>

<sup>a</sup> INL - International Iberian Nanotechnology Laboratory, Braga 4715-330, Portugal.

<sup>b</sup> Department of Chemistry, Humboldt-Universität zu Berlin, Brook-Taylor-Straße 2, 12489 Berlin, Germany.

Abstract:

Surface Enhanced Raman Scattering (SERS) has rapidly evolved into a pivotal tool for molecular analysis across various domains, including medical diagnostics. Innovative top-down techniques, such as electron-beam lithography, have been employed to create high-density SERS arrays. These arrays consist of gold nanostars with diameters ranging from 20 to 650 nm and controlled interparticle distances (200-700 nm). Notably, resulting in a significant signal amplification in SERS, due to high density of hot spots at their tips.

Our research encompasses a systematic evaluation of engineered SERS substrates. We employ a widely recognized Raman Reporter molecule, 1-Naphthalenethiol (1NAT), to assess their performance. Furthermore, we showcase the substrate's versatility by successfully detecting tryptophan, a crucial metabolite found in specific tumor microenvironments, serving as a compelling proof-of-concept.

## ACKNOWLEDGMENTS

This work was supported from through project BIOCELLPHE (H2020-FETOPEN-2018-2020, grant agreement 965018), and by the 3DSecret project, funded by the EU under the program HORIZON-EIC-2022-PATHFINDEROPEN-01-01 (ga 101099066) and by the UK Research and Innovation (UKRI) under the UK government's Horizon Europe funding guarantee (ga 10063360). A. T acknowledges the FCT studentship SFRH/BD/148091/2019

## REFERENCES

1. Abalde-Cela S. et al., "Adv Opt Mater.," 9, 2001171 (2021).
2. Abalde-Cela S. et al., "Adv Colloid Interface Sci.," 233, 255-270 (2016).
3. Pavlova N.N. et al., "Cell Metab.," 23, 27-47 (2016).

## Deciphering the effect of solvent polarity and wavepacket dynamics in TADF emitting molecule using Transient absorption and ultrafast Raman Loss spectroscopy

Nishant Dhiman<sup>1</sup>, Muhammed Munthasir A T<sup>1</sup>, Pakkirisamy Thilagar<sup>1</sup>, Siva Umopathy<sup>1,2</sup>

<sup>1</sup> Department of Inorganic and Physical Chemistry, IISc Bangalore, Karnataka, India

<sup>2</sup> Department of Instrumental and Applied Physics, IISc Bangalore, Karnataka, India

Email: [nishantd@iisc.ac.in](mailto:nishantd@iisc.ac.in)

Photoinduced charge transfer reactions are ubiquitous in nature [1]. Charge transfer molecules are important for making Organic Light-Emitting Diodes (OLEDs). Recently, the strategy of incorporating heteroatoms such as Boron (B) and Nitrogen (N) in a conjugated carbon-based system (non-polar) can be used to make TADF materials. These charge transfer processes in a molecular system can affect structural relaxation in the excited state. Finding and understanding these non-radiative structural decay pathways are crucial to improving the quantum efficiency of TADF materials. In the present work, we investigate the coherent nuclear dynamics of the excited state of 10-dixyleylboryl phenoxazine (BNO) and the effect of solvent parameters such as polarity, viscosity and polarizability on excited state by femtosecond transient absorption spectroscopy and ultrafast Raman loss spectroscopy (URLS).

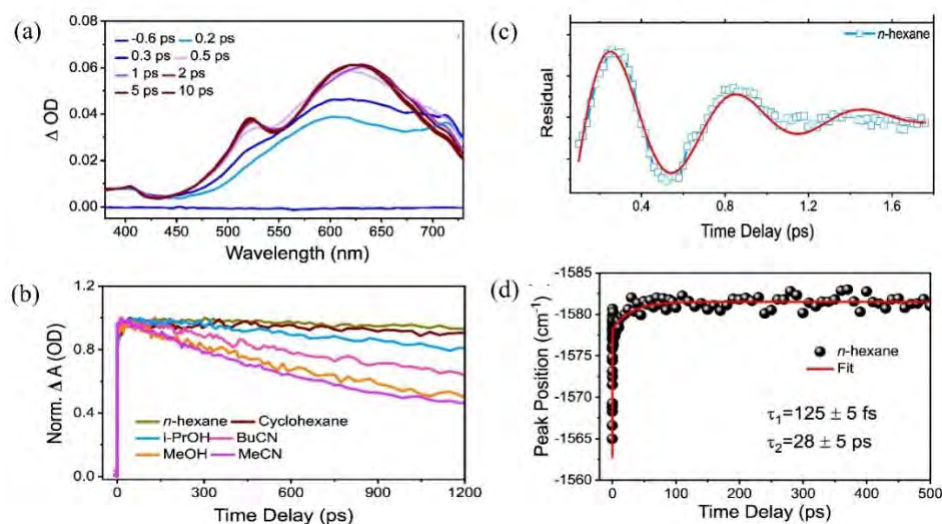


**Figure 1:** (a) Transient absorption spectrum at 320 nm photoexcitation in *n*-hexane (b) Normalized kinetics decay in solvents with different polarity (c) Coherent vibrational wave packet and (d) Raman peak position fitting at  $\sim 1582$   $\text{cm}^{-1}$  in *n*-hexane.

The coherent vibrational wave packet is observed in the kinetics trace of the transient absorption signal up to 1.5 ps as shown in Figure 1(c) which shows the real-time structural planarisation of the phenoxazine ring in the BNO molecule. Fourier Transformation of the observed oscillating signal results in low-frequency butterfly vibrations of  $\sim 60$   $\text{cm}^{-1}$  which is responsible for the Planarization of the phenoxazine ring. This work will provide an important reference for interpreting excited state dynamics in phenoxazine and BN-based charge transfer systems.

### References:

- [1] Grabowski, Zbigniew R., et al., Chemical reviews **103** (2003) 3899-4032.
- [2] Satoshi, Takeuchi, et al., J. Phys. Chem. A **109** (2005) 10199-10207.
- [3] Kalluvettukuzhy, Neena, et al., Chem comm **53** (2017) 3641.

# Spectroscopic imaging of Fabry disease-associated lipid accumulations in cardiac cells

Johann Dierks<sup>a</sup>, Nairveen Ali<sup>b</sup>, Irina Schuler<sup>a</sup>, Paula Arias-Loza<sup>c</sup> Peter Nordbeck<sup>c</sup>, Thomas Bocklitz<sup>b,d</sup>, Elen Tolstik<sup>a</sup> and Kristina Lorenz<sup>a,e,f</sup>

<sup>a</sup> *Leibniz-Institut für Analytische Wissenschaften – ISAS- e.V., Bunsen-Kirchhoff-Str. 11, 44139 Dortmund, Germany*

<sup>b</sup> *Leibniz Institute of Photonic Technology, Member of Leibniz Health Technologies, Albert-Einstein-Straße 9, 07745 Jena, Germany*

<sup>c</sup> *Department of Nuclear Medicine, University Hospital Würzburg, Josef-Schneider-Straße 2, 97080 Würzburg, Germany*

<sup>d</sup> *Institute of computer science, University of Bayreuth, Universitätsstraße 30, Bayreuth, Germany*

<sup>e</sup> *Institute of Pharmacology and Toxicology, University of Würzburg, Versbacher Str. 9, 97078 Würzburg, Germany*

<sup>f</sup> *Comprehensive Heart Failure Center, University Hospital of Würzburg, am Schwarzenberg 15, 97078 Würzburg, Germany*

**Introduction.** Fabry disease (FD) is a rare inherited lysosomal storage disorder due to alpha-galactosidase A ( $\alpha$ -Gal A) deficiency causing progressive multiorgan damage [1]. The leading cause of death in FD patients are cardiac manifestations. Cardiac involvement in FD is often diagnosed late, once irreversible damage already took place. All this makes a fast and reliable diagnostic tool necessary and desired. In our previous study it was shown that the use of coherent anti-Stokes Raman spectroscopy (CARS) enables differentiation between diseased and healthy mouse tissue samples with high sensitivity [2]. However more precise spectroscopic information is required to identify the type and stage of the disease.

**Objectives.** The aim of the current work is the application of Raman spectroscopy for accurate diagnosis of FD based on the disease-associated lipid biomarkers Gb3 and lyso-Gb3 in cardiac cells [3]. This would complement the previously described application of CARS spectroscopy on FD heart tissues of mice and would allow high specificity and accuracy by the investigation of cardiac involvement. Additionally, the behavior and lipid distribution between different cell types in FD is evaluated.

**Materials & methods.** Raman spectroscopy (RS) was applied to 50 isolated fibroblasts and 30 cardiomyocytes isolated from mouse hearts of  $\alpha$ -Gal A-knockout and wild type mice aiming to detect the disease-specific lipid accumulations of Gb3 and lyso-Gb3. Each cell measurement was preprocessed and grouped into several unique clusters based on spectral similarities utilizing hierarchical clustering analysis [4]. Afterwards for each cell, groups representing potential lipid candidates were selected by a house-written algorithm and afterwards compared with the lipid candidates of all other cell measurements. Finally, all candidates were grouped and sorted by the genotype with the goal to detect potential FD-specific biomarker lipids within certain cardiac cell types and compare the distribution between both groups.

**Results.** Since a spectroscopic signal is based on intrinsic molecular vibrations, the measurements using RS were highly specific and gave more precise definition of Gb3/lyso-Gb3 biomarkers compared to CARS imaging [1]. Certain lipid accumulations in cardiomyocytes were associated with Gb3 by comparing the cell signal to reference spectra and were exclusive in diseased mice. This is the first indication of the potential of RS to detect specific lipid-based biomarkers that accumulate intracellularly in Fabry disease. In contrast, a far higher lipid proportion compared to cell size and number was detected in fibroblasts, where they were often strongly localized around cell nucleus (Figure 1). This was detected for both genotypes of fibroblasts, isolated from knockout and wildtype mice, making a differentiation between the two groups difficult. Summarized, this work shows the potential of RS to detect and localize diseases-associated lipid accumulations even at early stages of FD disease. Additionally, cell-specific differences between cardiomyocytes and fibroblasts were obtained.

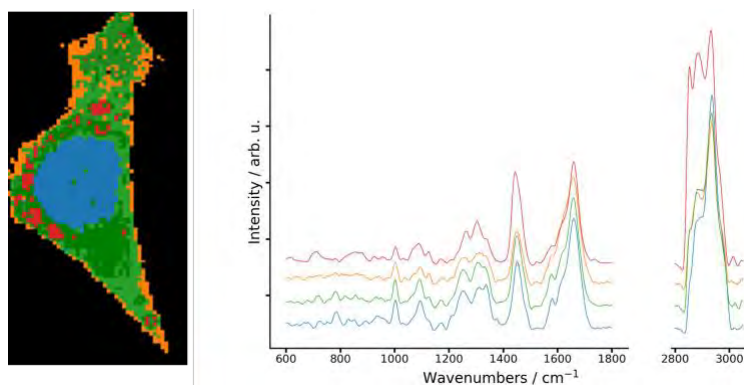


**Figure 1** Typical examples of reconstructed KO fibroblast (left) with corresponding mean spectra of k-Means clustering (right). Lipid clusters (depicted as a red group) are localized due to the lipid-specific Raman bands inside the cell.

## ACKNOWLEDGMENTS

We thank the support of the German Ministry of Research and Education (BMBF; ChinValue (03INT703AB), ERK-Casting (16GW0262K)), Deutsche Forschungsgemeinschaft's Collaborative Research Center SFB/TR 296 (#424957847) and SFB1525-B03 (#453989101) and the Drug Discovery Hub Dortmund (DDHD).

## REFERENCES

1. Oder et al. "α-Galactosidase A Genotype N215S Induces a Specific Cardiac Variant of Fabry Disease." *Circulation: Cardiovascular Genetics*, 2017, **10.5**,e001691
2. Tolstik et al. "CARS imaging advances early diagnosis of cardiac manifestation of Fabry disease." *International Journal of Molecular Sciences*, 2022, **23.10**,5345
3. Tolstik et al. "Cardiac multiscale bioimaging: from nano-through micro-to mesoscales." *Trends in Biotechnology*, 2023
4. Guo et al. "Chemometric analysis in Raman spectroscopy from experimental design to machine learning-based modeling." *Nature protocols*, 2021, **16**,5426-5459

# Quantitative and computational analysis, molecular docking studies, and in-vitro assays on 4-Isopropylbenzoic acid: A potential anti-parkinsonian drug

E. Eunice <sup>a, b</sup>, Johanan Christian Prasana <sup>a, b\*</sup>, S. Muthu <sup>c, d</sup>

<sup>a</sup> Department of Physics, Madras Christian College, East Tambaram 600059, Tamil Nadu, India.

<sup>b</sup> University of Madras, Chennai, 600005, Tamil Nadu, India.

<sup>c</sup> Department of Physics, Arignar Anna Government Arts College, Cheyyar, 604407, Tamil Nadu, India.

<sup>d</sup> Department of Physics, Puratchi Thalaivar Dr. M. G. R Govt. Arts and Science College, Uthiramerur, 603406, Tamil Nadu, India.

\* Corresponding author: [reachjcp@gmail.com](mailto:reachjcp@gmail.com)

Computational methods are extensively used for the in-depth characterization of compound binding and lead optimization [1]. Many computational methods have been employed in drug discovery. One of the most accurate and least time-consuming methods is the Density functional theory (DFT). A growing application of DFT is to understand the relationship between molecular structures, kinetics of binding, mode of action, and molecular interactions [2]. This has had a substantial impact on recognizing the importance of therapeutic action.

The research exploration of 4-Isopropylbenzoic acid (4-IPBA) extracted from plants *Libocedrus yateensis* (cypress) and *Bridelia retusa* (amla) involves investigating the structural, vibrational, bonding nature, electronic, topological and biological activity of 4-IPBA. Using Gaussian 16W software, this research is conducted at two levels: In the first level theoretical analyses were done on geometry, vibrational assignments (FT-IR, FT-R), UV-Vis, NBO, RDG, MEP, FMO, Drug likeness and Molecular docking. In the second level, experimental analyses were done on spectroscopic techniques (FT-IR, FT-Raman, and UV-Vis characterizing techniques) and in-vitro assays (Cytotoxicity). Finally, a comparison is drawn between the two levels and discussed.

Molecular geometry of 4-IPBA was fully optimized using the DFT B3LYP method with the 6-311++G(d,p) basis set. Figure 1 depicts 4-IPBA's optimized structure. The FT-IR and FT-R spectra were scaled, and prominent peaks were analyzed in detail. The complete vibrational assignments using Potential Energy Distribution (%PED) were calculated. All the experimental results were in line with the theoretical data. UV-Vis absorption spectrum for 4-IPBA was evaluated by the TD-DFT method in the gas and solvent phases. Stability and charge delocalization was studied by Natural Bond Orbital (NBO) analysis. The bonding zones and weakest interactions for 4-IPBA are seen in RDG studies. Local reactive properties of 4-IPBA have been addressed by MEP. Frontier molecular orbitals (FMO) analysis was performed. HOMO-LUMO energies, energy gap ( $\Delta E$ ), electronegativity ( $\chi$ ), chemical potential ( $\mu$ ), global hardness ( $\eta$ ), and softness ( $S$ ) were obtained. Low toxicity levels of 4-IPBA were calculated in terms of softness value (0.199 eV), and a high electrophilicity index (5.905 eV) describes the bioactivity. Lipinski's rule of five is an indicator that determines factors for a potent drug candidate. There is no violation found for the title compound. Analysing the parameters and comparing with the standard range suggests that, 4-IPBA is a good drug-like character. The Ramachandran plot was done to check the stereochemistry of



the protein (4BCB) structure. Docking studies of 4-IPBA were scrutinized to predict the preferred binding affinity and orientation. 4-IPBA was docked into the active site of protein 4BCB (antiparkinsonian), and a minimum binding energy of -5.1 kcal/mol was obtained. The commercially available drug Rivastigmine was theoretically studied for the same protein (4BCB), and its binding energy is -4.6 kcal/mol, which is comparable to the title compound. This predicts that 4-IPBA could be a suitable drug to treat Parkinson's dementia. To better understand the toxicity and bioavailability of the title compound, a cytotoxicity assay was also performed.

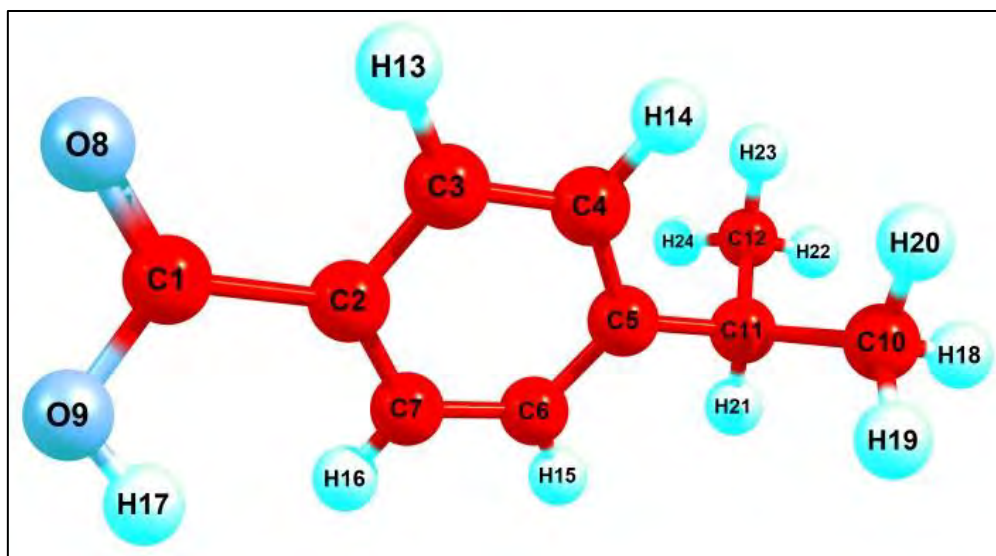


Fig. 1. Optimized structure of 4-Isopropylbenzoic acid

## REFERENCES

- [1] Copeland, Robert A., David L. Pompliano, and Thomas D. Meek. "Drug–target residence time and its implications for lead optimization." *Nature reviews Drug discovery* (2006) 5.9: 730-739.
- [2] Renaud, JP., Chung, Cw., Danielson, U. *et al.* Biophysics in drug discovery: impact, challenges and opportunities. *Nat Rev Drug Discov* (2016),**15**, 679–698.

# Data-driven infrared molecular fingerprinting: From *in silico* modeling to establishing a population-wide health screening platform

**Tarek Eissa**<sup>a,b,c</sup>, Marinus Huber<sup>a,b</sup>, Kosmas V. Kepesidis<sup>a,b,d</sup>, Cristina Leonardo<sup>a</sup>, Frank Fleischmann<sup>a,b</sup>, Birgit Linkohr<sup>e</sup>, Daniel Meyer<sup>b</sup>, Viola Zoka<sup>a,d</sup>, Liudmila Voronina<sup>a</sup>, Lothar Richter<sup>c</sup>, Annette Peters<sup>e,f,g,h</sup>, Mihaela Zigman<sup>a,b,d</sup>

<sup>a</sup> Ludwig Maximilian University of Munich, Department of Laser Physics, Germany

<sup>b</sup> Max Planck Institute of Quantum Optics, Laboratory for Attosecond Physics, Germany

<sup>c</sup> Technical University of Munich, School of Computation, Information and Technology, Germany

<sup>d</sup> Center for Molecular Fingerprinting, Hungary

<sup>e</sup> Helmholtz Zentrum München, Institute of Epidemiology, Germany

<sup>f</sup> Institute for Medical Information Processing, Biometry, and Epidemiology, Pettenkofer School of Public Health, Ludwig Maximilian University of Munich, Germany

<sup>g</sup> German Center for Diabetes Research, Germany

<sup>h</sup> German Centre for Cardiovascular Research, Partner Site Munich, Germany

Vibrational spectroscopy, with its ability to capture cross-molecular signatures of complex biological media in a holistic manner, offers a promising avenue for understanding and classifying a range of phenotypes linked to biological systems. Here, we explore the intersection of two recent studies where we harness the potential of infrared molecular fingerprinting to advance our understanding of personalized health diagnostics and establish a single-measurement multi-phenotype platform for populational screening.

We first delve into understanding the prospects and limits of infrared fingerprinting. Recently, we introduced an *in silico* modeling approach that draws on experimental observations and enables the generation of artificial infrared spectra of molecularly complex samples in arbitrary numbers [1]. Our approach provides the flexibility to fine-tune simulation parameters and generate realistic spectra that simulate diverse study setups and experimental paradigms. We apply machine learning methods to showcase how several, systematically-adjusted, parameters affect the performance of phenotyping biological systems using infrared spectroscopy of cell-free blood-based samples. Our results provide foundational insights into the effects of properties such as the noise introduced by measurement devices, biological variability and chemical complexity of analyzed samples. Applications of the *in silico* model which address different clinical questions, such as cancer detection and the prospects of personalized medicine, will be presented. We then discuss the current state of the published study and its future extensions.

In a parallel investigation, we extend the scope of infrared fingerprinting to population health screening. Recently, we carried out the largest cohort ( $n = 5184$ ) analysis involving infrared spectroscopy thus far, utilizing a population-based study which



reflects highly diverse individuals and true disease prevalence [2]. Coupling FTIR spectroscopy with machine learning analytics, we assessed the capacity of the combined approach to detect highly prevalent, coexisting phenotypes. Applying a custom multi-label classifier to simultaneously detect and distinguish between common health conditions, we found that the approach can accurately single out healthy individuals as well as characterize several chronic multimorbid states. Training and testing the classifier on spectra from different blood-based samplings (i.e., dataset-independent testing) led to very similar outcomes – underscoring the utility under realistic validation conditions. We further show that spectral data encode information that is conventionally retrieved by clinical laboratory test panels, which provides interpretability of the spectral data for the broader healthcare domain. Excitingly, we showcase how infrared fingerprinting has the capacity to detect pre-conditions and risk-stratify individuals at a time-critical stage, potentially preventing the development of further diseases.

Altogether, we present a data-driven approach to better understand the measurement characteristics of vibrational spectra, decode the biological information contained within them, and establish a high-throughput health screening platform. Although we focus on infrared spectroscopy of blood-based samples, the concepts and results presented extend to other sample types and molecular fingerprinting techniques.

## REFERENCES

1. T. Eissa, K. V. Kepesidis, M. Zigman, and M. Huber, “Limits and prospects of molecular fingerprinting for phenotyping biological systems revealed through *in silico* modeling,” *Analytical Chemistry*, vol. 95, no. 16. pp. 6523–6532, 2023. doi: 10.1021/acs.analchem.2c04711.
2. T. Eissa, C. Leonardo, K. V. Kepesidis, M. Huber, F. Fleischmann, B. Linkohr, D. Meyer, V. Zoka, L. Voronina, L. Richter, A. Peters, M. Zigman, “Integrative plasma infrared fingerprinting with machine learning enables single-measurement multi-phenotype health screening,” *Cell Reports Medicine*, 2023. Manuscript in Review.

# Application of surrogate minimal depth to unravel surface-enhanced Raman scattering data

Florian Gärber<sup>a</sup>, Stephan Seifert<sup>a</sup>

<sup>a</sup> *Hamburg School of Food Science, Grindelallee 117, University of Hamburg, Hamburg, Germany*

When surface-enhanced Raman scattering (SERS) is applied without labels or reporter molecules for the study of biological samples, complex data are obtained. This is due to the varying interaction of the molecules with the nanostructured metal substrate and is particularly the case when samples containing many different biomolecules are analyzed. Here we introduce a novel approach based on random forest that is very promising for the comprehensive exploitation of SERS data.

Random forest (RF) is a non-parametric machine learning approach that consists of a large number of individual binary decisions and has many advantages, such as flexibility in terms of input and output variables and the possibility of internal validation. Another advantage is the ability to generate variable importance measures that are used to select relevant features. However, the relationships between the predictor variables are usually not examined. We developed a novel RF based variable selection approach called Surrogate Minimal Depth (SMD) that incorporates relations into the selection process of important variables [1]. This is achieved by the exploitation of surrogate variables that have originally been introduced to deal with missing predictor variables. In addition to improving variable selection, surrogate variables and their relationship to the primary split variables can also be utilized as proxy for the relations between the different variables. This relation analysis goes beyond the investigation of ordinary correlation coefficients because it is based on the mutual impact on the outcome.

We present the basic concept of surrogate variables, SMD variable selection and relation analysis and their successful application to SERS data. We show that this approach can separate different co-occurring SERS signals, which facilitates the interpretation of complex SERS data [2].

## R PACKAGE

<https://github.com/AGSeifert/RFSurrogates>

## ACKNOWLEDGMENTS

This work is funded by the Deutsche Forschungsgemeinschaft (DFG, German Research Foundation) – 511107129.

## REFERENCES

1. S. Seifert, S. Gundlach, S. Szymczak, *Bioinformatics*, 2019, **35**, 3663-3671.
2. S. Seifert, *Scientific Reports*, 2020, **10**, 5436.

# Pregnancy Detection Based on Serum Samples Raman Spectroscopy

José Luis González-Solís<sup>1</sup>, Moisés Alejandro Lechuga-Zárate<sup>2</sup>, Francisco Hernandez-Salazar<sup>3</sup>

<sup>1</sup>Centro Universitario de los Lagos, Universidad de Guadalajara, Lagos de Moreno, México

<sup>2</sup>Centro Universitario de Ciencias Exactas e Ingenierías, Universidad de Guadalajara, Guadalajara, México

<sup>3</sup>Siena Clinic, Gynecology laboratory, León, México

In this research, we propose to use Raman spectroscopy as a pregnancy test using serum samples. Raman spectroscopy is a vibrational technique which provides information about the chemical structure. In particular, the Raman technique has impacted heavily on the study of various degenerative diseases, in particular cancer. However, this technique also has been used to study the health statuses of patients, which are difficult to diagnose with conventional techniques.

Serum samples were obtained from twelve women patients who were diagnosed pregnant and eleven control (no pregnant) volunteers. Spectra were collected at a Horiba Jobin-Yvon LabRAM HR800 Raman Spectrometer with a laser of 830 nm wavelength and 17 mW power. For each serum sample, 10 Raman spectra were obtained by focusing the laser on different points of the sample. Raw spectra were processed by carrying out baseline and smoothing correction to remove noise, fluorescence, and shot noise. Subsequently, they were normalized and analyzed using Principal Component Analysis (PCA).

In these spectra, we can observe characteristic bands of main biomolecules of serum samples as phenylalanine, tyrosine, amide III, phospholipid, carotene, and tryptophan. Furthermore, it is shown that the serum samples from control and pregnant patients can be discriminated against when PCA is applied to Raman spectra, obtaining two large clusters corresponding to the control and pregnant women.

The identification of the pregnant women based on serum samples Raman spectroscopy could be an alternative technique to traditional pregnancy tests. The results suggest that Raman spectroscopy technique can be used to study gynecological diseases.

# A mid-IR spectroscopic setup for identifying viruses in human saliva under high throughput conditions

J. Grzesiak<sup>a</sup>, A. Walter<sup>a</sup>, L. Fellner<sup>a</sup>, A. Brosig<sup>b</sup>, R. Horlacher<sup>b</sup>, R. Möller<sup>c</sup>, F. Duschek<sup>a</sup>

<sup>a</sup> German Aerospace Center (DLR), Institute of Technical Physic, 74239 Hardthausen, Germany

<sup>b</sup> trenzyme GmbH, 78467 Konstanz, Germany

<sup>c</sup> German Aerospace Center (DLR), Institute of Aerospace Medicine, 51147 Koeln, Germany

Mid-IR-Spectroscopy promises high selective capabilities for the detection of viruses such as SARS-CoV2 in human saliva. The motivation for this work was driven by the demand for enhanced COVID testing capabilities, especially in scenarios with large number of people passing, e.g. at airports. To achieve this, high and fast throughput of taken saliva samples is required. Additionally, high true positive rates are essential, when identifying the viral signatures e.g. by machine learning techniques.

In this progress report, we present our approach for a high and fast throughput detection setup: The mid-IR spectroscopy part is based on quantum cascade lasers (QCL) and attenuated total reflection flow cells. To enrich the concentration of the viral load in the saliva sample, we use functionalized magnetic beads. The sample handling part is designed to be automatized for the later application. This can allow for a much faster spectral scan than compared to for example FTIR methods and a possible higher throughput of samples, as for example for Raman microscopy approaches<sup>1</sup>. In our setting, detecting low concentrations of viral loads in aqueous solutions is challenging due to the dynamic range required for the detectors. We present a balanced detection approach to achieve a reasonable dynamic range and discuss the implications for the automatized identification.

The diversion of sample material during the cleaning procedure of the flow cells, the purification process with the protein-coated magnetic beads and other impurities can cause variations in the amide I and amide II vibration bands, disturbing the virus signatures. Along our measured spectra we discuss these upcoming challenges for the AI-based reliable identification of the viruses with respect to the creation of training datasets.

## REFERENCES

1. Pahlow, S.; Richard-Lacroix, M.; Hornung, F.; Köse-Vogel, N.; Mayerhöfer, T.G.; Hniopek, J.; Ryabchykov, O.; Bocklitz, T.; Weber, K.; Ehrlich, R.; et al., *Biosensors*, 2023, **13**, 594.

## Deep tissue single laser source multimodal microscopy

Hehl Gregor<sup>1</sup>, Goncharov Semyon<sup>1</sup>, Kadiwala Moinuddin<sup>1</sup>, Baltrusch Simone<sup>2,3</sup>, Pronin Oleg<sup>1</sup>

<sup>1</sup> Helmut-Schmidt-Universität/Universität der Bundeswehr Hamburg, Hamburg, Germany

<sup>2</sup> Institute of Medical Biochemistry and Molecular Biology, University Medicine Rostock, Rostock, Germany

<sup>3</sup> Department Life, Light & Matter, University of Rostock, Rostock, Germany

Various multimodal nonlinear laser scanning microscopy systems allowing the simultaneous detection of different imaging modalities like two- or three-photon fluorescence, FLIM, FCS, SHG, THG and/or CARS and SRS have been reported in the literature during the recent years [1],[2].

Often these reported systems need several individual laser sources for each imaging modality what makes these systems very expensive and complex to use. This rather complex realization also settles important laser parameters like e.g. the repetition rates, what makes e.g. a synchronization of all laser sources involved more and more difficult. However, such unsynchronized high repetition rate laser sources allow for the combination of a few imaging modalities but with certain drawbacks: one drawback is that considerably high average powers are needed for imaging, and as a second drawback no information regarding the individual photon detection events can be obtained because of both the high repetition rate and the lack of synchronized detection.

We report of the proceedings of our laser scanning microscopy system under development, capable of combining different imaging modalities using only one fs-laser source. Using appropriate laser sources allows to vary important laser parameters like eg. the repetition rates, chirp etc., but also to quickly replace or switch between laser sources. Furthermore the detection is fully synchronized with the laser source independent of the repetition rate chosen. This allows not only the simultaneous detection of SHG, two- and three photon fluorescence using up to four channels, but also the determination of fluorescence lifetimes (in the ns regime with sub-ns resolution).

Specifically, we demonstrate multimodal imaging with short pulses (< 50 fs) on human eye cornea tissue. Simultaneous forward and epi detection of SHG, THG, two- and threephoton fluorescence allows the characterization of the collagen structure as well as its rearrangement in patients with endothelial corneal

dystrophy[3]. The setup presented provides a wide range of excitation wavelengths ranging from below 800 nm and extending beyond 1200 nm by using a dual compression stage that greatly broadens the laser spectrum[4]. By selecting wavelengths around 930 nm, 1200 nm and 1300 nm respectively, a large penetration depth into the tissue is achieved (Figure). In addition, we ensure short pulse durations in the focal plane by pre-compensating the laser pulses. In combination, imaging deep in tissue is possible, and by selecting different excitation wavelength, we can infer the different substances involved and their local distribution. We furthermore demonstrate how on the other hand variable broadband excitation can be exploited to quickly determine how many compounds are present in the sample. Although not allowing as deep imaging as in the narrowband approach, variable broadband excitation allows us to determine how the compounds are arranged in 3D up to a certain depth. Both, the narrowband and the broadband approach together are thus completing the obtained information and help to verify the obtained findings.

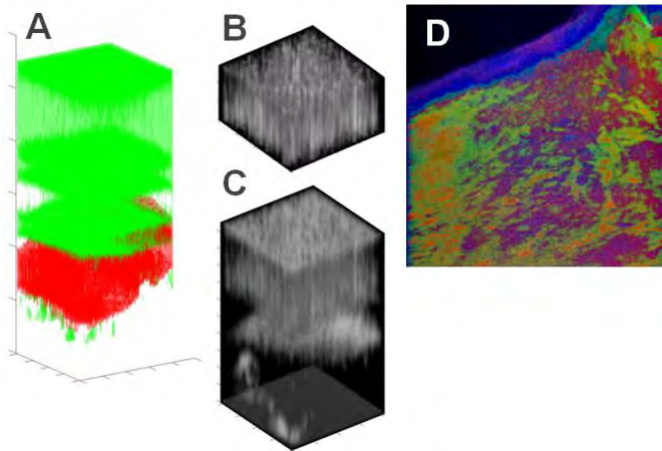


Fig.: Extracted isosurfaces of two-(red) and three-photon (green) fluorescence/SHG 3D images (A), enhanced contrast of the three-photon data (B, C, unlabeled human cornea tissue, narrowband excitation, 15 mW,  $207 \times 207 \times 540 \mu\text{m}^3$ ). RGB overlay of three identified Independent components as retrieved from two- and three-photon fluorescence / SHG 2D images by varying the excitation spectrum (unlabeled mouse cornea, broadband excitation, 15 mW).

[1] Chung Hsiang-Yu; Greinert, Rüdiger; Kärtner, Franz X.; Chang Guoqing. Multimodal imaging platform for optical virtual skin biopsy enabled by a fiber-based two-color ultrafast laser source. *Biomed. Opt. Express*. 2019 Jan 10;10(2):514-525.

[2] Schmitt, Michael; Meyer-Zedler, Tobias; Guntinas-Lichius, Orlando; Popp, Jürgen (2022): Multimodal spectroscopic imaging: A new, powerful tool for intraoperative tumor diagnostics. *Chirurgie*



[3] Walckling Marcus; Waterstradt Rica; Baltrusch Simone (2020): Collagen remodeling plays a pivotal role in endothelial corneal dystrophies. *Invest Ophthalmol Vis Sci.* 2020;61(14):1

[4] Semyon, Goncharov; Kilian, Fritsch; Oleg, Pronin (2022): White Light Generation and Few Cycle Pulse Compression in Cascaded Multipass Cells. In *Optics Letters.* 48(1), pp. 147-150.  
DOI:10.1364/OL.479248.

# Rapid electric-field molecular fingerprinting for infrared phenotype diagnostics

Philip Jacob<sup>a,b</sup>, Alexander Weigel<sup>a,b,c</sup>, Kosmas V. Kepesidis<sup>a,b,c</sup>, Wolfgang Schweinberger<sup>a,b,c</sup>, Marinus Huber<sup>a,b</sup>, Michael Trubetskov<sup>a</sup>, Patrik Karandušovský<sup>c</sup>, Frank Fleischmann<sup>a,b</sup>, Eric Griebinger<sup>b</sup>, Ferenc Krausz<sup>a,b,c</sup>, Ioachim Pupeza<sup>a,b,d</sup>, Mihaela Žigman<sup>a,b,c</sup>

<sup>a</sup> Max Planck Institute of Quantum Optics, Hans-Kopfermann-Str. 1, 85748 Garching, Germany

<sup>b</sup> Ludwig Maximilian University Munich, Am Coulombwall 1, 85748 Garching, Germany

<sup>c</sup> Center for Molecular Fingerprinting (CMF), 1093 Budapest, Czuczor utca 2-10, Hungary

<sup>d</sup> Leibniz Institute of Photonic Technology, Albert-Einstein-Straße 9, 07745 Jena, Germany

Human blood plasma is a very complex mixture of biomolecules. Compared to invasive clinical testing, which is often limited in molecular coverage and depth of molecular analysis, infrared spectroscopy of complex biofluids provides a valuable, minimally invasive, single-measurement diagnostic approach. Several recent studies have explored the efficacy of cell-free blood-based infrared molecular fingerprinting to determine the state of an individual's health [1-5]. The previously applied approach has involved the use of commercially available Fourier transform infrared spectrometers. Harnessing the potential of femtosecond laser technology, we developed a new rapid-scanning, field resolved infrared spectrometer that captures mid-infrared waveforms by the technique of electro-optic sampling.

The experimental setup consists of two mode-locked laser oscillators with an active repetition frequency synchronization lock. The first laser source, in combination with Herriott-cell compression stages, delivers few-cycle near-infrared pulses at a repetition frequency of 28 MHz, with an average power of 60 W. These pulses drive the formation of mid-infrared radiation in a LiGaS<sub>2</sub> crystal by the process of intra-pulse difference frequency generation. The mid-infrared beam is transmitted through a liquid flow-through cuvette to measure the sample, in this case, human blood plasma.

The pulses from the second mode-locked laser are spectrally broadened in a highly nonlinear fiber [6] and temporally compressed to 11 fs. The beam is spatially combined with the mid-infrared beam, and acts as a gate for electro-optic sampling. The relative optical delay between each pair of mid-infrared and gate pulses is controlled by tuning the pulse repetition frequency of laser 2 with respect to that of laser 1 using an electronic frequency lock [7]. We use the technique of electro-optic delay tracking to ensure attosecond timing precision for the optical delay axis [8].

The developed instrument was deployed in the *Lasers4Life* multi-centric clinical study (German Clinical Trial Register: DRKS00019844) to evaluate the accuracy in classifying individuals with cancer of the lung, prostate, breast and bladder at therapy

naïve states from the infrared molecular fingerprints of blood plasma. The results of the clinical sample measurements will be discussed.

## REFERENCES

1. M. Huber, K. V. Kepesidis, L. Voronina, F. Fleischmann, E. Fill, J. Hermann, I. Koch, K. Milger-Kneidinger, T. Kolben, G. B. Schulz, F. Jokisch, J. Behr, N. Harbeck, M. Reiser, C. Stief, F. Krausz, M. Žigman, *eLife*, 2021, **10**, e68758.
2. K. M. G. Lima, K. B. Gajjar, P. L. Martin-Hirsch, F. L. Martin, *Biotechnology Progress*, 2015, **31**, 832-839
3. D. Sheng, X. Liu, W. Li, Y. Wang, X. Chen, X. Wang, *Spectrochimica Acta Part A: Molecular and Biomolecular Spectroscopy*, 2013, **101**, 228-232
4. J. Backhaus, R. Mueller, N. Formanski, N. Szlama, H.-G. Meerpohl, M. Eidt, P. Bugert, *Vibrational Spectroscopy*, 2010, **52**, 173-177
5. M. Huber, K. V. Kepesidis, L. Voronina, M. Božić, M. Trubetskov, N. Harbeck, F. Krausz, M. Žigman, *Nature Communications*, 2021, **12**, 1511
6. D. Brida, G. Krauss, A. Sell and A. Leitenstorfer, *Laser & Photonics Reviews*, 2014, **8**, 409-428
7. S. Kray, F. Spöler, T. Hellerer, H. Kurz, *Opt. Express*, 2010, **18**, 9976-9990
8. A. Weigel, T. Buberl, P. Jacob, T. Amothckina, C. Hofer, et al., *Conference on Lasers and Electro-Optics Europe and European Quantum Electronics Conference*, 2021, paper cf\_9\_5

# Portable confocal POCT Raman spectrometer for biological/biomedical applications

Izabella J. Jahn<sup>a</sup>, Henry John<sup>a</sup>, Sebastian Bierwirth<sup>a</sup>, Jürgen Popp<sup>a,b</sup>,  
Walter Hauswald<sup>a</sup>

<sup>a</sup> Leibniz Institute of Photonic Technology, Albert-Einstein-Straße 9, D-07745 Jena, Germany, member of the Leibniz Research Alliance Leibniz Health Technology and of the Leibniz Centre for Photonics in Infection Research (LPI) Jena, Germany

<sup>b</sup> Institute of Physical Chemistry and Abbe Center of Photonics, Friedrich Schiller University Jena, Helmholtzweg 4, 07743 Jena, Germany

Raman spectroscopy is usually associated with the image of a large and expensive laboratory equipment. During the last years, multiple low-cost, portable Raman systems have been developed. The driving force behind this is the ability of the technique to probe the biochemical composition of samples in a non-destructive, non-invasive and label-free fashion yielding information on the molecular level. The great majority of these devices are dedicated to the identification of bulk materials, such as powders or liquids for forensic applications. Therefore, they are not equipped with a sample positioning unit or a widefield camera; they offer poor confocality and low spectral resolution. For biological applications of Raman spectroscopy all these aspects are crucial in order to obtain reliable results.

In a previous study [1] we showed that biosensor applications based on Raman spectroscopy do not in every case profit from the most expensive equipment. Namely, when the sample causes an auto fluorescence background, the fluorescence shot noise will play a decisive role. This is the case for most biological samples investigated with Raman spectroscopy. Therefore, there is no need to reduce the dark current shot noise of the detector significantly below the fluorescence shot noise of the sample by cooling the CCD below the freezing point. This paves the way to potent, economic, and portable confocal Raman biosensors.

Within this contribution the development, optimization and characterization of a confocal point of care (POCT) Raman device for biomedical applications is presented. An excitation laser emitting at 785 nm, a widefield unit, a xyz sample positioning unit, a spectrometer and all other optical and electrical elements are integrated in one device with a footprint of an A4 paper sheet.

In order to test the performance of the confocal POCT Raman device, reference Raman samples (such as silicon wafer, polymers and powders) as well as biological samples (human blood plasma, tissue) are measured. The results are compared with the performance of the laboratory grade Raman setup. Parameters, such as signal quality, spectral resolution and optical sectioning were assessed. In **Figure 1** the Raman spectra of polypropylene and human blood plasma, measured with the confocal POCT Raman spectrometer and with the reference device, are illustrated. Based on these results, it can be concluded that the confocal POCT Raman device yields spectral performances suitable for biomedical applications.

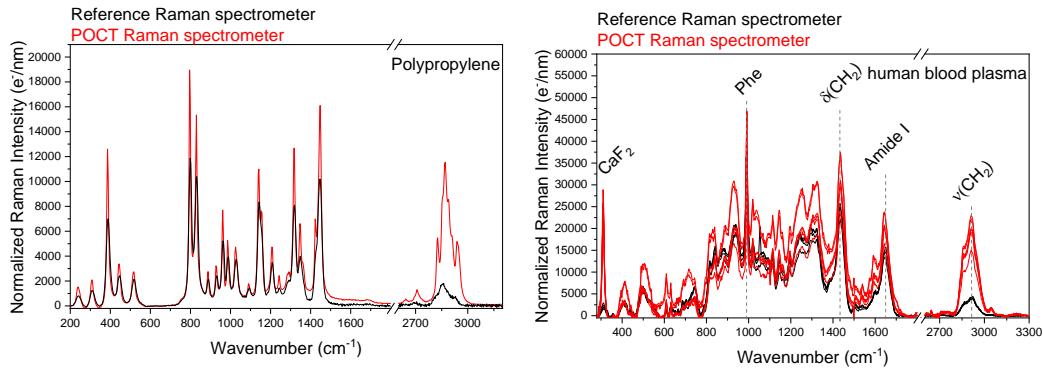


**Figure 1** Raman spectra of polypropylene and human blood plasma measured with the confocal POCT Raman device and a laboratory grade Raman spectrometer. In order to compare the light efficiency of both instruments, the raw data was converted into photoelectrons per nm. The conversion factors and the spectral resolution of the respective spectrometers were taken into account.

## ACKNOWLEDGMENTS

This work is supported by the BMBF, funding program Photonics Research Germany (13N15704) and is integrated into the Leibniz Center for Photonics in Infection Research (LPI). The LPI initiated by Leibniz-IPHT, Leibniz-HKI, UKJ and FSU Jena is part of the BMBF national roadmap for research infrastructures.

## REFERENCES

1. I. J. Jahn, A. Grjasnow, H. John, K. Weber, J. Popp, W. Hauswald, *Sensors*, 2021, 21, 5067.

# Autofluorescence spectral analysis for detecting urinary stone composition in emulated intraoperative ambient

Xing Li<sup>a,b</sup>, Siji Song<sup>b</sup>, Jiwei Yao<sup>c</sup>, Xiang Liao<sup>c</sup>, Min Chen<sup>b</sup>, Jinliang Zhai<sup>a</sup>, Lang Lang<sup>b</sup>, Chunyan Lin<sup>b</sup>, Na Zhang<sup>b</sup>, Chunhui Yuan<sup>d</sup>, Chunxia Li<sup>b</sup>, Hui Li<sup>b</sup>, Xiao Jun Wu<sup>b</sup>, Jing Lin<sup>b</sup>, Chunlian Li<sup>b</sup>, Yan Wang<sup>e</sup>, Jing Lyu<sup>e</sup>, Zhenqiao Zhou<sup>e</sup>, Mengke Yang<sup>e,f</sup>, Hongbo Jia<sup>a,e,g</sup>, Junan Yan<sup>b,c,d</sup>

<sup>a</sup> Advanced Institute for Brain and Intelligence, School of Physical Science and Technology, Guangxi University, Nanning, China

<sup>b</sup> Department of Urology, Southwest Hospital, Third Military Medical University, Chongqing, China

<sup>c</sup> Center for Neurointelligence, School of Medicine, Chongqing University, Chongqing, China.

<sup>d</sup> Chongqing Institute for Brain and Intelligence, Guangyang Bay Laboratory, Chongqing, China

<sup>e</sup> Brain Research Instrument Innovation Center, Suzhou Institute of Biomedical Engineering and Technology, Chinese Academy of Sciences, Suzhou, China

<sup>f</sup> UK Dementia Research Institute at UCL, University College London, WC1E 6BT London, UK.

<sup>g</sup> Leibniz Institute for Neurobiology, Magdeburg, Germany

The prevalence and disease burden of urolithiasis has increased substantially worldwide in the last decade, and intraluminal holmium laser lithotripsy has become the primary treatment method. However, inappropriate laser energy settings increase the risk of perioperative complications, largely due to the lack of intraoperative information on the stone composition, which determines the stone melting point. To address this issue, we developed a fiber-based fluorescence spectrometry method that detects and classifies the autofluorescence spectral fingerprints of urinary stones into three categories: calcium oxalate, uric acid, and struvite. By applying the support vector machine (SVM), the prediction accuracy achieved 90.28 % and 96.70% for classifying calcium stones versus non-calcium stones and uric acid versus struvite, respectively. High accuracy and specificity were achieved for a wide range of working distances and angles between the fiber tip and stone surface in an emulated intraoperative ambient. Our work establishes the methodological basis for engineering a clinical device that achieves real-time, in situ classification of urinary stones for optimizing the laser ablation parameters and reducing perioperative complications in lithotripsy.

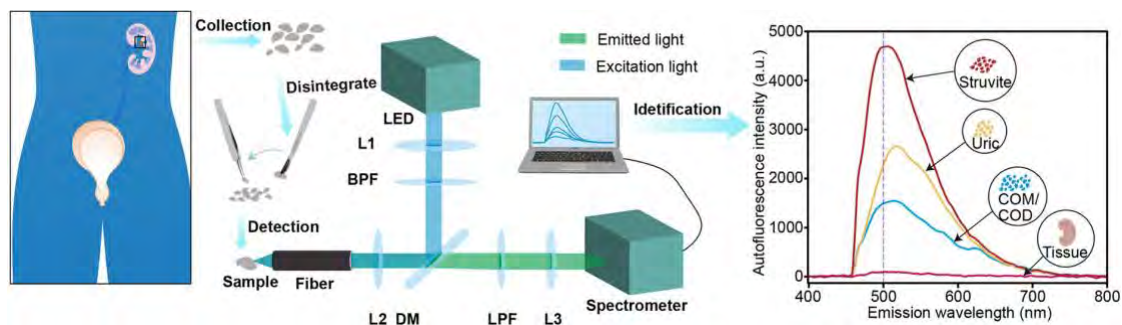


**Figure 1** The urinary stones were segmented to ~ 1 mm in size after urinary stone samples were collected from patients. Then, the autofluorescence spectrum of each sample was acquired with the custom-built fluorescence spectrometry device. Calcium oxalate, uric acid, struvite, and kidney tissues were successfully distinguished with high accuracy and specificity by analyzing the characteristics of fluorescence spectra.

## **ACKNOWLEDGMENTS TIMES NEW ROMAN- BOLD 14 PT**

This project was supported by grants from the National Natural Science Foundation of China (31970946, 61705251, 32127801); the Talent Project of Chongqing (4246ZP1252); the Youth Innovation Promotion Association, Chinese Academy of Sciences (No. 2022328); the Scientific Instrument Developing Project of the Chinese Academy of Sciences (YJKYYQ20200052); the Major scientific research facility project of Jiangsu Province, China (BM2022010); the Jiangsu Innovation and Entrepreneurship Team Fund.

## **REFERENCES**

1. A. Authors, *Journal*, Year, **Volume**, 1stPage-lastpage.



# Effect of non-resonant background on the CARS data analysis

Rajendhar Junjuri<sup>a,b</sup>, Tobias Meyer-Zedler<sup>a,b</sup>, Michael Schmitt<sup>b</sup>, Jürgen Popp<sup>a,b</sup>, Thomas Bocklitz<sup>a,b,c</sup>

<sup>a</sup> Leibniz Institute of Photonic Technology, Member of Research Alliance “Leibniz Health Technologies”, 07745 Jena, Germany

<sup>b</sup> Institute of Physical Chemistry and Abbe Center of Photonics (IPC/ACP), Friedrich-Schiller University (FSU), Helmholtzweg 4, D-07743 Jena, Germany

<sup>c</sup> University of Bayreuth, Institute of Computer Science, 95447 Bayreuth, Germany

Coherent Anti-Stokes Raman Spectroscopy (CARS) is a label-free analytical technique that provides vibrational fingerprint information of the molecule. Higher signal strength and no fluorescence effects are the advantages of the CARS over the spontaneous Raman technique. All these capabilities enabled it as a rapid imaging and spectroscopic tool for various applications<sup>1</sup>. However, non-resonant background (NRB) signals originating from electronic resonances significantly distort the spectral line shapes and impact the accuracy of CARS measurements. Various experimental approaches were proposed to reduce the effect of NRB but at the cost of increasing experimental complexity<sup>2</sup>. However, these techniques also reduced the measured CARS signal intensity. Hence, numerical phase retrieval approaches, such as the maximum entropy method (MEM)<sup>3</sup> and Kramers-Kronig (KK)<sup>4</sup>, were proposed, but they require optimization of the input parameters. Very recently, deep learning (DL) models such as convolutional neural network (CNN)<sup>5</sup> and long short-term memory (LSTM)<sup>6</sup> networks were explored to remove the NRB from the CARS signal. All these recent works were devoted to removing NRB, but no one studied its effect on the Raman signal retrieval<sup>7</sup>.

Hence, in this work, we have systematically investigated the effect of NRB variation on the CARS data simulation and corresponding Raman signal retrieval. The NRB is assumed as a linear function with different strengths of 0.01, 0.1, 1, 10, 100, and 1000 compared to the resonant Raman signal. Also, the variance is changed in the range of 0.001-100 for each NRB strength. First, the CARS data is simulated by considering different NRB strengths and variance combinations. For example, the CARS data simulated with  $\text{NRB } 100 \pm 1$  is shown in Figure 1a. Then, the corresponding Raman signal is retrieved by four different methods: MEM, KK, CNN, and LSTM. The MEM prediction is shown in Figure 1b. The background corrected prediction is shown in Figure 1c where the predicted imaginary part closely resembles the ground truth. Further, the predictive performance of the model is evaluated by measuring Pearson correlation coefficients (PCC) for the predictions. The PCCs estimated for MEM predictions for all the NRB combinations are shown in Figure 1d. The PCCs are decreasing with increasing NRB strength. Finally, the PCC measurements revealed that MEM and KK methods have an edge over LSTM and CNN for higher NRB strengths. It is also demonstrated background removal from the predictions significantly influenced the Pearson correlation for MEM and KK.

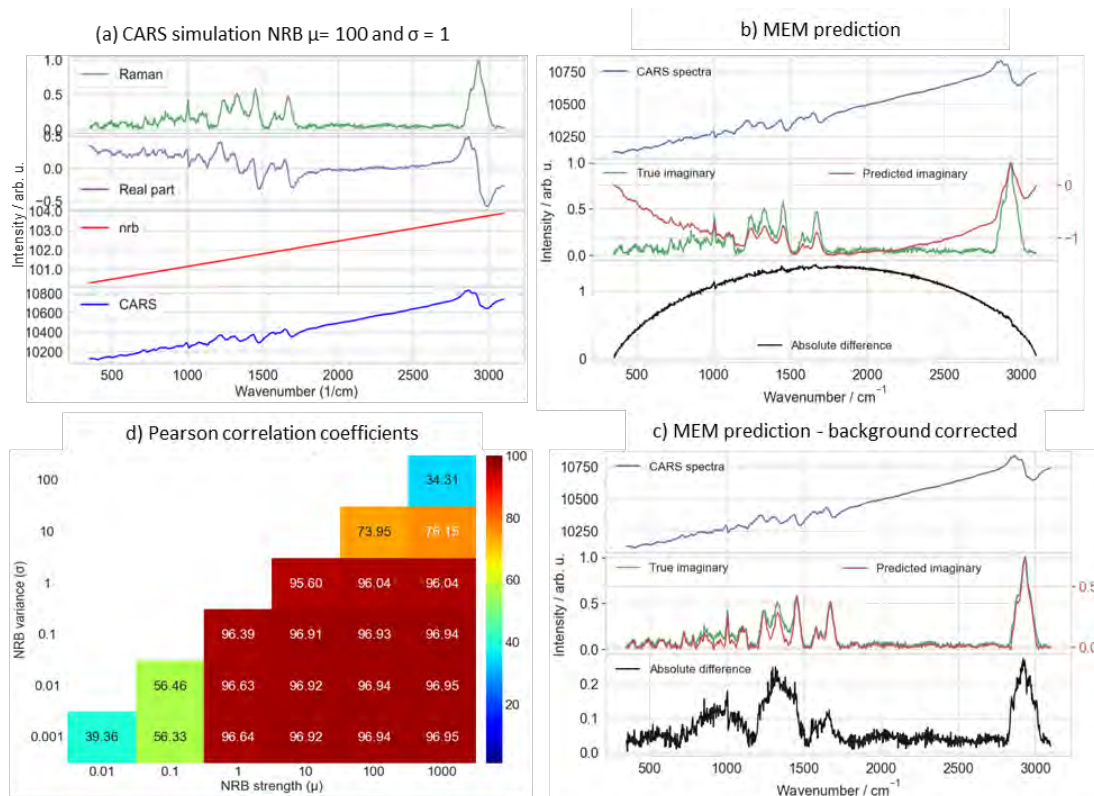


**Figure 1** a) Represents the different steps involved in the CARS data simulation. Green and purple lines represent the background corrected Raman spectrum and the corresponding real part extracted by the KK algorithm. The red line is the NRB spectrum simulated with a strength of 100 and a variance of 1. The last blue corresponds to the final simulated CARS signal. b) Represents the MEM prediction. A blue line at the top represents the input CARS data. In the middle row, the predicted imaginary and ground truth is shown in red and green colour. The last row visualizes the absolute difference between the predicted output and ground truth. c) Background corrected MEM prediction. d) Represent the average of Pearson correlation coefficients (PCC) obtained from the MEM predictions for different NRB strength combinations. Here, PCC values represent the similarity percentage between the predicted and true spectrum. PCCs decreased with increasing NRB strength. The correlation also increased after background correction from the prediction.

## ACKNOWLEDGMENTS

This work is supported by the EU funding program with grant number 101016923 for the project CRIMSON.

## REFERENCES

1. Tolles, W. M., Nibler, J. W., et al., *Applied Spectroscopy*, 1977, **31**, 253-271
2. Müller, M., Zumbusch, A., *ChemPhysChem*, 2007, **8**, 2156-2170
3. Vartiainen, E. M., Rinia, H. A., et al., *Optics Express*, 2006, **14**, 3622-3630
4. Lucarini, V., Saarinen, J. J., et al., Springer Science & Business Media: 2005; Vol. **110**.
5. Valensise, C. M., Giuseppi, A., et al., *Apl Photonics*, 2020, **5**, 0613051-0613058.
6. Houhou, R., Barman, P., et al., *Optics Express*, 2020, **28**, 21002-21024.
7. Junjuri, R., Saghi, A., et al., *Phys Chem Chem Phys*, 2023, **25**, 16340-16353

# Ultrabroadband two-beam CARS on organic fluids – a comparison with Raman spectroscopy

Timea Koch<sup>a</sup>, Roland Ackermann<sup>a</sup>, Axel Stoecker<sup>b</sup>, Tobias Meyer-Zedler<sup>c,d</sup>, Thomas Gabler<sup>a</sup>, Tom Lippoldt<sup>a</sup>, Jeannine Missbach-Guentner<sup>e</sup>, Christoph Russmann<sup>b,f</sup>, Stefan Nolte<sup>a,g</sup>

<sup>a</sup> *Institute of Applied Physics, Abbe Center of Photonics, Friedrich-Schiller-Universität Jena, Albert-Einstein-Straße 15, D-07745 Jena, Germany*

<sup>b</sup> *Faculty of Engineering and Health, University of Applied Sciences and Arts, Von-Ossietzky-Str. 99, D-37075 Goettingen, Germany*

<sup>c</sup> *Institute of Physical Chemistry and Abbe Center of Photonics, Friedrich-Schiller-Universität Jena, Albert-Einstein-Straße 6, D-07745 Jena, Germany*

<sup>d</sup> *Leibniz Institute of Photonic Technology, Albert-Einstein-Straße 9, D-07745 Jena, Germany*

<sup>e</sup> *Department of Diagnostic and Interventional Radiology, University Medical Center Göttingen, Robert-Koch-Str. 40, D-37075 Goettingen, Germany*

<sup>f</sup> *Brigham and Women's Hospital, Harvard Medical School, 75 Francis Street, Boston, MA, USA*

<sup>g</sup> *Fraunhofer Institute for Applied Optics and Precision Engineering IOF, Albert-Einstein-Straße 7, D-07745 Jena, Germany*

Spontaneous Raman spectroscopy is a diagnostic tool with a broad range of applications, e. g., the medical diagnostics<sup>1</sup> or industrial combustion<sup>2</sup> analysis, as all Raman active species can be identified with a single spectrum. On the downside, Raman scattering may suffer from fluorescent background and low signal intensities<sup>3</sup>. A nonlinear technique like coherent anti-Stokes Raman scattering (CARS) overcomes such issues, as it creates high intensity and laser-like signals. However, the traditional CARS approach lacks the multiplex capability of spontaneous Raman spectroscopy, as the laser wavelengths must be adjusted to individual Raman transitions. Ultrabroadband CARS<sup>4</sup> unites a laser-like signal with the multiplex feature of spontaneous Raman spectroscopy by providing an excitation pulse with sufficient bandwidth to probe transitions in multiple species.

In the present study, we use an ultrabroadband two-beam CARS setup<sup>5</sup>, which aims at exciting both the region below 1000 cm<sup>-1</sup> as well as the typical CH-stretching modes (~3000 cm<sup>-1</sup>). A dual-output optical parametric amplifier (venteon OPCPA, Laser Quantum GmbH) provides ~ 7 fs pulses (650 - 1030 nm) as pump/Stokes and a narrowband ~ 700 fs (517 nm) as probe pulse. Pulse energies are typically E<sub>pump/Stokes</sub> = 151 - 215 nJ and E<sub>probe</sub> = 5 - 67 nJ at the sample position. The beams are focused (NA = 0.7) and recollimated (NA = 0.5) by reflective objectives. The CARS signal is detected in transmission by a spectrograph (Shamrock 500i, Oxford Instruments, UK). Additionally, the Raman decay is measured by an automated delay stage (M-414.1PD, Physik Instrumente (PI) GmbH & Co. KG) shifting the probe pulse. The spectra are compared with spontaneous Raman spectroscopy, for which we use a commercial Raman microscope (inVia Raman microscope, Renishaw plc, UK) at an excitation wavelength of 473 nm.

Exemplarily, Fig. 1a presents CARS and Raman spectra of 99.9% dimethyl sulfoxide (DMSO) and of perylene in ethanol (50  $\mu\text{g/g}$ ), showing great agreement of the CARS measurements with the Raman microscope spectra. Furthermore, the fluorescence marker perylene does not affect CARS. On the other hand, signals from the Raman microscope are almost completely overshadowed by fluorescence, making ethanol undetectable for shifts below 2500  $\text{cm}^{-1}$ . Additionally, the CARS setup is used to measure the decay of individual Raman transitions. Two such measurements are shown in Fig. 1b for the two peaks at  $\sim 3000 \text{ cm}^{-1}$  in DMSO. These peaks exhibit an exponential decay with clearly different time constants.

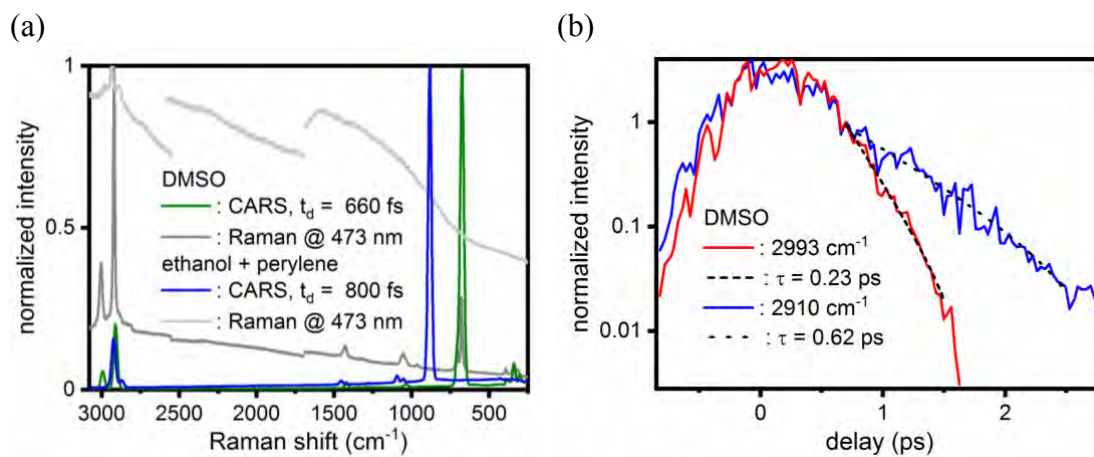


**Figure 1** (a) Raman and CARS spectra for DMSO and ethanol/perylene mixture. All spectra are corrected by a dark acquisition (laser-off). They are composed of 3 different grating positions. (b) Delay scan for the peaks at 2993  $\text{cm}^{-1}$  and 2910  $\text{cm}^{-1}$  of DMSO with exponential fits.

In conclusion, we have shown that ultrabroadband two-beam CARS generates background-free Raman spectra in organic liquids up to shifts of  $\sim 3000 \text{ cm}^{-1}$ . In addition, probing individual Raman decays provides a further approach for sample characterization. Future investigations focus on signal optimization for tissue analysis in reflection mode.

## ACKNOWLEDGMENTS

Funding: Deutsche Forschungsgemeinschaft (DFG) MI 1512/3-1, NO 462/14-1, RU 2156/3-1.

## REFERENCES

1. K. Kong, C. Kendall, N. Stone, I. Nottingher, *Adv Drug Deliv Rev*, 2015, **89**, 121-134.
2. A. C. Eckbreth, Laser diagnostics for combustion temperature and species, Gordon & Breach, Amsterdam, 1996.
3. C. Krafft, B. Dietzek, J. Popp *Analyst*, 2009, **134**, 1046-1057.
4. N. Dudovich, D. Oron, Y. Silberberg, *Nature*, 2002, **418**, 512-514.
5. Y. Ran, M. Junghanns, A. Boden, S. Nolte, A. Tünnermann, R. Ackermann, *J Raman Spectrosc*, 2019, **50**, 1268-1275.

# Optofluidic adaptive optics in confocal Raman microscopy

Juan David Muñoz Bolaños<sup>1</sup>, Maximilian Sohmen<sup>1</sup>, Pouya Rajaeipour<sup>2</sup>, Caglar Ataman<sup>3</sup>,  
Monika Ritsch-Martel<sup>1</sup>, Alexander Jesacher<sup>1</sup>

<sup>1</sup>Biomedical Physics, Physiology and Medical Physics, Innsbruck, Austria

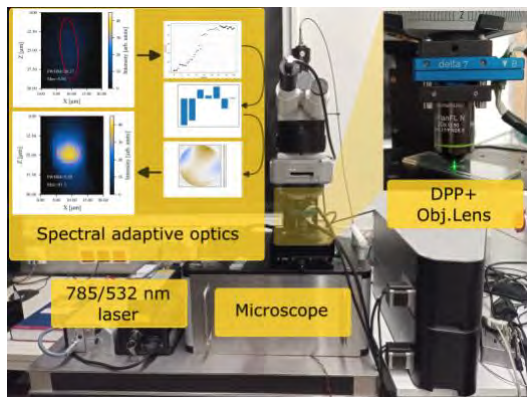
<sup>2</sup>Phaseform GmbH, Freiburg, Germany

<sup>3</sup>Dept. of Microsystems Engineering - IMTEK, Freiburg, Germany

Collecting the weak Raman signals can be a lengthy process, which can take anywhere from a few minutes to several hours. Confocal Raman microscopy is a technique used for capturing volumetric images, however, optical aberrations from the sample can degrade spatial resolution and signal quality, resulting in longer acquisition times.

Adaptive Optics (AO) is a technique used to correct optical aberrations and restore the signal and resolution even at deep focal points. In Confocal Raman imaging, we use AO in combination with an optofluidic adaptive element [1]. This element can be easily coupled with a commercial confocal Raman microscope. Please refer to the attached figure for more details.

We carried out a proof-of-concept experiment using an indirect wavefront sensing technique and a polystyrene bead placed under an aberrated beam. This allowed us to correct the aberrations caused by an artificial scatterer, leading to a five-fold signal enhancement. Presently, we are evaluating this setup for biosamples, including brain and vegetable tissues.



[1] K. Banerjee, P. Rajaeripour, C. Ataman & H. Zappe, „Optofluidic adaptive optics“, applied optics, 2018.



# Temperature-dependent Raman spectroscopic characterization of poly(furfuryl alcohol)

Bertoldo Menezes D.<sup>a</sup>, D'Amico F.<sup>b</sup>, Sepperer T.<sup>c</sup>, Benisek A.<sup>d</sup>,  
Musso M.<sup>d</sup>

<sup>a</sup> Instituto Federal do Triângulo Mineiro, Campus Uberlândia, 38.400-970 Uberlândia, Minas Gerais, Brazil

<sup>b</sup> Elettra-Sincrotrone Trieste S.C.p.A., Strada Statale 14 – km 163,5 in AREA Science Park, 34149 Basovizza, TS, Italy

<sup>c</sup> Salzburg University of Applied Sciences, Department Green Engineering and Circular Design, Markt 136a, 5431 Kuchl, Austria

<sup>d</sup> University of Salzburg, Department of Chemistry and Physics of Materials, Jakob-Haringer-Strasse 2a, 5020 Salzburg, Austria

Recently [1] we employed FTIR and Resonant Raman spectroscopy to investigate the chemical constitution of the polymer polyfurfuryl alcohol (PFA) synthesized in different ways, and appearing macroscopically different: the first one being a liquid and viscous commercial sample, the second one, produced following a thermosetting procedure, being a self-prepared solid and rigid sample. As a continuation of [1], we have performed a set of temperature dependent Raman spectroscopic measurements in order to study the evolution of these Raman spectra during the glass transition in thermosetted PFA [2], adopting the same spectral analysis previously performed to infer about the glass transition of the polymer poly(methyl methacrylate) (PMMA) [3].

At the University of Salzburg the Raman measurements were performed in the temperature range between  $-160^{\circ}\text{C}$  and  $+300^{\circ}\text{C}$  with laser excitation in the blue spectral range at 455 nm, while at the IUVSOFF beamline of the Elettra synchrotron in Trieste a series of Resonant Raman measurements were performed in the UV spectral range with laser excitation at 266 nm. The Raman and Resonant Raman spectra recorded for the thermosetted PFA close to room temperature were comparable with those published in [1], which were obtained for PFA samples also at room temperature. Figure 1a shows as example the Raman spectrum of thermosetted PFA, collected at  $20^{\circ}\text{C}$  with 455 nm laser excitation (compare in [1] Figure 3 and Table 1), and Figure 1b shows the synchronous two-dimensional correlation spectrum (2DCoS) obtained from all the recorded temperature dependent 455 nm Raman spectra of the thermosetted PFA.

Figure 1c shows Differential Scanning Calorimetry (DSC) data for the thermosetted PFA from  $10^{\circ}\text{C}$  to  $180^{\circ}\text{C}$ , having the glass transition temperature at around  $82^{\circ}\text{C}$ ,

Compatible with this DSC behaviour, Figure 1d shows how the normalized intensity of the Raman peak at around  $1610\text{ cm}^{-1}$  of the thermosetted PFA [1] changes with temperature, this spectral evolution being also an indication of the PFA glass transition [2], meaning that the PFA molecular structure and the associated cross-linking change with temperature, leading therefore to changes of the associated spectral features.



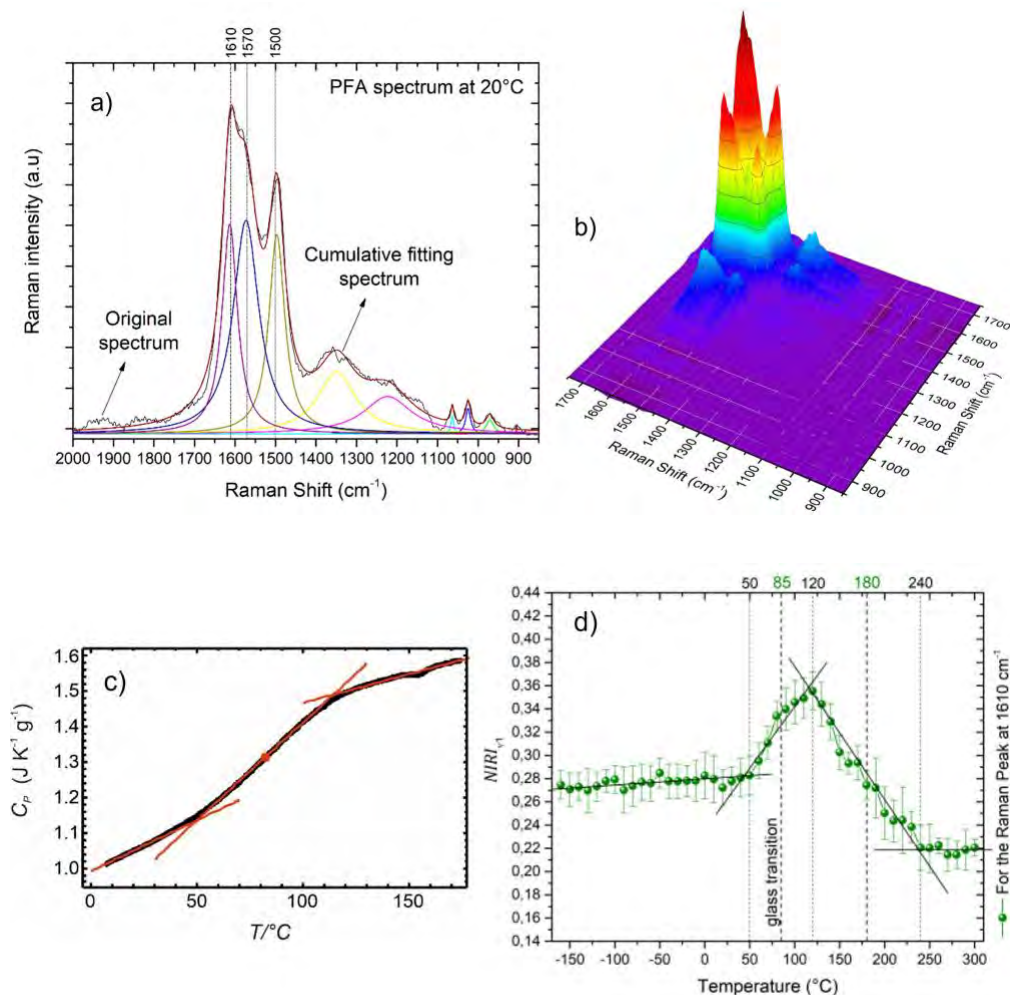


**Figure 1** a) Raman spectrum of thermosetted PFA, collected at 20°C with 455 nm laser excitation, highlighting the Raman peaks at around 1610  $\text{cm}^{-1}$ , 1570  $\text{cm}^{-1}$  and 1500  $\text{cm}^{-1}$ , peak assignments see in [1] Table 1. b) Synchronous two-dimensional correlation spectrum in the temperature range from  $-160^\circ\text{C}$  to  $300^\circ\text{C}$ . c) Differential Scanning Calorimetry (DSC) for thermosetted PFA from  $10^\circ\text{C}$  to  $180^\circ\text{C}$ , with the onset glass transition temperature at around  $50^\circ\text{C}$ , the midpoint (glass transition temperature) at around  $82^\circ\text{C}$ , and the endset temperature at around  $114^\circ\text{C}$ , compare [2]. d) Normalized Raman peak intensity  $NIRI_{1610}$  as a function of temperature for the Raman peak at around 1610  $\text{cm}^{-1}$ .

## ACKNOWLEDGMENTS

We thank for the financial support provided by the European Regional Development Fund and Interreg V-A Italy Austria 2014–2020 through the Interreg Italy Austria projects ITAT 1023 InCIMA and ITAT 1059 InCIMA4, and by CERIC 20197097.

## REFERENCES

1. F. D’Amico, et al., *Spectrochimica Acta Part A*, 2021, **262**, 120090.
2. J.M. Sadler, et al., *Journal of Applied Polymer Science*, 2018, **135**, 46608.
3. D. Bertoldo Menezes, et al., *Physical Chemistry Chemical Physics*, 2021, **23**, 1649-1665

## **Linear and non-linear microspectroscopy: a powerful tool to study polymer-based nanoparticles in fibrotic liver cells.**

Julian Plitzko<sup>a,b</sup>, Franziska Adermann<sup>c</sup>, Thorben Köhler<sup>c</sup>, Klea Mehmetaj<sup>d</sup>, Stephanie Schubert<sup>c</sup>, Adrian T. Press<sup>e,f</sup>, Michael Schmitt<sup>a</sup>, Michael Bauer<sup>e,f</sup>, Juergen Popp<sup>a,b</sup>

<sup>a</sup> Institute of Physical Chemistry and Abbe Center of Photonics, FSU Jena, Germany

<sup>b</sup> Leibniz Institute of Photonic Technology (IPHT), Member of Leibniz Health Technologies, Member of the Leibniz Centre for Photonics in Infection Research (LPI), Jena, Germany

<sup>c</sup> Laboratory of Organic and Macromolecular Chemistry (IOMC), FSU Jena, Jena, Germany

<sup>d</sup> Jena Center of Soft Matter (JCSM), FSU Jena, Jena, Germany

<sup>e</sup> Department of Anesthesiology and Intensive Care Medicine, Jena University Hospital, Jena, Germany

<sup>f</sup> Center for Sepsis Control and Care, Jena University Hospital, Jena, Germany

A promising way to address liver fibrosis is to utilize functionalized polymer-based Nanoparticles (NPs) to target the natural vitamin A receptor of liver cells, STRA6 (stimulated by retinoic acid 6). Those NPs are designed to encapsulate drugs in the necessary concentration to inhibit the signaling pathway inside the hepatic stellate cells that are responsible for inflammation.

To investigate such functionalized nanoparticles (NPs) within cells and tissue, molecular selective microspectroscopic techniques are well suited. Here, we report about the application of confocal fluorescence microscopy (Fig.1b) and coherent anti-Stokes Raman scattering (CARS) microscopy to study the localization of NPs in liver cells and tissue (Fig.1c). Furthermore, Raman spectroscopy in combination with two-dimensional correlation analysis (2DCOS) is utilized for the characterization of polymers, NPs, and drugs prior to its analysis in biological environments. Such a detailed Raman spectroscopic analysis of the polymers and the corresponding NPs allows for the identification of characteristic vibrations that enables a label-free localization of the functionalized NPs by CARS microscopy within cells. Fluorescence-lifetime imaging microscopy (FLIM) providing insights into the release of the encapsulated drug compounds of the functionalized NPs has also been applied.

These microspectroscopic approaches are aimed for a spatiotemporal localization of the NPs is supported by tailor-made image analysis routines to further characterize the NP uptake processes and induced metabolic influence.

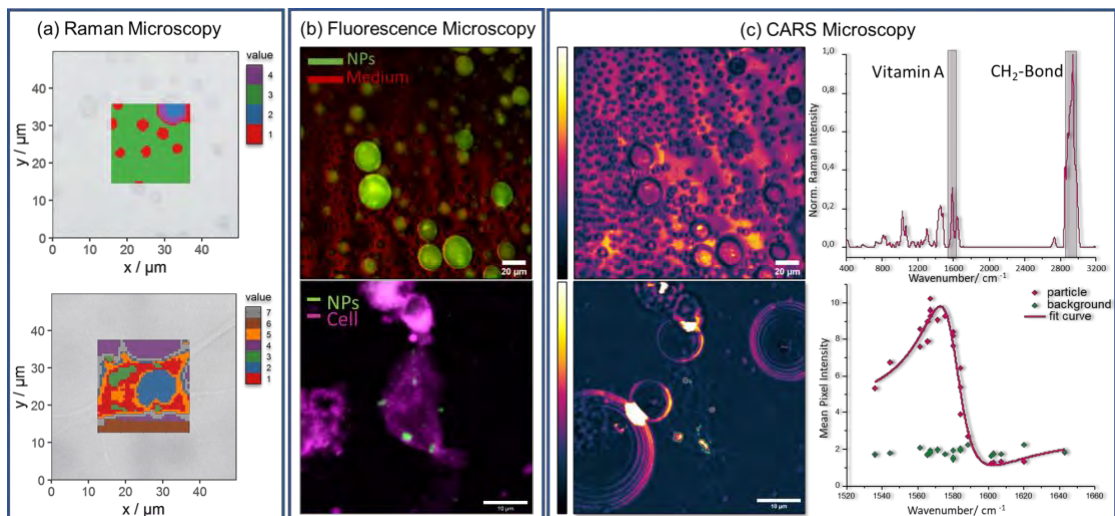


**Figure 1:** (a) Raman microspectroscopy enables to characterize clusters of NPs (top) and cell samples (bottom) on their chemical distribution. (b) Imaging with two-channel fluorescence microscopy of NPs accumulation in a fixation medium (top) and their distribution inside of cell (bottom). (c) CARS microscopy combines positive aspect of both techniques by focussing on one Raman band (here Vitamin A at  $1585\text{ cm}^{-1}$ ).

## ACKNOWLEDGMENTS

This study was funded by the German Research Foundation (DFG) through the Collaborative Research Centre PolyTarget 1278 “Polymer-based nanoparticle libraries for targeted anti-inflammatory strategies” (project C01) under DFG project number 316213987.

# Probing Structural Phase transitions in a Molecular Ferroelectric hexane-1,6-diammonium pentaiodobismuth using Raman Scattering

Monalisa Pradhan<sup>a</sup>, Aiswarya Abhisek Mohapatra<sup>b</sup>, Ashish Anand<sup>b</sup>, Diptikanta Swain<sup>c\*</sup>, Gopal K. Pradhan<sup>a\*</sup>

<sup>a</sup> Department of Physics, KIIT Deemed to be University, Bhubaneswar, 751024, Odisha, India

<sup>b</sup> Solid State and Structural Chemistry Unit, Indian Institute of Science, Bangalore, 560012, India

<sup>c</sup> Institute of Chemical Technology, Indian Oil Odisha Campus, Bhubaneswar, 751013, Odisha, India

## ABSTRACT

Hybrid organic–inorganic perovskite (HOIP) based molecular ferroelectrics hold great promise in photovoltaic and optoelectronic applications which combine the best from both materials offering a new way of tailoring the band structure.<sup>1,2,3</sup> The understanding of electron-phonon coupling is essential for their performance in optoelectronic applications as variety of interactions and structural disorder, which may significantly affect the material's characteristics.<sup>4</sup> Thus, it is crucial to study the thermodynamic structure-property relationship to get important insights towards improving their functionality. In this work, we carried out temperature-dependent Raman scattering studies of single crystal hexane-1,6-diammonium pentaiodobismuth (HDA-BiI<sub>5</sub>) HOIP in the 200 °C to -195 °C temperature ranges to study possible structural phase transition, electron-phonon interaction and change in the molecular symmetry during the transition. The analysis of temperature-dependent Raman data revealed that with increasing the temperature from room temperature to higher, the anomalous changes of Raman shift and line width has been observed at around 110 °C which confirms ferroelectric to paraelectric transition, while decreasing the temperature from room temperature to lower, the appearance of new Raman modes and splitting of peaks has been observed at around -45 °C suggesting the structural phase transition. In particular, the phase transition in HDA-BiI<sub>5</sub> is associated with tilting of BiI<sub>6</sub> octahedra and the changes of dynamics of hexane-1,6-diammonium cations is clearly established from our Raman analysis.

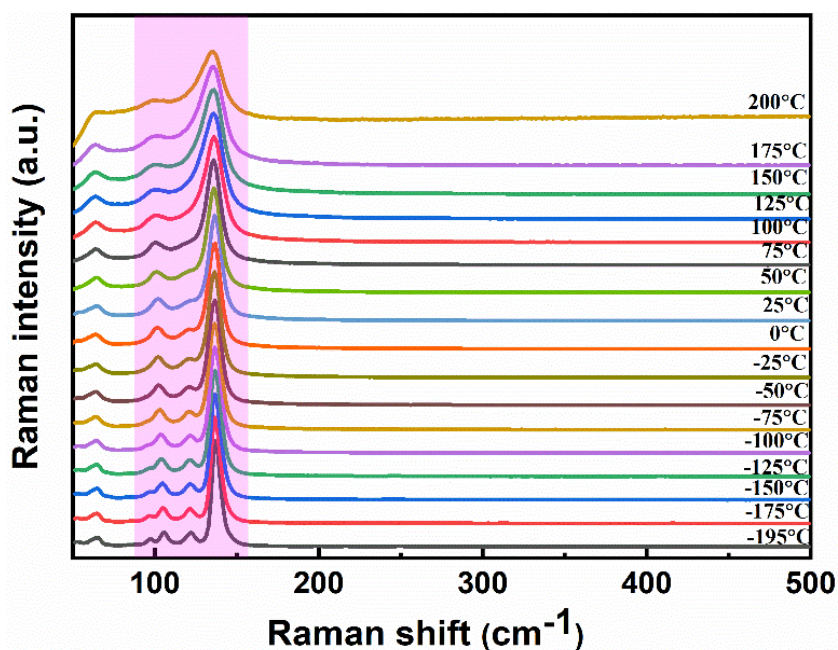


FIGURE 1 Temperature dependent Raman spectra of HDA-BiI<sub>5</sub> at 785nm laser excitation in the region 50 to 500 cm<sup>-1</sup>.

## ACKNOWLEDGMENTS

We would like to acknowledge DST ,India and Elettra Sincrotrone Trieste, Italy.

## REFERENCES

1. Li, Wei, et al., *Nature Reviews Materials*, (2017) ,**2(3)**,1-18.
2. Li, Peng-Fei, et al., *NPG Asia Materials*,2017,**9(1)**, e342-e342.
3. Saparov, Bayrammurad, and David B. Mitzi., *Chemical reviews*, (2016), **116(7)**, 4558-4596.
4. Zhao, Daming, et al., *ACS nano*, (2019),**13(8)**,8826-8835.

## Raman imaging of endothelial cells: searching for biochemical markers of hypoxia

Aleksandra Pragnaça<sup>a,b</sup>, Anna Antolak<sup>a</sup>, Zuzanna Krysiak<sup>c</sup>, Monika Leśniak<sup>c</sup>, Robert Zdanowski<sup>c</sup>, Kamilla Małek<sup>a</sup>

<sup>a</sup> Jagiellonian University, Faculty of Chemistry, Department of Chemical Physics, Raman Imaging Group, Gronostajowa 2 Street, 30-387 Krakow, Poland

<sup>b</sup> Jagiellonian University, Doctoral School of Exact and Natural Sciences, prof. S. Lojasiewicza 11 Street, 30-348 Krakow, Poland

<sup>c</sup> Military Institute of Medicine National Research Institute, Laboratory of Molecular Oncology and Innovative Therapies, Szaserów 128 Street, 04-141 Warsaw, Poland

Due to society's progressive ageing, the ratio of older people in the world's population is constantly growing, which results in an increase in the demand for research on diseases mainly affecting this social group. Over the previous two decades, the contribution of neurodegenerative diseases to the causes of mortality has grown significantly<sup>1</sup>. Furthermore, the etiology of these diseases remains poorly understood.

Brain endothelial cells are the primary structural component of the blood–brain barrier, a physical barrier that separates blood vessels from brain tissue<sup>2</sup>. Because they constitute the inner layer of the microvascular network, they are exposed to stress conditions accompanying neurodegenerative processes. The primary *in vitro* model reflecting neurological dysfunction is the hypoxia model<sup>3</sup>, which involves the cultivation of appropriate cells in a state of oxygen deficiency.

Spectroscopic methods of imaging biological materials, due to their non-invasive nature and lack of labelling, have great potential in *in vitro* research. Raman spectroscopy enables a detailed examination of the spectral characteristics of brain tissue cells, including the endothelium that forms the blood–brain barrier, under both normoxic and hypoxic conditions, allowing for the assessment of endothelial cell malfunction.

In this study, we evaluated the effect of oxygen deficiency (hypoxia) on 2D cultures of human brain endothelial cells using Raman spectroscopy. Because of its non-invasive nature, this approach has significant potential in *in vitro* research. Based on the analysis of specific bands of Raman spectra, the use of this technique in this study allowed us to identify and analyse changes in the content of macromolecules such as lipids, proteins, and nucleic acids in the organelles of brain endothelial cells.

The experiment was performed on a cerebral microvascular endothelial cell line (HBEC 5i) under normoxic and hypoxic conditions (1% oxygen in the culture environment). Cells were examined using high-resolution Raman microscopy. Spectroscopic methods assisted with chemometric analysis enabled the establishment of characteristic spectral



biomarkers of the investigated cells. The effect of oxygen deficiency was mainly observed in the nucleus and lipid droplets.

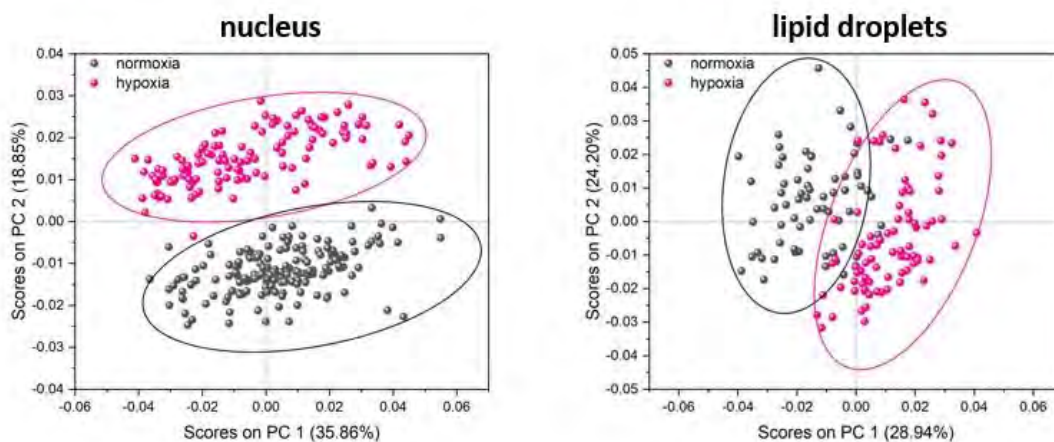


**Figure 1** The scores plots from Principal Component Analysis performed on Raman spectra of the cell nucleus (left) and lipid droplets (right) ( $500\text{-}3050\text{ cm}^{-1}$ ) of the brain endothelial cells under normoxic and hypoxic conditions. Each point refers to a single cell.

## ACKNOWLEDGMENTS

The authors acknowledge the financial support from OPUS 21 project (No. 2021/41/B/ST4/02000) funded by the National Science Center (Poland).

## REFERENCES

1. J.S. Rana, S.S. Khan, D.M. Lloyd-Jones, S. Sidney, *Journal of General Internal Medicine*, 2021, **36**, 2517–2518.
2. J.J. Lochhead, J. Yang, P.T. Ronaldson, T.P. Davis, *Frontiers in Physiology*, 2020, **11**, 1-17.
3. I. Olmez, H. Ozyurt, *Neurochemistry international*, 2012, **60**, 208-212.



# Detection of Oncometabolites in Hodgkin Lymphoma Cells using SERS and GC-MS

Daniel Zimmermann<sup>a</sup>, David Lilek<sup>a</sup>, Lukas Steininger<sup>a</sup>, Agnes Grünfelder<sup>a</sup>, Alfred Minarik<sup>a</sup>, Birgit Herbinger<sup>a</sup>, Katerina Prohaska<sup>a</sup>

<sup>a</sup> *Fachhochschule Wiener Neustadt – Biotech Campus Tulln, Konrad-Lorenz-Straße 10, Tulln, Austria*

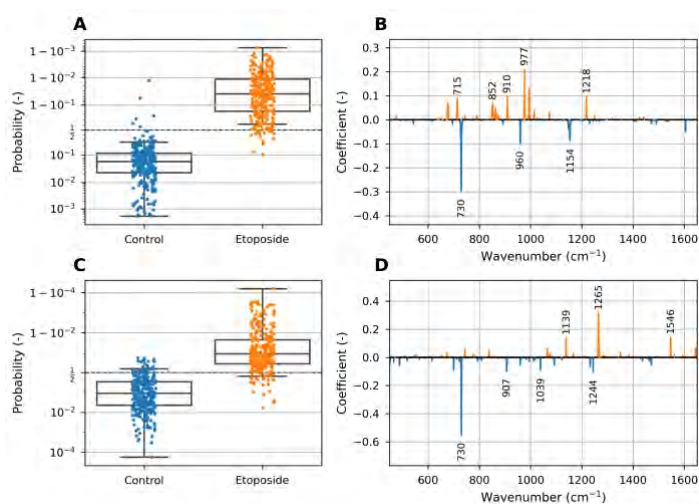
Surface-enhanced Raman spectroscopy (SERS) using colloidal nanoparticles serves as a powerful tool for fast and reliable measurement of cultivated cancer cells, providing a “chemical fingerprint” which contains information about the status of individual cells<sup>1</sup>. With this non-targeted technique, ensuring reproducible enhancement of the Raman signal remains challenging<sup>2</sup>. To successfully evaluate the collected spectra and apply SERS for diagnostics in future, it is furthermore crucial to establish a well optimized and validated data analysis workflow<sup>3</sup>.

Here, we studied the effect of two different substances – Etoposide and Resveratrol – on Hodgkin lymphoma (HL) cells using SERS and GC-MS. Etoposide is a chemotherapeutic medication which primarily affects rapidly dividing cancer cells by inhibiting the relaxation of supercoiled DNA strands<sup>4</sup>. Resveratrol is a polyphenol found in high levels in red wine which is being studied for its potential use in cancer treatment<sup>5</sup>.

HL cell lines L-428 and L-540 were treated with Resveratrol, Etoposide, and a combination of both, in addition to an untreated control. Data analysis of SERS spectra was performed using an open-source Python-based workflow<sup>6</sup>. Tentative band assignments were supported by spectra of pure substances using an in-house database. For GC-MS, metabolites were extracted using methanol and water and derivatized by methoximation and silylation. After data acquisition, we used an R-based data analysis script to identify significant differences between treatments.

**Figure 1** Classification probabilities (A, C) and logistic regression model coefficients (B, D) of L-428 (top) and L-540 (bottom) cells. Blue – untreated cells; Orange – Etoposide-treated cells

In both examined cell lines, we found significant differences between the SERS spectra of the untreated control and all three treatments (Figure 1 A, C). Based on the higher

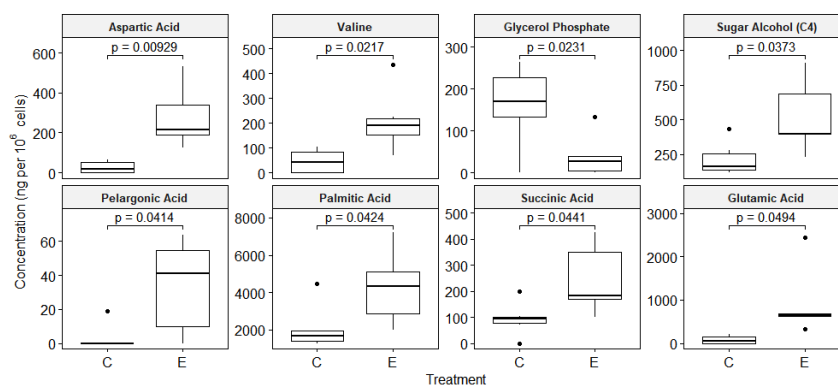


classification accuracy, these differences were more pronounced in the cell line L-428, which is known to contain a mutation of the p53 protein<sup>8</sup>. p53 plays a crucial role in DNA repair, cell cycle control and apoptosis<sup>9</sup>, which could relate to a greater susceptibility to Etoposide treatment in the mutated cell line.

We also identified the Raman bands which contribute to the classification of treated and untreated cells (Figure 1 B, D). At  $\sim 730\text{ cm}^{-1}$ , which has been tentatively assigned to the nucleobase adenine<sup>10</sup>, the signal intensity is diminished in all treated cells. The signal  $\sim 1265\text{ cm}^{-1}$  is more pronounced in treated L-540 cells, and most likely corresponds to the amide III vibration of proteins<sup>11</sup>.

**Figure 2** Metabolites with significantly different concentration between control (C) and Etoposide-treated (E) L-540 cells.

Metabolic profiling by GC-MS identified several



metabolites with significantly different concentrations in treated and untreated cells (Figure 2). Among these metabolites are multiple amino acids, as well as the recognized oncometabolite succinate.

In summary, both SERS and GC-MS were able to identify differences in the cellular composition caused by the chemotherapeutic treatment. While SERS can quickly provide a general overview of the chemical conditions in individual cells, GC-MS allows resolving specific compounds. Further research is needed to correlate the results from these two complementary techniques.

## ACKNOWLEDGMENTS

We thank the consortium of the project Ra-Dia-M for their support and expertise.

## REFERENCES

1. D. Cialla-May et al., *Chemical Society Reviews*, 2017, **46**, 3945–3961.
2. C. Zong et al., *Chemical Reviews*, 2018, **118**, 4946–4980.
3. F. Lussier et al., *TrAC - Trends in Analytical Chemistry*, 2020, **124**, 115796.
4. K. R. Hande, *European Journal of Cancer*, 1998, **34**, 1514–1521.
5. A. P. Singh et al., *Medicinal Research Reviews*, 2019, **39**, 1851–1891.
6. D. Zimmermann et al., in *Scientific Computing*, 2023.
7. C. A. Sellick et al., *Nat Protoc*, 2011, **6**, 1241–1249.
8. A. Feuerborn et al., *Leukemia and Lymphoma*, 2006, **47**, 1932–1940.
9. K. Hientz et al., *Oncotarget*, 2017, **8**, 8921–8946.

10. U. Neugebauer et al., *Journal of Biophotonics*, 2010, **3**, 579–587.
11. A. B. Veloso et al., *Scientific Reports*, 2017, **7**, 1–12.

# Clinical diagnostics of diseases and infections by optical photothermal mid-IR spectroscopy

Shravan Raghunathan<sup>a</sup>, Michael Kiehntopf<sup>b</sup>, Susann Piehler<sup>b</sup>, Jürgen Popp<sup>a,c</sup>, Christoph Krafft<sup>a</sup>

<sup>a</sup> Leibniz Institute of Photonic Technology, Member of the Leibniz Center for Photonics in Infection Research, Albert-Einstein-Straße 9, 07745 Jena, Germany

<sup>b</sup> Jena University Hospital, Institute for Clinical Chemistry and Laboratory Diagnostics, Member of the Leibniz Center for Photonics in Infection Research, Am Klinikum 1, 07747 Jena, Germany

<sup>c</sup> Friedrich Schiller University, Institute of Physical Chemistry and Abbe Center of Photonics, Member of the Leibniz Center for Photonics in Infection Research, Helmholtzweg 4, Jena, Germany

Laboratory diagnostics for the identification of diseases and infections require a standard tool for studying cell specimen. Reproducibility of identifying diseases and infections patterns is of particular interest to pathologists. Understanding drug delivery and antibiotic action is also an essential study in biomedical cell research. Large samples must be studied in high-throughput configurations for developing standard libraries for cell screening. Infrared (IR) spectroscopy and imaging can be a possible solution for the above-mentioned challenges. The chemical information obtained by IR spectroscopy provides specific molecular information of both microorganisms and medicines alike and can be used to understand infections and counter-mechanisms. Fourier transform infrared spectroscopy (FTIR) and laser-direct infrared spectroscopy (LDIR) are modalities that provide chemical and morphological information in the mid-infrared region for most biological samples. Although they provide label-free probing of samples, they are limited by resolution due to wavelength of mid-IR irradiation, large acquisition times, limited sensor sizes, dispersive effects, and inherent water absorption. Commercial high throughput microscopy systems can be used, but the fluorescent labeling of samples often leads to photo-bleaching and chemical alteration of samples under consideration.

Optical mid-IR photothermal spectroscopy (O-PTIR) overcomes the limitations in standard IR modalities, by which label-free chemical information and precise sub- $\mu\text{m}$  imaging can be performed simultaneously [1]. A pulsed quantum cascade laser (QCL) excites the sample in the mid-IR region which activates the vibrational modes of the sample, thereby leading to absorption of incident radiation. This absorption leads to a thermal modulation of refractive index, which changes the optical scattering properties at the local environment within the sample. A visible laser probes this change at the same focus of the mid-IR focus using lock-in detection principle, which then records and scales with the absorption of the sample. The tunability of the QCL and the wavelength of the visible probe enables simultaneous discrete wavenumber imaging and spectral measurement that can be analyzed by standard IR libraries and chemometrics.

In this work, we study full blood and peripheral blood mononuclear (PBMC) smears as a model sample to study for disease and infections. The primary reason for studying them is that liquid biopsies contain the active state of the individual from which the samples are collected from. We studied them in three different configurations: a) blood smear on  $\text{CaF}_2$  substrate, stained by May-Grunwald

Giemsa and methylene blue stains for leukocyte identification b) unstained blood smear on glass substrate c) unstained PBMC smear on a glass substrate. We chose multiple field-of-views  $500 \times 500 \mu\text{m}^2$  in size and performed discrete wavenumber imaging at two wavenumbers  $1660$  and  $2922 \text{ cm}^{-1}$ . The resolution was set at  $2 \mu\text{m}/\text{pt}$  and speed at  $250 \mu\text{m}/\text{s}$ . the total time for acquiring a single wavenumber image in this configuration was approx. 12 min. A contrast is obtained by producing an RGB channel for the two IR images to locate leukocytes among erythrocytes. A point-by-point spectral measurement is then carried out by probing the individual leukocytes identified. The leukocytes could also be distinguished from red blood cells by their size distribution: mean size,  $11\text{--}13 \mu\text{m}$  in diameter as compared to RBCs which are smaller: mean size,  $6\text{--}8 \mu\text{m}$ . A similar measurement approach is also applied to the PBMC smears for leukocyte subtypes counting.

A 2<sup>nd</sup> derivative spectrum was calculated for the blood and PBMC smears on glass substrates to suppress a large background in the low wavenumber region ( $900\text{--}1200 \text{ cm}^{-1}$ ). Staining of blood smears also allows for the samples to be analyzed by a commercial throughput system as a reference standard. A widefield IR microscope which offers large sample measurement through high-throughput cell screening is further introduced [2].

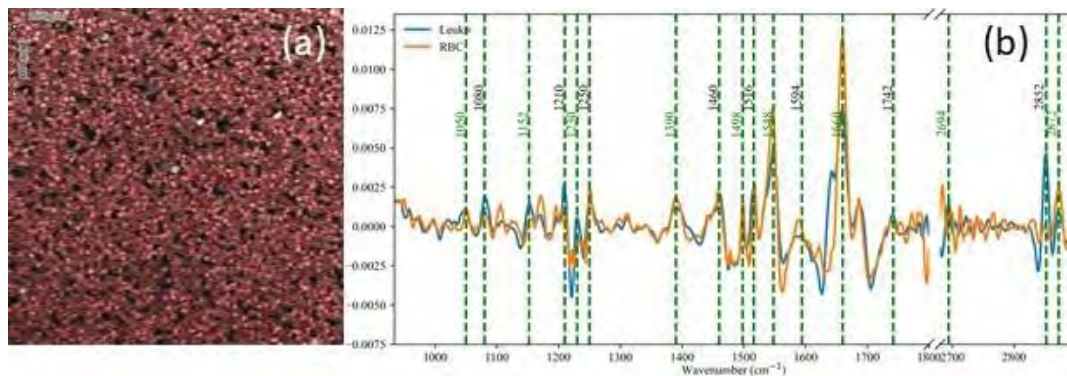


**Figure 1** (a) RGB overlay of unstained blood smear on a glass substrate, images obtained at  $1660$  and  $2922 \text{ cm}^{-1}$  respectively. (b) negative 2<sup>nd</sup> derivative spectra of leukocytes and red blood cells obtained from unstained blood smear on a glass substrate.

## ACKNOWLEDGMENTS

This work is supported by the BMBF, funding program Photonics Research Germany (13N15464) and is integrated into the Leibniz Center for Photonics in Infection Research (LPI). The LPI initiated by Leibniz-IPHT, Leibniz-HKI, UKJ and FSU Jena is part of the BMBF national roadmap for research infrastructures.

## REFERENCES

1. Delong Zhang et al., *Sci. Adv.*, 2016, **(2)** e1600521.
2. Yeran Bai et al., *Sci. Adv.*, 2019, **(5)** eaav7127.



## Characterizing the lipid composition of breast cancer cells resistant to neoadjuvant treatments by Raman spectroscopy: assessing background removal performance

José Javier Ruiz<sup>1</sup>, Neus Carbó<sup>2,3</sup>, Patricia Fernández-Nogueira<sup>4,5,6</sup>, Merche Rivas<sup>1</sup>, Mónica Marro<sup>1</sup>, Gemma Fuster<sup>2,3,6,7</sup>, Pablo Loza-Álvarez<sup>1</sup>

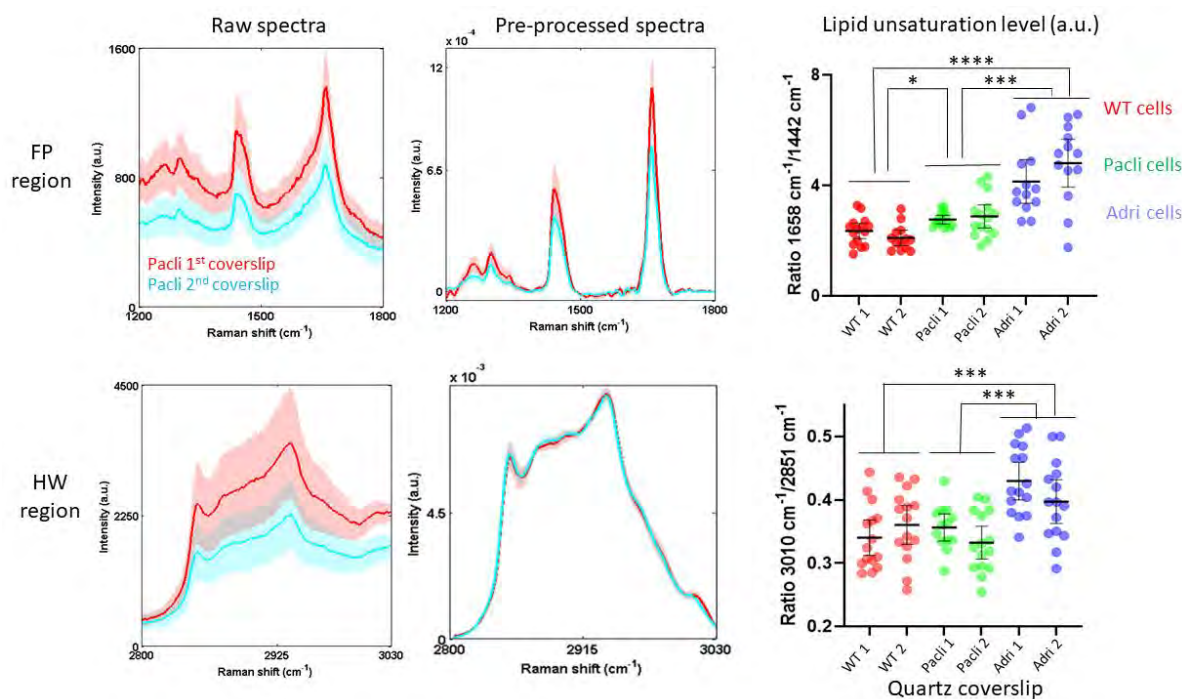
<sup>1</sup>ICFO-Institut de Ciències Fotòniques, The Barcelona Institute of Science and Technology, Castelldefels, 08860, Barcelona, Spain. <sup>2</sup>Department of Biochemistry and Molecular Biomedicine, Universitat de Barcelona, 08028, Barcelona, Spain. <sup>3</sup>Institute of Biomedicine of the University of Barcelona (IBUB), 08028, Barcelona, Spain. <sup>4</sup>Department of Biomedicine, School of Medicine, University of Barcelona (UB), 08036, Barcelona, Spain. <sup>5</sup>Unit of Biophysics and Bioengineering, Department of Biomedicine, School of Medicine and Health Sciences, Universitat de Barcelona, 08014, Barcelona, Spain. <sup>6</sup>Biosciences Department, Sciences Technology and Engineering Faculty, FUBalmes, UVIC.UCC, Vic, Spain. <sup>7</sup>Tissue Repair and Regeneration Group, IRIS-CC, Vic, Spain

**Objective:** Characterize the lipidic profile of triple-negative BT-549 breast cancer cells that developed resistance to Paclitaxel (Pacli) or Adriamycin® (Adri) neoadjuvant treatments, and of non-resistant wild-type (WT) BT-549 cells. This way, we can unravel the metabolic pathways that confer cells this resistance, which are not completely understood yet. To do so, a correct pre-processing must be done to guarantee a robust and reliable profiling.

**Methodology:** Cells were seeded and fixed with PFA 4% in quartz coverslips. For each cell type (WT, Pacli and Adri), we measured cells in the two different coverslips and in different days, to assess the robustness of the analysis under variations due to spectrometer status and human practice during sample preparation. A fluidic magnetic chamber filled with PBS was used to measure. We used a 532nm laser and measured in the fingerprint (FP) and high-wavenumber (HW) spectral region. In total, 30 cells of each type were measured.

Spectra were first normalized with Savitzky-Golay algorithm. Then, fluorescence background was removed in the FP region with the rolling circle method. After, background coming from quartz and PBS was removed in both FP and HW regions by carefully implementing a fitting with background spectra. Later, spectra were normalized with respect to the total biomass, calculated as the area under the curve in the HW region. Finally, a gaussian fitting of the bands of interest was done to consider band overlapping, and lipid unsaturation levels were calculated in both FP and HW to provide more robustness. Statistics was done with GraphPad Prism.

**Results and conclusions:** Significant differences are found in lipid unsaturation levels between resistant and non-resistant cells. Also, the proposed pre-processing corrects intensity differences due to background variations, since no significant differences are found within cells of the same type measured in different coverslips and days.



# Experimental and computation challenges of combining data from different sources

Oleg Ryabchykov<sup>a,b</sup>, Ute Neugebauer<sup>a,b,c</sup>, Juergen Popp<sup>a,b</sup>, Thomas Bocklitz<sup>a,b,d</sup>

<sup>a</sup> Leibniz Institute of Photonic Technology, Albert-Einstein-Straße 9, Jena, Germany

<sup>b</sup> Institute of Physical Chemistry and Abbe Center of Photonics, Friedrich-Schiller-University, Helmholtzweg 4, D-07743 Jena, Germany

<sup>c</sup> Jena University Hospital, Am Klinikum 1, Jena, Germany

<sup>d</sup> University of Bayreuth, Nürnberger Str. 38, Bayreuth, Germany

It was previously shown that combining various types of data into a single model improves the model performance in comparison to using either of the modalities alone [1]. Despite obvious advantages, an approach of combining different data types may be challenging and the complexity of the needed data fusion pipeline largely depends on the experimental data and the initial design of the experiment.

The focus of this contribution will be on the relations between the design of the experiments and the applied data fusion methods in different scenarios. From the data analyst's perspective, the most straight-forward combined data analysis can be performed when the different modalities are acquired simultaneously. In the case of multimodal imaging, data from different modalities is acquired pixel-by-pixel, which enables pixel-level data fusion without excessive steps of image co-registration. In such case, multimodal images after minor preprocessing steps can be treated similarly to RGB color images [2]. On the other side, if the acquired data is not aligned, it might require manual alignment and data interpolation for centralized pixel-level data fusion (Figure 1a) [3]. Automation of image co-registration remains a challenging topic, especially for the imaging techniques with large number of channels. In some cases, such alignment might not be possible due to the design of the experiment and only distributed (or decision-level) data combination (Figure 1c) can be applied in a straight-forward manner. Combining such data on lower levels can be, however, enabled by random sampling or data aggregation [4].

Besides the different data fusion scenarios, introduction of experimental factors that may introduce bias in the analyzed data will be discussed within the frame of the classic chemometrics [1] and the artificial neural networks. We will discuss different approaches for reducing the bias of the models via data weighting and the incorporation of the secondary data in the supervised model.



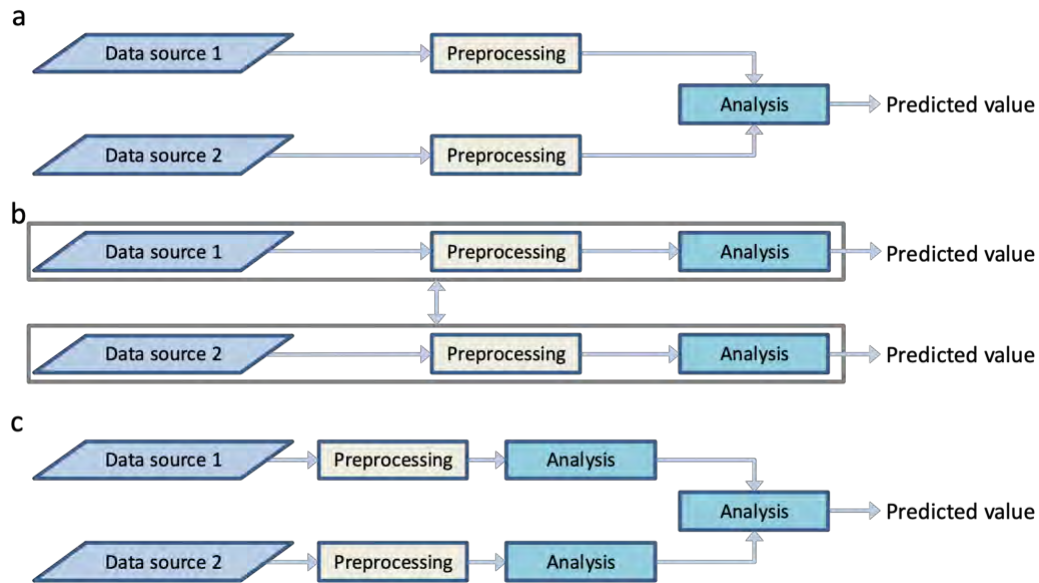


**Figure 1** Types of data fusion approaches. Centralized (a), decentralized (b), and distributed (c) architectures. Adapted from reference [3].

## ACKNOWLEDGMENTS

Financial support from the EU, the TMWWDG, the TAB, the BMBF, the DFG, the Carl-Zeiss Foundation, and the Leibniz Association is greatly acknowledged. This work is supported by the BMBF, funding program Photonics Research Germany (13N15708 (LPI-BT3-IPHT), 13N15715 (LPI-BT4-FSU), and 13N15710 (LPI-BT3-FSU)) and is integrated into the Leibniz Center for Photonics in Infection Research (LPI). The LPI initiated by Leibniz-IPHT, Leibniz-HKI, Friedrich Schiller University Jena and Jena University Hospital is part of the BMBF national roadmap for research infrastructures.

## REFERENCES

1. Ramoji, Anuradha, et al., *Critical care explorations*, 2021, **3(5)**.
2. Pradhan, Pranita, et al., *ICPRAM*, 2021, 495-506.
3. Ryabchykov, Oleg, et al., *Frontiers in Chemistry*, 2018, **6**, 257.
4. Kirchberger-Tolstik, Tatiana, et al., *Analyst*, 2021, **146.4**, 1239-1252.

# Quantum computational studies, spectroscopic (FT-IR, FT-Raman and UV–Vis) profiling, molecular docking and topology (ELF,LOL,RDG) analysis on Isobutyl 4-Hydroxybenzoate

S. Kaleeswaran<sup>a,b</sup>, Johanan Christian Prasana<sup>a,b\*</sup>, S. Muthu<sup>c,d</sup>

<sup>a</sup> Department of Physics, Madras Christian College, East Tambaram, Chennai 600059, Tamil Nadu India.

<sup>b</sup> University of Madras, Chennai 600005 Tamil Nadu, India.

<sup>c</sup> Department of Physics, Arignar Anna Govt. Arts College, Cheyyar 604407, Tamil Nadu, India.

<sup>d</sup> Department of Physics, Puratchi Thalaivar DR.MGR. Govt. Arts and Science College, Uthiramerur-603406, Tamilnadu, India.

\*Corresponding author: [reachjcp@gmail.com](mailto:reachjcp@gmail.com)

Isobutyl 4-Hydroxybenzoate (IB4HB) is a derivative of benzoate chemical structure. The chemical formula of isobutyl 4-Hydroxybenzoate is C<sub>12</sub>H<sub>16</sub>O<sub>3</sub> with molecular weight of 194.23 g/mol. IB4HB consists of a benzene ring (the hexagonal ring on the right side) with a hydroxyl (OH) group attached to the carbon atom. The presence of the ester group shows its antimicrobial properties [1,2]. IB4HB's bioactivity revolves around its ability to inhibit the growth of microorganisms, particularly bacteria and fungi.

Density Functional Theory (DFT) is a widely used computational method in quantum chemistry and condensed matter physics. It is employed to understand and predict the electronic structure and properties of molecules, atoms, and solids.

In this research, an organic compound Isobutyl 4-Hydroxybenzoate was evaluated theoretically using spectroscopy profiling. Density Functional Theory (DFT) B3LYP method with 6-311++G(d,p) basis set was employed to calculate vibrational (IR, Raman) studies were compared with experimental data. Prominent peaks were analyzed in detail. PED values were analysed using the VEDA program for a detailed interpretation of vibrational spectra. Stability of the molecule, resulting from hyper-conjugative interactions and charge delocalization was analyzed using Natural Bond Orbital (NBO) analysis. DFT functions were computed using Gaussian 16W, enabling quantum mechanical calculations to determine the linear polarizability ( $\alpha$ ) and first-order hyperpolarizability ( $\beta$ ) values for the title compound. TD-DFT was employed to assess the electronic properties of IB4HB with solvents such as acetone, ethanol, water, ethylethanoate. The energy gap, chemical softness and hardness were obtained from the Frontier Molecular Orbital analysis, indicating biological activity. Molecular Electrostatic Potential (MEP) were calculated to study the charge distribution within the molecule. Topological analyses such as ELF, LOL and RDG were carried out using MULTIWFN software in order to identify bonding zones and the weakest interactions in IB4HB. Furthermore, Drug likeness values were analyzed to assess the title compound's potential as an active pharmaceutical drug. Biological nature of the compound was observed by molecular docking studies. The results of molecular docking analysis using the antifungal protein (1Z3Q) indicate that the studied ligand exhibits strong potential with a binding

energy of -5.63 kcal/mol, comparable with commercially available drug Penlac, which has a binding energy of -5.23 kcal/mol.

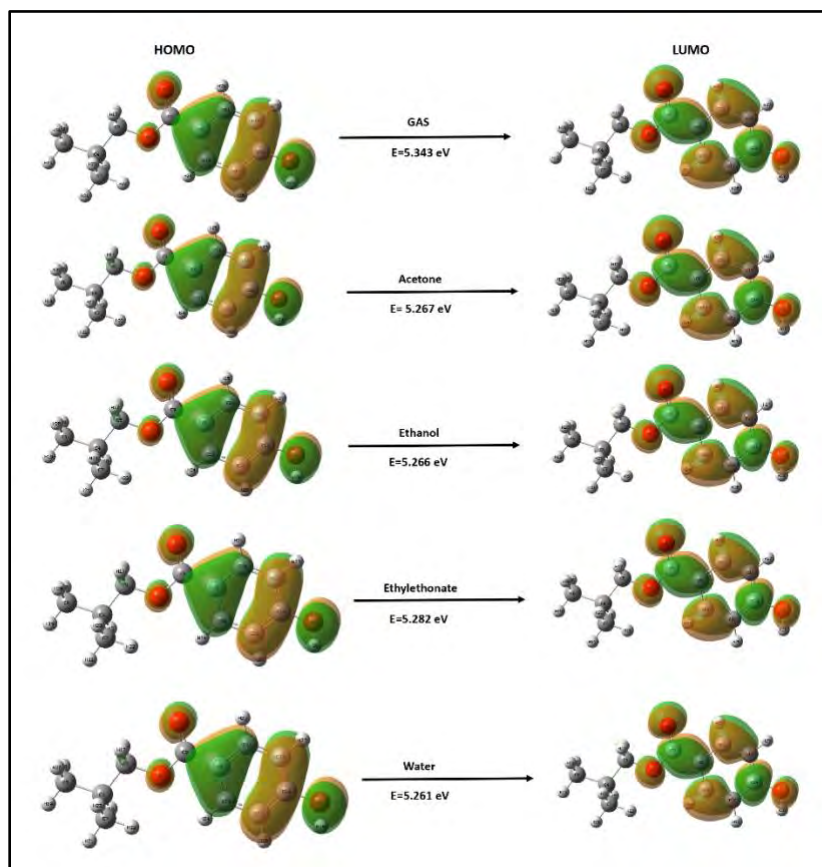


**Figure 1.** Frontier Molecular Orbital diagram of IB4HB.

## REFERENCES

1. M. Teresa Garcia, Isabel Ribosa, Lourdes Perez, Angeles Manresa, and Francesc Comelles, *Langmuir*, 2013, **29** (8), 2536-2545.
2. Huiying Zou, Guangying Chen and Shiyang Zhou, *RSC Advances*, 2019, **9**, 6627-6635.

# Comparative analysis of multispectral imaging of T and B cells in murine spleen utilizing LDIR, FTIR, and OPTIR spectroscopy techniques

A. Shydlukh<sup>a</sup>, S. Deinhardt-Emmer, J. Popp<sup>a,b</sup>, C. Krafft<sup>b</sup>

<sup>a</sup> Leibniz Institute of Photonic Technology (IPHT), Member of the Leibniz Center for Photonics in Infection Research, Albert-Einstein-Straße 9, 07745 Jena, Germany

<sup>b</sup> Friedrich Schiller University Jena, Institute of Physical Chemistry and Abbe Center of Photonics, Member of the Leibniz Center for Photonics in Infection Research, Jena, Germany

Multispectral imaging techniques based on infrared (IR) spectroscopy have become pivotal in biomedical research, offering insights into the spatial distribution and chemical composition of cells within biological tissues. A previous FTIR imaging study already identified vessels, red pulp, white pulp, and B and T lymphocytes in spleen tissue sections[1]. In 2019, new generations of IR instruments were introduced that were coupled to quantum cascade lasers (QCL) namely Laser Direct Infrared (LDIR, Agilent) and Optical Photothermal Infrared (OPTIR, Photothermal Inc.) spectroscopy. A comparative application of these three IR approaches for spectroscopy and imaging to murine spleen tissue sections with and without infection by influenza virus A will be presented.

FTIR microspectroscopic imaging with focal plane array detection is well-regarded for its precise chemical analysis via molecular vibrational frequencies offering high specificity and providing a full spectrum for each image pixel (900–4000  $\text{cm}^{-1}$ ). LDIR spectroscopy is notable for its rapid scan speed at discrete wavenumbers, making it a preferred choice for time-sensitive imaging tasks, but it's restricted to operating in reflection mode and a narrower spectral range (975–1800  $\text{cm}^{-1}$ ). OPTIR spectroscopy combines excitation by infrared laser pulses followed by induction of a photothermal effect which is probed by visible light, and the infrared absorption is obtained by lock-in detection schemes. Main OPTIR advantage is submicron resolution which enables to identify single cell nuclei.

To compare the distribution of white pulp and red pulp in both infected and non-infected spleen tissue on IR-transmissive  $\text{CaF}_2$  and reflective MirrIR (Kevley Technologies) slides, FTIR and OPTIR data were collected both in transmission and reflection modes while LDIR data could only be recorded in reflection. Similar than in reference [1], the FTIR spectra were normalized to the intensities to the amide I band of proteins followed by k-means cluster analysis in the spectral range 990–1340  $\text{cm}^{-1}$  that contains the most intense nucleic acid bands.

Figure 1 shows the microscope image and the color-coded chemical image of IR intensities from 990 to 1340  $\text{cm}^{-1}$ . White pulp (yellow to red) is clearly separated from red pulp (blue to cyan). The fine structure is further visualized in the cluster membership

map where cyan and green clusters are assigned to red pulp, red cluster to follicle margin (T lymphocytes) and the light blue and beige clusters are assigned to the follicle center (B lymphocytes).

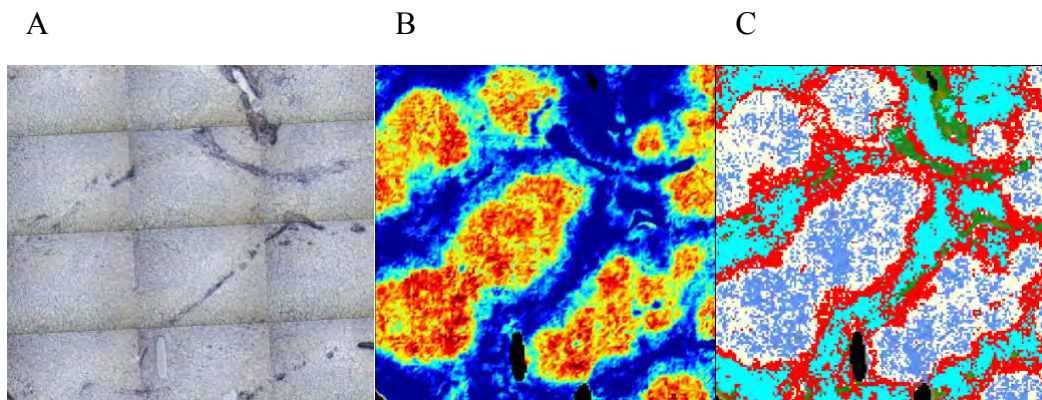


**Figure 1** A) Microscopic image, B) FTIR image of non-infected spleen on  $CaF_2$  at  $990-1340\text{ cm}^{-1}$  C) K-means cluster image

Similar contrast can be obtained by IR imaging of discrete wavenumbers using LDIR and OPTIR. This comparative analysis sheds light on the strengths and weaknesses of each spectroscopy technique, elucidating their suitability for various research applications. By providing an in-depth understanding of these techniques, this study equips researchers in the field of multispectral imaging with the knowledge to make informed decisions tailored to their specific experimental requirements. This analysis serves as a valuable resource for selecting the spectroscopy method that best aligns with their research objectives.

## ACKNOWLEDGMENTS

This work is supported by BMBF and is integrated to QUANCER project

## REFERENCES

1. C. Krafft, R. Salzer, G. Soff, M. Ern, M. Meyer-Hermann. Identification of B and T cells in human spleen sections by infrared microspectroscopic imaging. *Cytometry A*, 2005, 64A, 53-61
2. Feng, Z., Jensen, S. M., Messenheimer, D. J., Farhad, M., Neuberger, M., Bifulco, C. B., & Fox, B. A. Multispectral Imaging of T and B Cells in Murine Spleen and Tumor. *Journal of immunology*, 2016, 196(9), 3943–3950.



# Wide-field optical photothermal infrared microscope for imaging and spectroscopy

A. Thayyil Raveendran<sup>a</sup>, J. Popp<sup>a,b</sup>, C. Krafft<sup>a</sup>

<sup>a</sup> Leibniz Institute of Photonic Technology (IPHT), Member of the Leibniz Center for Photonics in Infection Research, Jena, Germany

<sup>b</sup> Friedrich Schiller University Jena, Institute of Physical Chemistry and Abbe Center of Photonics, Member of the Leibniz Center for Photonics in Infection Research, Jena, Germany

Optical photothermal infrared (OPTIR) spectroscopy is an innovative vibrational spectroscopic method that combines excitation by a pulsed infrared quantum cascade laser, induction of a photothermal effect by infrared absorption and its detection by visible light sources. A first OPTIR instrument has been commercialized to collect IR spectra and acquire images in point-based scan mode (see Figure 1A). The image shows a white pulp in the center surrounded by red pulp of the murine spleen tissue section. Cell nuclei of B- and T-lymphocytes of white pulp are resolved by elevated phosphate band at  $1083\text{ cm}^{-1}$  relative to the protein band at  $1658\text{ cm}^{-1}$  [1]. Compared to previous Fourier transform infrared images, OPTIR images offer higher lateral resolution and are less affected anomalous scattering effects.

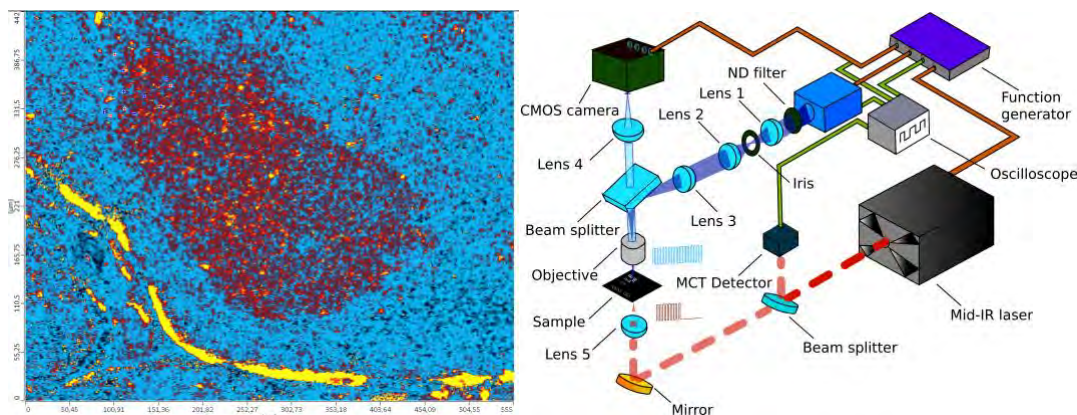


**Figure 1** A) OPTIR Image of murine spleen section (region of interest  $442 \times 555\ \mu\text{m}^2$ ) registered in the scanning mode with  $2\ \mu\text{m}$  step size. B) Instrumental and optical set-up of the new wide-field system

Widefield OPTIR approaches were described in the literature [1] to capture images in milliseconds at submicron spatial resolution. Inspired by these developments, a novel implementation will be presented. For wide-field detection at sub-micron resolution, a CMOS camera was used in conjunction with visible light source (see Figure 1B). The CMOS camera was employed in a time-gated manner to capture images during the on and off periods of the IR beam. Photothermal contrast is provided by the differences between the photographs. A spatial resolution of roughly  $600\text{ nm}$  was demonstrated by the system using a  $40\times$ ,  $0.6\text{ NA}$  objective. With a field of approximately  $300 \times 300\ \mu\text{m}^2$ ,

OPTIR images can be captured at 200 ms using a 5 mega-pixel CMOS camera. The new system is expected to capture the photothermal contrast from biomedical sample as shown in Figure 1A within a second. Furthermore, rapid hyperspectral imaging of the samples can be achieved by series of images and IR spectra can be reconstructed.

The perspectives of widefield OPTIR imaging will be demonstrated in the biomedical context for tissue sections and cell screening.

## **ACKNOWLEDGMENTS**

This work is supported by BMBF, funding program Photonics Research Germany (13N15464) and is integrated into the Leibniz Center for Photonics in Infection Research (LPI).

## **REFERENCES**

1. C. Krafft, R. Salzer, S. Seitz, C. Ern, M. Schieker. Differentiation of individual human mesenchymal stem cells probed by FTIR microscopic imaging. *Cytometry A*, 2005, **64A**, 53-61
2. Y. Bai, J. Yin, and J.X. Cheng. "Bond-selective imaging by optically sensing the mid-infrared photothermal effect." *Science Advances*, 2021, **7.20**, eabg1559



# Interaction of a synthetic bio-relevant drug-molecule with C<sub>24</sub> and B<sub>12</sub>N<sub>12</sub> fullerene: A first-principles quantum chemical investigation

A. K. Vishwkarma<sup>a</sup>, T. Yadav<sup>a</sup>, A. Pathak<sup>a</sup>, G. Brahmachari<sup>b</sup>

<sup>a</sup>*Department of Physics, Institute of Science, Banaras Hindu University, Varanasi, India*

<sup>b</sup>*Laboratory of Natural Products & Organic Synthesis, Department of Chemistry, Visva-Bharati (A Central University), Santiniketan, India*

## Abstract

This research deals with the interaction of a synthetic bio-relevant drug-molecule with fullerene like nanocages specifically C<sub>24</sub> and B<sub>12</sub>N<sub>12</sub> to explore their potential as carrier in drug delivery systems [1-4]. The efficacy of C<sub>24</sub> and B<sub>12</sub>N<sub>12</sub> nanocages as an effective drug carrier has been investigated by computing electronic and geometric properties along with adsorption energies in different possible configurations. The *ab initio* calculations have been performed at DFT/B3LYP/6-31G (d, p) level of theory. The adsorption energy for the target molecule over the surface of C<sub>24</sub> nanocage in the most favorable configuration has been calculated to be -1.324kcal/mol. However, the target molecule when adsorbs over the surface of B<sub>12</sub>N<sub>12</sub> nanocage then its adsorption energy is -20.659kcal/mol for the most favorable configuration in the gas phase, which suggests that B<sub>12</sub>N<sub>12</sub> nanocage can be used as an effective drug carrier for target molecule. In contrast, C<sub>24</sub> nanocage due to its low value of adsorption energy cannot be used as a drug carrier for the target molecule. We have computed various electronic properties viz HOMO-LUMO energy gap, Fermi level and work function. Moreover, the effect of aqueous media on these electronic properties and adsorption energy has been explored.

**Keywords:** DFT, Fullerene nanocages, Adsorption Energy, Electronic properties.

Email of authors: [akv1993.au@gmail.com](mailto:akv1993.au@gmail.com), [tarunyadavbly@gmail.com](mailto:tarunyadavbly@gmail.com), [amitpah@gmail.com](mailto:amitpah@gmail.com), [brahmg2001@yahoo.co.in](mailto:brahmg2001@yahoo.co.in)

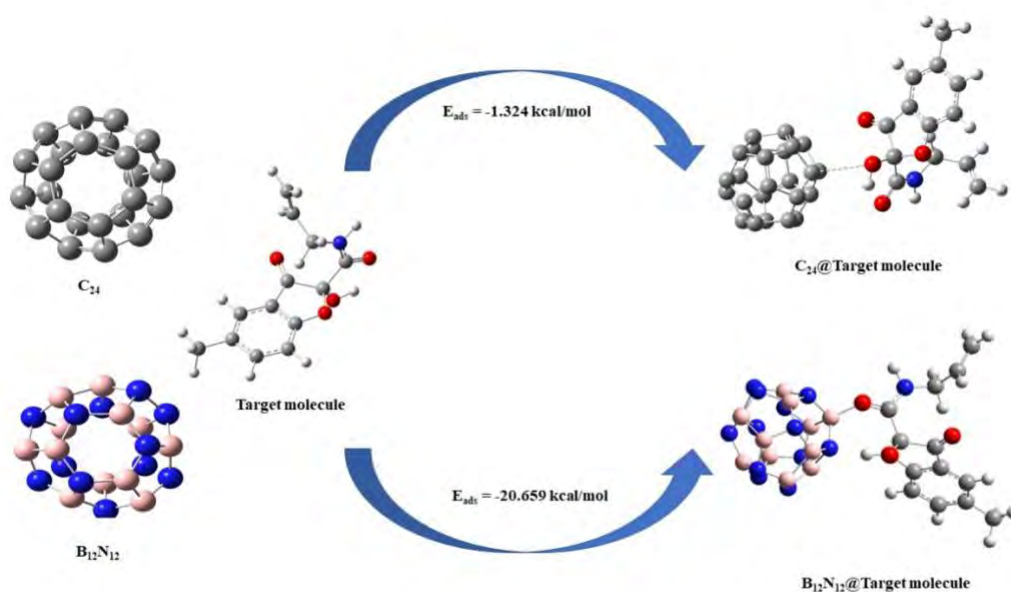


**Figure1** Optimized structures of  $C_{24}@target$  and  $B_{12}N_{12}@target$  molecule for the most favorable configuration.

## Acknowledgements

The author A. K. Vishwkarma is grateful to UGC India to provide financial support in form of UGC-JRF/SRF (Award Number:1499/ (CSIR-UGC NET DEC.2018). A. Pathak acknowledges financial support from the IoE grant of Banaras Hindu University (R/Dev/D/IoE/Incentive/2021-22/32439) and financial support through the Core Research Grant of SERB, New Delhi (CRG/2021/000907).

## References

1. A. Al-Jumaili, S. Alancherry, K. Bazaka, M. Jacob, *Materials*, 10(9), (2007), 1066.
2. R. Ahmadi, M.R.J. Sarvestani, B. Sadeghi, *Int. J. Nano. Dimens.*, 9(4), (2018), 325-335.
3. Q. Sun, R. Zhang, J.Qiu, R.Liu, W.Xu, *Adv. Mater.*, 30(17), 1705630.
4. B. T. Tomic, C.S. Abraham, S. Pelemis, S. J. Armakovic, S. Armakovic, 21, (2019), 23329.

# Infrared molecular fingerprinting of blood plasma glycoproteins.

Liudmila Voronina<sup>a,b</sup>, Frank Fleischmann<sup>a,b</sup>, Mihaela Žigman<sup>a,b,c</sup>

<sup>a</sup> Max Planck Institute of Quantum Optics, Garching, 85748 Germany

<sup>b</sup> Ludwig Maximilian University of Munich, Garching, 85748 Germany

<sup>c</sup> Center for Molecular Fingerprinting, Budapest, 1093 Hungary

Vibrational spectroscopy is well suited for studying protein post-translational modifications: the corresponding functional groups produce characteristic absorption bands that arise at different spectral ranges than the major signals from the protein backbones.<sup>1</sup> Therefore, intact proteins can be investigated, eliminating the need for protein digestion. This approach is especially promising for protein glycosylation, which carries a wealth of information about the health state of an individual.<sup>2</sup>

So far, infrared spectroscopy has mostly been applied to purified glycoproteins.<sup>3</sup> Here we extend its use to classes of proteins separated from blood plasma using ion exchange chromatography. We demonstrate that infrared spectroscopy identifies different patterns and global levels of glycosylation of intact proteins obtained from crude clinical samples. As an example, we use global glycosylation index<sup>3</sup> to quantify the percentage of protein mass contributed by the glycans and compare glycosylation patterns of human and bovine orosomucoid.

Next, we perform spiking experiments that model a biomarking scenario: glycosylation of a particular protein is affected by a disease and this change is spectroscopically detected. We confirm that chromatographic separation significantly improves the detection capabilities.

Stepping away from the model system, we present the results of a pilot case-control study, comparing the glycosylation patterns of blood plasma proteins in lung cancer patients and control individuals. Although aberrant protein glycosylation has been detected in lung cancer patients previously,<sup>4</sup> to our knowledge, it is the first time that it has been observed in top-down manner using vibrational spectroscopy.

In addition to using conventional Fourier-transform infrared spectroscopy, we present the first evidence that the high sensitivity of field-resolved laser-based infrared spectroscopy developed in our group<sup>5</sup> contributes to improved signal-to-noise ratio in protein glycosylation analysis.

Generally, in this work we aim to combine the simplicity of a spectroscopic measurement with the richness of the biological information contained in glycans.

## **ACKNOWLEDGMENTS**

This work was funded by the Center for Advanced Laser Applications (CALA) of the Ludwig Maximilians University Munich (LMU), Department of Laser Physics, and the Max Planck Institute of Quantum Optics (MPQ), Laboratory for Attosecond Physics, Germany.

The authors thank Prof. Ferenc Krausz for his continuous support and fruitful discussions.

## **REFERENCES**

1. M. Khajepour, J.L. Dashnau, J.M. Vanderkooi, Infrared spectroscopy used to evaluate glycosylation of proteins, *Anal. Biochem.* 348 (2006) 40-48.
2. Reily, C., Stewart, T.J., Renfrow, M.B. & Novak, J. Glycosylation in health and disease. *Nat. Rev. Nephrol.* 15 (2019) 346-366.
3. Derenne, A. et al. Mass Spectrometry of Glycoproteins. in *Mass Spectrometry of Glycoproteins* (ed. Delobel, A.) 401 (Humana Press, 2021).
4. Arnold, J. N. et al. Novel glycan biomarkers for the detection of lung cancer. *J. Proteome Res.* 10, 1755-1764 (2011).
5. Pupeza, I. et al. Field-resolved infrared spectroscopy of biological systems. *Nature* 577 (2020) 52-59.

# **Integrating Optical Coherence Tomography Localization with Spatially Offset Raman Spectroscopy: A New Approach to Enhance Skin Tissue Examination**

Di Wu<sup>a</sup>, Anatoly Fedorov Kukk<sup>a</sup>, Bernhard Roth<sup>a,b</sup>

<sup>a</sup> *Hannover Centre for Optical Technologies, Leibniz University Hannover, Nienburger Str. 17, 30167 Hanover, Germany*

<sup>b</sup> *Cluster of Excellence PhoenixD, Leibniz University Hannover, Welfengarten 1, 30167 Hannover, Germany*

Skin cancer, particularly cutaneous melanoma, is a significant global health concern due to its increasing incidence and potential lethality. Early detection is critical for effective intervention and improved patient outcomes. A new multi-modal optical imaging system integrating optical coherence tomography (OCT) and spatially offset Raman spectroscopy (SORS) is proposed, utilizing the OCT scanning mode to achieve the spatial offset of the acquisition point required by SORS, see Figure 1.

Skin phantoms were created by dissolving gelatin in distilled water and adding carotenoids and melanin (the latter being insoluble in water was dissolved in dimethyl sulfoxide before being added to the phantom) to simulate normal skin and cutaneous melanoma, respectively. For SORS measurements, a 10 mm thick melanin phantom was stacked on top of a carotenoid phantom. Without offset, the spectral peaks of the carotenoids were almost invisible, but when the offset was gradually increased to 2 mm, the peaks of the carotenoids became stronger and more visible, proving that SORS has the ability to detect deeper layers of the skin that are impenetrable by normal Raman spectroscopy, see Figure 2. This indicates that SORS has the ability to complement the information required by dermatologists compared to ordinary Raman spectroscopy.

The combination of SORS with OCT further enhances its diagnostic capabilities. OCT provides high-resolution imaging of tissue microstructure, offering complementary morphological information to the chemical insights provided by SORS. The integration of these two modalities enables a comprehensive evaluation of skin lesions, including structural, depth, and chemical composition information, and presents a promising avenue for advancing non-invasive skin cancer diagnosis. This new capability will be presented and discussed based on selected examples.

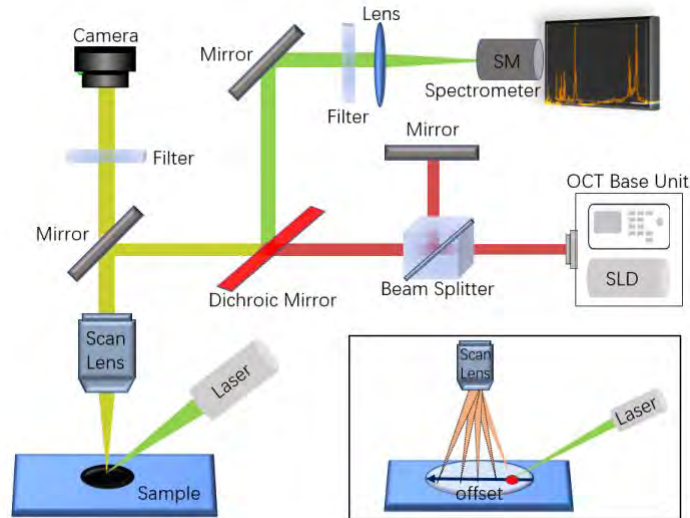


**Figure 1** Sketch of the OCT-SORS multi-modal setup, the small box in the lower right corner demonstrates the process of achieving the spatial offset of the acquisition point using the OCT scanning lens.

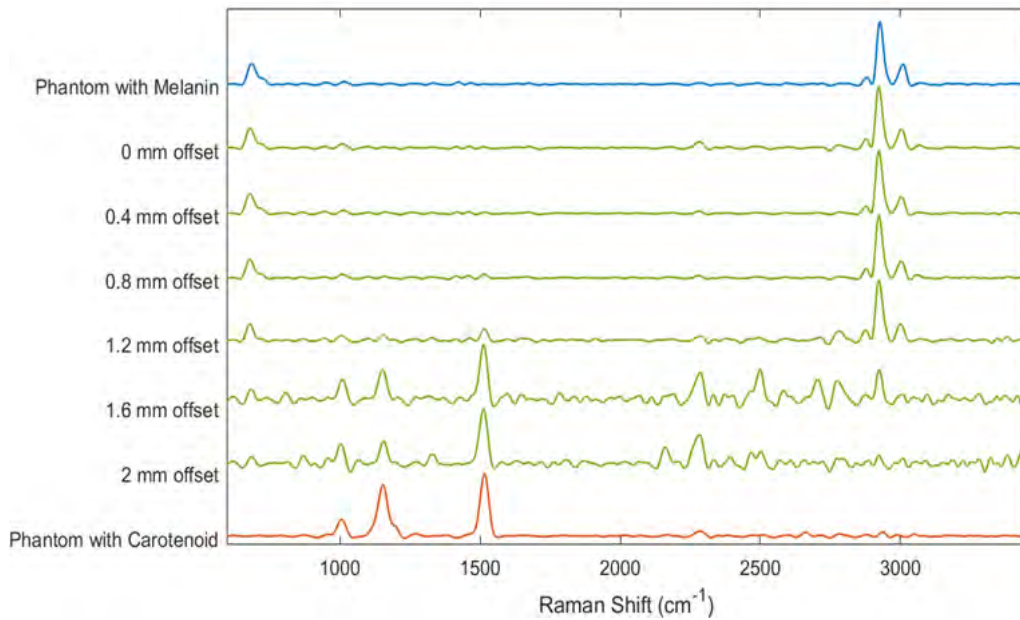


**Figure 2** SORS spectra obtained by stacking a 10 mm gelatine phantom with melanin added on top of a gelatine phantom containing carotenoids. As the offset increases, the three peaks of the carotenoids become more and more obvious.

## ACKNOWLEDGMENTS

We thank the financial support from the German Research Foundation DFG (German Research Foundation, Project ID RO 3471/18-1 and EM 63/13-1). Also, financial support from the German Research Foundation (DFG) under Germany's Excellence Strategy within the Cluster of Excellence PhoenixD (EXC 2122, Project ID 390833453) is acknowledged.

# Unraveling Genetic Secrets: RNA Modification detection of single nucleotides by AI methods after ONT sequencing

Jannes Spangenberg<sup>a</sup> and Manja Marz<sup>a,b,d</sup>

<sup>a</sup> RNA Bioinformatics and High-Throughput-Analysis, Friedrich Schiller University Jena, Germany

<sup>b</sup> European Virus Bioinformatics Center 2, Leutragraben 1, 07743 Jena, Germany

<sup>c</sup> FLI Leibniz Institute for Age Research, Beutenbergstraße 11, 07745 Jena, Germany

Nanopore sequencing techniques have emerged as powerful tools for deciphering the composition of genomes and transcriptomes of e.g. pathogenic agents. The ONT MinION method enables even direct RNA sequencing, allowing us to read chemical modifications of single nucleotides. This breakthrough is currently leading us into a new era of genetic analysis.

We have developed AI-based, context sensitive deep neural networks capable of reading individual RNA modifications. I will introduce a method enabling researchers to discover any of the 340 described RNA modifications throughout the epitranscriptome. Our focus is on the identification and characterization of RNA modifications, a field of increasing importance, as these modifications play a pivotal role in gene regulation and expression.

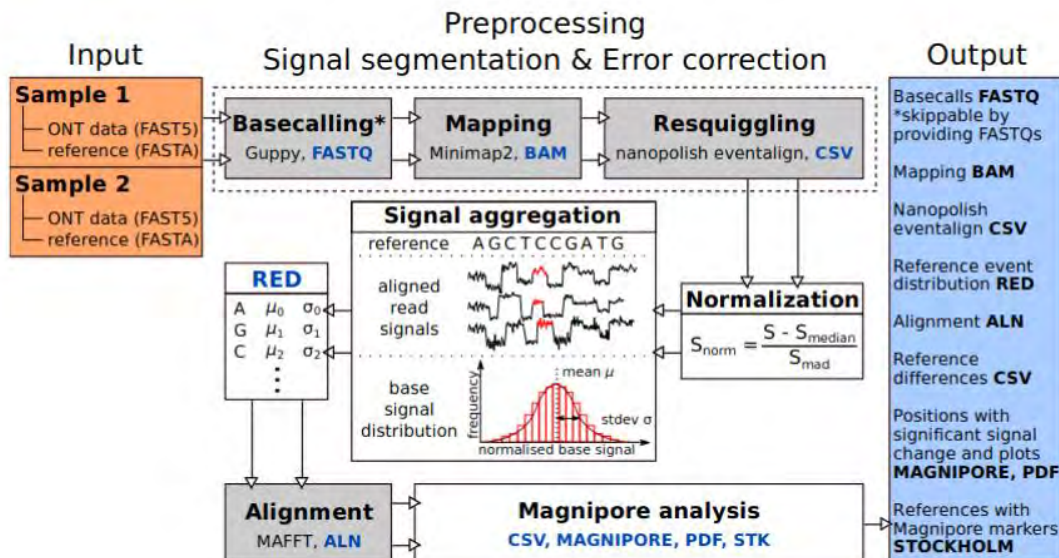
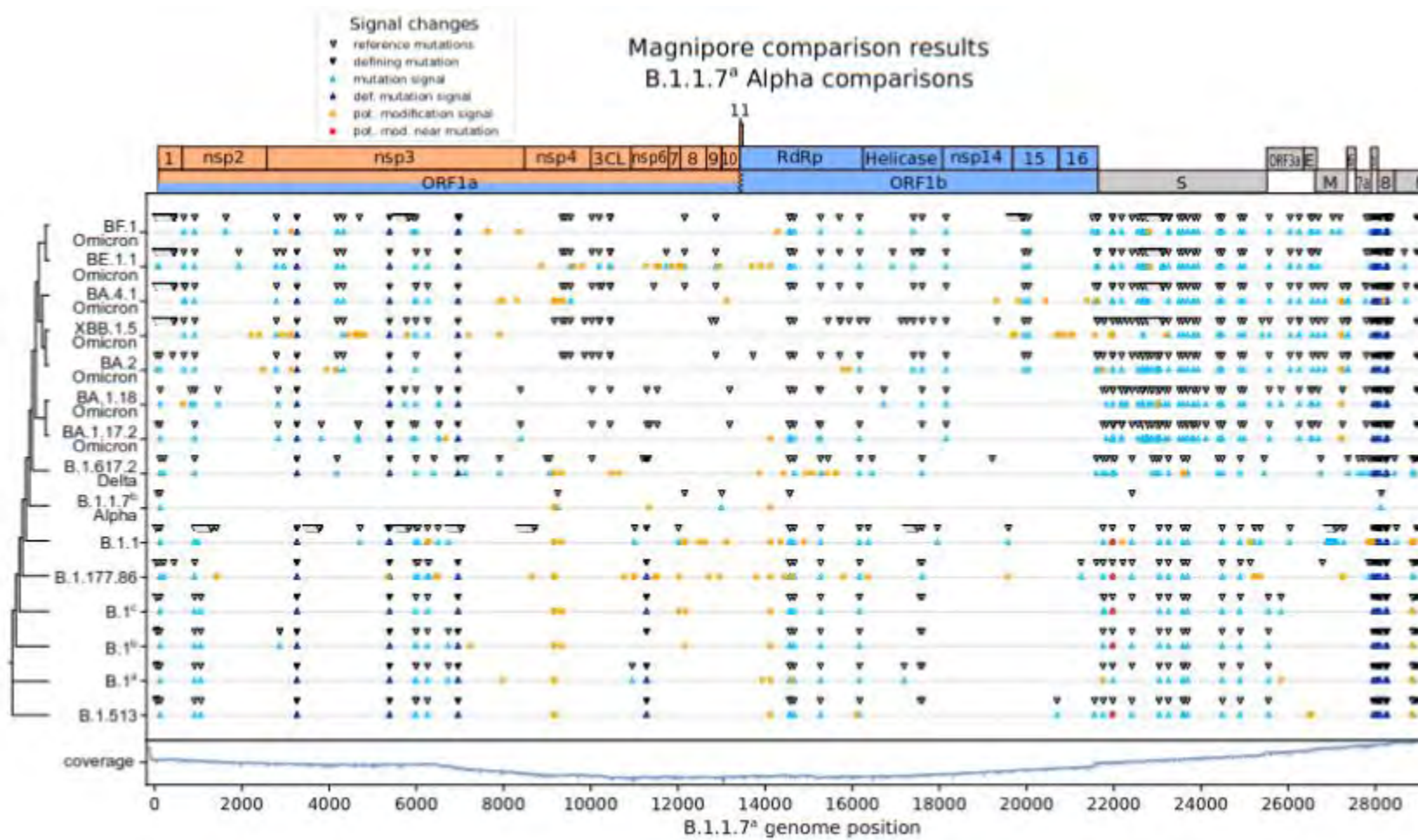




**Figure 1** Overview of the tool Magnipore, ready to use for direct application of sequenced cellular or viral RNA.

Additionally, we have created 'Magnipore', a novel tool designed to detect significant signal shifts in ONT data between samples of similar or related pathogenic species. Magnipore classifies these shifts into mutations and potential modifications. We used Magnipore to compare SARS-CoV-2 samples, revealing an evolutionary impact reflected in the modification profiles. This discovery suggests a link between RNA modifications in viral genomes and their pathogenic potential. With Magnipore, we provide a rapid, high-throughput solution for tracking and understanding the spread and evolution of the virus at a genetic level.

**Figure 2** Magnipore shows defining mutations of the several SARS-CoV-2 types (e.g. Alpha, Omicron) and adds a new layer of information by presenting defining RNA modifications of the several virus variants.



## **ACKNOWLEDGMENTS**

The authors thank Dr. Barbara Mühlemann (Institute of Virology, Charité Berlin) for providing the Illumina reference sequences. Special thanks go to Dr. Thomas Lorentz (Labor Dr. Krause) and Prof. Helmut Fickenscher (Institute for Infection Medicine) for providing the equipment, reagents and facilities.